CHAPTER 1: INTRODUCTION

INTRODUCTION

OBJECTIVES AND METHODOLOGY

The objective of the present study was to document quantitatively the petrologic composition and porosity-permeability patterns of the Jurassic and Lower Cretaceous Surat Basin succession and to elucidiate the effect of detrital mineralogy and diagenetic overprints on sandstone reservoir characteristics. To this end 215 rock samples were collected from five Gelogical Survey of Queensland (GSQ) fully-cored stratigraphic test wells in a west-east transect (Figure 1.1, Table 1.1). The samples comprised the remnant surrounds of core-plugs on which porosity and permeability were measured by Bureau of Mineral Resources (BMR) personnel, Canberra. Thin-sections impregnated with blue epoxy resin and cut normal to bedding were made from these samples, and were stained with potassium ferricyanide and alizarin red-S to highlight the presence of carbonate minerals and to simplify their identification. One thousand points were counted in each thin-section including detrital framework grains, interstitial material and the genetically different porosity categories (see Appendix 1.1). A count of 1000 points ensures a two-sigma (2σ) statistical confidence range of +/- 3% or less for any modal component (Van der Plas and Tobi, 1965). A further 26 modal analyses were made on an additional subset of thin-sections stained for K-feldspar using sodium cobaltinitrite solution (cf. Friedman, 1971) and employing a count of 600 points per thin-section to better resolve the feldspar mineralogy. Average grainsize was determined by measurement of the long axis dimension of 10 grains in the dominant size mode in each thin-section. Thin-section studies were supplemented by BMR quantitative porosity and permeability data from GSQ open-file reports and publications (Noon and Coote, 1983;

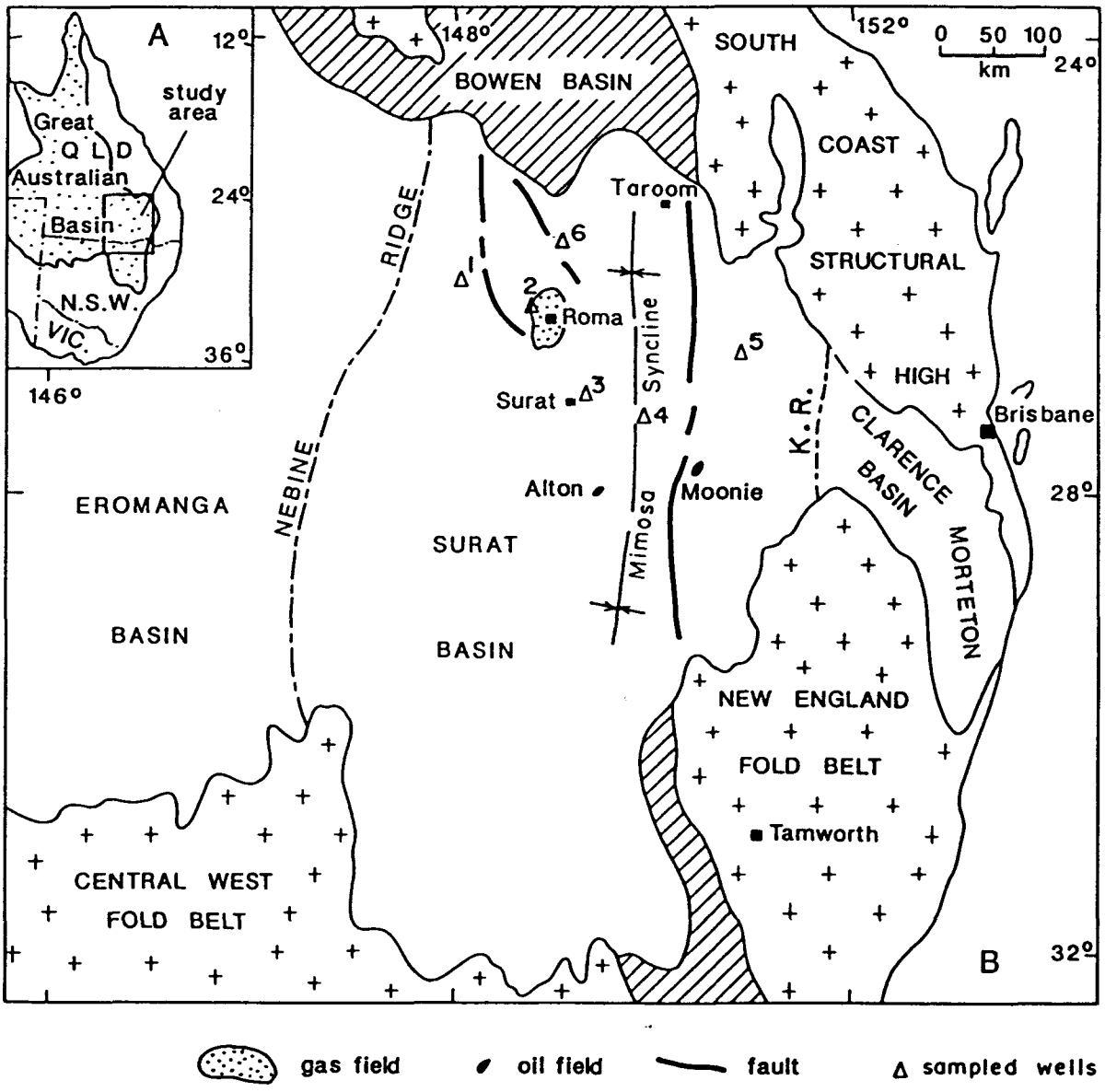

Figure 1.1. Location (A) and major structural elements (B) of the Surat Basin (after Exon, 1976). Sampled GSQ wells are: 1 - Mitchell 2; 2 - Roma 8; 3 - Surat 1; 4 - Surat 3; 5 - Chinchilla 4. Well 6 is GSQ Taroom 17, used as a source of vitrinite reflectance data (together with GSQ Mitchell 2, Roma 8, and Chinchilla 4; cf. Appendix 2.8) for assessing the thermal maturation characteristics of the basin. K.R. - Kumbarilla Ridge.

Table 1.1 Name and location of the stratigraphic wells with sample distribution on formation basis. Well locations, elevations, total depth and intersected formations are from Noon and Coote (1983) and Coote (1986).

Well name	Year completed	Location (o & ')	Elevation (m)	Total Depth (m)	Formation intersected	Number of samples taken	Number of samples with Porosity-permeability data	
							Measured by BMR	Measured by author
GSQ Surat 1	1968	27 05 S 149 12 E	N. R.[1]	351	Surat Siltstone	—[2]	—[2]	—[2]
					Wallumbilla Formation	4	4	
					Bungil Formation	5	2	
GSQ Surat 3	1968	27 33 S 149 39 E	N. R.	460	Griman Creek Formation	26	26	
					Surat Siltstone	2	2	
					Wallumbilla Formation	3	2	1
GSQ Roma 8	1983	26 33 S 148 36 E	312	1163	Wallumbilla Formation	—	—	—
					Bungil Formation	4	4	
					Mooga Sandstone	4	4	
					Orallo Formation	11	11	
					Gubberamunda Sandstone	6	6	
					Westbourne Formation	3	3	
					Springbok Sandstone	2	2	
					Birkhead Formation	9	8	1
					Hutton Sandstone	22	5	17
					Evergreen Formation	4	—	4
					Precipice Sandstone	2	—	2
					Basement	—	—	—
GSQ Mitchell 2	1984	26 21 S 148 08 E	400	1004	Wallumbilla Formation	—	—	—
					Bungil Formation	3	3	
					Mooga Sandstone	1	—	1
					Orallo Formation	11	11	
					Gubberamunda Sandstone	4	4	
					Westbourne Formation	7	7	
					Springbok Sandstone	2	—	1
					Birkhead Formation	2	1	1
					Hutton Sandstone	25	25	
					Evergreen Formation	2	2	
					Precipice Sandstone	1	1	
					Bowen Basin Sequence	—	—	—
					Basement	—	—	—
GSQ Chinchilla 4	1984	26 44 S 150 12 E	295	1255	Orallo Formation	2	2	
					Gubberamunda Sandstone	7	7	
					Westbourne Formation	3	—	3
					Springbok Sandstone	2	—	2
					Walloon Coal Measures	16	12	4
					Hutton Sandstone	4	4	
					Evergreen Formation	10	10	
					Precipice Sandstone	6	6	
					Bowen Basin Sequence			

Footnotes to Table 1.1

1 Not reported.

2 Not sampled.

Coote, 1986). Additional porosity and permeability measurements were made by the author at the BMR on the same equipment to that used for the existing GSQ data to check their reproducibility and to extend the data-base. Porosity was measured with helium as the saturating medium and permeability with dry nitrogen as the flowing medium. Fresh, artificially fractured small samples from the remnants of core materials after thin-section preparation were coated with gold and examined under the scanning electron microscope (SEM). About 500 SEM photomicrographs of different diagenetic minerals and pore geometry were taken. The compositions of certain diagentic minerals were determined using an energy dispersive X-ray (EDX) facility fitted with a SEM. Orientated X-ray diffraction (XRD) samples of the clay fraction (<2 um) were prepared and analysed from 11 sandstone samples following procedures described by Drever (1973), Brindley and Brown (1980) and Carroll (1970). Additionally, identification of certain diagenetic and detrital minerals was facilitated by electron microprobing. Various statistical procedures (e.g., factor, simple and multiple regression analyses) were performed on petrographic and petrophysical data using SPSSX software (SPPS Inc, 1983) on the Macquarie University VAX mainframe computer system. A more detailed version of the methodology employed in the thesis is given in Appendix 1.11.

The author commenced work on this project on a full-time basis in January, 1986 and continued until March, 1989 with the exception of a period of four-weeks recreation leave in October, 1987. The study was undertaken under the general supervision of Dr. P. J. Conaghan of the School of Earth Sciences.

The chapters in this thesis are written as a series of self-contained papers which has led to some unavoidable repetition of certain background material. The data on which the chapters are based are presented in the accompanying appendices, and supporting documentation in

the body of the report. Chapter 8 and part of Chapter 9 stem from a literature survey undertaken during the earlier phase of my candidature at the suggestion of Associate Professor John Veevers.

This report represents a substantial contribution to the study of sandstone petrology and reservoir evolution of the Surat Basin clastics. Despite being Australia's first commercial oil-producing basin, virtually no comprehensive published or unpublished record exists on the petrology and reservoir aspects of the Surat Basin succession. Allen and Houston (1964) and Houston (1972) provided a semiquantitative reconnaisance petrography of the Surat Basin sandstones. Mason (1980) described the stratigraphy and petrography of the Walloon Coal Measures sandstones in the Taroom area. Martin (1976, 1981) studied the petrology and diagenesis of the Precipice Sandstone which constitutes the major hydrocarbon reservoir in the Surat Basin. However no such study exists for the other stratigraphic units, some of which are hydrocarbon producing in the Surat Basin. The present work describes in a quantitative manner the reservoir potential of all the formations of the Surat Basin succession many of which are presently barren of hydrocarbons but whose lateral equivalents constitute reservoirs in the neighbouring Eromanga Basin.

The study of sandstone diagenesis in this report is pursued in the context of the basin's overall geologic evolution, tectonics, depositional environments, and thermal history. Many of the supposed influencing factors on the evolution of reservoir characteristics have been quantified and the interpretations and conclusions substantiated by petrographic and petrophysical data.

GEOLOGIC SETTING

The Jurassic to mid-Cretaceous Surat Basin is a segment of the Great Australian (Artesian) Basin that extends across southeastern Queensland (Qld) and northeastern New South Wales (NSW), Australia (Figure 1.1). It was formed in the Early Jurassic as a retro-arc foreland basin in response to a magmatic arc which lay along what is now the Great Barrier Reef in offshore Queensland. A convergent plate boundary existed several hundred km east of the arc where the Pacific Plate subducted under the eastern Gondwanaland Plate (Jones and Veevers, 1983). It is a composite basin and overlies the Permo-Triassic Bowen Basin (Figure 1.1). The average thickness of the Jurassic and Lower Cretaceous succession of the basin is 1.5 km which increases to 2.5 km in the Mimosa Syncline (Figure 1.1). The Surat Basin is separated from the neighbouring Eromanga Basin to the west by a linear basement culmination called the Nebine Ridge whereas to the east it is separated from the Clarence-Moreton Basin by the Kumbarilla Ridge (Figure 1.1).

The Surat Basin succession is a record of continuous sedimentation from the Early Jurassic onward up to Albian (Figure 1.2) but there had been a considerable degree of difference in the style and rate of sedimentation between the Jurassic and the Early Cretaceous. Jurassic sedimentation was mainly terrestrial (with the possible exception of a brief marine incurson during deposition of the Evergreen Formation) and the rate of sedimentation was slower (40 m/Ma) compared to the environmentally 'wet' Lower Cretaceous succession which was deposited in a dominantly paralic/shallow-marine environment (Figure 1.2) and where the sedimentation rate reaches 150 m/Ma (cf. Exon, 1976).

According to Exon (1976) the structural features of the Surat Basin are mainly due to differential compaction of the underlying Bowen Basin sediments. In post-Cretaceous times the basin's northern margin was

uplifted and eroded, resulting in a significantly southerly tilt to the succession (Battersby, 1981), subsequently to be followed during the Plio-Peistocene by the inception of the artesian system (Bowering, 1982).

STRATIGRAPHY

The stratigraphy of the Surat Basin has been described by many workers. Whitehouse (1954) was the first to conduct a regional survey of the Great Artesian Basin. Mack (1963) reviewed the surface and subsurface geology of the southern part of the Surat Basin; Day (1964) mapped the Roma - Wallumbilla area in detail. The work of Power and Devine (1970) is regarded as the most extensive subsurface stratigraphic study of the Surat Basin. They carried out detailed basinwide correlations and also discussed the geologic history of the Surat Basin and its petroleum potential. The geology of the Great Artesian Basin in NSW was reviewed by Hind and Helby (1969) and more recently by Hawke and Cramsie (1984). Other detailed stratigraphic and sedimentological studies include those of Moran and Gussow (1963), and Porter (1979). Exploration in the Roma area is documented by Swindon (1965, 1968), Traves (1971) and Sell et al (1972). Allen (1976) and Groves (1976) provided comprehensive summaries of the hydrocarbon fields and petroleum geology of the Surat Basin. Battersby (1981) reviewed the status of hydrocarbon exploration including new discoveries. The most comprehensive recent review of the Geology of the Surat Basin is that of Exon (1976). The stratigraphy of the Surat Basin used herein (Figure 1.2) follows that of Exon (ibid.).

PETROLEUM EXPLORATION HISTORY

Gas and condensate were discovered unexpectedly during the sinking of a water bore at Hospital Hill, Roma in 1900. Reserves were, however, limited and the results of further drilling were disappointing. The modern phase of exploration began in 1960 with the discovery of oil and gas at

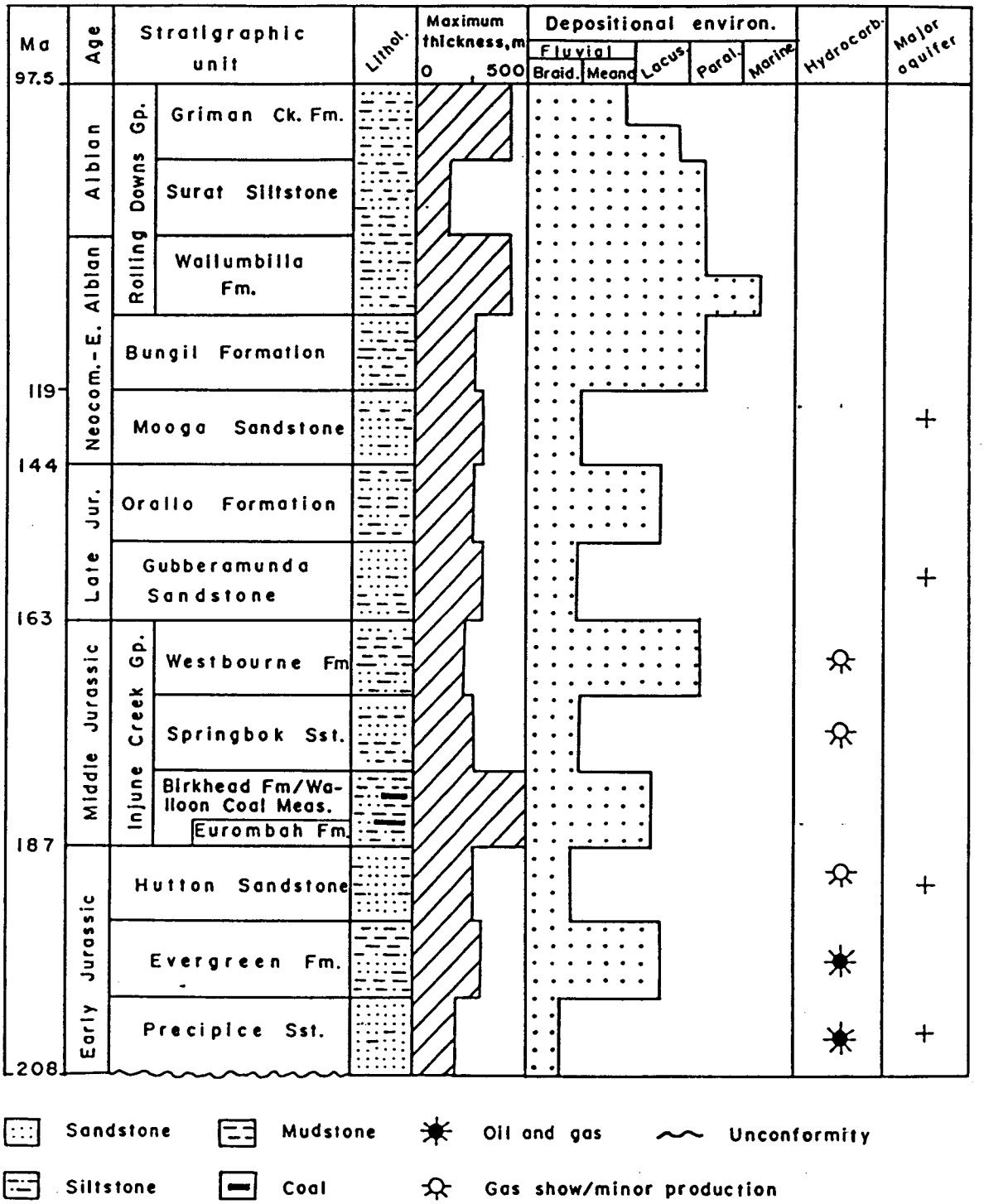

Figure 1.2. Generalised stratigraphic column and the distribution of hydrocarbons and aquifers in the Surat Basin (after Exon, 1976 with modifications). Time scale after Palmer (1983).

Cabawin (1960) followed by commercial oil at Moonie (1961). At about the same time, gas was discovered in the Roma Shelf at Timbury Hills 1 (1960) and Pickannjinnie 1 (1960). Since then more than 700 exploration and development wells have been drilled resulting in the discovery of more than 50 oil and gas fields (Battersby, 1981). The Surat Basin is now considered as the most densely drilled basin in Australia. Exploration activity has stabilized and slowed to some extent in recent years in view of the depletion of older fields and fewer new discoveries.

HYDROCARBON OCCURRENCE

Most known hydrocarbons in the Surat Basin occur in the Precipice Sandstone and Basal Evergreen Formation (Figure 1.2). Gas has been discovered in the Hutton Sandstone only in the Leichhardt field and very minor gas production has been reported from the Springbok Sandstone and the Westbourne Formation in the Roma area (Allen, 1976; Groves, 1976). Sandstones with good reservoir characteristics exist throughout the Surat Basin Mesozoic succession as evidenced by their functioning as aquifers (Figure 1.2). Lack of adequate seals over many of these formations and thermal immaturity of hydrocarbon source-rocks are held responsible for their general barrenness.

REFERENCES

Allen, R. J., and Houston, B. R., 1964, Petrology of Mesozoic sandstones of the Carnarvon Highway section, Western Bowen and Surat Basins. Geol. Surv. Qld. Rpt. 6. 25 p.

Allen, R. J., 1976, Surat Basin. In Leslie R. B., Evans H. J., and Knight C. L., (eds.) Economic geology of Australia and Papua New Guinea. Australas. Inst. Min. Metall. Monogr. 7, pp. 262-272.

Battersby, D. G., 1981, New discoveries in the Surat/Bowen Basin. Austral. Petrol. Expln Assoc. Jour., v. 21, pp. 39-44.

Bowering, O. J. W., 1982, Hydrodynamics and hydrocarbon migration - a model for the Eromanga Basin. Austral. Petrol. Expln Assoc. Jour. v. 22, pp. 227-236.

Brindley, G. W., and Brown, G., 1980, Crystal structures of clay minerals and their X-ray identification. Mineral. Soc. Monogr. 5, 495 p.

Carroll, D., 1970, Clay minerals - a guide to their X-ray identification. Geol. Soc. of Amer. sp. paper 126.

Coote, S. M., 1986, Departmental stratigraphic drilling in Queensland, 1983 to 1986. Qld. Govt. Min. Jour., v. 87/1017, pp. 306-326.

Day, R. W., 1964, Stratigraphy of the Roma - Wallumbilla area. Geol. Surv. Qld. Publ. 318, pp. 1-23.

Drever, J. I., 1973, The preparation of oriented clay mineral specimens for X-ray diffraction analysis by a filter-membrane peel technique. Amer. Mineral., v. 58, pp. 553-554.

Exon, N. F., 1976, Geology of the Surat Basin in Queensland. Bureau Miner. Res. Bull. 166, 160 p.

Friedman, G. M., 1971, Staining. In Carver, R. E. (ed.) Procedures in sedimentary petrology. Wiley-Intersc., New York, pp. 511-530.

Groves, R. D., 1976, Roma Shelf petroleum fields. In Leslie R. B., Evans H. J., and Knight C. L., (eds.) Economic geology of Australia and Papua New Guinea. Australas. Inst. Min. Metall. Monogr. 7, pp. 280-302.

Hawke, J. M., and Cramsie, J. W. (eds.) Contributions to the Geology of the Great Artesian Basin in New South Wales. Geol. Surv. NSW Bull. 31, 295 p.

Hind, M. C., and Helby, R. J., 1969, The Great artesian Basin in New South Wales. In Packham, G. H., (ed). The Geology of New South Wales. Jour. Geol. Soc. Austral. v. 16, pp. 481-497.

Houston, B. R., 1972, Petrology of subsurface samples of Mesozoic arenites of the Bowen and Surat Basins. In Gray, A. G. R., (ed.) Stratigraphic drilling in the Surat and Bowen Basins, 1967-70. Geol. Surv. Qld. Rpt. 71, pp. 89-98.

Jones, G. J., and Veevers, J. J., 1983, Mesozoic origins and antecedents of Australia's Eastern Highlands. Jour. Geol. Soc. Austral. v. 30, pp. 304-322.

Mack, J. E., 1963, Reconnaissance geology of the Surat Basin, Queensland and New South Wales. Bureau Min. Res. Austral. Petrol. Search Subsidy Acts Publ. 40.

Mason, J. D., 1980, Stratigraphy and petrology of the Jurassic sediments, Taroom, south-central Queensland. B.Sc (Hons) thesis. Univ. of Qld., 59 p.

Martin, K. R., 1976, Sedimentology of the Precipice Sandstone, Surat Basin, Queensland. Unpubl. Ph.D thesis. Univ. Qld. 224 p.

Martin, K. R., 1981, Deposition of the Precipice Sandstone and the evolution of the Surat Basin in the Early Jurassic. Austral. Petrol. Expln Assoc. Jour., v. 21, pp. 16-23.

Moran, W. R., and Gussow, W. C., 1963, The history of the discovery and the geology of the Moonie oil field, Queensland, Australia. Proceed. 6th World Petrol. Congr., Geophys. Geol. Sec. 1. pp. 595-609.

Noon, T. A., and Coote, S. M., 1983, Review of departmental stratigraphic drilling in Queensland. Qld. Govt. Min. Jour., v. 84/985, pp. 417-453.

Palmer, A. R., 1983, The decade of North American geology - 1983 geologic time scale. Geol., v. 11, pp. 503-504.

Porter, C. R., 1979, Fluvio-deltaic deposition in Lower Jurassic sediments of the Surat Basin, Queensland. Austral. Petrol. Expln Assoc. Jour. v. 19, pp. 37-50.

Power, P. E., and Devine, S. B., 1970, Surat Basin, Australia - susurface stratigraphy, history and petroleum. Bull. AAPG v. 54/12, pp. 2410-2437.

Sell, B. H., Brown, L. N., and Groves, R. D., 1972, Basal Jurassic sands of the Roma area. Qld. Govt. Min. Jour. v. 73, pp. 309-321.

SPSS Inc., 1983, SPSSX user guide. McGraw-Hill, New York, 806 p.

Swindon, V. G., 1965, Exploration methods in the Roma area. Austral. Petrol. Expln Assoc. Jour. v. 5, pp. 133-138.

Swindon, V. G., 1968, Case history - Roma area, Austral. Petrol. Expln Assoc. Jour., v. 8, pp. 120-129.

Traves, D. M., 1971, Stratigraphic traps in the Roma area, Queensland, Australia. Proceed. 8th World Petrol. Congr., Applied Sc., London, pp. 275-284.

Whitehouse, F. W., 1954, The geology of the Queensland portion of the Great Artesian Basin. Appendix G, In Artesian water supplies in Queensland. Dep. Co-ord. Gen. Publ. Works, Qld. Parl. pap. A., pp. 56-955.

Van der Plas, L., and Tobi, A. C., 1965, A chart for judging the reliability of point-counting results. Amer. Jour. Sci., v. 263, pp. 87-90.

CHAPTER 2: PETROLOGY AND PROVENANCE OF THE SURAT BASIN SANDSTONES

PETROLOGY AND PROVENANCE OF THE SURAT BASIN SANDSTONES

ABSTRACT

The mineralogic composition of the Jurassic-Lower Cretaceous Surat Basin sandstones ranges from quartzarenite through sublitharenite and feldsarenite/lithic feldsarenite to feldspathic litharenite. With respect to the composition they are subdivided here into two petrofacies: *quartzose*, having more than 50% QFR quartz; and *labile*, with less than 50% QFR quartz content. The labile sandstones are derived from an andesitic magmatic arc which lay to the east of the basin and which intermittently shed volcanogenic detritus into the subsiding foreland basin throughout most of its geologic history. The quartzose facies contains mainly plutonic quartz, has a higher K-feldspar to total feldspar ratio and contains variable amounts of volcanic components. Consideration of likely source-rocks together with limited palaeocurrent data for some formations suggest that the ingredients of the quartzose petrofacies are derived mainly from the craton to the west and southwest but with some input from the arc to the east which presumably was dissected to varying degrees during periods of relative tectonic quiescence when the quartzose facies formations are thought to have accumulated. The compositional spectrum of the Surat Basin sandstones is essentially cyclic beginning with the deposition of the craton-derived quartz-rich sandstones and ending with the arc-derived volcanogenic labile sediments. These petrologic cycles probably reflect episodic tectonic activity of the magmatic arc which waxed and waned through the Jurassic and Early Cretaceous until its death in the later Cretaceous, 80 Ma ago.

INTRODUCTION

Despite being the first commercial oil-producing basin of Australia, no comprehensive petrologic study of the Surat Basin rocks has been made to

date except for the reconnaissance and semi-quantitative work of Allen and Houston (1964) and Houston (1972). Martin (1976, 1981) studied the composition, depositional settings, and diagenesis of the Precipice Sandstone which constitutes the most important hydrocarbon reservoir of the Surat Basin. Arditto (1982, 1983) described the diagenetic alteration of the southern lateral equivalent of the Springbok Sandstone and Westbourne Formation (i.e., the Pilliga Sandstone) in the NSW portion of the Surat Basin. The remaining stratigraphic units of the basin gained little, if any, coverage in published and unpublished studies, which is surprising in view of their in some cases economic potential as regional groundwater aquifers and the fact that many of their lateral equivalents in the neighbouring Eromanga Basin constitute hydrocarbon reservoirs (cf. Figure 2.7).

The present study attempts to describe in a quantitatively rigorous manner the detrital composition of the sandstones of the whole sedimentary succession of the Surat Basin, from the Jurassic Precipice Sandstone at the bottom to the Cretaceous Griman Creek Formation at the top (Figure 1.2). The objectives of the present study are to decipher sandstone provenance from the detrital mineralogy and to relate the control that detrital mineralogy has exerted on diagenetic processes and reservoir porosity and permeability. As will be shown in Chapter 6, detrital mineralogy is found to exert a first-order control on sandstone porosity. Hence, knowledge of detrital composition coupled with other relevant parameters can have excellent predictive capability as to the temporal and spatial distribution of potential hydrocarbon reservoirs.

FACTORS AFFECTING SANDSTONE COMPOSITION

The composition of sandstone is related to four variables, namely: provenance, mineralogical modification during transport and deposition, and

modification during diagenesis (Suttner, 1974). The provenance of sediments includes all aspects of source-area, such as source-rocks, climate and relief (Pettijohn et al, 1972, p. 297). Detrital composition is likely to be affected more by climate and relief in areas where tectonism/magmatism is absent (Basu, 1976). In areas of intense tectonic/magmatic activity such as magmatic arcs and collision orogens, source-rock types determine sediment composition in the flanking basins more than do climate and relief (cf. Dickinson, 1970; see also Potter, 1986). Being a retro-arc foreland basin the detrital mineralogy of the Surat Basin sandstones are influenced more by the source-rock composition and the influence of climate is likely to be minimal, since there is no evidence to suggest that there were drastic changes in climate during the Jurassic and Early Cretaceous, the evidence suggesting instead that the climate remained mainly cool to temperate (Quilty, 1984).

The effect of depositional environment

The effect of depositional environments on sediment composition has been demonstrated by Davies and Ethridge (1975), Ethridge (1977), and Mack (1978). The major changes on sediments that are effected environmentally are progressive increase in quartz content (or siliceous resistates) and decrease in mean grainsize consequent upon prolonged mechanical reworking particularly in littoral environments. But its effect on ancient sandstone is difficult to isolate from that of geologic age and provenance - a problem which has been noted by Mack (1978). Due to the overall environmental shift in the Surat Basin from terrestrial conditions during the Jurassic to paralic/marine conditions during the Early Cretaceous (Figure 1.2), it is likely that sediment composition might have been influenced by this in some way. One formation in the Surat Basin where depositional environment might have contributed to the sediment

compositional maturity is the Bungil Formation which is the second most quartzose formation of the Lower Cretacous succesion in this basin (after the Mooga sandstone; cf. Figures 2.3 and 2.4C). The Bungil Formation was deposited in a near-shore/littoral environment as evidenced by the presence of glauconie pellets and a marine fauna (Exon, 1976). Its relatively quartzose composition compared to the other volcanogenic formations presumably reflects prolonged reworking in near-shore environments (cf. Ferree et al, 1988) possibly reflecting a period of slower sediment influx into the basin and perhaps slower subsidence. This is also evidenced by the generally good sorting and grain-rounding in some samples (Appendix 1.5) relative to that in all other formations. However, it has been generally assumed in provenance determinations that the environmental processes that bring about grain-destruction (and hence compositional change) are minimal (Pettijohn et al, 1972; p. 304).

Dagenetic alterations

With regard to diagenesis, it has played an important role in altering the original sediment composition of the Surat Basin sandstones. Therefore every attempt was made to mentally reverse the diagenetic overprints so as to 'see through' the veil of alterations to the original composition at the time of deposition (cf. Dickinson, 1970; Wolf, 1971).

The major diagenetic changes that occur in the Surat Basin sandstones are mineralogical alterations of framework grains (especially rock-fragments and feldspars), replacement of detrital grains by carbonates, kaolinitization/sericitization of detrital feldspar, minor quartz overgrowth, and varying degrees of occlusion of original pore space by epimatrix, phyllosilicate and other cements (cf. Chapter 3). Although most of the interstitial clay minerals are present either as detrital allogenic clays or chemically precipitated/recrystallized authigenic clays,

a small proportion possibly resulted from the mechanical breakdown of labile detrital grains (diagenetic matrix; Cummins, 1962). Clay is present in all stratigraphic units in varying amounts and there are gradations in the mode of its occurrence ranging from partially altered rock-fragments, partially altered feldspars and mica showing relict features such as grain-shape and cleavage and coherent grain-wide extinction (each of which grain-type was assigned to its respective category in the modal analyses), to deformed lithic grains of epiclastic mudrock squeezed between more competent grains. All other clay, including that comprising both detrital non-epiclastic bed-load-sized grains (i.e., intraclasts) and interstitial matrix lacking diagnostic evidence of a chemically precipitated void-filling origin was regarded as representing allogenic (i.e., detrital) material. Some detrital framework grains have been partially or completely replaced by carbonate cement and such grains (and perhaps other mineralogic grain-types as well) have in places been dissolved completely with the creation of secondary grain-dissolution (moldic) porosity. Moldic porosity is present in varying proportions in all stratigraphic units (Appendix 1.9). However, the total amount of detrital grains completely lost by dissolution (so as to render their original genetic nature undecipherable) hardly exceeds 5% in any formation, which is rather small compared to the variation of framework mineralogy within individual formations.

GRAINSIZE - COMPOSITION RELATIONSHIPS AND THE POINT-COUNTING METHOD

The apparent dependence of sandstone detrital modes on grainsize has been demonstrated by several workers (Blatt et al, 1972, fig. 8-19, p. 301; Mack and Suttner, 1977). The traditional view is that grainsize change is accompanied by compositional change as original clasts are altered in size through chemical and physical weathering (Basu, 1976). However, some

workers (e.g., Dickinson, 1970; Graham et al, 1976; Ingersoll and Suczek, 1979) believe that control of grainsize on modal composition can be excluded and argue that identification and recording of mineral crystals of sand size whether present in a sediment within coarser-grained lithic fragments or as distinct phenoclasts reduces the compositional dependence on grainsize. Notwithstanding the merits of this tack, the present study followed the traditional approach of point-counting and coarsely crystalline polymineralic grains were counted as individual lithic fragments rather than as separate component minerals. The effect of grainsize on sediment composition in the present study is also minimized by the fact that most of the sandstones are medium- to fine-grained with only a few samples lying outside this range within the coarse- and very fine-grained grades (cf. Appendix 1.5; Figure 3.6).

DETRITAL GRAIN-TYPES

The major petrographic grain-types recognised during the point-counting procedure are shown in Table 2.1. A more detailed tabulation of the grain-types together with the porosity categories is shown in Appendix 1.1. Petrographic modal analyses and porosity and permeability data are tabulated in Appendix 1.5. Among the difficulties inherent in the study of labile and sublabile sandstones is the identification of fine-grained lithic fragments, and interpretation of the interstitial matrix - problems that have been discussed by Cummings (1962), Hawkins and Whetten (1969), Dickinson (1970), Wolf (1971), and Dickinson et al (1979). There are gradational grain categories, for instance, chert and felsite grains. To discriminate among such grains of intergradational nature, rigorous thin-section operational criteria were used (cf. Appendix 1.2).

Table 2.1. A classification scheme of petrographic grain-types of the Jurassic - Lower Cretaceous snadstones of the Surat Basin[1].

DETRITAL QFR CATEGORIES

Megaquartz

Common/plutonic	Unstrained/slightly strained; Moderately/highly strained
Volcanic	
Vein	Monocrystalline/polycrystalline
Polycrystalline	Unimodal/bimodal/polymodal

Microquartz

Chert	Clear/cloudy/silty/argillaceous
Metachert	
Microvein	
Chalcedony	

Feldspar

- Perthitic/antiperthitic
- Untwinned
- Carlsbad twinned
- Albite/pericline twinned
- Cross-twinned K-feldspar
- Glomeroporphyritic
- Radiaxial
- Quartz-feldspar intergrowth

Plutonic/metaplutonic/volcanic/hypabyssal

Vitric	Clastic/non-clastic
	Pumiceous, vesicular
	Semiopaque

- Microlitic
- Microgranular
- Felsitic
- Siliceous-granular
- Vapour-phase quartz
- Lathwork
- Spherulitic
- Mesocrystalline-granular
- Other

Carbonate rock-fragments

Tectonite

- Slate/phyllite/semi-schist
- Quartz-mica schist/gneiss
- Ribbon/mylonitic quartz schist
- Calc-schist, Chlorite schist
- Other

Table 2.1 (contd.)

DETRITAL QFR CATEGORIES

Metamorphic, other	Non-foliated types
	Hornfels/metaquartzite
Sedimentary clastic (Extraclastic only)	
Quartzose	
Labile	
Argillite/mudrock	
Extraclastic detrital grains of ambigious/uncertain provenance affinity	
Equant/semiequant massive chlorite/?chamosite	
Non-organic, non-minerogenic opaques/semiopaques	
Wholly replaced pseudomorphous rock-fragments	
Polymineralic rock-fragment of insdeterminate source-rock affinity	
Pseudomatrix	

DETRITAL NON-QFR GRAIN CATEGORIES: EPICLASTIC/INTRACLASTIC

Mica	Biotite/muscovite/chlorite (detrital)
	Degraded indeterminate
Heavy minerals	Pyrobole
	Detrital opaque/semi-opaque heavy minerals
	Transparent/translucent heavy minerlas
Sedimentary intraclasts	
Protomatrix	
Orthomatrix	Pseudomatrix

DETRITAL NON-QFR CATEGORIES: ALLOCHEMICAL/AUTHIGENIC

Bioclasts	
Oolites	
Detrital organics	
Glauconie	
Superficial oolitic coatings of epiclastic grains	
Fecal pellets/peloids	
Void-filling phyllosilicate (epimatrix)[2]	
Dickite	
Kaolin	Clear, discoloured, fine-/coarse-grained
Sheetwork ?smectite	
Illite	
Other	
Other void-lining/filling chemically-precipitated cements	
Phyllosilicate cements	
Quartz overgrowth	
Feldspar overgrowth	
Carbonate	Calcite/ferroan calcite/dolomite
	Ferroan dolomite/ankerite/siderite
Pyrite	
Chert/metaquartz	
Zeolite	Heulandite/clinoptilolite/laumontite
Iron oxide/hydroxide	
Other	

Footnotes to Table 2.1.

1 A more detailed version of the table together with the porosity categories and designated verbal codes used during the point-counting analyses is shown in Appendix 1.1.

2 Terminology of Dickinson (1970).

The types of rock-fragments

Unstable lithic fragments are identified by joint observation of texture and mineralogy. Volcanogenic types display microlitic/lath-like, microgranular, felsitic, vitric, and pyroclastic textures. Microlitic grains are characterised by microlites or tiny laths of plagiclase crystals arranged in either random or fluidal fabrics (Figure 2.1C). Many lithic grains contain euhedral phenocrysts of twinned and/or apparently untwinned feldspar set in a cryptocrystalline groundmass. In the main they are probably representative of volcanic rocks of intermediate composition on the basis of additional mineralogical evidence to be discussed in later sections. Vitric rock-fragments in many cases show clastic and porphyritic textures and are commonly chloritized to varying degrees. Sandstones rich in volcanogenic detritus (e.g., the Rolling Downs Group) also contain sand-size grains of massive chlorite as distinct from chlorite flakes and glauconie pellets. These grains of massive chlorite (grain-type category Achm; cf. Appendix 1.1) are interpreted as volcanic rock-fragments due to their common association with formations rich in unambigious volcanogenic detritus and the presence of relict volcanic textures (e.g., ghost axiolites, shards and small phenocrysts) in some of them. Felsite grains display fine-grained microcrystalline mosaics of quartz and feldspar and are commonly difficult to distinguish from chert. Criteria for distinction include internal relief between quartz and feldspar in plane light and the presence of microphenocrysts visible under crossed nicols. Distinction is facilitated if the groundmass is coarse enough to show the contrast in birefringence between tiny quartz and feldspar crystallites (cf. Appendix 1.2).

Epiclastic sedimentary rock-fragments are present in all formations in varying amounts and range up to 13% in individual samples (cf. Appendix 1.3). They are represented mainly by argillaceous rock-fragments with some

Figure 2.1. Thin-section photomicrographs showing the composition and detrital grain-types of some Surat Basin sandstones.

A: Zoned plagioclase (centre-left) and microlitic volcanic rock-fragments (top-centre and bottom-right). Crossed polars. Springbok Sandstone, GSQ Chinchilla 4/50, depth - 265.68 m.

B: Angular broken feldspar grains (top-centre and bottom-left) and microlitic volcanic rock-fragments (centre). Crossed polars. Orallo Formation, GSQ Roma 8/12, depth - 222.18 m.

C: Lathwork volcanic rock-fragments. Plane light. Orallo Formation, GSQ Mitchell 2/7, depth - 166.34 m.

D: A relatively quartzose sandstone seen under crossed polars. Gubberamunda Sandstone, GSQ Mitchell 2/21, depth - 299.30 m.

A

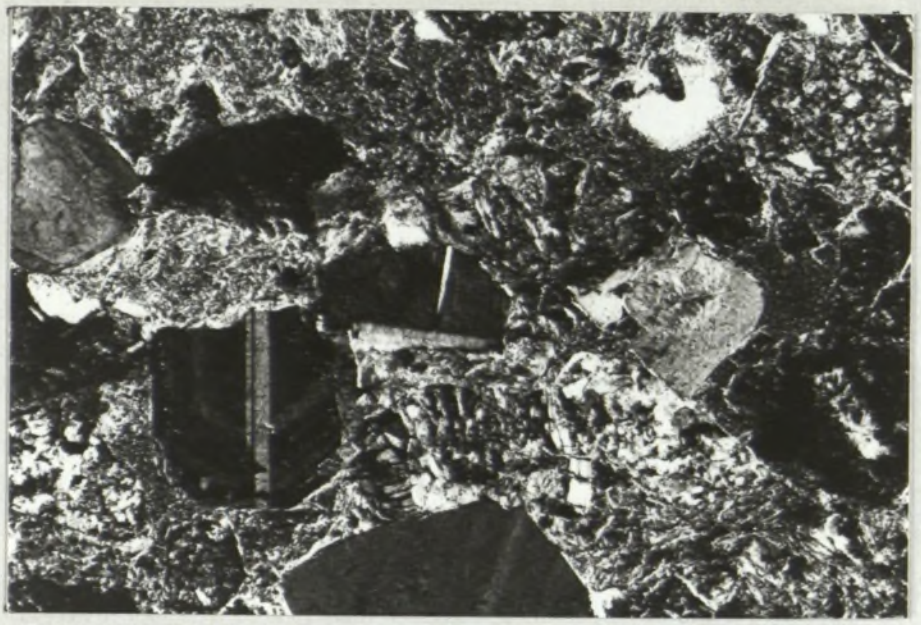

0.1 mm

B

0.1 mm

C

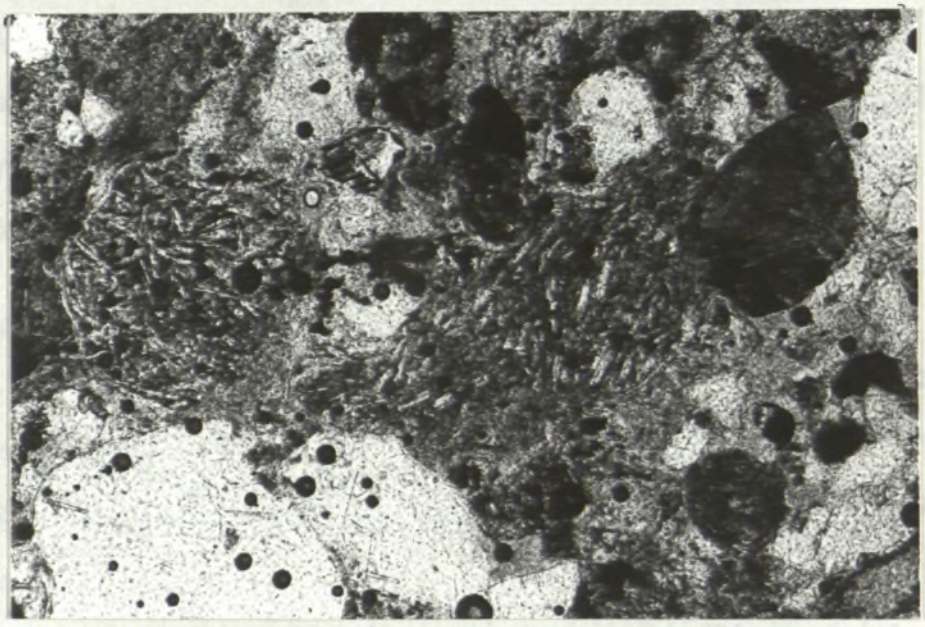

0.1 mm

D

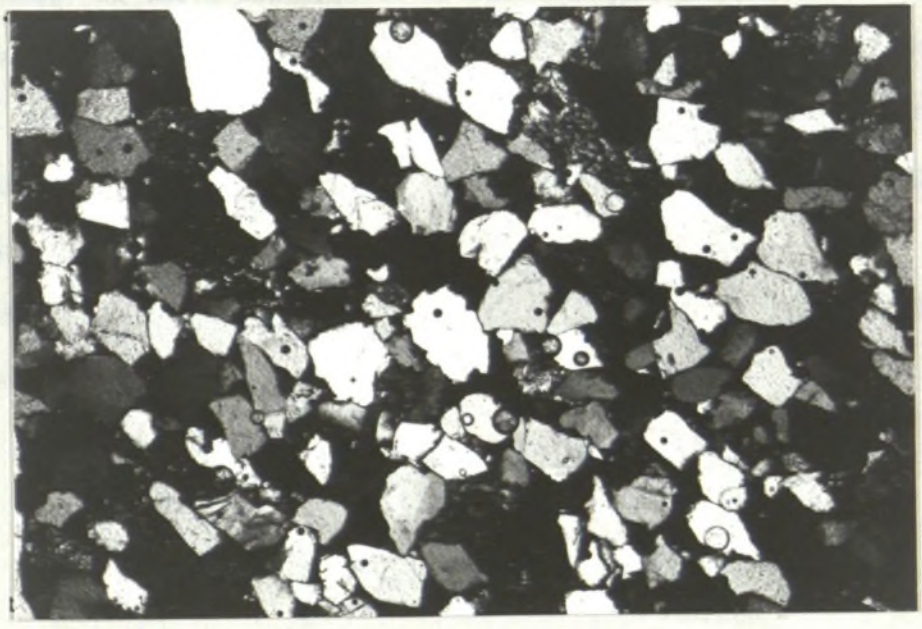

0.5 mm

siltstone and minor sandstone and chert (Appendix 1.8.1). Gradations from chert to argillite are also common (cf. Table 2.1, Appendix 1.2). Metamorphic rock-fragments comprise mainly slate, phyllite and semischist (Appendix 1.8.1). They are present in minor amounts and rarely exceed 5% in any sample (cf. Appendix 1.3). Plutonic rock-fragments were very rarely encountered in the Surat Basin sandstones (Appendix 1.8.1).

The types of feldspar

Staining of thin-sections for alkali feldspar shows that the predominant feldspar type present in the lithic and feldspathic sandstones is plalgioclase, represented dominantly by andesine as confirmed by electron microprobe analyses (Appendix 1.6). They are commonly remarkably fresh and many crystals show conspicuous zoning (Figure 2.1A). In these same rocks plagioclase feldspar also occurs as phenocrysts in volcanic rock-fragments. The average K-feldspar to total feldspar ratio in the litho-feldspathic formations does not exceed 0.20 (Figure 2.10, Table 2.2) and most of the K-feldspar is thought to be represented by sanidine as evidenced by their commonly euhedral and broken shapes and lack of twinning types characteristic of microcline and orthoclase. Such grains appear uniform internally with no suggestion of exsolution to a perthitic or microperthitic texture. Smaller sanidine grains (yellow in stained samples) are probably broken fragments or cleavage pieces, and are noticeably more angular than coarser ones.

Table 2.2. Average detrital quartz percentage and K-feldspar to total feldspar ratio of some Surat Basin sandstones based on a count of 600 points (= grains) in each thin-section. A more detailed tabulation of petrographic categories is given in Appendix 1.4 (p. 394).

Stratigraphic Unit	N[1]	Detrital quartz (whole-rock %)	K-feldpar/Tot.feldspar
Griman Creek Fm.	2	10.33	0.09
Wallumbilla Fm.	2	16.13	0.10
Bungil Formation	2	38.30	0.20
Mooga Sandstone	2	60.05	0.67
Orallo Formation	2	32.65	0.17
Gubberamunda Sst.	4	58.37	0.45
Westbourne Fm.	2	42.25	0.22
Walloon Coal M.	2	23.30	0.07
Hutton Sandstone	4	58.01	0.50
Evergreen Fm.	2	74.23	0.19
Precipice Sst.	2	85.65	0.36

[1] N = Number of samples analyzed.

Contrastingly, in the relatively quartzose sandstones, the K-feldspar content is variable but typically they have higher K-feldspar to total feldspar ratios than the labile sandstones, with an average of 0.35-0.65 (Table 2.2, Figure 2.10) and reaching up to 0.90 in individual samples (Appendix 1.4)). The K-feldspars in these relatively quartzose sandstone units mostly lack twinning, but in some cases show perthitic lamellae, and on this basis appear to comprise mainly orthoclase. Microcline, recognised on the basis of its characteristic twinning, is also present in small amounts, mostly in the quartzose petrofacies (Table 2.3). The fact that the yellow-stained K-feldspars show a preferred association with detrital (predominantly plutonic) quartz at a first-order level (cf. Table 2.2, see also Figure 2.10) is suggestive of a plutonic provenance (cf. Pettijohn et al, 1972, p. 302).

Some plagioclase and K-feldspar in both quartz-rich and labile fomations are kaolinitized and sericitized to varying degrees (although to a markedly lesser degree in the Bungil and younger Formations) and exhibit a murky/cloudy appearance in plane light under the microscope. This pattern of alteration is especially noticeable in the quartzose facies sandstones, particularly in the coarser-grained ones. In unstained thin-sections feldspars of this kind where lacking twinning usually could not be identified during the point-counting either as alkali feldspar or plagioclase with any degree of confidence. However electron microprobe analyses of unaltered remnants of some of these altered feldspars show that most of them comprise albite and only a few were found to be K-feldspar (cf. Appendix 1.7). Many feldspar grains in both labile and quartzose petrofacies were corroded to varying degrees giving rise to skeletal grain shapes. These partially dissolved feldspars are due either to preferential leaching of the calcic cores in the zoned plagioclases (Figure 3.12A) (present mostly in sandstones rich in juvenile volcanogenic materials;

Table 2.3. Means of modal analyses (whole-rock percentage) of the Surat Basin sandstones based on thin-section point-counting (1000 points per slide). Symbols as in Appendix 1.1.

Formation	N	QUARTZ							FELDSPAR							
		Q_{V1}	Q_{V2}	Qc	Qv	Qp	qc	qcd	Fans	Fas	Fz	Funs	Fus	Fx	Fp	Fo
Griman Ck. Fm.	26	0.00	0.11	5.28	0.04	0.41	0.09	0.02	5.57	0.59	1.07	18.87	0.98	0.02	0.06	0.64
Surat Siltst.	2	0.15	0.10	10.75	0.00	0.90	0.10	0.00	1.60	0.30	0.10	18.45	1.4	0.00	0.05	0.15
Wallumbilla Fm.	7	0.03	0.00	6.27	0.00	0.31	0.04	0.03	0.72	0.01	0.18	18.74	1.61	0.00	0.01	0.67
Bungil Fm.	12	0.39	0.00	29.40	0.32	1.00	0.25	0.07	0.75	0.06	0.01	14.16	1.61	0.00	0.08	0.31
Mooga Sst.	5	0.00	0.00	43.62	0.06	0.64	0.18	0.04	0.72	0.00	0.00	11.24	0.54	0.30	0.06	0.06
Orallo Fm.	24	0.09	0.01	21.39	0.21	1.37	0.37	0.06	3.76	0.51	0.49	13.00	3.03	0.07	0.05	1.04
Gubberamunda Sst.	17	0.00	0.00	37.02	0.07	1.87	0.28	0.02	1.46	0.10	0.39	10.83	2.20	0.63	0.52	1.27
Westbourne Fm.	13	0.46	0.06	28.38	0.23	1.05	0.71	0.08	1.83	0.45	0.17	10.76	3.14	0.19	0.20	1.87
Springbok Sst.	6	0.11	0.08	8.75	0.00	0.60	0.25	0.05	4.13	0.72	2.47	16.16	3.78	0.13	0.05	1.61
Walloon Coal M.	27	0.08	0.02	16.51	0.24	0.84	0.53	0.07	2.16	0.08	0.23	15.82	1.04	0.05	0.05	1.96
Hutton Sst.	51	0.00	0.00	45.88	0.13	2.09	2.17	0.04	0.95	0.04	0.00	10.43	0.69	0.28	0.22	1.10
Evergreen Fm.	16	0.00	0.00	40.50	0.21	1.39	0.17	0.00	1.11	0.00	0.00	14.39	1.08	0.07	0.17	1.03
Precipice Sst.	9	0.00	0.00	70.51	0.53	1.99	0.26	0.00	0.02	0.00	0.00	2.50	0.00	0.13	0.14	0.26

Table 2.3. (contd.)

		⟨—— VOLC. ROCK-FRAGS. ——⟩					⟨—— CLASTIC SED. ROCK-FRAGS.—⟩					⟨—— METAMORPHIC ROCK-FRAGS.—⟩					
Formation	N	Vv	Vf	Vm/Vl	Achm	Vo	Ksq	Kzq	Ksl	Kzl	Ka	Tp	Ts	Tq	Mkq	Mo	P
Griman Ck. Fm.	26	21.92	2.46	3.44	1.10	4.77	0.44[1]		0.27[2]		0.18	1.10	0.04	0.01	0.00	0.00	0.04
Surat Siltst.	2	13.60	1.85	1.10	0.00	0.75	0.10		0.20		0.10	0.35	0.00	0.00	0.00	0.00	0.00
Wallumbilla Fm.	7	19.10	2.38	1.98	0.08	1.2	0.24		0.58		0.34	0.61	0.00	0.00	0.00	0.00	0.00
Bungil Fm.	12	8.92	2.36	0.65	0.08	0.83	0.41		0.21		0.09	0.07	0.00	0.03	0.01	0.00	0.08
Mooga Sst.	5	2.58	1.54	0.00	0.10	0.18	0.00	0.00	0.00	0.00	0.64	0.24	0.00	0.00	0.00	0.00	0.00
Orallo Fm.	24	19.06	2.14	3.30	0.00	1.65	0.12	0.62	0.26	0.36	1.65	0.74	0.00	0.04	0.00	0.02	0.00
Gubberamunda Sst.	17	10.23	1.67	1.64	0.13	0.77	0.00	0.04	0.03	0.49	1.49	0.49	0.00	0.03	0.00	0.00	0.00
Westbourne Fm.	13	10.67	1.61	1.27	0.00	1.09	0.10	0.93	0.20	0.16	2.47	0.80	0.00	0.04	0.02	0.04	0.07
Springbok Sst.	6	13.85	2.36	5.61	0.38	1.76	0.08	0.40	0.88	0.98	3.83	0.48	0.00	0.00	0.01	0.00	0.00
Walloon Coal M.	27	17.88	3.14	1.93	0.11	1.50	0.09	1.10	0.26	0.58	4.22	0.58	0.00	0.00	0.15	0.03	0.00
Hutton Sst.	51	6.38	1.68	0.82	0.02	0.77	0.00	0.08	0.07	0.20	1.23	1.35	0.33	0.04	0.02	0.00	0.00
Evergreen Fm.	16	10.87	1.48	1.50	0.00	1.02	0.00	0.07	0.02	0.04	1.05	1.27	0.00	0.00	0.15	0.06	0.00
Precipice Sst.	9	0.27	0.36	0.00	0.00	0.17	0.10	0.48	0.00	0.00	1.46	0.49	0.14	0.04	0.04	0.02	0.00

Table 2.3 (contd.)

		⟨——— MICA ———⟩				⟨-HEAVY MINERALS-⟩		
Formation	N.	Zb	Zw	Zch	Zdi	HP	HT	HO
Griman Ck. Fm.	26	2.51	0.22	0.12	0.00	0.14	0.18	0.13
Surat Siltst.	2	1.40	0.00	0.00	0.00	0.05	0.05	0.00
Wallumbilla Fm.	7	3.30	0.00	0.01	0.00	0.11	0.06	0.04
Bungil Fm.	12	2.15	0.39	0.00	0.14	0.10	0.07	0.19
Mooga Sst.	5	0.06	0.20	0.14	4.52	0.00	0.10	0.02
Orallo Fm.	24	0.68	0.74	0.01	0.00	0.02	0.06	0.06
Gubberamunda Sst.	17	0.19	0.08	0.05	0.63	0.02	0.44	0.05
Westbourne Fm.	13	0.57	0.50	0.00	0.00	0.01	0.15	0.07
Springbok Sst.	6	0.25	0.08	0.18	0.38	0.01	0.06	0.01
Walloon Coal M.	27	0.50	0.43	0.07	0.13	0.02	0.02	0.09
Hutton Sst.	51	0.17	0.34	0.03	1.15	0.00	0.09	0.02
Evergreen Fm.	16	0.66	1.22	0.03	0.00	0.00	0.15	0.06
Precipice Sst.	9	0.23	0.88	0.01	0.88	0.00	0.03	0.00

Footnotes to Table 2.3.

1 Mean of Kq including sum of Ksq and Kzq, and undifferentiated Kq.

2 Mean of Kl including sum of Ksl and Kzl, and undifferentiated Kl.

e.g. the Rolling Downs Group and the Orallo Formation), or to partial leaching along cleavage planes thereby giving rise to 'cockscomb' skeletal shapes (Figure 3.12B). The latter variety also presumably are derived from originally more calcic varieties of plagioclase but electron microprobe analyses show them to now consist of pure albite in all cases (Appendix 2.1). Under the petrographic microscope they are optically clear, commonly lacking any alteration, and have white birefringence (Figure 3.12B). SEM examinations show delicate subgrain boundaries of the cockscomb feldspar suggesting later healing by authigenic albite (Figures 3.12C and D; see also Pittman, 1988). Authigenic feldpars are always represented by the pure Na or K end-members (Kastner and Siever, 1979). In the Surat Basin these two kinds of corroded feldspar can coexist in the same formation. In many formations feldspar grains of either composition were completely or partly replaced by diagenetic carbonate mineral(s) which include some ferroan varieties. However, petrographic evidence such as dust-line preservation of detrital grain-outlines, presence of unreplaced remnants of the original mineral, and relict cleavage traces permitted reliable identification of their detrital grain-type and they were tallied as such.

SEDIMENT COMPOSITION AND PROVENANCE

Existing concepts on sediment provenance in the Surat Basin

As mentioned previously, petrologic and provenance studies on the Surat Basin succession are surprisingly sparse. The only study which addressed the question of provenance in any detail is that of Martin (1976, 1981) who studied the sedimentology of the Precipice Sandstone and on the basis of detrital mineralogy and consistent west to east palaeocurrent pattern (cf. Martin, 1981, his fig. 4) suggested that the source of the Precipice Sandstone lay to the west and south of the Great Artesian Basin in the bordering Precambrian areas (Figure 2.12, herein). The compilation

of the geology of the Surat Basin by Exon (1976) does not address the problem of provenance in detail except in regard to some gross generalisations. Exon (ibid.) however, recognised the major change in provenance style towards the Early Cretaceous which began with the deposition of dominantly volcanogneic sediments. Exon (1976) and Exon and Burger (1981) also noted the essentially cyclic nature of the Surat Basin succession where each of their inferred cycles begins with coarser-grained fluvial sediments and ends with finer-grained lacustrine/paralic/shallow-marine sediments (cf. Figures 9.2 and 1.2). Similar cycles have been recognised in the neighbouring Eromanga Basin as well (cf. Burger, 1986). Exon and Burger (ibid.) attributed these cycles to eustatic sea-level changes which they argued can account for the upsequence variation in grainsize and sedimentary structures; Exon and Burger's (ibid.) scheme in essence involves the operation of eustatic sea-level changes on an inert craton. Jones and Veevers (1983) were the first to suggest a tectonic/provenance interpretation of Exon and Burger's (ibid.) sedimentary cycles and introduced the concept of environmental 'wetness'; they found a correlation between the sediment composition and the environmental wetness. In the Surat Basin the coarser-grained sediments are dominanltly fluvial ('dry') whereas the finer-grained sediments have paludal/brackish/shallow-marine ('wet') environmental affinities. The detrital composition of the former is predominantly quartzose whereas the sandstone units within the finer-grained sediments are predominantly labile comprising overwhelmingly volcanogenic components, and these labile sandstones are associated with tuffs and coals. Jones and Veevers (1983) suggested that the 'dry' quartzose sediments have cratonic provenance in contrast to the 'wet' labile sediments which have an orogenic/magmatic arc provenance. Jones et al (1984) subsequently elaborated this concept in a foreland basin model

which suggests that in a retro-arc foreland basin fronting a volcanically active orogen (arc) both the foreland and the orogen act in synchrony - i.e., the times of orogeny are also the times of foreland subsidence; and conversely, times of quiescence in the orogen/arc are accompanied by a gentle rise of the foreland (see also Jones and Veevers, 1982). During the waxing phase of magmatism/orogeny the arc sheds into the foreland pulses of volcanogenic sediments which are deposited in 'wet' depositional environments (accompanied by concomitant foreland subsidence). During the waning phase of magmatism/orogeny this labile pulse is opposed by the flux of quartz sand derived from the gently rising craton and both petrofacies are deposited in a fluvial setting. The presence of coal, tuff and relatively abundant dispersed organic matter within the finer-grained labile sediments is characterisitic of all late Palaeozoic and Mesozoic foreland basins in eastern Australia as well as the Cainozoic Papuan Basin of Papua New Guinea (cf. Jones et al, 1987) and such an association reflects optimal conditions for accumulation of peat and/or kerogen by establishing high water tables and/or anoxia as a consequence of increased rates of basin subsidence and rapid sedimentation.

Figure 2.2 portrays four instances of a typical foreland basin cycle on the scale of about 5-25 Ma. Orogenic and magmatic activity in the arc/orogen initiates the growth of a mountain range and piedmont alluvial fans prograding into a concomitantly subsiding foreland basin (Figure 2.2A). High water tables (in marine/lacustrine/paludal depositional settings) give rise to favourable condition for the preservation of peat/dispersed organic matter (Chapter 9). With continued uplift and outward expansion of the orogen (involving thrusting and folding of the proximal outwash) the clastic wedge progrades further cratonward pushing back the domain of craton-derived quartzose sediment (Figure 2.2B). Ultimately marine/lacustrine/paludal conditions are eliminated as the

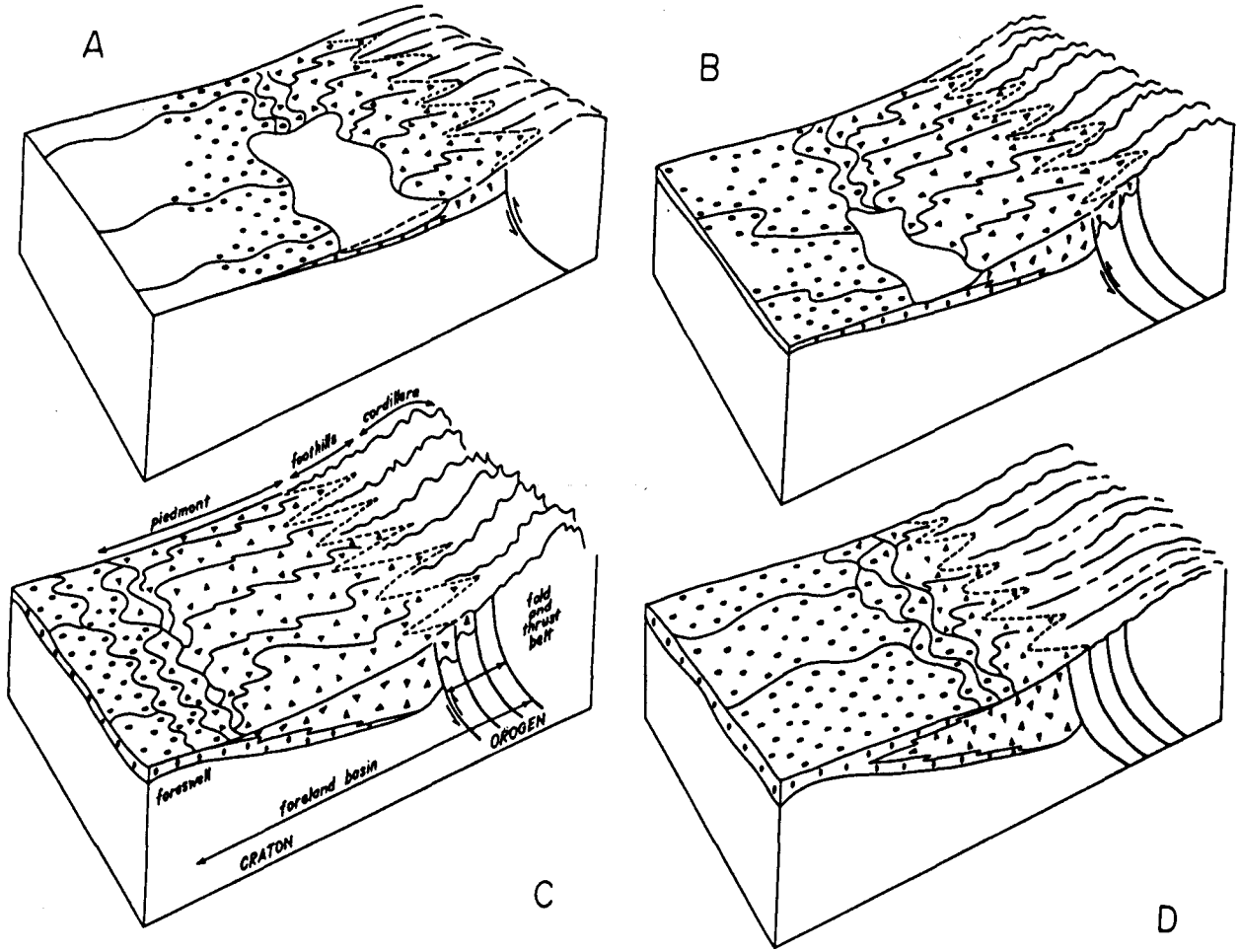

Figure 2.2. Schematic diagrams showing the single-cycle evolution of a foreland basin and the resulting basin-fill pattern. Open circles indicate dominantly quartzose sediments; solid triangles - dominantly volcanogenic sediments with tuff and coal; open triangles - dominantly volcanogenic sediments without tuff or coal. Lettering on C indicates topographic and tectonic elements common to all block diagrams. From Jones et al (1984, fig. 167).

orogen/arc-derived labile sediments overwhelm the foredeep (Figure 2.2C). With the decline of magmatism/tectonism the arc/orogen settles (quiescence) and the foreland basin gently rises (tectonic relaxation) resulting in intervals characterised by falling or low water tables and nondeposition/mild erosion. The tuffs, coals, and high organic content that are characteristic of the prograding piedmont are no longer formed and/or preserved and the piedmont begins to retreat with the dwindling of orographic relief in the arc/orogen through continued erosional denudation; and eventually the domain of cratonic quartz sand advances orogenward (Figure 2.2D). Thus in terms of the postulated basin-fill pattern in time/space the foreland basin model of Jones et al (1984) involves essentially an interfingering of orogen-derived environmentally 'wet' labile sediments and craton-derived environmnetally 'dry' and compositionally mature quartzose sediments. Jones et al's (ibid.) model was derived principally from their focus on the Late Cainozoic history of the Papuan Basin of Papua New Guinea and the mid-Permian to mid-Triassic succession of the Sydney Basin and rests, in respect of the latter basin, on a detailed petrographic and palaeocurrent data-base (cf. Conaghan et al, 1982; McDonnell, 1983; Cowan, 1985). The extension of the model to the Surat-Eromanga Basins (cf. Jones et al, 1982) which were formed by similar mechanisms of arc migration away from the craton (cf. Veevers, 1984, p. 351-364) rested on a scanty petrographic data-base but neverthesless is found to be in excellent agreement with the petrologic data assembled in this report as will be shown in the following sections.

Mineralogy and classification of the Surat Basin sandstones

Sandstones of the the Surat Basin succession vary markedly in composition from one formation to another (Figure 2.3) and in general show relatively minor intraformational compositional variation (Figures 2.4A-C). The compositional range is from quartzarenite through sublitharenite and feldsarenite/lithic feldsarenite to feldspathic litharenite (Figures 2.3, 2.4A-C), the scatter of individual sample plots spreading over much of the QFR triangle (Appendix 1.10.2). On a first-order level the Surat Basin sandstones are subdivided here into a quartzose petrofacies having an average detrital megaquartz content of 50% or more (on a QFR basis), and a labile petrofacies with less than 50% QFR detrital megaquartz. According to this classification the Precipice Sandstone, Evergreen Formation, the Hutton, Gubberamunda and Mooga Sandstones all belong to the quartozose facies and the Bungil Formation almost so (Figures 2.3, 2.4A-B, and 2.9). It is noteworthy that, with the execption of the Precipice Sandstone, the feldspar content of all of the sandstone formations is similar, averaging about 38% (cf. Figure 2.3) against a variable quartz and lithic content.

Provenance fingerprints from framework-grain composition

A magmatic arc provenance for the labile sandstones can be supported by several lines of evidence such as the following:

(1) The predominance of volcanic rock-fragments as can be seen from the LvLsLm plots (Figures 2.5A-C and 2.11).

(2) The dominantly plagioclase (andesine) composition of the feldspar population (cf. Appendix 1.6), their juvenile phenocrystic textures (euhedral and broken shape), their relatively smaller grainsize compared to the feldspar grains in the quartzose facies, and their obvious association with abundant volcanic rock-fragments. A volcanic origin of the plagioclase grains is also indicated by their commonly zoned nature (cf.

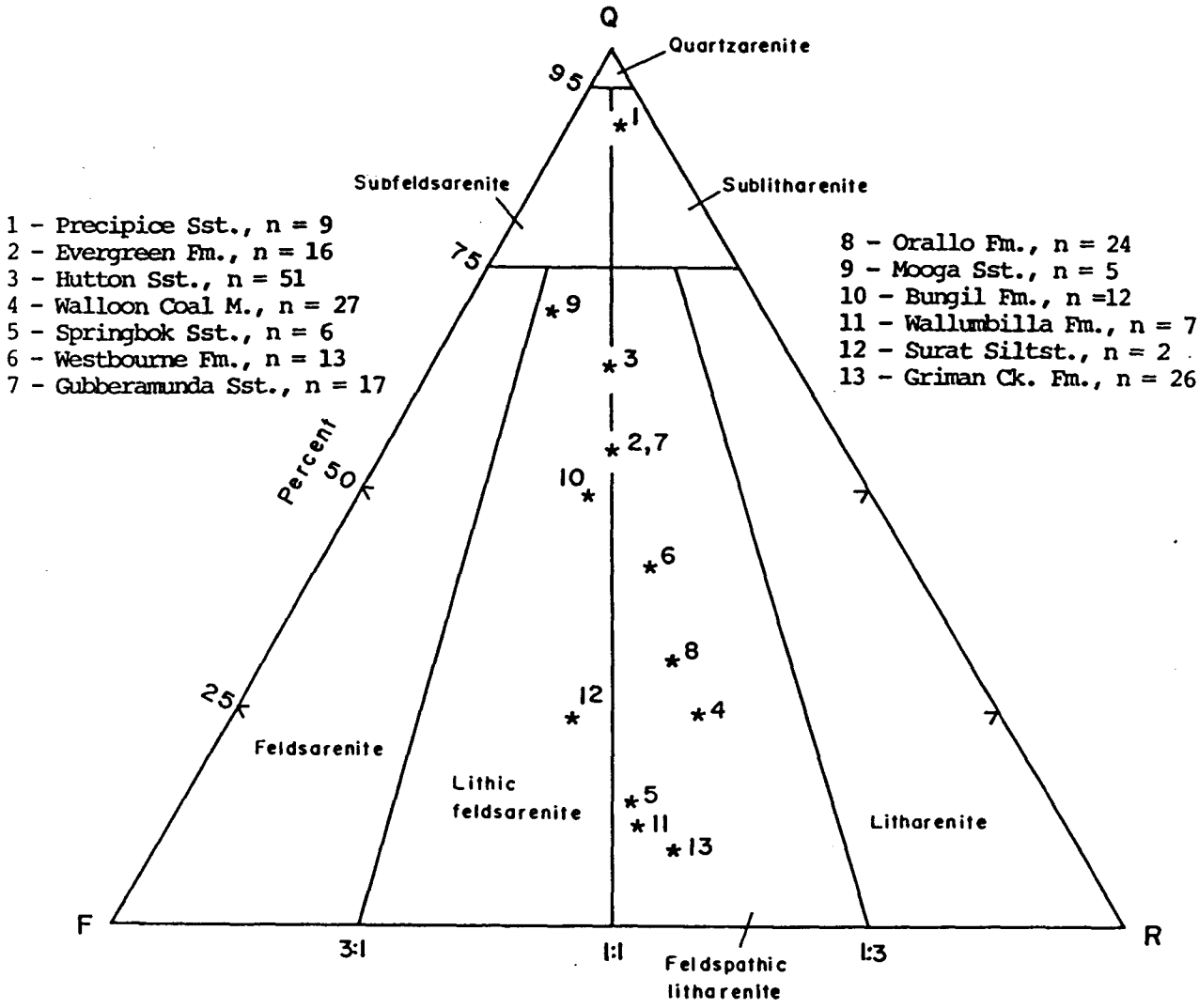

Figure 2.3. Average QFR detrital composition of the Surat Basin sandstones on a formation basis. Sandstone classification after Folk et al (1970). Numerical symbols indicate formations; n - number of samples.

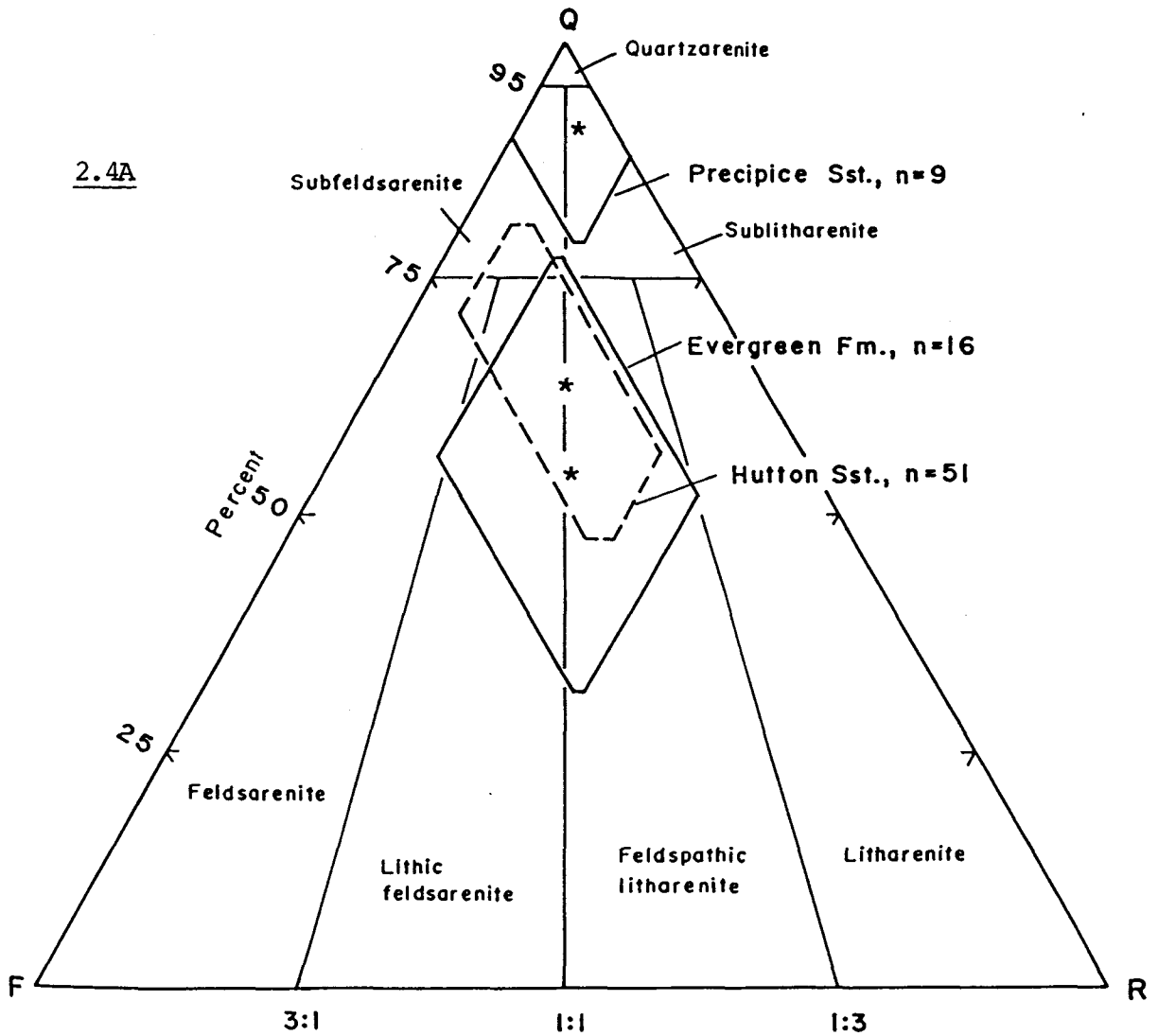

Figure 2.4A-C. Means and one standard deviation (cf. Ingersoll, 1978) of the lower Jurassic (A), Middle and Upper Jurassic (B), and Lower Cretaceous sandstones (C) of the Surat Basin; n - number of samples.

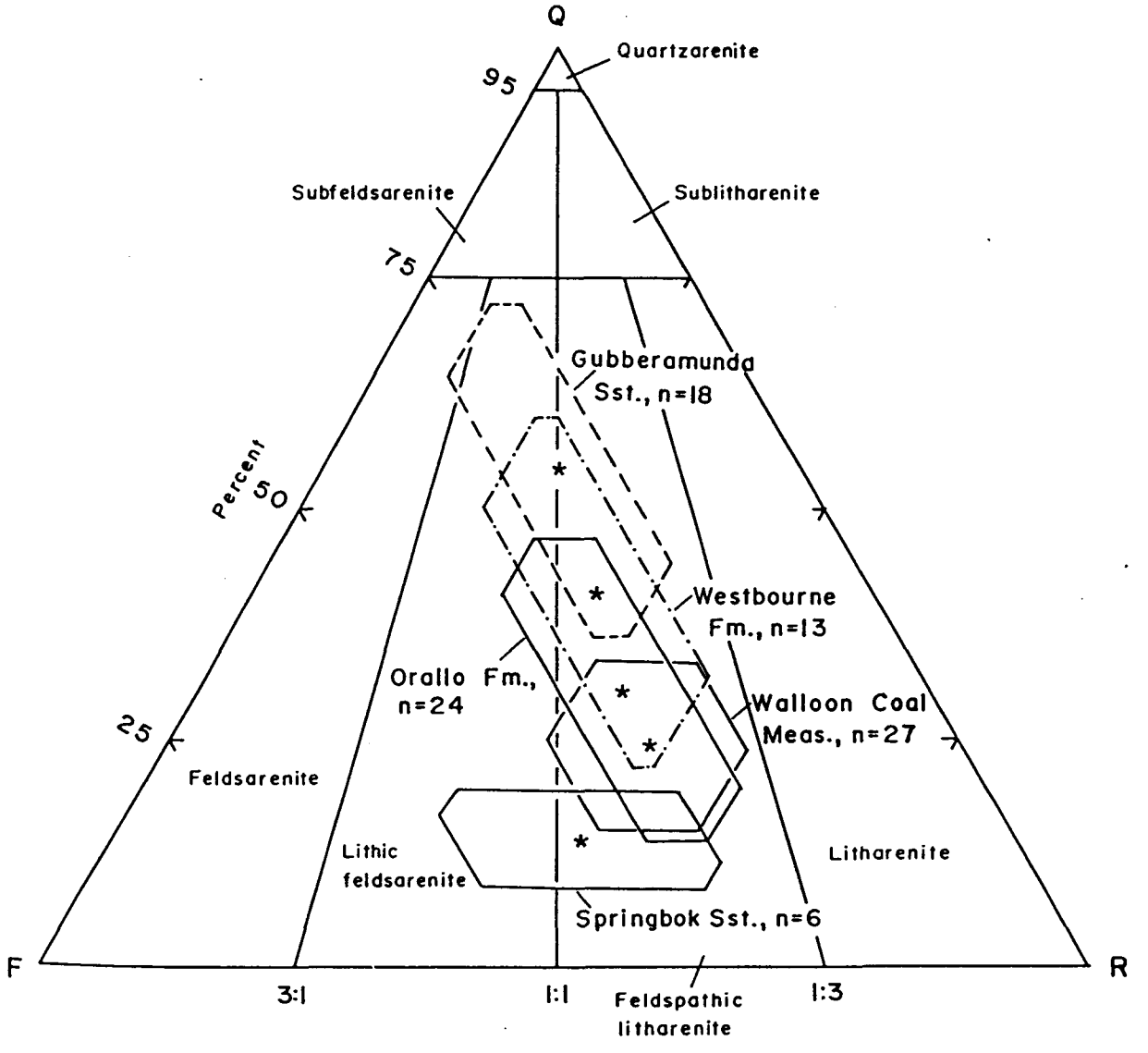
Q
Quartzarenite
95
Subfeldsarenite
Sublitharenite
75
Gubberamunda
Sst., n=18
Percent
50
Westbourne
Fm., n=13
Orallo Fm.,
n=24
Walloon Coal
Meas., n=27
25
Feldsarenite
Lithic
feldsarenite
Litharenite
Springbok Sst., n=6
F
R
3:1
1:1
1:3
Feldspathic
litharenite

Figure 2.4B.

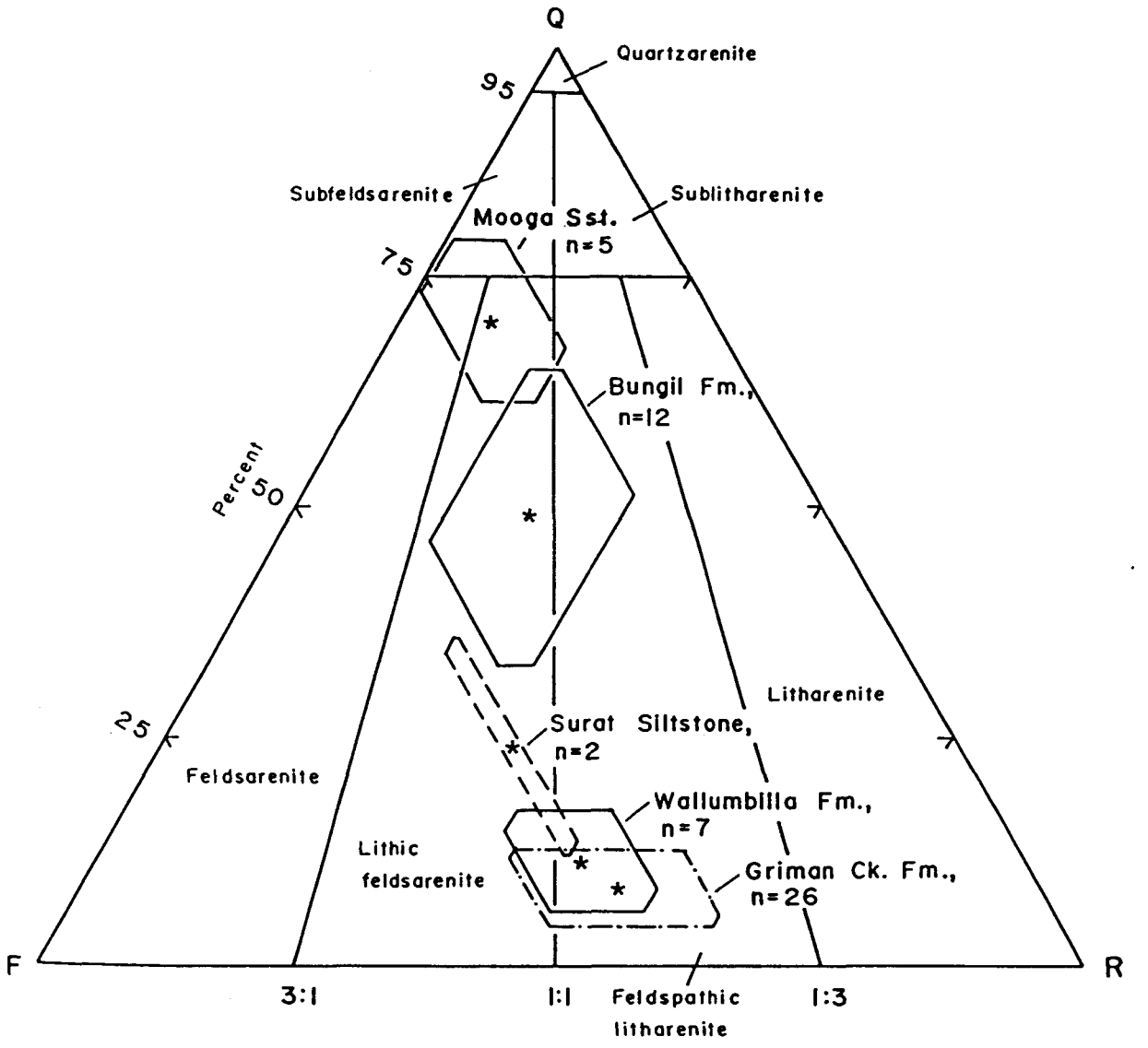
Q
Quartzarenite
95
Subfeldsarenite
Sublitharenite
Mooga Sst.
n=5
75
Bungil Fm.,
n=12
Percent
50
Litharenite
25
Surat Siltstone,
n=2
Feldsarenite
Wallumbilla Fm.,
n=7
Lithic
feldsarenite
Griman Ck. Fm.,
n=26
F
R
3:1
1:1
Feldspathic
litharenite
1:3

Figure 2.4C.

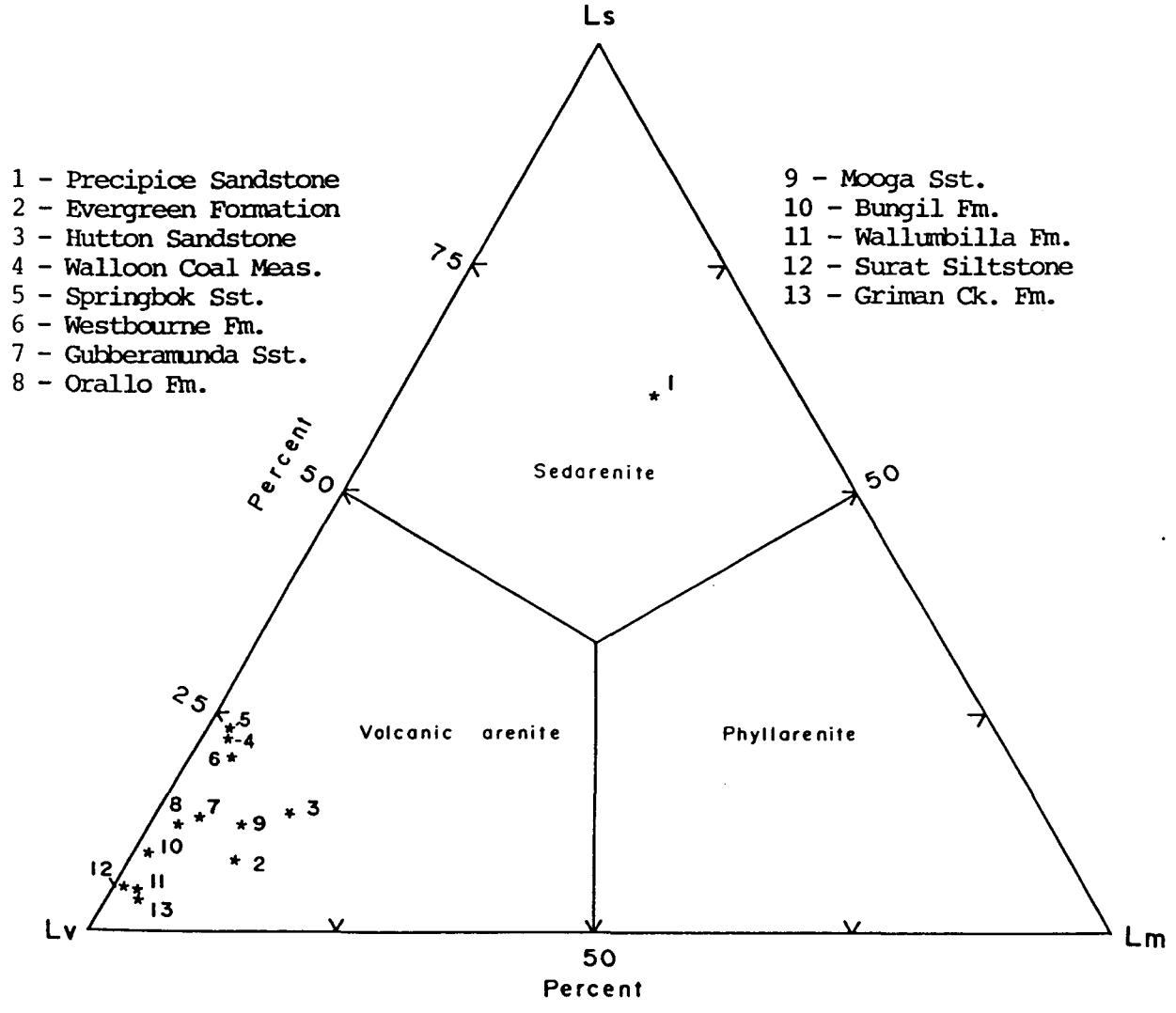

Figure 2.5A. Average rock-fragment composition of the Surat Basin sandstones on a %LvLsLm plot; n values are the same as for Figure 2.3. Lv - volcanic rock-fragments; Ls - sedimentary rock-fragments; Lm - metamorphic rock-fragments.

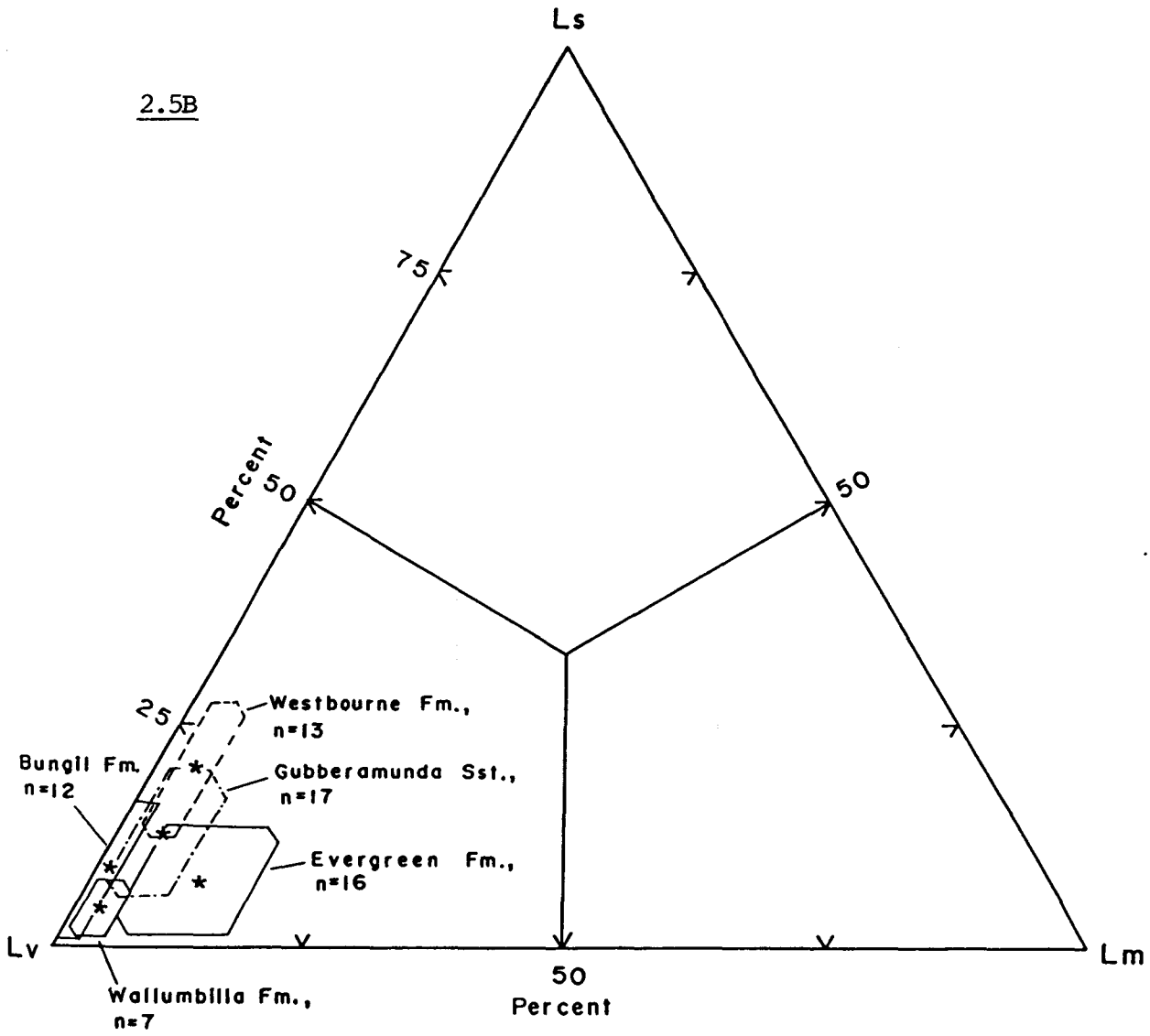

Figure 2.5B-C. Means and envelopes of one standard deviation of the Surat Basin sandstones on %LvLsLm plots. n - number of samples.

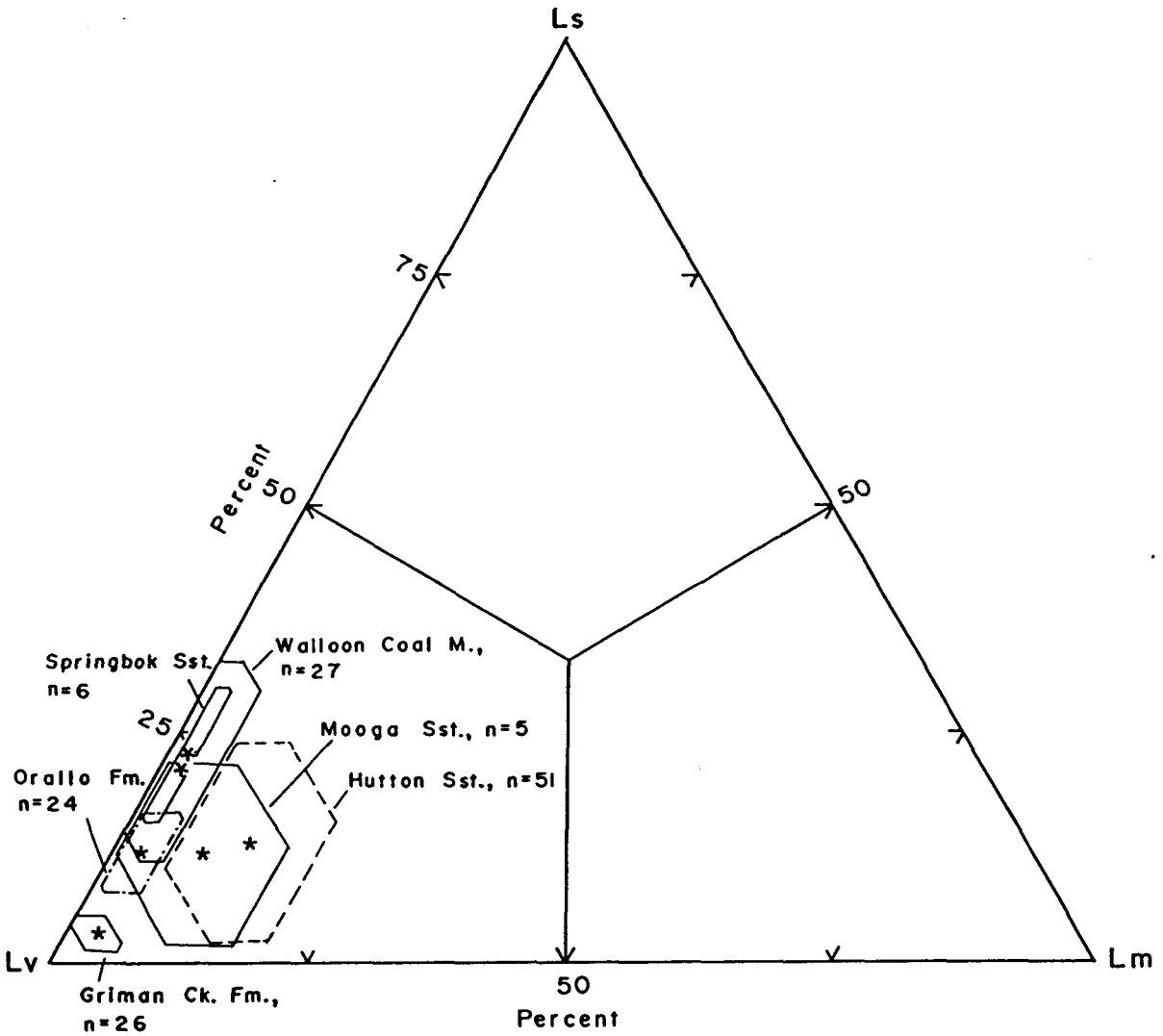
Ls
75
50
Percent
50
Springbok Sst.
n=6
Walloon Coal M.,
n=27
25
Mooga Sst., n=5
Hutton Sst., n=51
Orallo Fm.
n=24
Lv
Lm
Griman Ck. Fm.,
n=26
50
Percent

Figure 2.5C.

Pittman, 1963; Figure 2.1A herein). The dominantly andesitic feldspar composition (Appendix 1.6) together with the abundant associated microlitic volcanic rock-fragments also suggest that the chemistry of the magmatism was andesitic (cf. Dickinson, 1985).

(3) The presence of volcanic (beta-form) quartz in the labile facies contrasting with its virtual absence in the quartzose facies (Table 2.3).

(4) Some of the labile facies formations (e.g., the Injune Creek Group and the Orallo Formation) also contain bentonite beds (Exon, 1976) suggesting contemporaneous volcanism.

(5) The Bungil Formation, the Rolling Downs Group, and the Injune Creek Group (Figure 1.2) contain variable amounts of pyroboles whereas other stratigraphic units either lack these heavy minerals or their content is an order of magnitude less than in the above formations attesting to the juvenile nature of the volcanogenic material in the former (cf. Table 2.3). The relatively lower content of pyroboles in the Jurassic Injune Creek Group compared to the Lower Cretaceous Rolling Downs Group may be attributed to the relative instability of these minerals in non-marine sedimentary environments and to their susceptibility to alteration in older rocks (Folk, 1980, p. 96-97).

(6) The Bungil and younger formations also contain abundant biotite (cf. Table 2.3) some of which in places shows pseudohexagonal outlines and remarkable freshness suggesting a volcanic origin (cf. Pettijohn et al, 1972, p. 302).

Contrastingly, the likely cratonic provenance of the quartzose petrofacies is attested by the following observations:

(1) The predominance of common quartz among total megaquartz (Figure 2.10, Table 2.3)

(2) The high K-feldspar to total feldspar ratio (Figure 2.10)

(3) The anhedral shape and commonly large size of feldspar grains (especially in the Hutton and Gubberamunda Sandstones; cf. Figures 3.13B), and the dominantly albitic composition (cf. Appendix 1.7) of the plagioclase population (as opposed to dominant andesine in the labile petrofacies; cf. Appendix 1.6)

(4) The predominance of garnet in the heavy mineral population in some quartzose sandstones (e.g., the Hutton and the Gubberamunda Sandstones; Appendix 1.8.2). Garnet is also reported from the Precipice Sandstone by Martin (1979) which he considered to have been derived through single-cycle erosion of the Willyama Block to the southwest of the Surat Basin (Figure 2.12).

Evidence from facies relationships

An examination of the facies relationships in a west-to-east transect across the Eromanga-Surat Basins shows the interfingering nature of the quartzose and labile petrofacies (cf. Figures 2.6 and 2.7). Most of the labile facies formations grade laterally into more quartzose sandstones towards the west and southwest before finally giving way to quartzose sandstone. For instance, the volcanogenic Orallo Formation is not present on the Nebine Ridge where the quartzose Mooga Sandstone rests directly on the quartzose Gubberamunda Sandstone. On the Nebine Ridge it is consequently not possible to distinguish between the Mooga and Gubberamunda Sandstones and the term Hooray Sandstone is used for the combined equivalent interval. This is more a "change of name than a change of facies, as the Mooga and Gubberamunda Sandstones are indistinguishable once the Orallo Formation piches out" (Exon, 1976; Figure 2.7 herein). Formation isopach patterns show that most, if not all, of the labile facies

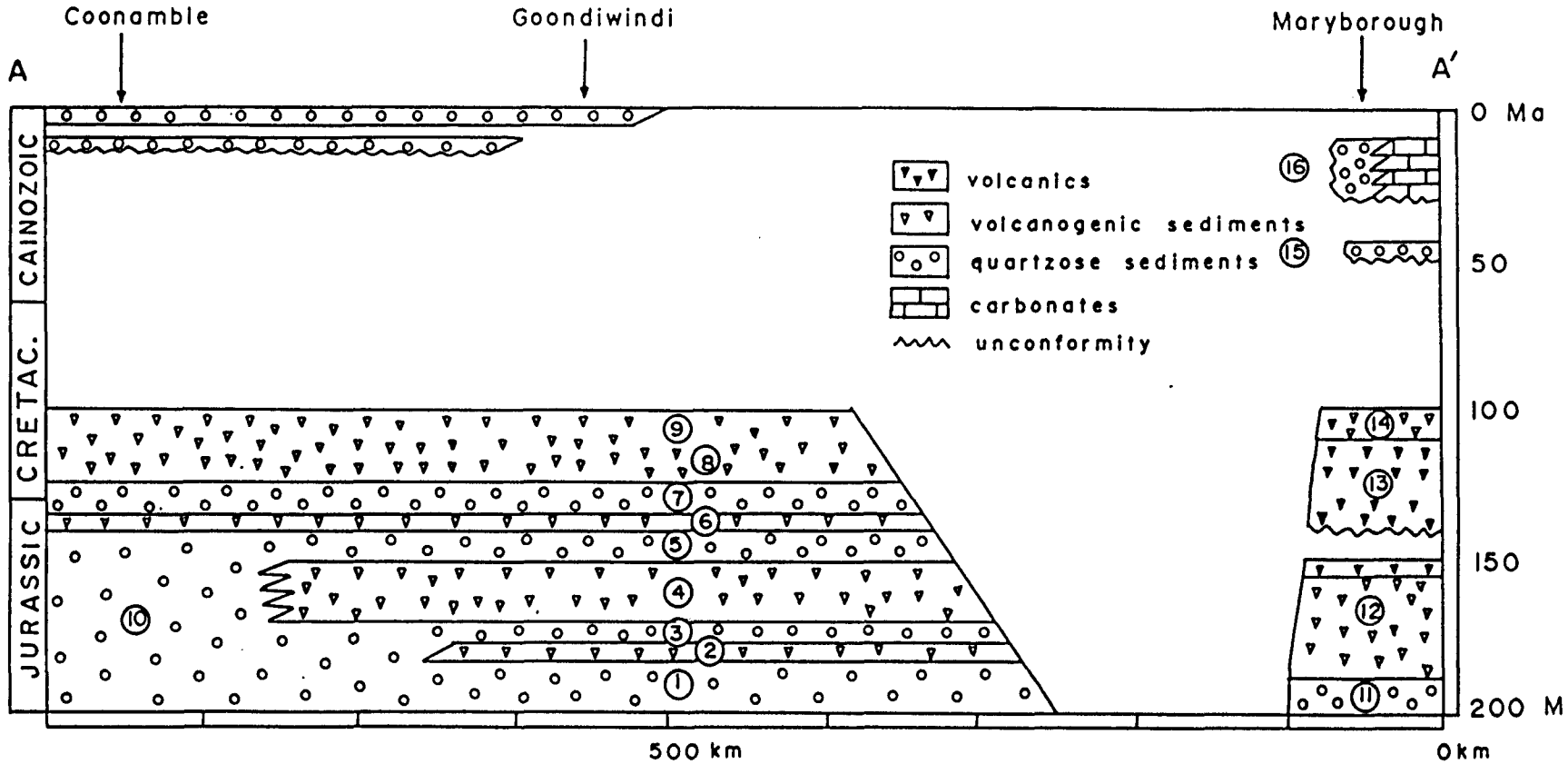

Figure 2.6. Time-space diagram of the Surat and Maryborough Basins (section AA' in Figure 9.1) showing the distribution of preserved petrofacies and lacunae (shown blank). Circled numbers indicate stratigraphic units: 1 - Precipice Sandstone; 2 - Evergreen Formation; 3 - Hutton Sandstone; 4 - Injune Creek Group; 5 - Gubberamunda Sandstone; 6 - Orallo Formation; 7 - Mooga Sandstone; 8 - Bungil Formation; 9 - Rolling Downs Group; 10 - Pilliga Sandstone; 11 - Myrtle Creek Sandstone; 12 - Tiaro Coal Measures; 13 - Grahams Creeek Formation; 14 - Maryborough Formation and Burrum Coal Measures; 15 - Fairymead Beds; 16 - Elliott Formation. Redrawn from Jones and Veevers (1983; fig. 5).

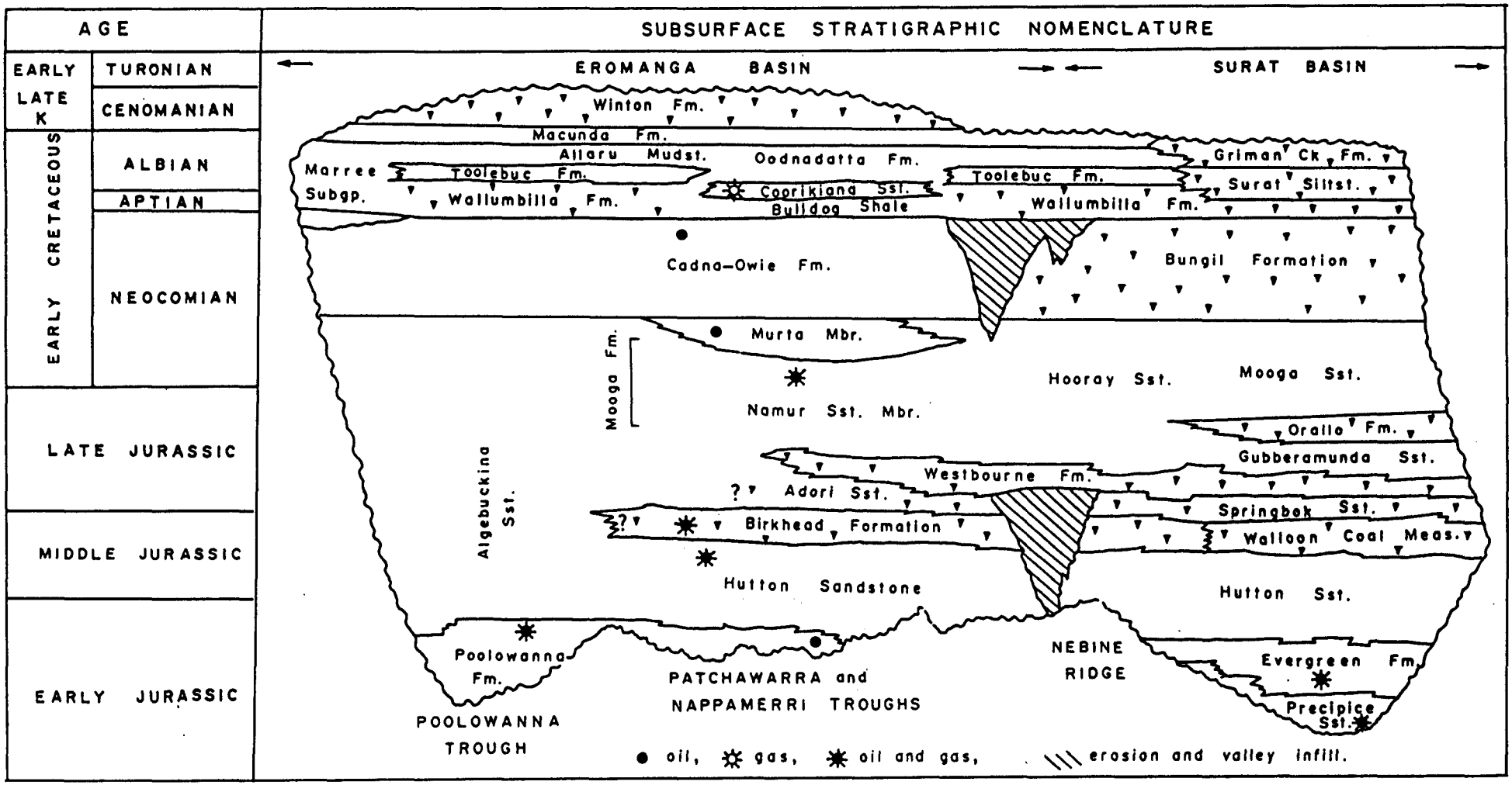

Figure 2.7. Generalised stratigraphy of the Eromanga and Surat Basins (modified after Moore et al, 1986) showing the distribution of different petrofacies and hydrocarbons. Eromanga Basin petrofacies are known only on reconnaissance-level and mostly semi-quantitative/qualitative petrography from Wopfner et al (1970), Senior et al (1978) and Watts (1987). Solid triangles indicate labile petrofacies, and blank indicates quartzose petrofacies.

intervals increase in thickness towards the orogen[1] whereas the quartzose formations thicken towards the craton (Exon, 1976; see also Watts, 1987, his fig. 12).

The volcanolithic Springbok Sandstone intertongues (according to Exon, 1976) across the Nebine Ridge with the sublabile to labile Adori Sandstone of the Eromanga Basin (Figure 2.7) and in the south-southwest of the Surat Basin with the lower part of the coarse quartzose highly porous Pilliga Sandstone (Figure 2.6). Likewise the Westbourne Formation which is volcanolithic in the Surat Basin grades laterally into quartzose sandstone in the type area (Amoseas Westbourne 1) in the Eromanga Basin (Exon, 1976) and finally gives way to the quartzose Mooga Formation (in Qld; and Hooray Sandstone in S.A.; Figure 2.7). The Bungil Formation comprises juvenile volcanogenic material and is absent on the Nebine Ridge (Figure 2.7) probably because of intra-Cretaceous erosion there. Its lateral equivalent in the Eromanga Basin, the Cadna-Owie Formation is quartzose, but contains silicic and intermediate volcanic rock-fragments in the upper part (i.e., the Mt. Anna Sandstone Member; Wopfner et al, 1970).

Possible sources of the volcanic rock-fragments in the quartzose facies

Rock-fragments are present in varying proportions in all formations of the quartzose petrofacies (Table 2.4). On the LvLsLm triangle only the Precipice Sandstone plots in the Ls field (Figure 2.5A). Very minor content of volcanic rock-fragments characterizes this formation (Table 2.4,

---

1 The most comprehensive and recent isopach compilation for the Surat Basin (i.e., Exon, 1976) combines some formations of contrasting petrofacies character for isopach purposes (such as the Hutton Sandstone and Walloon Coal Measures). This makes it difficult to isolate the thickness pattern of some individual formations.

Table 2.4. Mean and one standard deviation[1] of %QFL and %LvLsLm of the Surat Basin sandstones based on a consistent count of 1000 points in each thin-section.

Stratigr. Unit	Q[2]	F	L	Lv	Ls	Lm	N
	←——— %QFL ———→			←——— %LvLsLm ———→			
Griman Ck. Fm.	8.5 ± 3.8	40.5 ± 9.0	51.0 ± 11.2	93.8 ± 2.1	2.9 ± 1.8	3.3 ± 1.1	26
Surat Siltstone	23.8 ± 13.2	42.4 ± 1.2	33.8 ± 12.1	94.1 ± 3.3	4.5 ± 1.4	1.4 ± 1.9	2
Wallumbilla Fm.	11.7 ± 5.8	41.7 ± 5.8	46.6 ± 10.2	93.2 ± 4.2	4.5 ± 2.9	2.3 ± 1.8	7
Bungil Formation	48.9 ± 16.0	28.3 ± 10.9	22.8 ± 8.5	89.7 ± 8.5	9.1 ± 7.6	1.2 ± 1.2	12
Mooga Sandstone	69.8 ± 9.0	20.9 ± 5.4	9.3 ± 8.6	79.2 ± 8.5	11.7 ± 10.3	9.1 ± 8.5	5
Orallo Formation	30.6 ± 16.8	29.1 ± 5.9	40.3 ± 17.1	85.5 ± 5.8	11.8 ± 4.7	2.7 ± 1.7	24
Gubberamunda Sst.	53.6 ± 18.2	23.5 ± 5.8	22.9 ± 15.9	82.4 ± 8.2	13.1 ± 7.1	4.5 ± 3.8	17
Westb'ne Formation	40.7 ± 19.1	26.2 ± 6.1	33.1 ± 15.3	75.9 ± 8.3	19.9 ± 7.6	4.2 ± 2.0	13
Springbok Sst.	14.1 ± 5.4	41.0 ± 12.2	44.9 ± 14.8	75.1 ± 8.2	23.1 ± 7.7	1.8 ± 0.9	6
Walloon Coal M.	24.5 ± 9.2	29.6 ± 9.1	45.9 ± 10.1	75.7 ± 10.9	22.0 ± 10.9	2.3 ± 3.0	27
Hutton Sandstone	64.0 ± 16.4	18.3 ± 5.7	17.5 ± 13.7	73.8 ± 9.6	13.2 ± 10.9	13.0 ± 6.9	51
Evergreen Fm.	53.7 ± 23.2	23.3 ± 11.3	23.0 ± 13.4	82.3 ± 9.7	7.7 ± 6.2	10.0 ± 6.2	16
Precipice Sst.	91.0 ± 12.6	4.0 ± 5.9	5.0 ± 6.8	13.8 ± 29.2	61.4 ± 35.8	24.8 ± 19.5	9

Footnotes to Table 2.4.

1 The means and standard deviation shown in this table and plotted in Figures 2.1A-C, 2.3A-D, 2.5 and 2.10B are not statistically rigorous values because the data represent a constant sum and are therefore constrained. The exact meaning of the standard deviation fields depicted in the abovementioned tables and figures is statistically ambigious. Nevertheless, the fields are measures of the dispersion of the data and are useful in visually illustrating the contrasts between different stratigraphic units. For more discussion see Ingersoll (1978).

2 Q - Sum of mono and polycrystalline quartz (excluding chert), F - Total feldspar grains, L - total rock-fragments, Lv - Volcanic rock-fragments, Ls - Sedimentary rock-fragments, Lm - Metamorphic rock-fragments, N - Number of samples analysed.

Appendix 1.3) and Martin (1976, p. 202) suggested the derivation of these rock-fragments from the Adavale Basin to the northwest (Figure 2.12). The Adavale Basin contains silicic to intermediate volcanics and volcanogenic sediments (Day et al, 1983, p. 72-73, 77). In contrast to the Precipice Sandstone, the quartzose Evergreen Formation, and the Hutton, Gubberamunda and Mooga Sandstones all plot in the Lv field of the LvLsLm triangle (Figure 2.5A-C), but there is no commentary in the literature on the likely derivation of the volcanogenic components in these formations. The only other quartzose sandstone in the Surat-Eromanga Basins with volcanic rock-fragments having definitive provenance other than from the eastern arc is the Lower Cretaceous Cadna-Owie Formation (the Bungil Formation equivalent; Figure 2.7). The Cadna-Owie Formation is predominantly quartzose but contains silicic volcanic grains present mostly in the upper part of the formation (the Mt. Anna Sandstone Member) in the south and southwest part of the basin which Wopfner et al (1970) showed convincingly to have been derived from the Proterozoic Gawler Ranges Volcanics in South Australia (cf. Gawler Block in Figure 2.12). Apart from volcanic rocks (rhyolite to rhyodacite; Turner, 1975) in the Gawler Ranges, volcanics and volcanogenic sediments are present in the Adavale Basin (Day et al, ibid.) but much of it is covered by the Permo-Triassic sedimentary rocks of the Gallile Basin (Figure 2.12; cf. Armstrong and Barr, 1986, fig. 2) and Early Jurassic sediments (e.g., the Hutton Sandstone and Evergreen Formation) of the Eromanga Basin (Burger, 1986, fig. 2; see also Day et al, 1983, p. 128). Therefore it is unlikely that it contributed any volcanic rock-fragments to sediments younger than the Precipice Sandstone in the Surat Basin. Moreover, contribution of volcanic rock-fragments to the quartzose formations from sources other than the eastern arc can not be substantiated because in the quartzose petrofacies the proportion of volcanic components,

in most cases, increases orogenward but thickness of individual quartzose formations increases cratonward with concomitant increase in quartz content[1] (Appendix 1.12, see also Watts, 1987). The only possible sources of volcanic components in the east (other than the Jurassic-Cretaceous magmatic arc) are the Bowen and possibly Drummond Basins to the northeast which contain intermediate to silicic volcanics and volcanogenic sediments (Olgers, 1972, Jensen, 1975). The Bowen Basin is believed to have formed a pathway for arc-derived sediment dispersal into the Eromanga and possibly Surat Basins as supported by the presence of reworked Permian and Triassic palynomorphs in the Birkhead Formation in the Eromanga Basin (cf. Watts, 1987); but any such contribution to the quartzose facies formations (e.g., Hutton Sandstone) would be obscured by the overwhelmingly greater sedimentary contribution from the arc, the arc possibly having been dissected to varing degrees during these periods of relative tectonic quiescence (cf. Figure 2.2D). Furthermore, the major periods of erosion in the Drummond and Bowen Basins preceded deposition of the Lower Jurassic basal units of the Surat Basin (Veevers, 1984, p. 359; Day et al, 1983, p. 116), so any significant sediment contribution from these basins to the Surat-Eromanga Basins is unlikely. Likewise, contribution of volcanic rock-fragments from the Sydney Basin in the south (which contains volcanogenic sediments; cf. Leitch, 1969; and McDonnell, 1983) can not be substantiated as there is no evidence of southward increase in lithic

---

1 Although the trend of cratonward increase of detrital quartz content in the Hutton Sandstone within the Surat Basin appears to be less conspicious than the other quartzose formations (particularly in GSQ Chinchilla 4, Appendices 1.12.2 and 1.13.1), the overall trend holds true on a first-order level; e.g., in the Surat Basin the average detrital quartz content of the Hutton Sandstone is 64% (%QFR, cf. Table 2.4) whereas in the Eromanga Basin the figure lies between 80 and 90% (cf. Watts, 1987, his fig. 4).

content in the quartzose sandstones of the Surat Basin (Figure 2.6) and the evidence is to the contrary. Moreover, the volcanic rock-fragments in the quartzose facies do not appear to be reworked. On the contrary, wherever present, they are relatively fresh, comparable to those in the labile facies and, like the latter, are suggestive of a first-cycle origin. From the above discussion it follows that, except perhaps for the Precipice Sandstone, it is unlikely that a major proportion of the volcanic rock-fragments in the quartzose facies formations came from the older sedimentary basins in the various adjacent regions. The Precipice Sandstone is an exception in that it is the most quartzose of all the formations (Figure 2.4); it contains a consistently small but variable amount of rock-fragments (the latter present mainly in GSQ Roma 8 and Chinchilla 4 in terms of the sample control embodied in this report) most of which are of sedimentary affinity (Table 2.4; Figure 2.5A). The very quartzose character of this formation suggests that it formed in a typical passive margin/cratonic sheet sandstone setting. The Precipice Sandstone was deposited before initiation of the Jurassic arc magmatism and has uniform composition throughout the Surat and Clarence-Moreton Basins (Exon, 1976). Volcanic rock-fragments comprise only minor proportions of the Precipice Sandstone and are about an order of magnitude less than in the stratigraphically higher quartzose Hutton Sandstone (Table 2.4). According to Martin (1976, p. 202) these volcanic rock-fragments in the Precipice Sandstone are derived from the Devonian volcanogenic sediments in the Adavale Basin. However, those in GSQ Chinchilla 4 which are confined to the upper part of the formation in the transitional zone with the overlying Evergreen Formation (cf. Appendix 1.3) would appear to have had an eastern provenance (cf. Appendix 1.13).

Upsequence and lateral petrographic trends

Upsequence and lateral petrographic trends in terms of detrital megaquartz and total volcanic components are shown in Appendices 1.12 and 1.13. These trends can be satisfactorily explained by the basin-fill pattern elaborated in Jones et al's (1984) foreland basin model. Formations with dominantly fluvial environmental affinity (e.g., the Jurassic System and lowermost unit of the Lower Cretaceous succession) show petrographic trends consistent with the dynamic fluvial model of Conaghan et al (1982) as exemplified by the Permo-Triassic Sydney Basin in eastern NSW. In the Sydney Basin upsequence variation in quartz content is accompanied by a concomitant swing of palaeocurrent direction from cratonward to orogenward and vice versa as a function of sediment supply from these geographically opposed source-regions and the tectonic activity of the arc-craton couplet. This is schematically depicted in Figure 2.8 in which are shown the orogenward-flowing tributaries bearing craton-sourced quartz sands and the cratonward-flowing tributaries bearing arc/orogen-sourced labile sands, each of which petrologic suites is blended in an axial trunk stream. Migration of the drainage-net results from the balance of sediment supply from the arc/orogen and craton respectively as magmatism waxes and wanes in the arc/orogen (cf. Figure 2.2C and D). If operating in an essentially steady-state mode, such a model requires that change from the quartzose facies to the labile facies and vice-versa in time/space is not drastic but gradational through a sublabile petrofacies domain having intermediate compositional (and palaeocurrent) characteristics (cf. Conaghan et al, 1982) resulting from the blending of sediments of both provenance. To illustrate this point, on a second-order level the concept of an intermediate (sublabile or mixed) petrofacies having an arbitrary QFR megaquartz content between 30 to 50% (cf. Appendices 1.12 and 1.13) is

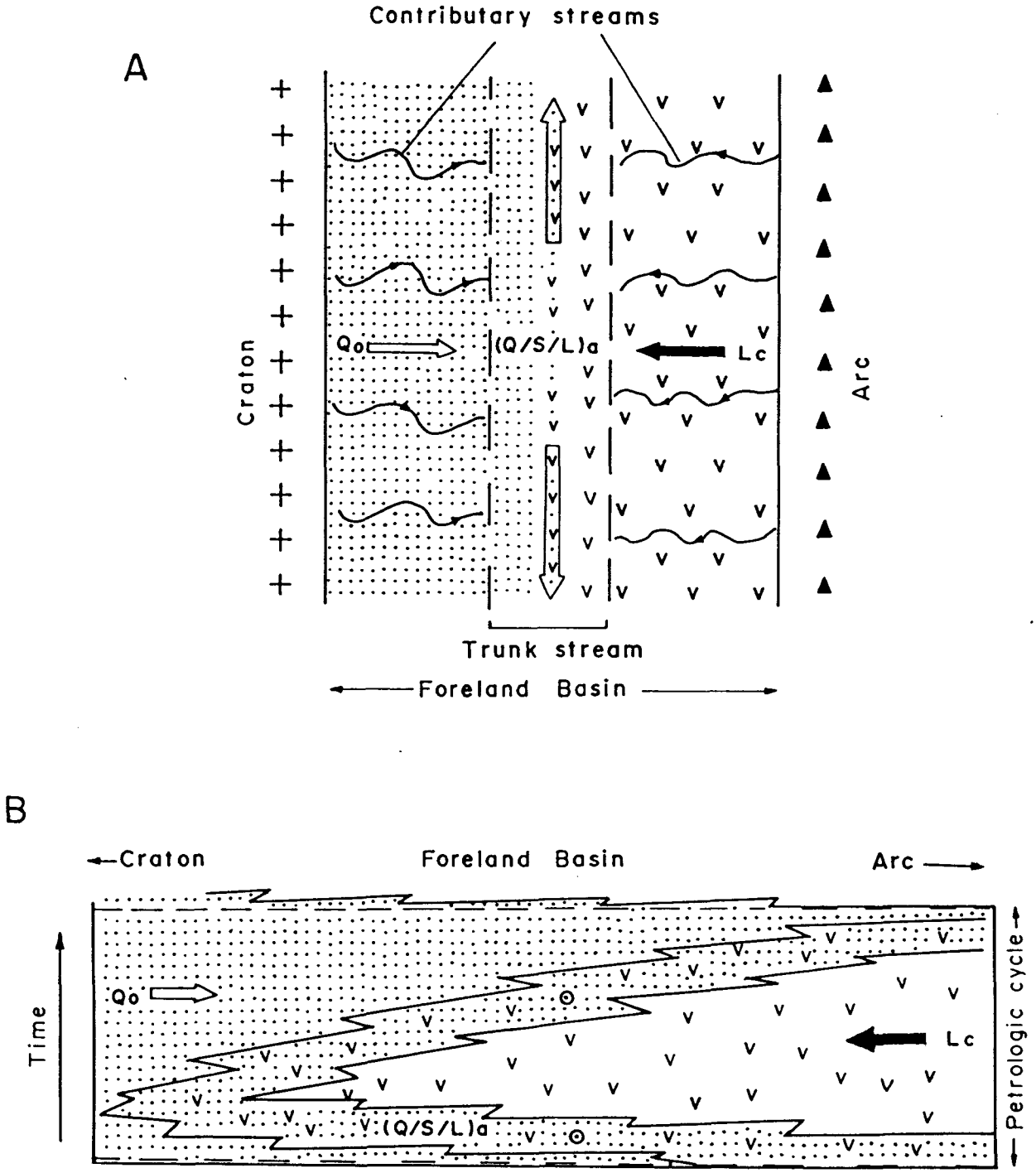

Figure 2.8. Schematic time-space cross-section (B) of a retro-arc foreland basin (A) showing the distribution of gross petrofacies and sediment-transport directions (arrows and circled dots) within a single petrologic cycle. Circled dots indicate transport normal to the plane of the figure. Qo - quartzose petrofacies (orogenward-directed palaeocurrents); Lc - labile petrofacies (cratonward-directed palaeocurrents); (Q/S/L)a - intermediate (sublabile/mixed) petrofacies with or without envelopes of quartzose (Q) and labile (L) domains (axial palaeocurrents). From Coanghan et al (1982, fig. 6) with additions.

introduced. This is shown schematically in Figure 2.8. The domains of the contributary streams are the sites of deposition of either quartzose (Qo) or labile (Lc) petrofacies whereas the axial or trunk stream carries sediments of either cratonic or orogenic/arc provenance or a mixture of both (Q/S/L)a depending on the location and relative width of the trunk system on the basin floor and relative balance/imbalance of sediment supply from the opposing source-lands as a function in large part of the phase of the tectonic cycle (Figure 2.2). Such a scheme is valid for sediments with fluvial environmental affinities and plotting of the detrital megaquartz content in most of the formations in the Surat Basin with fluvial affinities suggests the operation of similar mechanism (see Appendices 1.12 and 1.13). Thus the upsequence variation of sandstone mineralogy that is illustrated in the petrologic logs of individual formations (Appendix 1.12) and west-east transect of petrologic logs of the full stratigraphic succession (Appendix 1.13) demonstrates (notwithstanding some second-order complexity) a first-order pattern of sublabile sediment envelopes separating or interleaved between the quartzose and labile petrofacies in all cases. This is also shown in summary form in Figure 2.9 which defines the major or first-order petrologic cycles. Notwithstanding the absence of any palaeocurrent (i.e., dipmeter-derived) data-control in these stratigraphic test wells, this upsequence compositional pattern strongly suggests a basin-fill pattern in which the lithic petrofacies entered the basin from the east, the quartzose petrofacies from the west, and the intermediate/sublabile petrofacies resulted from the blending of these two sediment suites in an axial stream system which must have flowed either generally towards the south or towards the north (cf. Figure 2.8). Reconnaissance palaeocurrent mapping in the surface exposures of the various sublabile petrofacies (Appendix 1.14) indicates the above disspersal relationships to hold true, and further indicates that the axial

dispersal direction was towards the south rather than towards the north. In stratigraphic intervals that accumulated under marine conditions such as the Rolling Downs Group, there is little blending of the sediment of either provenance (cf. Figure 2.2A) as evidenced by the overwhelmingly labile nature of the Rolling Downs Group (Appendix 1.13.3). Detailed palaeocurrent study in the Surat Basin is beyond the scope of the present report but reconnaissance palaeocurrent data from the surface exposures lend support to the applicability of the model, especially for the non-marine part of the succession (Figure 9.2). The quartzose formations show consistent orogenward palaeocurrent patterns whereas the labile formations show either cratonward or axial (but, with the exception of the Eurombah Formation, not orogenward) patterns (cf. Figure 9.2). Moreover, the model seems to be valid for similar quartzose-labile petrologic cycles in the subsurface of the neighbouring Eromanga Basin as shown by the petrologic and dipmeter-derived palaeocurrent data of the Hutton-Birkhead interval documented by Watts (1987). These data from the central Eromanga Basin (in Qld) show that the average dispersal direction of the quartzose Hutton Sandstone is towards the northeast and that of the lithic Birkhead Formation is towards the west (cf. Watts, 1987, his fig. 11).

SEDIMENTARY AND PETROLOGIC CYCLES WITH RESPECT TO PROVENANCE

On the basis of detrital composition, the Surat Basin succession can be divided into four petrologic cycles, each commencing with the deposition of relatively quartzose sediment, and ending with relatively labile sediment (Figure 2.9). These cycles[1] can be satisfactorily differentiated by the detrital QFR quartz content (Figure 2.9), K-feldspar to total feldspar ratio (Figure 2.10), and total vocanic components (Figure 2.11B) but less satisfactorily so with such categories as Qc/Q (Figure 2.10) and Lv (as pecentage of LvLsLm; Figure 2.11A). It is interesting to note that the whole of the Injune Creek Group (Walloon Coal Measures, the Springbok Sandstone and Westbourne Formation) constitutes the labile phase of one petrologic cycle (Figures 2.9, 2.10 and 2.11B; Appendix 1.13). In terms of content of total volcanic components, this half-cycle reaches its climax in the Springbok Sandstone (Figure 2.11B; Appendix 1.13.2). In fact in some places in the Surat Basin the Springbok Sandstone is indistinguisable from the Westbourne Formation and essentially represents the "... different facies of the same fluvial cycle - the Springbok Sandstone laid down by vigorous stream and the Westbourne Formation by sluggish stream" (Exon, 1976, p. 98). Likewise the Bungil Formation and the Rolling Downs Group is best considered as a single pulse of labile sediment (rather than two pulses notwithstanding the relatively less labile nature of the Surat Siltstone compared to the Griman Creek and Wallumbilla Formations; Figures 2.9, 2.10 and 2.11B; Appendix 1.13.3). The less

---

1 Although the Evergreen Formation has been assigned to the quartzose facies on the basis of the detrital megaquartz content, it is relatively labile compared to the underlying Precipice and overlying Hutton Sandstones and is best viewed as the labile phase of the first and oldest petrologic cycle. With respect to its provenance, it received contribution from both the craton and the arc and the labile content is a function of its proximity to the orogen (cf. Appendix 1.12) and increases orogenward before giving way to the volcanogenic Tiaro Coal Measures in the Maryborough Basin to the east (cf. Figure 2.6).

Figure 2.9. Stratigraphic distribution of mean and one standard deviation of the detrital quartz content (%QFR) for each formation in the Surat Basin succession. Stratigraphic units: 1 - Precipice Sandstone; 2 - Evergreen Formation; 3 - Hutton Sandstone; 4 - Walloon Coal Measures; 5 - Springbok Sandstone; 6 - Westbourne Formation; 7 - Gubberamunda Sandstone; 8 - Orallo Formation; 9 - Mooga Sandstone; 10 - Bungil Formation; 11 - Wallumbilla Formation; 12 - Surat Siltstone; 13 - Griman Creek Formation. The construction of this and following diagrams (i.e., Figures 2.10 and 2.11) is schematic with respect to the vertical scale and is not meant to imply compositional non-uniformity within individual formations. Labile petrofacies (i.e., QFR quartz content <50%) is further subdivided into a sublabile/ intermediate (S) and labile (L) field. Q - quartzose petrofacies field.

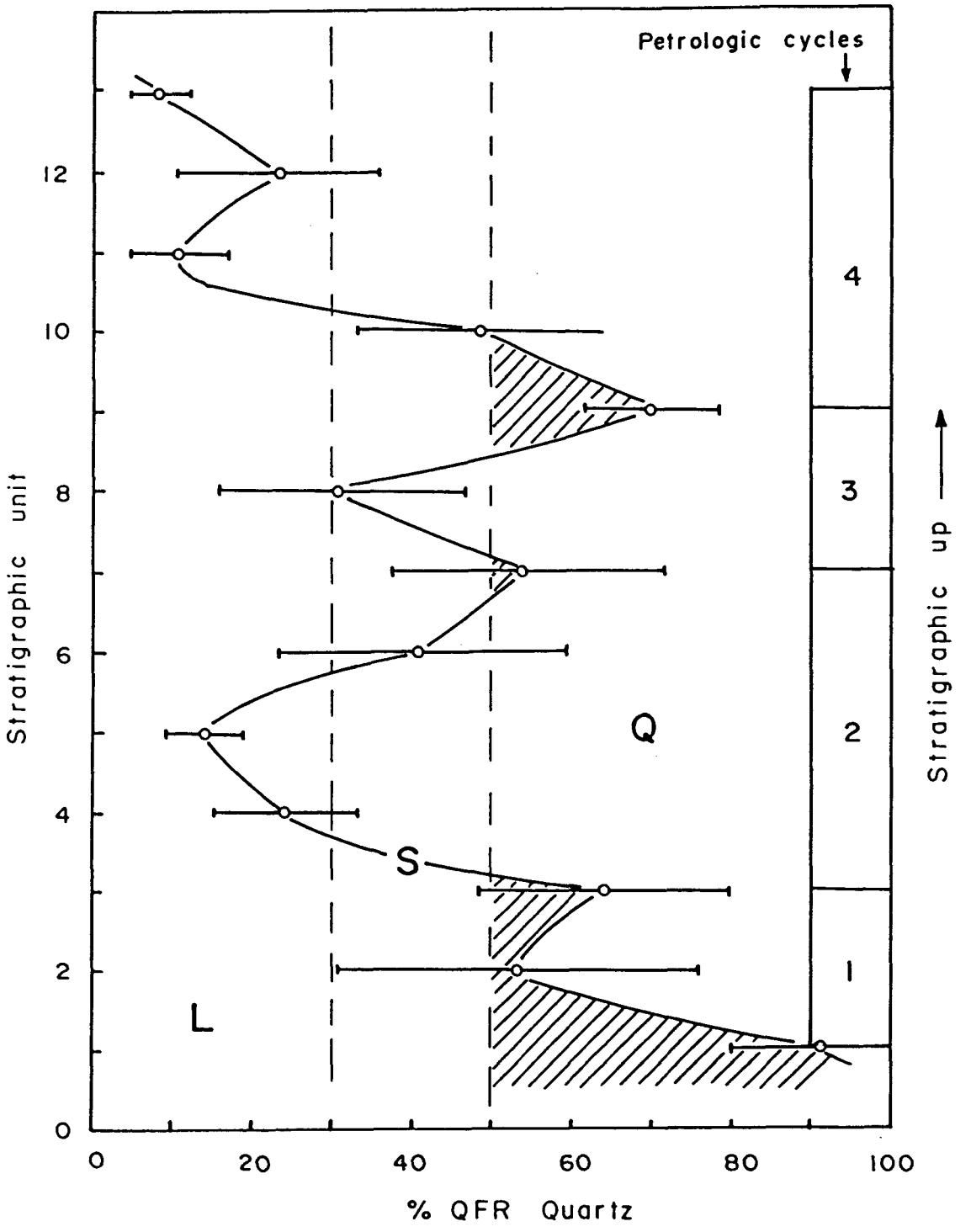
Petrologic cycles
4
3
2
1
Q
S
L
Stratigraphic unit
Stratigraphic up
0
2
4
6
8
10
12
0
20
40
60
80
100
% QFR Quartz

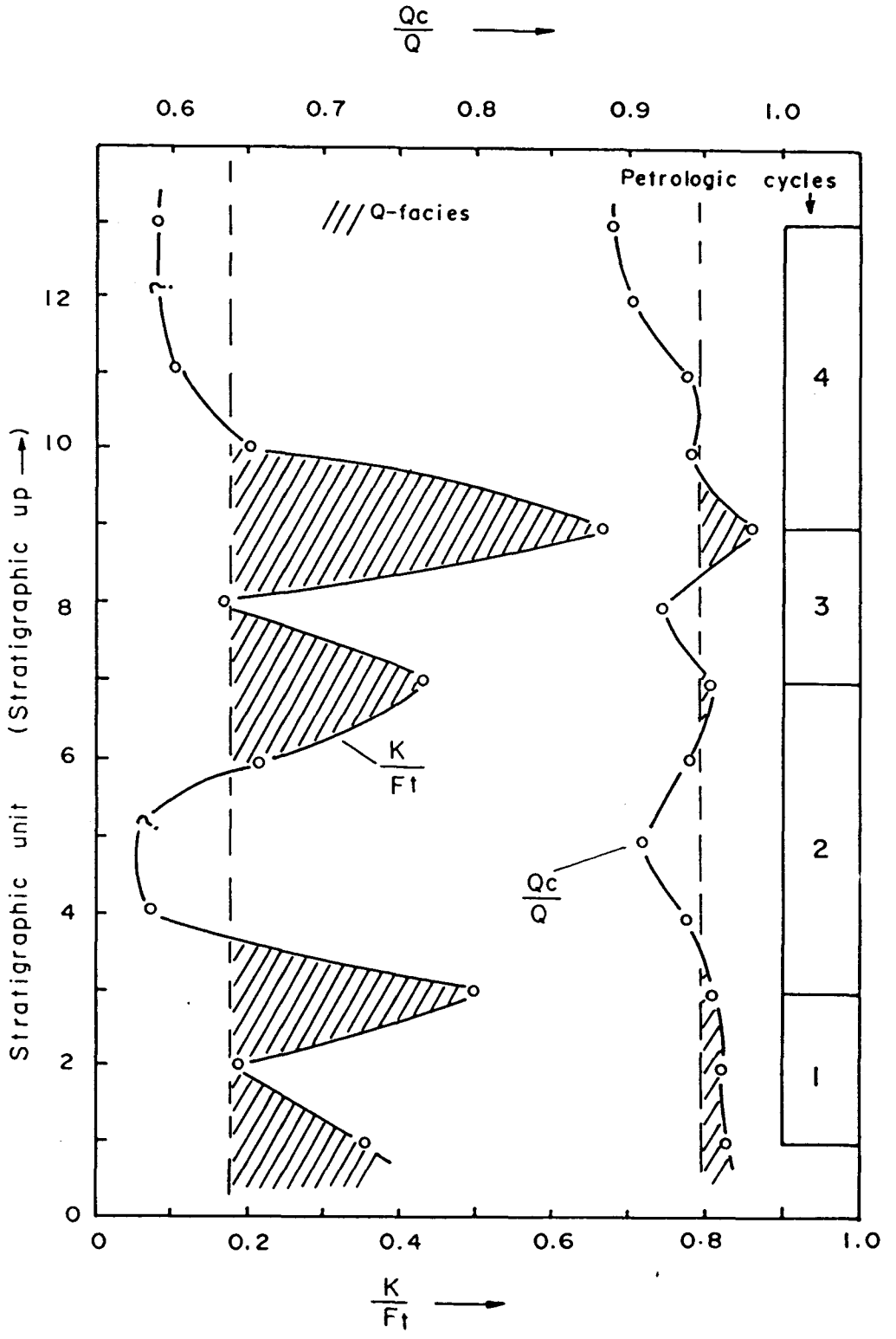

Figure 2.10. Average K-feldspar to total feldspar (K/Ft), and common (plutonic) quartz to total megaquartz (Qc/Q) ratios in sandstones of each formation of the Surat Basin succession. K/Ft ratios are from Table 2.2. Symbols as in Figure 2.9.

Figure 2.11. Stratigraphic distribution of the mean and one standard deviation of the volcanic rock-fragments (Lv, as %LvLsLm) (A), and total volcanic component, Lvt (B), in the Surat Basin sandstones. Numerical symbols of stratigraphic units are the same as in Figure 2.5. Total volcanic components (Lvt) are calculated using the following formulae:

In the labile petrofacies:
$Lvt = Lv + QV_1 + QV_2 + Fans + Fas + Fz + Funs\ (1-r) + F_O\ (1-r)$,
where r is the average K-feldspar to total feldspar ratio (cf. Table 2.3). The Springbok Sandstone and the Surat Siltstone lack data on the value of r, hence r values of the Westbourne and Wallumbilla Formations were used respectively for these on the basis of their stratigraphic proximity (cf. Figure 1.2) and general mineralogic (including feldspar content) similarity (Figure 2.3).

In the quartzose petrofacies:
$Lvt = Lv + QV_1 + QV_2 + Fz$.
(Symbols as in Appendix 1.1 and Table 2.3)
Considering the juvenile nature, euhedral and broken shapes, zoning and conspicious association with abundant volcanic rock-fragments, most, if not all feldspars in the labile petrofacies are presumably volcanic in origin (the minor K-feldspar that has been recorded in this petrofacies appears to comprise sanidine but is excluded from Lvt (cf. r-factor in the first equation above). Hence the estimates of Lvt for the labile petrofacies are on the conservative side.
Most untwinned and albite twinned feldspars in the quartzose petrofacies are euhedral in shape and in some formations are characteristically larger in grainsize than the feldspar grains in the labile petrofacies, and presumably are plutonic in origin. They have been excluded from the calculation of Lvt.

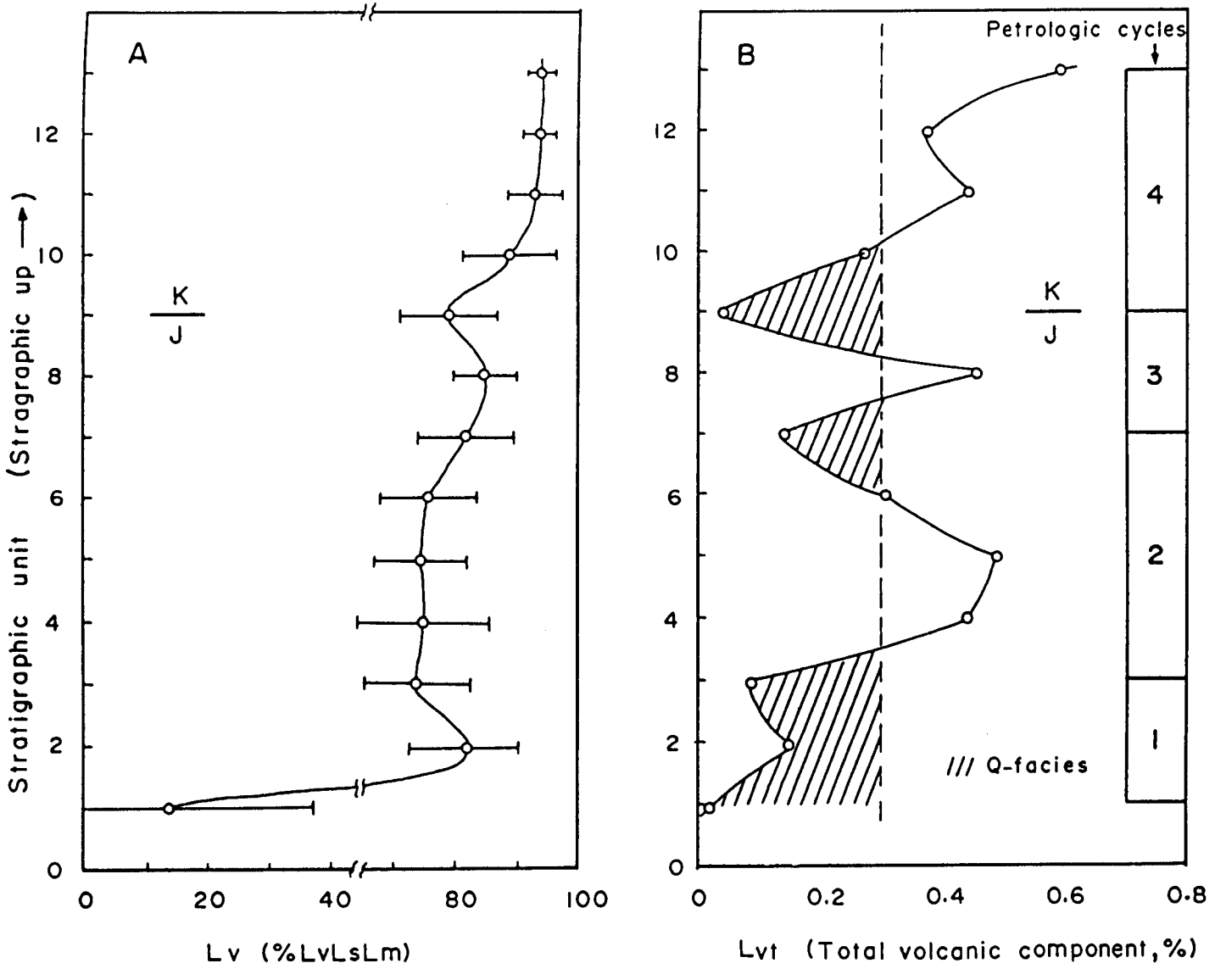
A
B
Petrologic cycles
K/J
K/J
Stratigraphic unit (Stragraphic up ⟶)
0
2
4
6
8
10
12
0
20
40
80
100
Lv (%LvLsLm)
0
0.2
0.4
0.6
0.8
Lvt (Total volcanic component, %)
4
3
2
1
/// Q-facies

labile character of the Surat Siltstone probaly reflects the overall finer mean grainsize of its component sandstones and possibly also the small sample size (n = 2; see Figure 2.4C). These petrologic cycles are different in number but are analogous to the sedimentary (environmental) cycles of Exon and Burger (1981; Figure 9.2 herein). It is noteworthy that these petrologic cycles are excellent matches to those postulated by Jones and Veevers (1983; Figure 2.6 herein) and are better indicators of the episodic activities of the arc-craton couplet, and therefore provenance.

DISCUSSION

Results of the modal analyses of the Surat Basin sandstones suggest that the basin-fill pattern is characterised by a dual source - an andesitic magmatic arc in the east-northeast and a stable craton consisting of plutono-metamorphic terrains and sedimentary and some volcanic rocks in various adjacent basins (Figure 2.12).

In terms of the basin-fill pattern, the whole Jurassic-Cretaceous history of the Surat Basin is one of episodic activities of the arc and the craton as depicted in the speculative palaeogeographic maps of eastern Australia during Jurassic-Cretaceous (Figure 2.13). This episodic activity of the arc-craton couplet is manifested by the petrologic cylces, each of which consists of a cratonic-sourced quartzose sandstone at the base and arc-derived quartz-poor labile sediments above (Figures 2.9 - 2.11; Appendix 1.13).

The magmatic arc commenced its activity during the Early Jurassic as manifested by deposition of the Evergreen Formation but in terms of distance of sediment dispersal away from the arc, this pulse is rather weak compared to most of the successively later pulses of labile sediment (Figures 2.6 and 2.7). The Evergreen Formation pinches out against the Nebine Ridge (Figure 2.7) but undergoes an increase in its thickness and

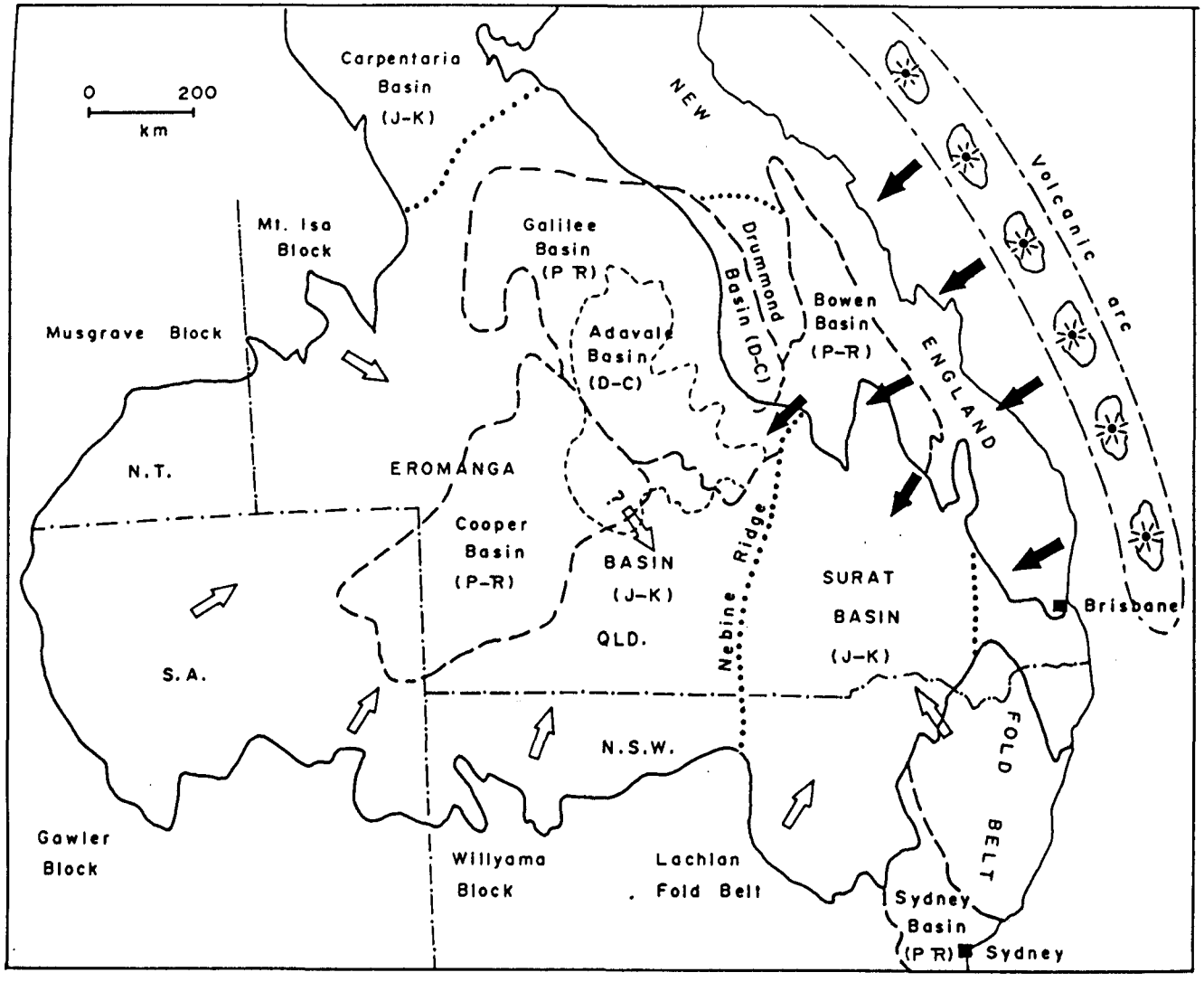

Figure 2.12. Geologic setting of the Surat-Eromanga Basins with interpreted areas of sediment input (modified from Moore et al, 1986, and Watts, 1987, with additions). Solid arrows indicate transport directions of volcanogenic labile sediments and open arrows those of quartzose sediments.

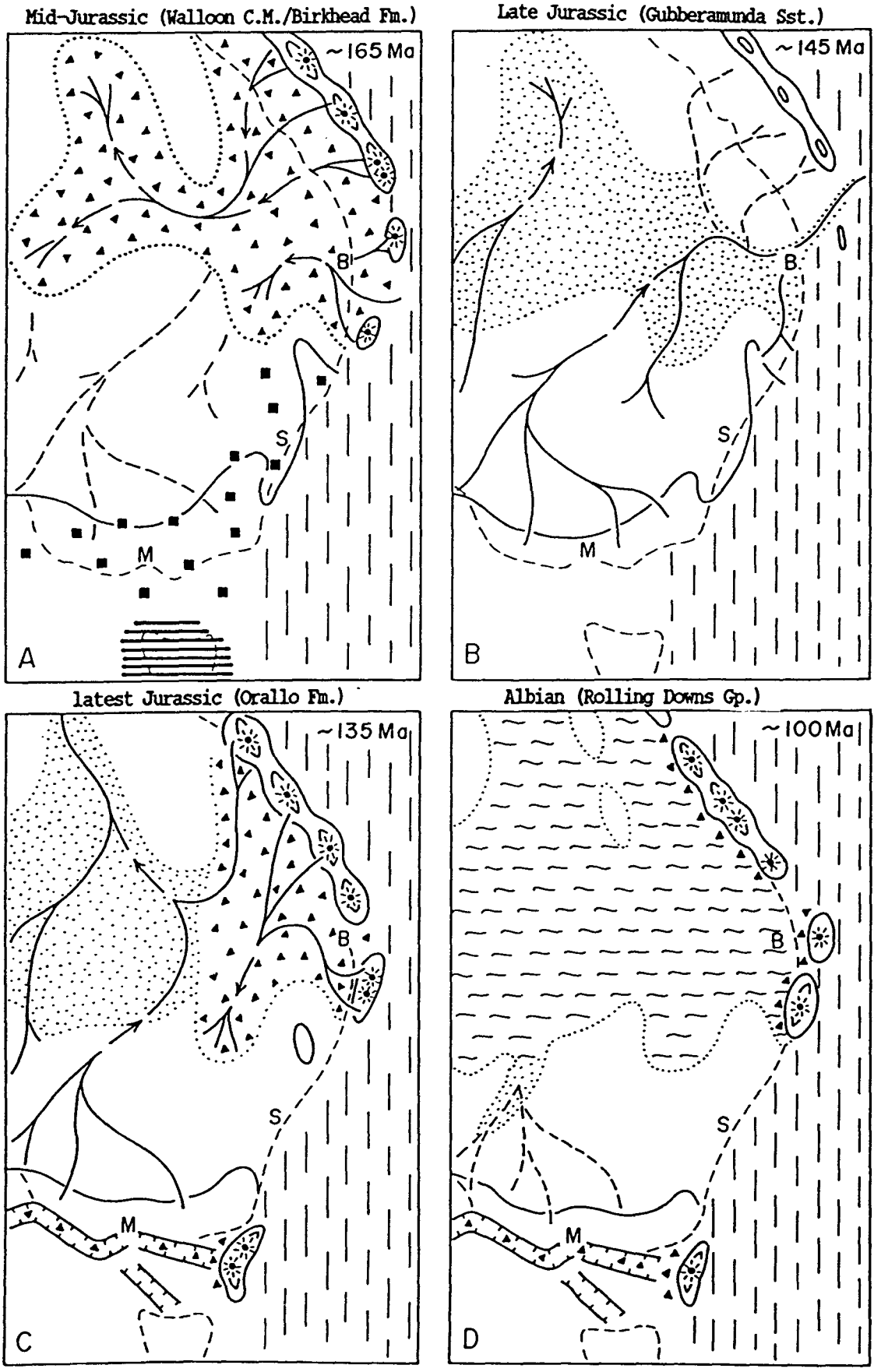
Mid-Jurassic (Walloon C.M./Birkhead Fm.)
~165 Ma
B
S
M
A
Late Jurassic (Gubberamunda Sst.)
~145 Ma
B
S
M
B
latest Jurassic (Orallo Fm.)
~135 Ma
B
S
M
C
Albian (Rolling Downs Gp.)
~100 Ma
B
S
M
D

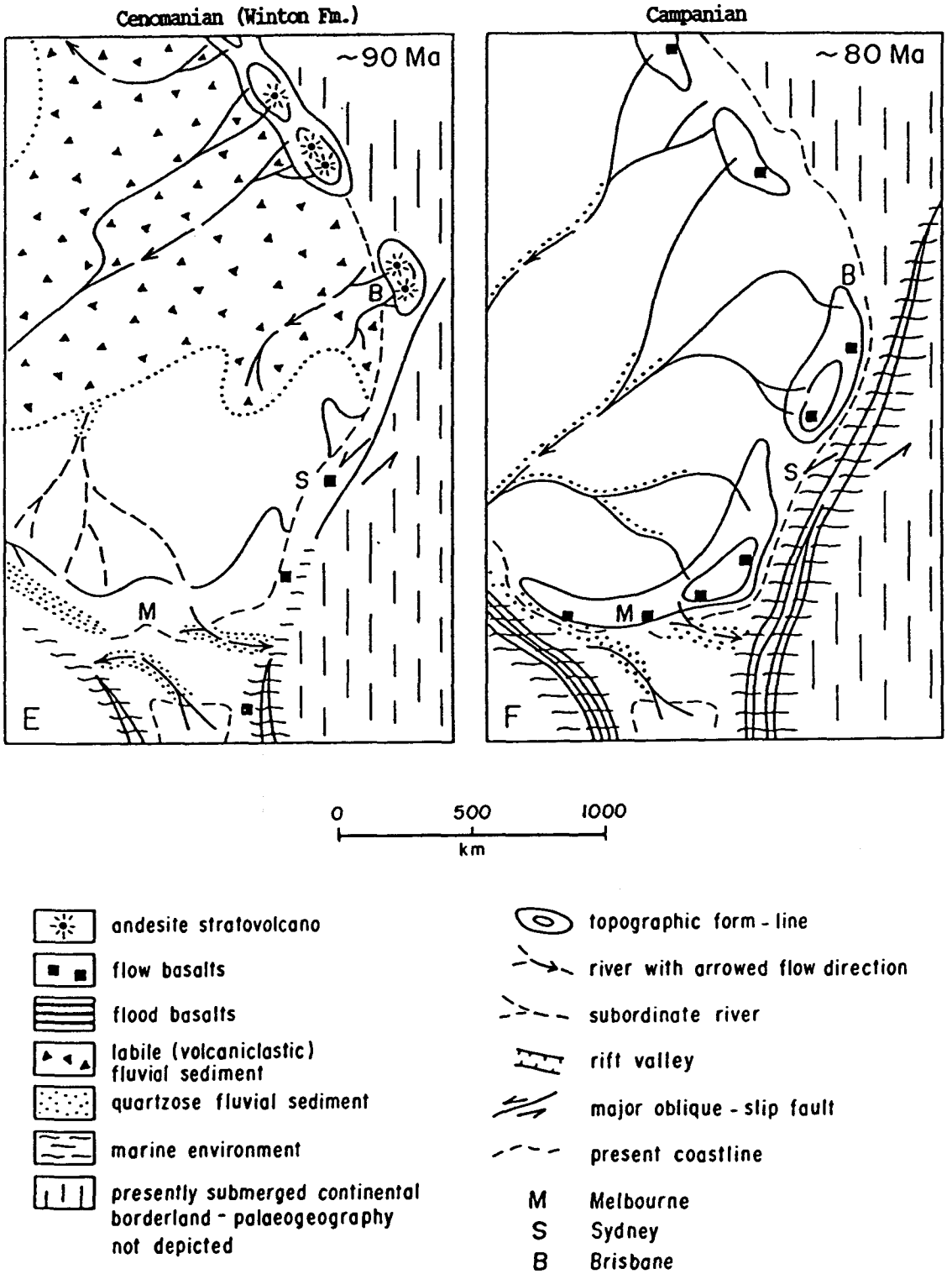

Figure 2.13. Speculative Jurassic-Cretaceous palaeogeographies of eastern Australia. From Jones and Veevers (1983, fig. 8). See text for explanation. The absolute time scale used in this figure is from Veevers (1984, p. 2) and the ages are not identical to those of Palmer (1983) depicted in Figure 1.2 in this report. For ease of comparison formation names representing corresponding times of deposition are shown in parentheses.

volcanic content towards the east as represented by the volcanogenic Tiaro Coal Measures of the Maryborough Basin (cf. Figure 2.6). The Walloon Coal Measures/Birkhead Formation is the first intense pulse of volcanic activity during the Middle Jurassic (Figure 2.13A) when the arc shed ample volcanogenic detritus which spilt past the Nebine Ridge into the epicratonic Eromanga Basin as far west as the Birdsville Track Ridge (Moore, 1982; Paton, 1982; Figure 2.12 herein). This is followed by deposition of the craton-derived Gubberamunda Sandstone - the quartzose counter-phase of the earlier labile pulse (Figure 2.13B). The next labile pulse in the Late Jurassic is much smaller in magnitude and is represented by the volcanogenic Orallo Formation which terminates on the Nebine Ridge and interfingers with the cratonic quartzose Hooray Sandstone (Figures 2.13C and 2.7). The arc resumed its activity during the Early Cretaceous with the deposition of the marine Bungil Formation and the Rolling Downs Group (Figure 2.13D) and reached its climax in the Cenomanian with the deposition of the Winton Formation (Figure 2.13E) that is presrved only in the Eromanga Basin (Figure 2.7) and contains juvenile andesitic debris (Veevers, 1984, p. 269). As measured by the distance travelled by the volcanogenic sediment from the arc, this terminal spasm had the greatest effect, its products extending at least 400 km further west than that of the Mid-Jurassic (Callovian) Walloon Coal Measures/Birkhead Formation. The arc became extinct towards the Late Cretaceous with the inception of sea-floor spreading in the east (Figure 2.13F).

REFERENCES

Allen, R. J., and Houston, B. H., 1964, Petrology of Mesozoic sandstones of the Carnarvon Highway section, western Bowen and Surat Basins. Geol. Surv. Qld. Rpt. 6, 25 p.

Arditto, P. A., 1982, Deposition and diagenesis of the Jurassic Pilliga Sandstone in the southeastern Surat Basin, New South Wales. Jour. Geol. Soc. Austral. v. 29, pp. 191-203.

Arditto, P. A., 1983, Mineral-goundwater interactions and the formation of authigenic kaolinite within the southeastern intake beds of the Great Australia (Artesian) Basin, NSW. Sedim. Geol., v. 35, pp. 249-261.

Armstrong, J. D., and Barr, T. M., 1986, The Eromanga Basin, an overview of exploration and potential. In Contributions to the geology and hydrocarbon potential of the Eromanga Basin. Geol. Soc. Austral. Sp. Publ. 12, pp. 25-38.

Basu, A., 1976, Petrology of Holocene fluvial sand derived from plutonic source rocks: implications to paleoclimate interpretation. Jour. Sedim. Petrol., v. 46, pp. 694-709.

Blatt, H., Middleton, G., and Murray, R., 1972, Origin of sedimentary rocks. Prentice-Hall, Englewood Cliff, NJ. 634 p.

Burger, D., 1986, Palynology, cyclic sedimentation, and palaeoenvironments in the Late Mesozoic of the eromanga Basin. In Contribution to the Geology and hydrocarbon potential of the Eromanga Basin. Geol. Soc. Austral. Sp. Publ. 12, pp. 53-70.

Conaghan, P. J., Jones, J. G., Mcdonnell, K. L, and Royce, K., 1982, A dynamic fluvial model for the Sydney Basin. Jour. Geol. Soc. Austral., v. 29, pp. 55-70.

Cowan, E. J., 1985, A basin analysis of the Triassic System, central coastal Sydney Basin. Unpubl. B.Sc (Hons) thesis. Macquarie University, 255 p.

Cummins, W. A., 1962, The greywacke problem. Liverpool and Manchester Geol. Jour., v. 3, pp. 51-72.

Davies, D. K., and Ethridge, F. G., 1975, Sandstone composition and depositional environments. AAPG Bull., v. 59/2, pp. 239-264.

Day, R. W., Whitaker, W. G., Murray, C. G., Wilson, I. H., and Grimes, K. G., (1983), Queensland Geology - a companion volume to the 1:2 500 000 scale geological map (1975). Geol. Surv. Qld. 194 p.

Dickinson, W. R., 1970, Interpreting detrital modes of greywacke and arkose. Jour. Sedim. Petrol., v. 40, pp. 695-707.

Dickinson, W. R., Helmold, K. P., and Stein, J. A., 1979, Mesozoic lithic sandstones in central Oregon. Jour. Sedim. Petrol., v. 49, pp. 501-516.

Dickinson, W. R., 1982, Compositions of sandstones in circum-Pacific subduction complexes and forearc basins. AAPG Bull., v. 66, pp. 121-137.

Dickinson, W. R., 1985, Interpreting provenance relations from detrital modes of sandstones. In Zuffa, Z. Z. (ed.) Provenance of arenites. D. Reidl, Dordrecht, pp. 333-361.

Ethridge, F. G., 1977, Petrology, transport, and environment in isochronous Upper Devonian sandstone and siltstone units, New York. Jour. Sedim. Petrol., v. 47, pp. 53-65.

Exon, N. F., 1976, Geology of the Surat Basin in Queensland. Bureau Miner. Res. Bull. 166, 160 p.

Exon, N. F., and Burger, D., 1981, Sedimentary cycles in the Surat Basin and global changes in sea-level., Bureau Min. Res. Jour. Austral. Geol. Geophy., v. 6, pp. 153-159.

Ferree, R. A., Jordan, D. W., Kertes, R. S., Savage, K. M., and Potter P. E., 1988, Comparative petrographic maturity of river and beach sand, and origtin of quartz arenites. Jour. Geol. Educ., v. 36, pp. 79-87.

Folk, R. L., Andrews, P. B., and Lewis, D. W., 1970, Detrital sedimentary rock classification and nomenclature for use in New Zealand. NZ Jour. Geol. Geoph., v. 13/14, pp. 937-968.

Folk, R. L., 1980, Petrology of sedimentary rocks. Hemphill. Austin, Texas. 182 p.

Graham, S. A., Ingersoll, R. V., and Dickinson, W. R., 1976, Common provenance for lithic grains in Carbiniferous sandstones from Quachita Mountains and Black Warrior BAsin. Jour. Sedim. Petrol., v. 46, pp. 620-632.

Hawkins, J. W., and Whetten, J. T., 1969, Graywacke matrix minerals: hydrothermal reactions with Columbia River sediments. Science, v. 166, pp. 868-870.

Houston, B. R., 1972, Petrology of subsurface samples of Mesozoic arenites of the Bowen and Surat Basins. In Gray, A. G. R., (ed.) Stratigraphic drilling in the Surat and Bowen Basins, 1967-70. Geol Surv. Qld. Rpt. 71, pp. 89-98.

Ingersoll, R. V., 1978, Petrofacies and petrologic evolution of the late Cretaceous forearc basin, northern and central California. Jour. Geol., v. 86, pp. 335-352.

Ingersoll, R. V., and Suczek, C. A., 1979, Petrology and provenance of Neogene sand from Nicobar and Bengal fans, DSDP sites 211 and 218. Jour. Sedim. Petrol., v. 49, pp. 1217-1228.

Jensen, A. R., 1975, Permo-Triassic stratigraphy and sedimentation in the Bowen Basin, Queensland. Bureua Min. Res. Bull. 154, 187 p.

Jones, J. G., and McDonnell, K. L., 1981, Papua New Guinea analogue for

the Late Permian environment of northern New South Wales, Australia. Palaeogeogr., Palaeoclimatol., Palaeoecol., v. 34, pp. 191-205.

Jones, J. G., and Veevers, J. J., 1982, A Cainozoic history of Australia's Southeast Highlands. Jour. Geol. Soc. Austral., v. 29, pp. 1-12.

Jones, G. J., and Veevers, J. J., 1983, Mesozoic origins and antecedents of Australia's Eastern Highlands. Jour. Geol. Soc. Austral. v. 30, pp. 304-322.

Jones, J. G., Conaghan, P. J., McDonnell, K. L., Flood, R. H., and Shaw, S. E., 1984, Papuan Basin analogue and a foreland basin model for the Bowen - Sydney Basin. In Veevers, J. J. (ed.) Phanerozoic earth history of Australia. Cleardon Press, Oxford., pp. 243-262.

Jones, J. G., Conaghan, P. G., and McDonnell, K. L., 1987, Coal measures of an orogenic recess: Late Permian Sydney Basin, Australia. Palaeogeogr. Palaeoclimatol. and Palaeoecol., v. 58, pp. 203-219.

Kastner, M., and Siever, R., 1979, Low temperature feldspars in sedimentary rocks. Amer. Jour. Sci., v. 279, pp. 435-479.

Leitch, E. C., 1969, Igneous activity and diastrophism in the Permian of New South Wales. Geol. Soc. Austral. Sp. Publ. 2, pp. 21-33.

Mack, G. H., and Suttner, L. J., 1977, Paleoclimate interpretation from a petrographic comparison of Holocene sands and the Fountain Formation (Pennsylvania) in the Colorado Front Range. Jour. Sedim. Petrol., v. 47, pp. 89-100.

Mack, G. H., 1978, The survivability of labile light-mineral grains in fluvial, aeolian and littoral marine environments: the Permian Cutler and Cedar Mesa Formations. Maob, Utah. Sedimentology, v. 25, pp. 587-604.

Martin, K. R., 1976, Sedimentology of the Precipice Sandstone, Surat Basin, Queensland. Unpubl. Ph.D thesis. Univ. Qld., 224 p.

Martin, K. R., 1979, Early Jurassic sedimentation in the Surat Basin. Coal Geol., v. 1/3, pp. 71-81.

Martin, K. R., 1981, Deposition of the Precipice Sandstone and the evolution of the Surat Basin in the Early Jurassic. Austral. Petrol. Expln Assoc. Jour., v. 21, pp. 16-23.

McDonnell, K. L., 1983, The Sydney Basin from Late Permian to Middle Triassic - a study focussed on the coastal transect. Unpubl. Ph.D thesis. Macquarie University, 347 p.

Moore, P. S., 1982, Mesozoic geology of the Simpson desert region, northern South Australia. In Moore, P. S., and Mount, T. J., (eds.) Eromanga Basin symposium - summary papers. Geol. Soc. Austral. and Petrol. Expln Soc. Austral., Adelaide. pp. 46-57.

Moore P. S., Hobday, D. K., Mai, H., and Sun, Z. C., 1986, Comparison of selected non-marine petroleum-bearing basins in Australia and China. Austral. Petrol. Expln Assoc. Jour. v. 26, pp. 285-309.

Olgers, F., 1972, Geology of the Drummond Basin, Queensland. Bureau Min. Res. Bull. 132, 78 p.

Palmer, A. R., 1983, The decade of North American geology - 1983 geologic time scale. Geology, v. 11, pp. 503-504.

Paton, I. M., 1982, The Birkhead Formation - a Jurassic petroleum reservoirs. In Moore, P. S., and Mount, T. J., (eds.) Eromanga Basin symposium - summary papers. Geol. Soc. Austral. and Petrol. Expln Soc. Austral., Adelaide. pp. 346-355.

Pettijohn, F. J., Potter, P. E., and Siever, R., 1972, Sand and sandstone. Springer-Verlag, New York. 618 p.

Pittman, E. D., 1963, Use of zoned plagioclase as an indicator of provenance. Journ. Sedim. Petrol., v. 33, pp. 380-386.

Pittman, E. D., 1988, Diagenesis of Terry Sandstone (Upper Cretaceous), Spindle Field, Colorado. Jour. Sedim. Petrol., v. 58/5, pp. 785-800

Potter, P. E., 1986, South America and a few grains of sand: part 1 - beach sands. The Jour. Geol., v. 94, pp. 301-319.

Quilty, P. G., 1984, Phanerozoic climates and environments of Australia. In Veevers, J. J. (ed.) Phanerozoic earth history of Australia. Clarendon Press. Oxford. pp. 48-57.

Senior, B. R., Mond, A., and Harrison, P. L., 1987, Geology of the Eromanga Basin. Bureau Min. Res. Geol. Geophy. Bull. 167, 102 p.

Suttner, L. J., 1974, Sedimentary petrographic provinces: an evaluation. In Ross, C. A., (ed.) Paleogeographic provinces and provinciality. Soc. Econ. Paleon. Miner. Sp. Publ. 21, pp. 75-84.

Turner, A. R., 1975, The petrology of the eastern Gawler Ranges volcanic complex. Geol. Surv. South Austral. Bull. 45, 135 p.

Watts, K. J., 1987, The Hutton Snadtone-Birkhead Formation transition, ATP 269P (I), Eromanga Basin. Austral. Petrol. Expln. Assoc. Jour., v. 27, pp. 215-228.

Wolf, K. H., 1971, Textural and compositional transitional stages between various lithic grain types (with a comment on "Interpreting detrital modes of greywacke and arkose"). Jour. Sedim. Petrol., v. 41, pp. 328-332.

Wopfner, H., Freytag, I. B., and Heath, G. R., 1970, Basal Jurassic-Cretaceous rocks of western Great Australian Basin, South Austrlia: stratigraphy and environment. AAPG Bull., v. 54/3, pp. 383-416.

Veevers, J. J (ed.), 1984, Phanerozoic earth history of Australia. Clarendon Press, Oxford. 418 p.

CHAPTER 3: DIAGENESIS AND THE GEOLOGIC EVOLUTION OF POROSITY AND PERMEABILITY OF THE SURAT BASIN SANDSTONES

DIAGENESIS AND THE GEOLOGIC EVOLUTION OF POROSITY AND PERMEABILITY OF THE SURAT BASIN SANDSTONES

ABSTRACT

The present-day porosity of the Surat Basin sandstones is diagenetically controlled. Compaction has significantly reduced primary depositional porosity but sporadic cementation locally halted further compaction and preserved moderate to good pre-cement bulk-volume. Some of these cementing phases were later dissolved creating secondary intergranular porosity accompanied by variable amounts of framework grain dissolution porosity. Compaction is strongly influenced by detrital composition and is more pronounced in the lithic sandstones. Present-day porosity of the Surat Basin sandstones is primarily a function of five variables; in order of decreasing importance these are: diagenetic cement, detrital mineralogy, geologic age, burial depth and depositonal environments. The evolved porosity of the Surat Basin clastics is a combination of both primary and secondary dissolution porosity. On the whole in the Surat Bsin the latter is volumetrically marginally more prevalent than the former. In specific formations, on average, secondary porosity constitutes up to 80% of the total thin-section porosity. Primary porosity is prevalent in the younger stratigraphic units, presumably reflecting relatively minor compaction compared to the more deeply buried formations. Nevertheless they also show variable amounts of secondary porosity created mainly by meteoric flushing after inception of the Great Artesian System. Secondary porosity is ubiquitous throughout the whole stratigraphic column. However, significant amounts of it occur within specific depth intervals where such enhancement is believed to have resulted from the action of organic maturation products emanating from the

intercalated mudrocks. The quality and quantity of organic matter, its level of thermal maturation, and the timing of hydrocarbon generation all played a vital role in the creation and preservation of secondary porosity at depth.

INTRODUCTION

Reduction of porosity and/or its subsequent restoration after initial reduction takes place through a complex interplay of numerous processes collectively known as diagenesis. Various parameters such as geologic age, sediment composition and texture, burial depth, geothermal and pressure gradients, fluid flux and chemistry, sand/shale ratio, level of organic maturation of the intercalated mudrocks and hydrocarbon saturation are some of the parameters deemed important for the evolution of sandstone porosity by many workers (cf. Chapter 6). It will be shown quantitatively in Chapter 6 that cementation, detrital mineralogy, geologic age, burial depth and depositional environments have exerted a first-order control in determining the porosity of the Surat Basin succession. The effect of cementation on porosity reduction becomes more important (as shown by the results of multiple regression anlysis; Chapter 6) after the volume of cement exceeds 5%. The present-day porosity of the Surat Basin sandstones is the result of a complex diagenetic history. Diagenesis as a physico-chemical process may be divided into three main pathways: compaction, cementation[1] and dissolution (Figure 3.1). In this chapter the factors controlling the porosity of the Surat Basin sandstones, various diagenetic processes involved and their products will be discussed.

---

1 In terms of its effect on porosity reduction, recrystallization may be viwed as a special case of cementation.

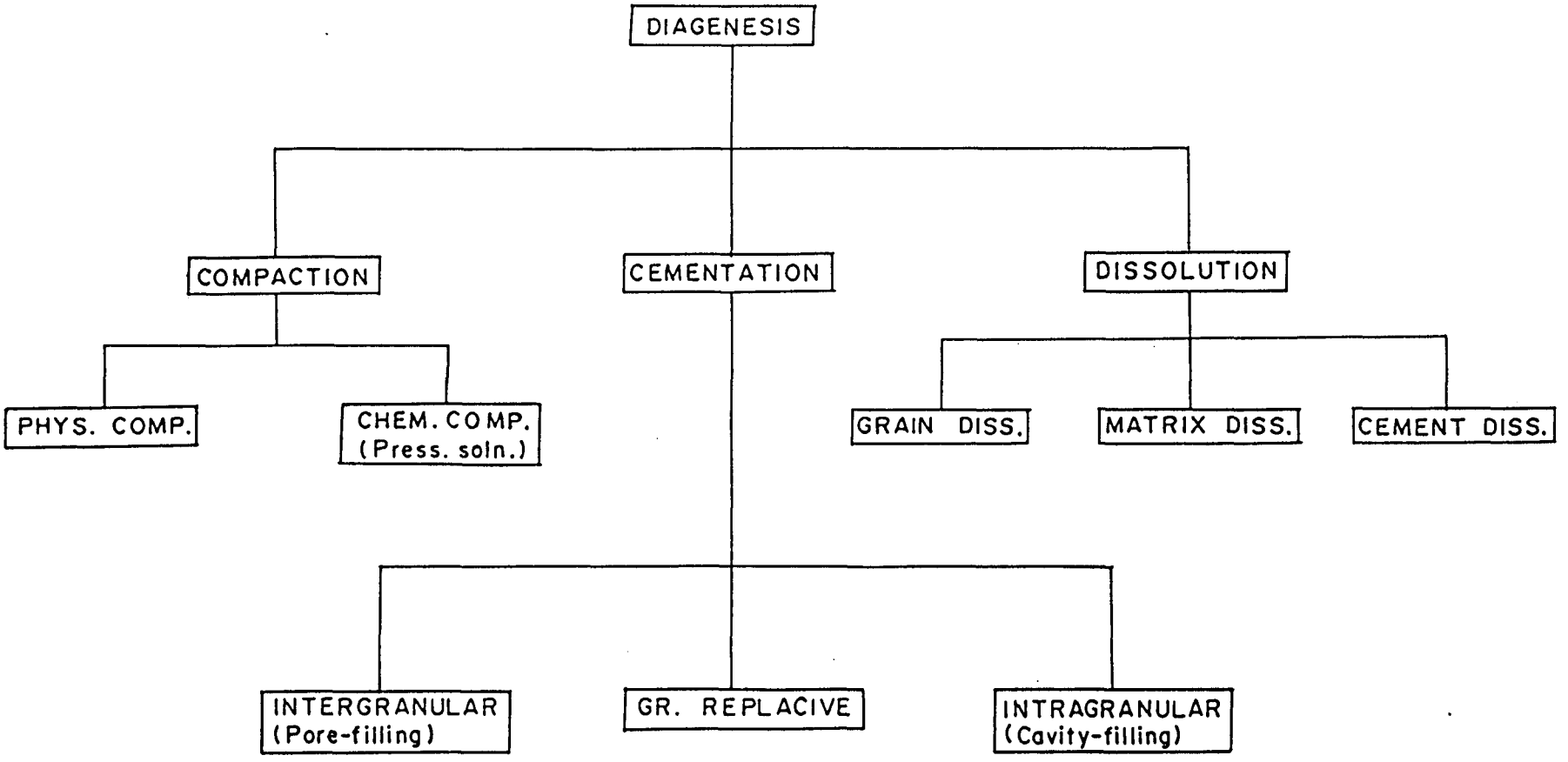

Figure 3.1. A general classification of diagenetic processes.

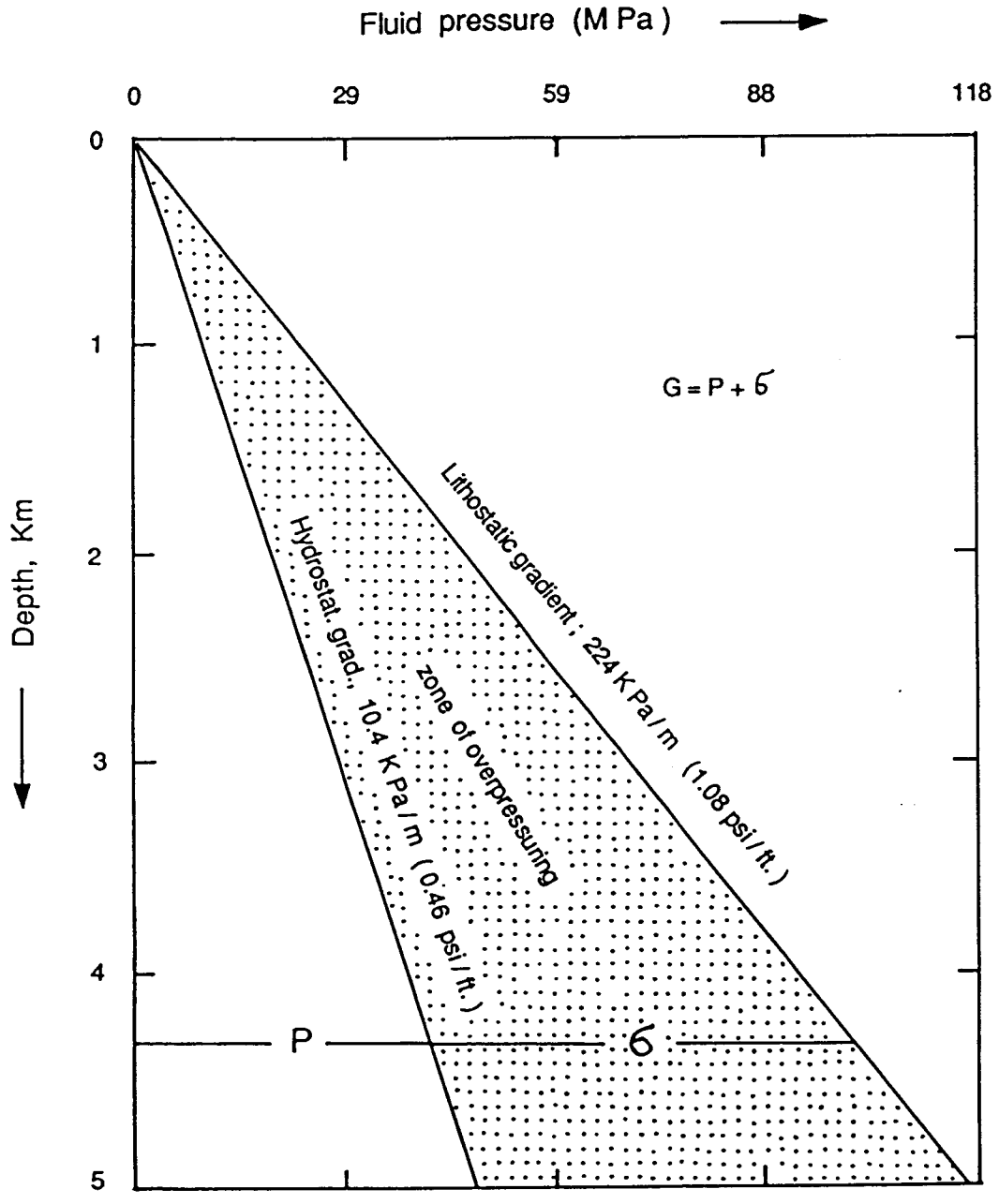

Figure 3.2. Distribution of overburden pressure as a function of pore-fluid pressure and grain-to-grain pressure. From Hunt (1979, fig. 6-5) with minor modifications.

FACTORS AFFECTING THE GEOLOGIC EVOLUTION OF POROSITY

Burial depth

The most obvious change of a body of sediment upon burial is compaction in response to overburden pressure which is transmitted partly by the pore-fluid pressure and partly by the grain-to-grain pressure (uniaxial effective stress). From Rubey and Hubbert (1959), the overburden or the petrostatic (geostatic) pressure G may be expressed as follows:

$$G = P + \sigma',$$

where P is the pore-fluid pressure and σ' is the grain-to-grain pressure (Figure 3.2). As more sedimentary load is added, pore pressure initially increases to support the additional overburden. With time the water is slowly expelled from the sediment pile resulting in a decrease in pore pressure to a minimum limit and a corresponding increase in grain pressure to a maximum limit. Pore pressure P at this time is equal to the hydrostatic pressure:

$$P = \rho_f gh,$$

where ρ_f is formation water density, g is acceleration due to gravity, and h is burial depth. However, the effect of compaction is not solely a factor of grain pressure because time (geologic age) also plays a role. The effect of both pressure and time can be approximated by using the time - pressure integral as a measure of compaction:

$$C = \int_{\cdot}^{t} \sigma'(t)\, dt.$$

where C is compaction, σ' is the grain pressure, and t is the time in My. The effect of geologic age on compaction has been demonstrated by Roll (1974) by matching actual sediment-compaction curves with mathematically calculated curves. His Tertiary examples fit better than the Palaeozoic

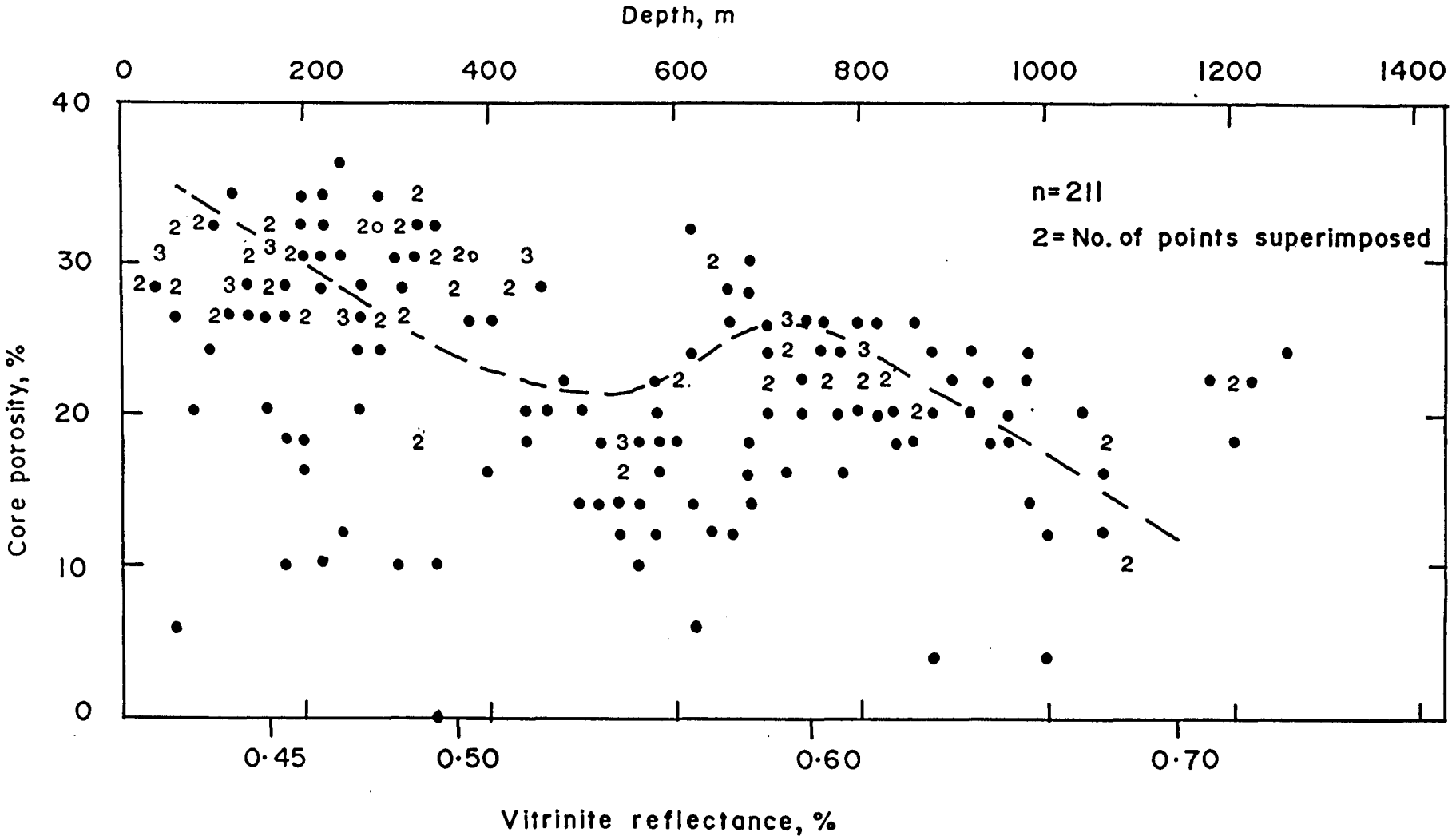

Figure 3.3. Core porosity - depth relationship of the Surat Basin sandstones (all formations) superimposed on vitrinite reflectance. Vitrinite reflectance is calculated from R_o - depth regression equation based on data from four stratigraphic wells (i.e., GSQ Mitchell 2, GSQ Roma 8, GSQ Chinchilla 4, and GSQ Taroom 17; cf. (Appendix 2.8.1.). A more detailed version of this plot which differentiates the quartzose and labile petrofacies is shown in Appendix 8.1.

records. He noted that compaction responds initially to the pressure of overlying sediments, but aging perhaps of 100 My will reduce pore space by another 2-3% (see also Harris, 1988).

The time-dependent tendency of pore pressure to become hydrostatic is a natural consequence of any body of sediment buried to a certain depth as exemplified by the general scarcity of overpressuring in sedimentary rocks older than Mesozoic (cf. Selley, 1985). As mentioned before, with the establishment of hydrostatic pressure, grain pressure attains the maximum value and inelastic deformation of the pore system may take place. With increasing grain pressure (i.e., decreasing pore pressure) in the course of commercial exploitation (i.e., production) of hydrocarbon fields inelastic collapse of pores and fractures (and in some cases also well casings; cf. Hammerlindl, 1971) occurs resulting in the destruction of porosity (Schatz and Ahmed, 1982). In many cases, inelastic collapse can be a dominant mechanism in reducing porosity and permeability even when the reservoir condition is hydrostatic (Schatz and Ahmed, ibid.). Abnormally high formation pressure associated with young basins of high geothermal gradient, high sedimentation rate, high shale/sand ratio and active hydrocarbon generation reduces grain-to-grain pressure thus preventing further compaction and sustains higher-than-average porosity.

The Surat Basin sandstones show a considerable scatter of porosity with depth (Figure 3.3) as might be expected for other basins. However, many workers put forward different porosity - depth curves. A linear relationship was favoured by some investigators (Proshlyakov, 1960; Maxwell, 1964). Selley (1978) interpreted Atwater and Miller's (1965) data as a straight line relationship although they can be represented by an exponential equation as well. Sclater and Christie (1980) proposed an exponential relationship and suggested that Athy's (1930) formula which was meant for shale compaction can be used for sandstone as well:

$P = P_o\ e^{-cz}$

where P is the porosity at depth z, P_o is the porosity at the surface and c is a constant. The exponent c and the pre-exponential factor P_o (i.e., initial porosity) depends on the lithology. It may be mentioned here that to seek a model curve is risky and can be misleading because of the widespread occurrence of secondary porosity in many sedimentary basins. However such a curve presumbaly simulates the loss of primary porosity upon burial. As it will be shown below the present-day porosity in the Surat Basin is both primary and secondary in origin, the latter being marginally more abundant as a whole. Compaction is the single most important cause of the loss of primary porosity and, other factors being equal, is a function of detrital mineralogy, the porosity gradient increasing with increasing labile content (Figure 3.4).

Temperature

The rate of any chemical reaction increases exponentially with temperature as demonstrated by the Arrhenius equation:

$K = A \exp(-E_a/RT)$

where K = reaction rate constant related to change in concentration of parent substance with change in time, A = a constant called the frequency factor, E_a = activation energy; T = temperature in degrees Kelvin and R = universal gas constant. The effect of temperature on porosity has always been portrayed to be detrimental (Maxwell, 1964; Galloway, 1974, 1979) which can be explained by the increased degree of compaction (Sprunt and Nur, 1977) and cementation with temperature. However, no comprehensive study on the effect of temperature on dissolution as a distinct diagenetic process has been done so far and it is proposed that, other factors being equal, dissolution will be enhanced by higher geothermal gradients.

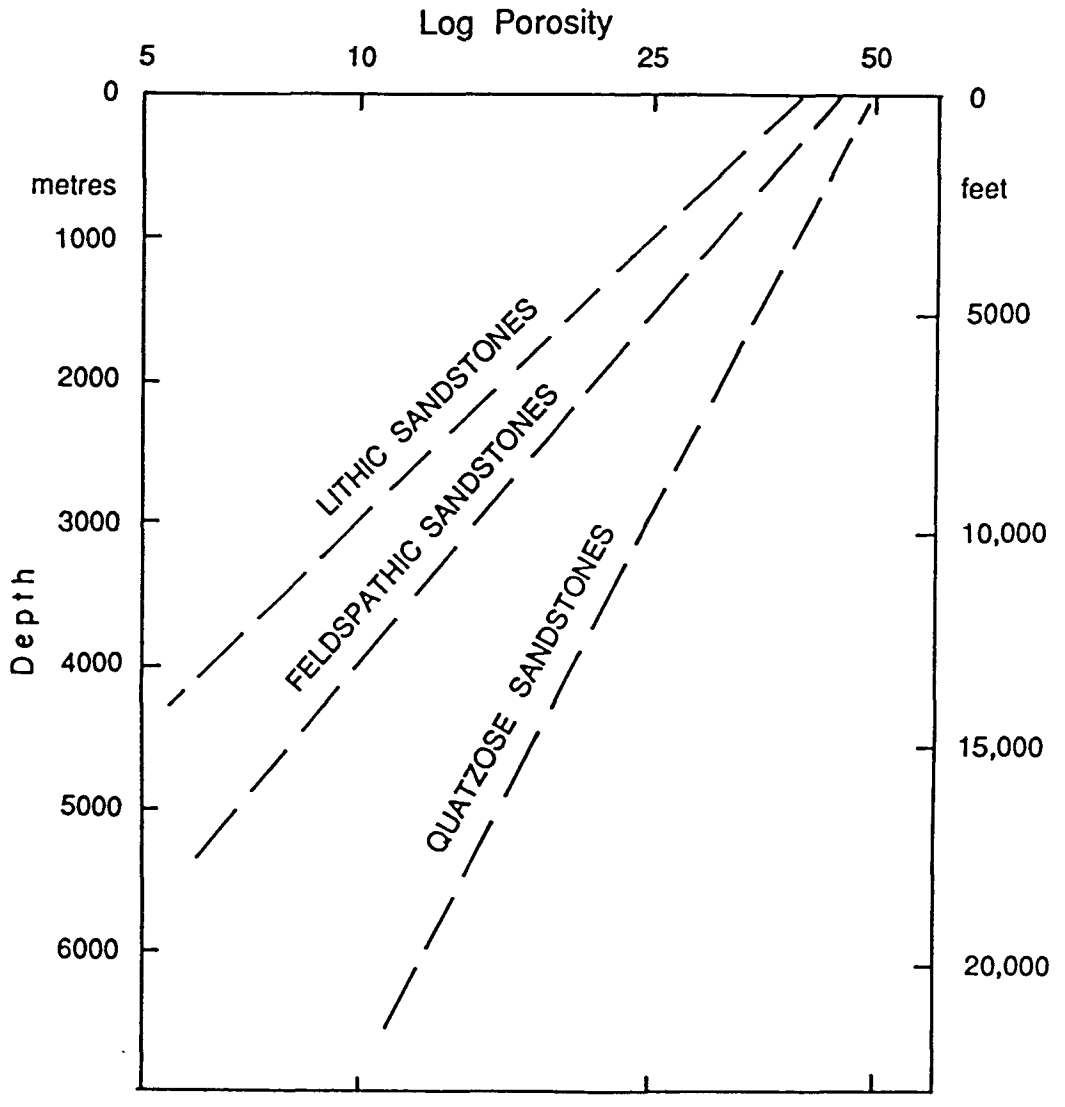

Figure 3.4. Depth - porosity relationship of sandstones with different mineralogic compositions. Redrawn from Dickinson (1985), based on data from Galloway (1974), Zieglar and Spotts (1978), and Sclater and Christie (1980).

Whether the net effect would be a gain or loss of porosity depends upon the relative importance of the three distinct mechanisms - i. e., compaction, cementation and dissolution.

Numerous geologic processes occur in response to the combined effect of temperature and geologic age and it is very difficult to isolate their individual effects. Quantification of the cumulative effect of temperature and geologic age was first attempted by Lopatin (1971) to account for its effect on the maturation of organic matter. Subsequently some workers used this concept outside organic geochemistry in the inorganic domain of clastic diagenesis. Thus Schmoker (1984) applied the concept of time - temperature index (TTI) of Lopatin (1971) to predict porosity at depth:

$$P = a\ (TTI)^b$$

where, P is the porosity at depth, the pre-exponential factor a incorporates all depositional and diagenetic parameters, and the exponent b is independent of rock matrix and may reflect rate-limiting processes of diffusive transport. The Time-Temperature Index (TTI) of Lopatin (1971) may be expressed as follows:

$$TTI = t.\gamma = t.2^n,$$

where t = time factor expressed by the time in My that the particular rock spent in the temperature interval defined by isotherms 10° C apart; γ is the temperature factor which reflects the exponential dependence of organic maturity on temperature; and n = 0 for 100-110° C interval. Schmoker (1984) used this concept for limestone and dolomite but concluded that the method may be equally valid for sandstone.

Subsurface temperature as manifested by geothermal gradient will be determined to a large extent by the tectonic setting of the basin. Thus basin-type will directly or indirectly affect such controlling parameters as geothermal gradient, subsidence/sedimentation rate, depositional

environment and provenance.

Temperature not only affects cementation and dissolution but also compaction. For example, Houseknecht (1984) has shown that pressure solution at comparable depth in finer-grained quartzose sandstone is more pronounced in regions of higher geothermal gradients. This observation has been supported by the experimental data of Sprunt and Nur (1977). No such differences in the style of compaction were, however, observed in the Surat Basin sandstones which may reflect relatively small geographic variation in geothermal gradients over the area from which the samples were derived. But with regard to dissolution of framework grains and cement, this is temperature controlled and therefore is of fundamental importance to the evolution of sandstone porosity in the Surat Basin.

Geologic age

Geologic age is a first-order parameter affecting porosity of the Surat Basin sandstones (see Chapter 6). As mentioned before, time is an important variable in controlling the fate of any physico-chemical environment. Connan (1974) has shown from the Arrhenius equation that after exceeding a certain threshold temperature, the rate of organic maturation increases linearly with time and exponentially with temperature. The rate of dissolution may be expected to display a similar relationship. Likewise the effect of compaction is also believed to be time-dependent (cf. Sprunt and Nur, 1977; Harris, 1987). The negative relationship (cf. Table 6.2) of the sandstone porosity with geologic age in the Surat Basin suggests that in general time- (and temperature-) induced compaction and cementation were more prevalent in controlling sandstone porosity than dissolution.

Depositional environment

The quantitative analysis of sandstone porosity by means of multiple regression analysis in Chapter 6 shows that the genetic character of the depositional environment is one of the predictor variables that affects porosity in the Surat Basin succession. This can be explained in the following manner: firstly, the type of depositional environment influences the texture and composition of the sediments (cf. Davies and Ethridge, 1975) which in turns controls the formation fluid flow behaviour. In the Surat Basin succession fluvial sandstones are prone to be more porous than the 'environmentally wet' lithic sandstones which are deposited in paludal/brakish/paralic/shallow-marine environments (cf. Figure 1.2). Apart from being deposited in fresh water (due either to tectonically elevated land level or eustatically lowered sea-level; cf. Exon and Burger, 1981) fluvial sandstones commonly experience post-depositional flux of vast quantities of meteoric water whereas marine sandstones unless raised relative to sea-level do not generally experience such throughput of freshwater. This is one of the fundamental and inevitable hydrological differences in the histories of the fluvial and marine sandstones. Dissolution by CO_2-charged corrosive pore-waters may be held responsible for the many examples of unusually high porosity reported from terrestrially-deposited labile sandstones (e.g., Hayes et al, 1976; Mathisen, 1984). This process has been the principal agent of secondary porosity development in many stratigraphic units of the Surat Basin (Arditto, 1982, 1983). Another explanation of the statistically negative correlation (at 4% significance level) between porosity and depositional environment (cf. correlation matrix, Table 6.2) is the relatively quartzose nature of the fluvial sandstones compared to their labile counterparts which probably accounted for lesser compactional porosity loss in the former than in the latter.

Detrital mineralogy

The mineralogical composition of the sandstone is one of the critical parameters in determinig porosity upon burial as has been stressed by many investigators (e.g., Griffiths, 1967; Nagtegaal, 1978; Galloway, 1974, 1979; Hayes, 1979; Loucks et al, 1984). Consistent with this it has been found to be one of the important predictor variables of porosity at depth in the Surat Basin sandstones (Chapter 6). Detrital mineralogy affects porosity in a variety of ways. For instance, sandstones containing significant amounts of ductile grains can undergo total loss of porosity as a result of plastic deformation of these grains and their conversion to diagenetic matrix and pseudomatrix (Hawkins and Whetten, 1969; Dickinson, 1970; Rittenhouse, 1971). Moreover, the amount of mechanically and chemically unstable framework grains is important in controlling the rate of compaction. For instance, a plot of thin-section porosity against detrital quartz for the Hutton Sandstone (Figure 3.5) shows that porosity increases at first gradually with increasing quartz content until a threshold value of quartz content of about 50% is reached, above which porosity seems to vary independent of detrital quartz content. The value 50% of detrital quartz is interpreted as the threshold quartz content necessary to provide the rock with a rigid framework sufficient to resist plastic deformation of the ductile grains (cf. Scherer, 1987). It is suggested that the minimum content of detrital quartz necessary to provide a resistant framework could be much lower if the labile components are represented by the mechanically stable (but chemically unstable) feldspars rather than rock-fragments.

Sediment texture

One of the important criteria controlling cementation and dissolution is sediment texture which influences initial porosity and

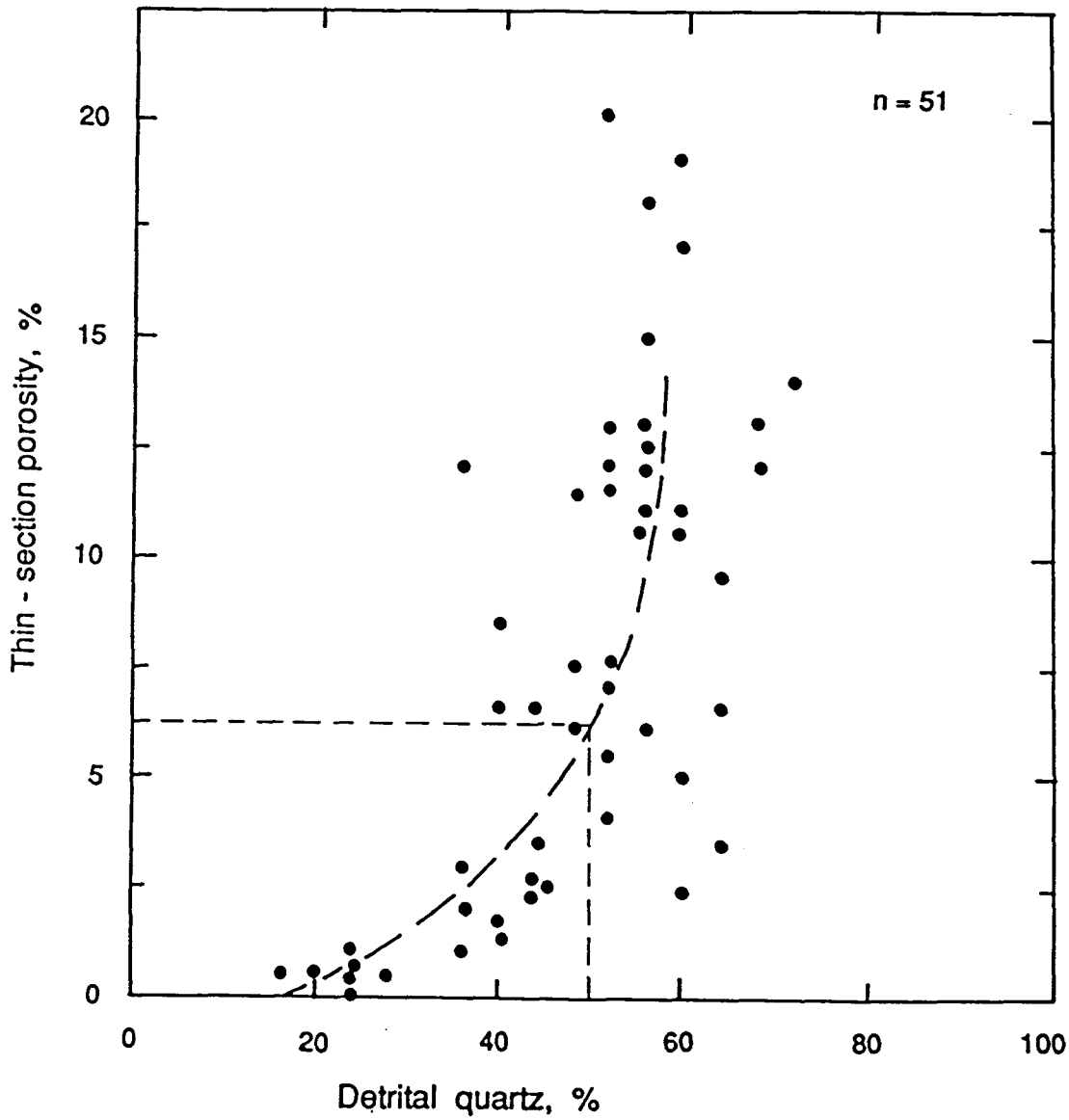

Figure 3.5. Thin-section porosity as a function of detrital quartz content in the Hutton Sandstone. Note that the magnitude of porosity seems to be independent of detrital quartz content beyond a threshold value of approximately 50% quartz.

permeability. Heald (1956) noted that pressure-solution and calcite cementation in sandstones are fabric-selective: finer-grained laminae are characterized by pressure solution whereas coarser-grained laminae by calcite cementation. Houseknecht (1984) came to a similar conclusion. The conclusions of the above workers are based on mature quartzose sandstones. The sandstones of the Surat Basin comprise a vast array of detrital composition encompassing much of the QFR compositional triangle (Chapter 2). Despite this variable mineralogical composition, a statistically significant positive correlation was observed between secondary dissolution porosity and grainsize (i.e., negative correlation with phi grainsize scale) which suggests that, other factors being equal, secondary porosity is likely to be best developed in coarser-grained sandstones (Figure 3.6). Similar relationships have been documented in other basins (e.g., Jonston and Johnson, 1987).

THE EFFECT OF TEMPERATURE ON RESERVOIR QUALITY: AN ALTERNATIVE APPROACH

As has been mentioned before, the effect of temperature has always been portrayed as an impediment to preserving porosity at depth. This conclusion seems rather logical when the increased rate of compaction and cementation that are expected to result from the higher temperature are considered to be the major porosity destroying phenomena. However, several investigators have offered alternative ideas and presented compelling facts and observations in favour of their views: i.e., higher temperature can be conducive to better hydrocarbon potential by way of preserving higher porosity. For example, Halbouty et al (1970) in their study of the formation of the giant oil and gas fields recognised that higher-than-normal geothermal gradients accounted for better efficiency of hydrocarbon generation from source rocks in basins such as the PreCaucasus, Los Angeles and Central Sumatra. Klemme (1972, 1975) has shown that yield of

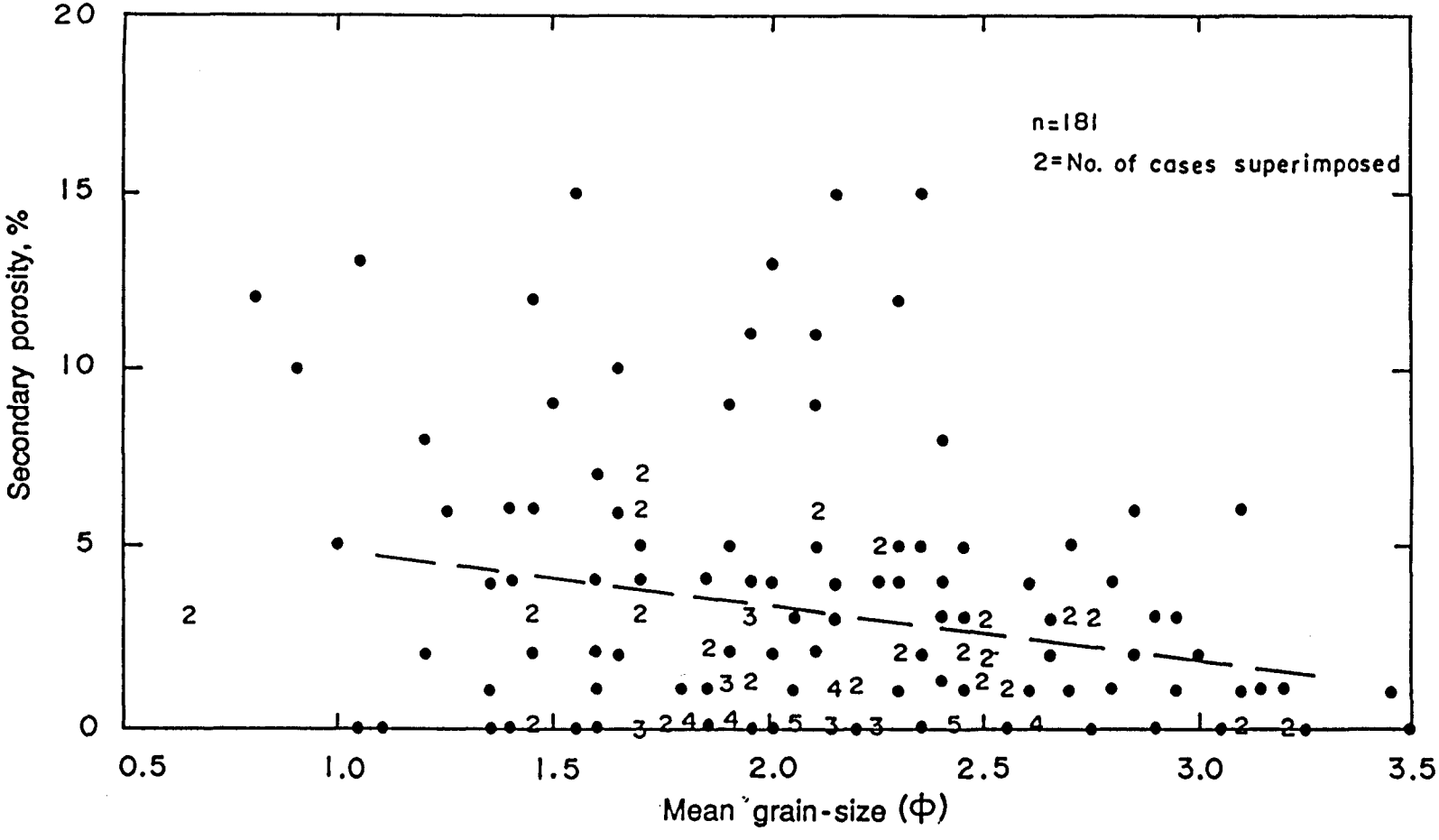

Figure 3.6. Relationship between the occurrence of secondary dissolution porosity and grainsize (phi units) of the Surat Basin sandstones (all formations). Note the statistically significant negative correlation. The regression line is computed. r = -0.24, sig. = 0.0009.

hydrocarbon per volume of sediment is higher in basins of high heat flow (geothermal gradient) than those of low heat flow. The effect was greatest for intermediate crustal zone basins that occupied the transitional area between continental and oceanic crusts. Klemme (1972) also made the interesting observation that in clastic sediments of high geothermal gradient the reservoir accumulation will be larger than those with low geothermal gradient because the average porosity is greater at depths equivalent to comparable temperatures. The relationship is shown in Figure 3.7. For example, at a gradient of 5.5°C/100 m, a sandstone at 120°C will have 38% porosity. In an area with a gradient 2.5° C/100 m the 120°C isotherm will be attained at a much greater depth (4000 m) where the average sandstone porosity will be 26%. What Klemme (1972) did not take into account however is that sandstone porosity is a factor of detrital mineralogy which is determined to a large extent by the tectonic setting. Tectonic setting in turn exerts a first-order control on geothermal gradient and generally basins with higher geothermal gradients are characterized by labile sandstone suites (i.e., arc-related or rift basins). Klemme (1972) argues that with the exponential effect of temperature on chemical reaction rate in the formation of hydrocarbons and the greater mobility of water expulsion from shales in basins with higher geothermal gradient (as opposed to linear or near-linear decrease of reservoir porosity with depth), it is apparent that a high geothermal gradient facilitates the early formation of oil at a relatively shallow depth. Klemme (1972) also pointed out that, trapping mechanism being similar, theoretically a high geothermal gradient might result in more than double the hydrocarbon accumulation than in areas of low thermal gradients, due not only to reservoir porosity but due also to the decrease in viscosity of the generated hydrocarbon, increase in fluid pressures and

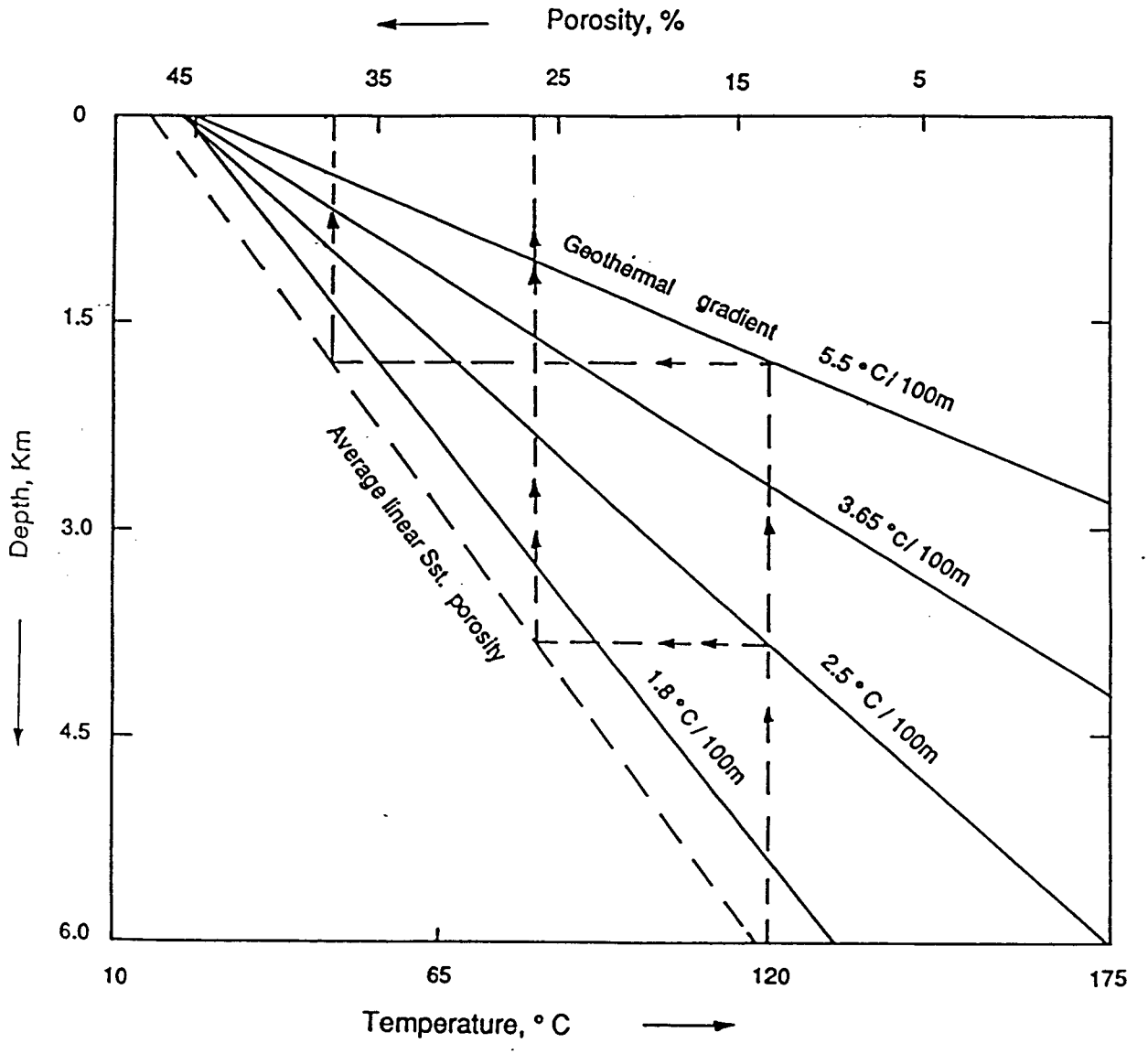

Figure 3.7. Relationship between geothermal gradient and sandstone porosity. Simplified from Klemme (1972). The porosity of a sandstone at a depth equivalent to 120° C with a geothermal of 5.5°C/100 m is 38%, whereas at the same temperature (i.e., 120°C) but experiencing a lower geothermal gradient, for example 2.5°C/100 m, the sandstone will have 26% porosity (cf. dashed pathways in diagram).

higher permeability in the carrier beds (i.e., much better migrational efficiency, a parameter difficult to quantify, cf. Dow, 1977). Also, Halbouty et al (1970) argue that a high geothermal gradient probably accounts for the better efficiency of hydrocarbon generation from source rocks in certain basins, such as the PreCausasus, Los Angeles and the Central Sumatra back-arc basin. In these 'active' basins sufficiently high temperature is reached at shallow depth and the hydrocarbon is enabled to migrate into sandstone reservoirs before greater depth of burial has reduced the porosity by cementation. As the Surat Basin is a retro-arc foreland basin high palaeoheat flow may be assumed for the magmatic arc and back-arc basin. This assumption is substantiated by the study of heat flow patterns in analogous modern arc-related basins. For example, Pigott (1985) reports that the geothermal gradient of the Sumatran fore-arc Basin averages 2.4° C/100 m and in the volcanic arc more than 20° C/100 m and decreasing gradually cratonward. In the central Sumatran back-arc basin it averages 6.01° C/100 m whereas in the Malyasian sector of the Sundaland craton it decreases to 4.8°C/100 m. The above approach of associating better hydrocarbon potential with relatively high geothermal gradient is contrary to the idea put forward by Galloway (1974, 1979) who attributed rapid porosity loss of compositionally immature sandstones in arc-related basins to high geothermal gradients. What Galloway (1974, 1979) has not taken into consideration is that the high geothermal gradient would likewise give rise to a shallower hydrocarbon kitchen and the higher porosity gradient will be greatly offset by early and shallow emplacement of hydrocarbons as schematically shown in Figure 3.8. If additionally products of organic maturation are taken as viable agents of secondary porosity development as discussed in a following section, the arguments and observations of Klemme (1972, 1975) become more compelling.

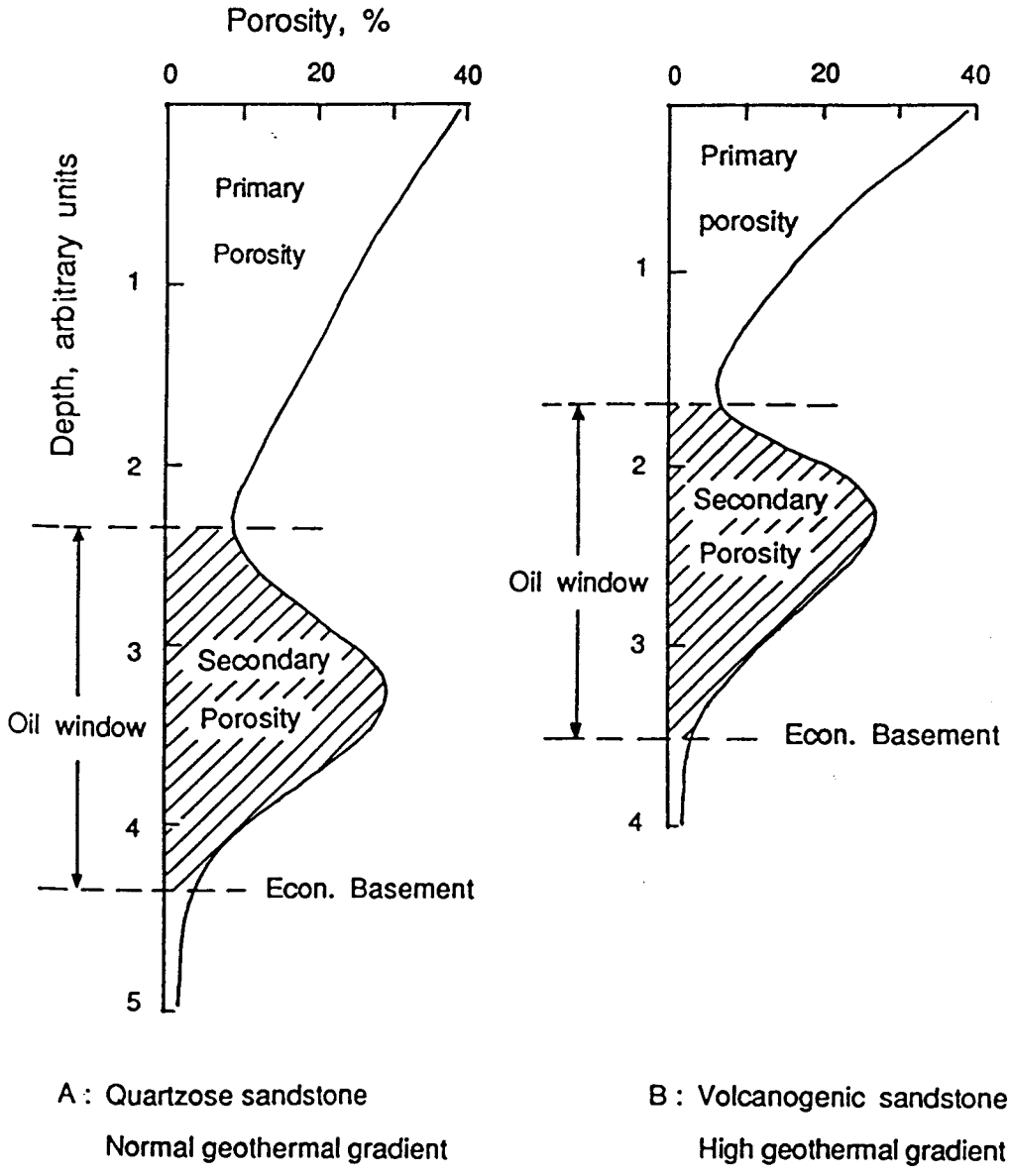

Figure 3.8. Schematic diagram showing the geologic evolution of porosity in sandstones with contrasting detrital composition. The varying depth of the oil window and the maximum zone of secondary porosity development as functions of sandstone mineralogy and geothermal gradient control the depth of economic basement. See text for explanation.

DIAGENETIC PROCESSES

The relative importance of compaction and cementation

Compaction and cementation are two diagenetic processes which invariably destroy porosity at depth. While porosity loss by the former process is most commonly irreversible, porosity loss by the latter, depending on the mineralogy of the cementing phase, may subsequently be reveresed (by decementation) under suitable geochemical conditions. This is explained by the fact that compaction destroys intergranular volume while cementation occludes but does not reduce it; later dissolution/decementation can restore/enhance intergranular porosity. Compaction takes place in response to overburden pressure and depends on the pore-fluid pressure (Figure 3.2). While lower hydrostatic pore pressures cause maximum grain-to-grain pressure (i.e., lithostatic pressure), overpressuring reduces it thus preventing porosity loss by compaction and facilitating preservation of high porosity. Higher grain pressure not only induces inelastic pore collapse and ductile deformation but also chemical compaction (pressure solution) at grain contacts. The amount of the latter, however, would be more pronounced in mineralogically mature quartzose sandstones. Ductile deformation is the most widespread compactional phenomenon in labile sandstones. Both pressure solution and ductile deformation are found to be relatively minor in the Surat Basin sandstones which is consistent with the comparatively shallow burial depth (up to 1225 m). Pressure solution and ductile deformation become important below a burial depth of 1000-1500 m above which mechanical compaction (mainly packing rearrangement) is believed to be prevalent (Füchtbauer, 1967, 1974). Ductile deformation above such depths is minor.

At the depositional surface a well-sorted sandstone has several thousand millidarcies of permeability and an initial porosity ranging from

Figure 3.9. Thin-section photomicrographs illustrating ductile deformation of soft framework grains.

A: A leached biotite grain 'flares' out both as a result of having been compressed between two adjacent rigid grains and through volume increase of the 'flames' due to leaching and alteration. Orallo Formation, GSQ Roma 8/20, depth - 306.38 m. Plane light.

B: A volcanic rock-fragment squeezed between two rigid grains. Orallo Formation, GSQ Roma 8/13, depth - 232.10 m. Crossed polars.

A

0.1 mm

B

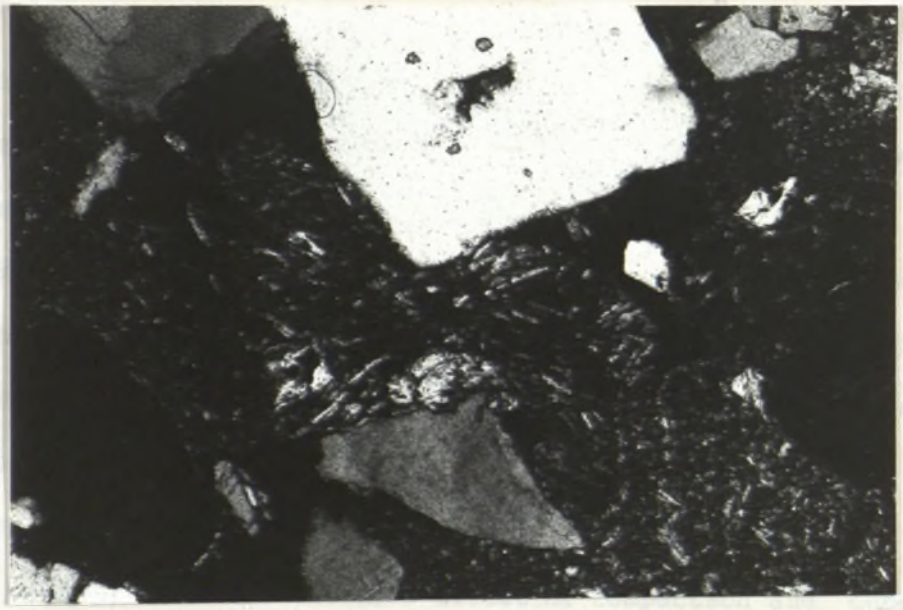

0.1 mm

17 tO 52% with an average of 41% depending on the depositional environments (Pryor, 1973). Porosities of Holocene barrier-island sand samples measured by Beard and Weyl (1973) range from 40 to 45% while porosities of unconsolidated sands from various modern environments measured by Fraser (1935) range from 35-45%. Initial depositional porosity of sand is essentially a function of grain packing which theoretically can vary from 26% having the tightest (i.e., rhombohedral) to 40% with the loosest (i.e., cubic) packing (Graton and Fraser, 1935). In nature, however, these extreme packing configurations rarely occur (Beard and Weyl, 1973; Pryor, 1973). But theoretically a sand deposited with an initial porosity of 40% can reduce its primary porosity to 26% by mechanical compaction alone (i.e., through packing rearrangements) which is believed to be significant down to burial depths of 1000-1500 m (Füchtbauer, ibid.), although to some extent both mechanical compaction and pressure solution go hand in hand. Füchtbauer (1967) has shown how small amounts of pressure solution can remove the corners of grains and allow them to slide past each other to assume a tighter packing thereby reducing porosity. However, pressure solution in quartzose sandstone is also grainsize controlled and is more pronounced in the finer-grained varieties which Füchtbauer (ibid.) explained in terms of the increased number of contacts per grain with decreasing size. Figures 3.9A-B and 3.13C respectively show some examples of plastic deformation and pressure solution observed in the Surat Basin sandstones. Early cementation under certain circumstances can locally 'freeze' the grain packing of sandstone bodies and thus halt these intergranular-volume-reducing processes (cf. Figure 3.12F).

To evaluate the relative effect of compaction and cementation in reducing intergranular (primary) porosity, Houseknecht (1987) advocated a plot of minus-cement porosity (term explained in text later) against total authigenic cement (Figures 3.10 and 3.11). Although Houseknecht (1987)

Figure 3.10. Plot of minus-cement porosity against total diagenetic cement. Note that both the horizontal and vertical scales here and in Figure 3.11 terminate at 40%. Note also the general importance of compaction over cementation. Plot construction after Houseknecht (1987). Data from all formations, Surat Basin.

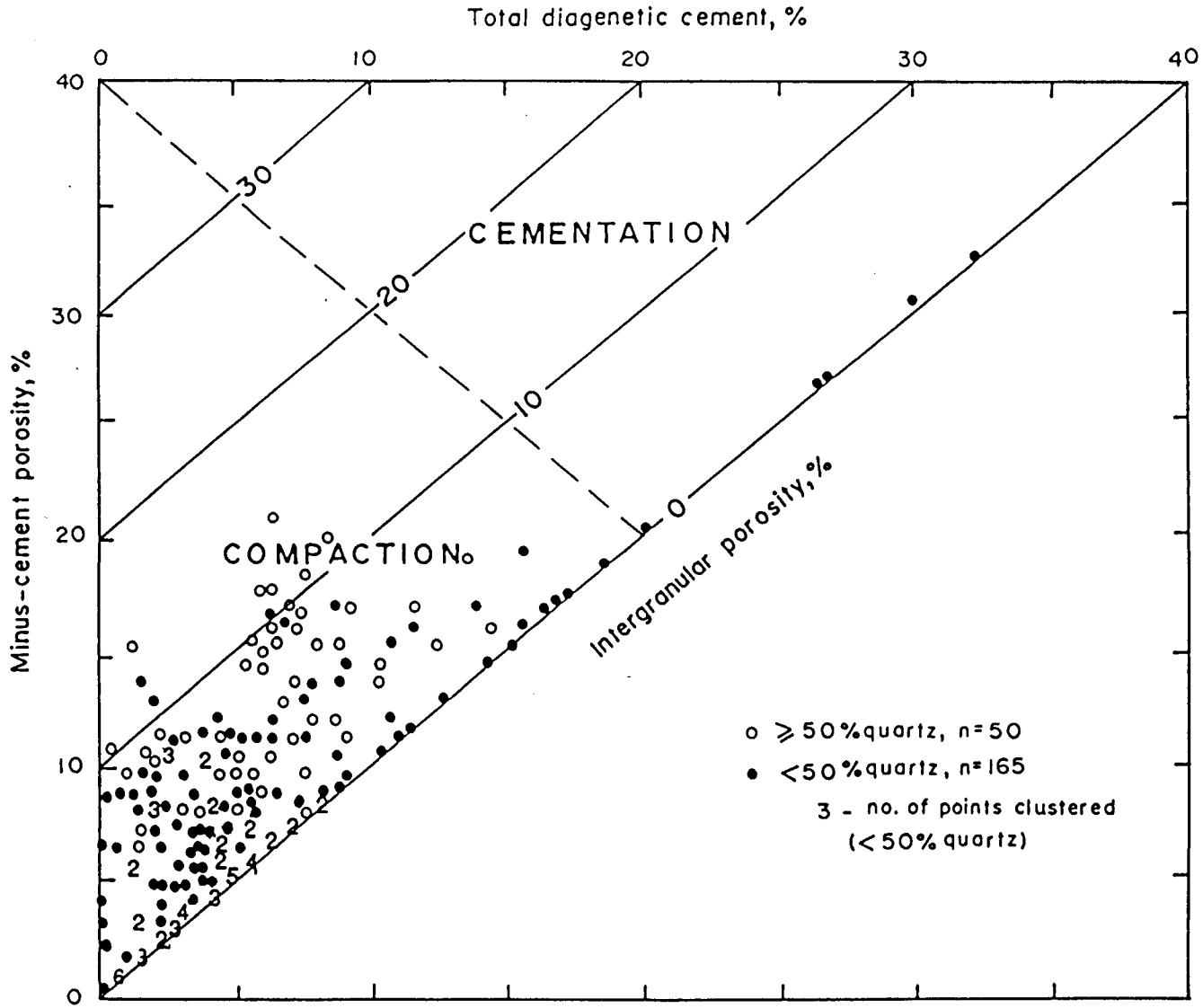
Total diagenetic cement, %
0
10
20
30
40
Minus-cement porosity, %
CEMENTATION
30
20
10
0
COMPACTION
Intergranular porosity, %
○ ≥ 50% quartz, n = 50
● < 50% quartz, n = 165
3 - no. of points clustered
(< 50% quartz)

Figure 3.11. Plot of minus-cement porosity against total diagenetic cement for the Evergreen Formation and Hutton Sandstone. Note the different degree of compaction of the two sandstone suites of contrasting detrital composition. See text for explanation. Plot construction after Houseknecht (1987).

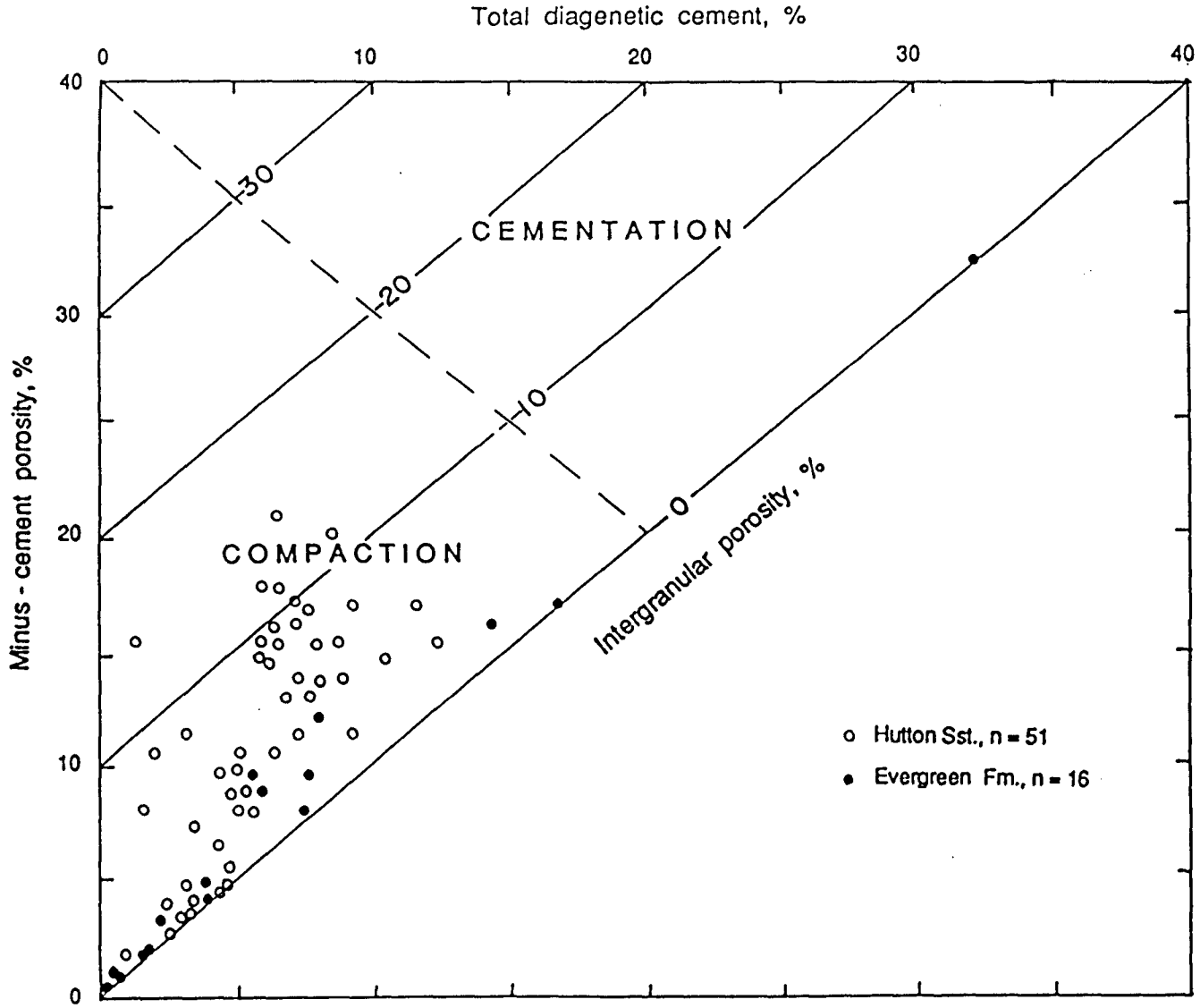
Total diagenetic cement, %
0
10
20
30
40
Minus - cement porosity, %
-30
-20
-10
0
CEMENTATION
COMPACTION
Intergranular porosity, %
Hutton Sst., n = 51
Evergreen Fm., n = 16

used this technique for mature quatzose sandstone, the writer believes that it is applicable to feldspathic and lithic sandstones as well as long as the degree of plastic/ductile deformation is relatively minor which is the case with the Surat Basin sandstones examined in the present work. Minus-cement porosity is a term first coined by Rosenfield (1949) to account for the loss of primary porosity due to compaction. It is the porosity which would exist if the specimen contained no cement and is the sum of the present intergranular porosity and the chemically precipitated intergranular cement. The term is synonymous with intergranular volume of Weller (1959) and pre-cement porosity of McBride et al (1987). Samples which have undergone significant compaction will plot in the compactional domain which is separated from the cementation domain by a diagonal line as shown in Figures 3.10 and 3.11. Minus-cement porosity is here calculated by adding total diagenetic cement to thin-section porosity (excluding fracture porosity) minus secondary dissolution porosity. Likewise, cements comprise all varieties including the grain-replacive category, the latter being of minor volumetric importance in any formation. Although this is a rather simplistic approach (due to the fact that some intergranular porosity could well be of secondary origin, but in the absence of any diagnostic criteria was tallied as intergranular primary porosity), the method is quick for plotting a large number of samples and for comparative purposes is found to be satisfactory. Diagenetic cements here represent quartz, carbonate, zeolite etc. and phyllosilicate cement and epimatrix (cf. Appendix 1.1). In the Surat Basin sandstones compaction seems to be more important than cementation in destroying primary porosity as can be seen from the plots of minus-cement porosity vs. total diagenetic cement (Figures 3.10 and 3.11). Furthermore, the distribution of many authigenic cements is patchy in these rocks. Certain types of cement such

as quartz (either as syntaxial overgrowth or as microcrystalline pore-filling druzy aggregates) and to some extent certain clay minerals destroy porosity almost irreversibly, whereas carbonates and zeolites are potential candidates for future dissolution under favourable geochemical environments. In Figure 3.10 sandstones with different quartz contents are plotted to show their different compactional behaviour. Despite the wide range of depth from which the samples are derived (i.e., from 17 to 1225 m) it clearly shows that the loss of primary porosity due to compaction in quartzose sandstone is less severe than in labile sandstones. This is further and more clearly illustrated by the contrasting compactional behaviour of the Hutton Sandstone and the Evergreen Formation (Figure 3.11). The more quartzose Hutton Sandstone has been compacted less severely than the Evergreen Formation sandstones which are more lihic-rich than the former (cf. Figure 2.3).

Dissolution and Cementation

Dissolution and cementation can be regarded as chemical processes the extent of which depends upon the time - temperature integral of the sediment body (cf. Siever, 1983). Whether a particular phase will be precipitated or dissolved depends upon the chemistry of the formation water, its Eh, PH and total dissolved contents. With geologic age formation water becomes saturated with dissolved chemical species and precipitation of minerals takes place, thus destroying porosity. This is one of the reasons why there is a general tendency of decreasing porosity with geologic age as observed in the Surat Basin clastics (cf. Table 6.2) and in other areas by numerous workers (Maxwell, 1964; Roll, 1974; Schmoker, 1984; Siever, 1983; Scherer, 1987). However, change in hydrogeologic regime (be it compactional, thermobaric or meteoric), products of organic maturation and change in clay-mineral composition

(e.g., illitization of smectite) in the intercalated mudrocks can drastically alter the pore-water chemistry leading to the dissolution of framework grains and/or previously deposited cements. On the other hand new mineral species can be precipitated, clogging pore space. Deviation from the normal porosity - depth relationship reflects such changes in geochemical environment in the evolutionary history of a body of sediment.

DIAGENETIC MINERALS

The major diagenetic minerals present in the Surat Basin sandstones are shown in Figure 4.1. There is a distinct stratigraphic association of the occurrence of diagenetic minerals - e.g., the quartzose sandstones are characterized by kaolinite and quartz overgrowth (e.g., Precipice and Hutton Sandstones) whereas the more labile sandstones contain montmorillonite, mixed-layer montmorillonite-illite, nontronite, zeolite and kaolinite. Minor authigenic feldspar was also noticed in some formations. All of the cockscomb skeletal feldspars[1] (Figures 3.12A and B) upon electron microprobing are found to be composed of pure albite (Appendix 2.1). Their delicate shape observed under the SEM (Figures 3.12C and D) and pure albitic composition is suggestive of their authigenic origin (Pettijohn et al, 1972, p. 429). Minor authigenic albite in the form of optically clear and continuous overgrowth is also observed in some formations (e.g., Hutton Sandstone). Authigenic carbonates occur sporadically throughout the Surat Basin succession; they are represented mainly by calcite although some ferroan calcite and dolomite are also present. Siderite is not uncommon (Figure 3.12G) and is generally

[1] The other kind of skeletal feldspar is the corroded zoned plagioclase in formations rich in volcanic detritus (cf. Chapter 2). They result from the selective dissolution of the more calcic cores leaving the relatively sodic outer rims intact. These feldspars are represented mostly by andesine.

Figure 3.12. Varieties of skeletal feldspar (A-D) and carbonate ement (E-G).

A: Thin-section photomicrograph of 'corroded' (upper-left) and 'cockscomb' (bottom-left and bottom-right) skeletal feldspars. The corroded feldspar grain presumably is the result of preferential dissolution of the more calcic core of a zoned volcanogenic andesine. The cockscomb feldspar was formed due to leaching along cleavage traces. Note also good intergranular porosity. Orallo Formation, GSQ Roma 8/14, depth - 242.88 m. Crossed polars.

B: High magnification view of a cockscomb skeletal feldspar. Note the characteristic fresh nature and the white birefringence of the remnants. The same sample as above. Crossed polars.

C and D: SEM photomicrographs of cockscomb skeletal feldspar grains similar to those illustrated in Figure 3.12A and B. Note the delicate shape and well-developed subcrystal boundaries which suggest later healing by authigenic feldspar after initial dissolution. Authigenic chlorite rosettes surround and partially engulf the feldspar grain in D. C - Mooga Sandstone, GSQ Roma 8/5, depth - 135.69 m. D - Hutton Sandstone, GSQ Roma 8/52, depth - 782.78 m.

E-G: Thin-section photomicrographs showing different aspects of carbonate cement. Plane light.
E: Grain-replacive (centre) poikilotopic ferroan calcite. Bungil Formation, GSQ Surat 1/18, depth - 351.05 m.

F: Diagenetic 'freezing' by pore-filling poikilotopic ferroan calcite cement. The sample has a high minus-cement porosity (26.7%) and almost no permeability. Griman Creek Formation, GSQ Surat 3/18, depth - 227.80 m.

G: Pore-filling siderite in the Precipice Sandstone. This kind of cement is acid-sensitive and acidizing (either by HCl or HF) may lead to precipitation of $Fe(OH)_3$ gel or CaF_2 (i.e., in the presence of Ca ions in solid substitution for Fe in the mineral siderite, $FeCO_3$), clogging pore-space and reducing permeability instead of increasing it. GSQ Chinchilla 4/44, depth - 1217.09 m.

A

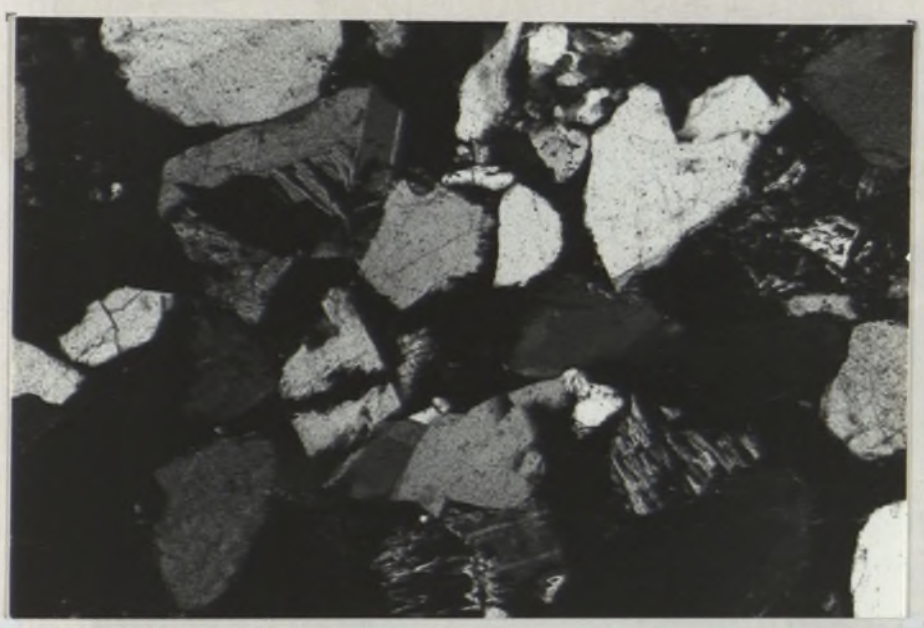

0·1 mm

B

0·1 mm

C

D

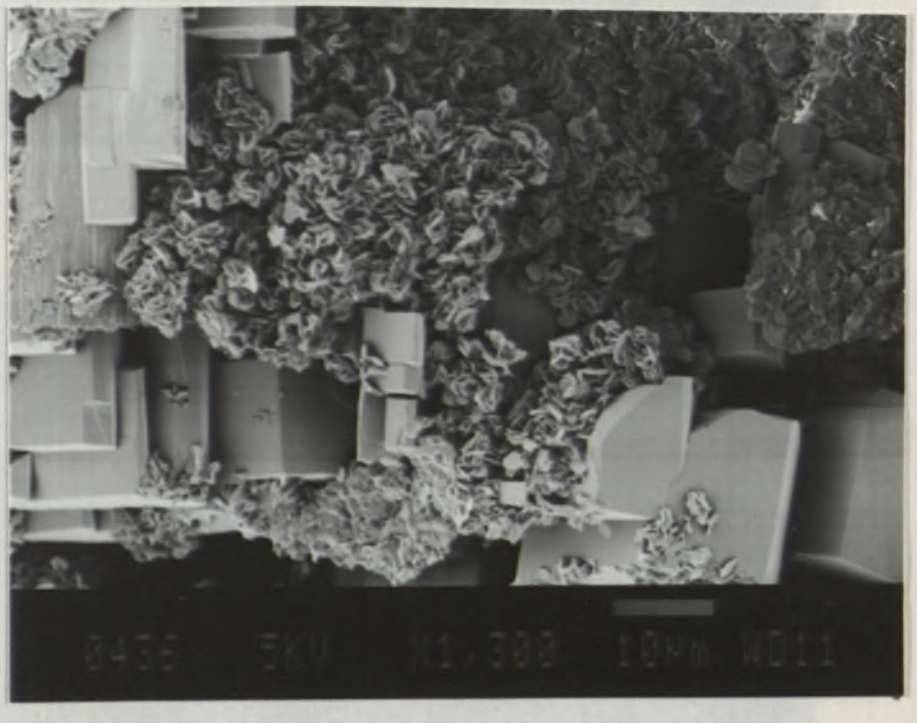

E

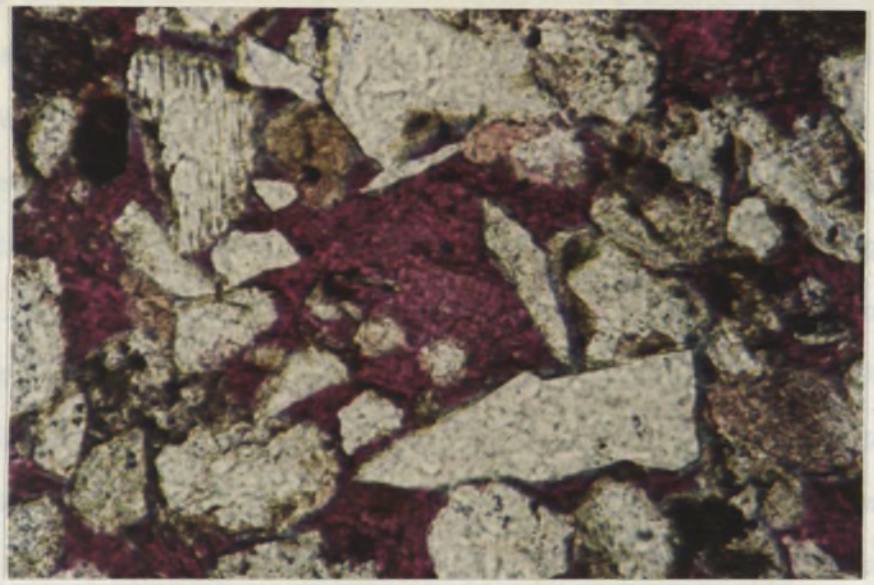

0.1 mm

F

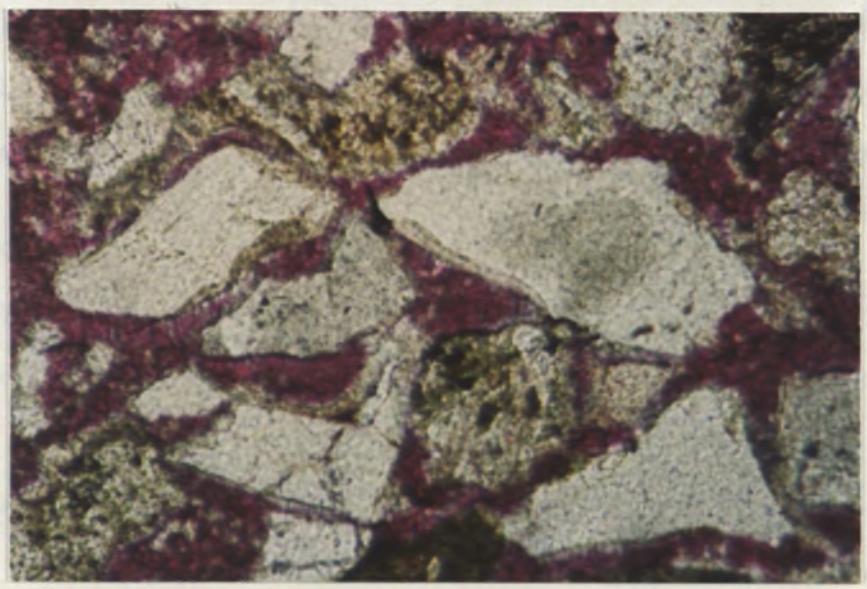

0.1 mm

G

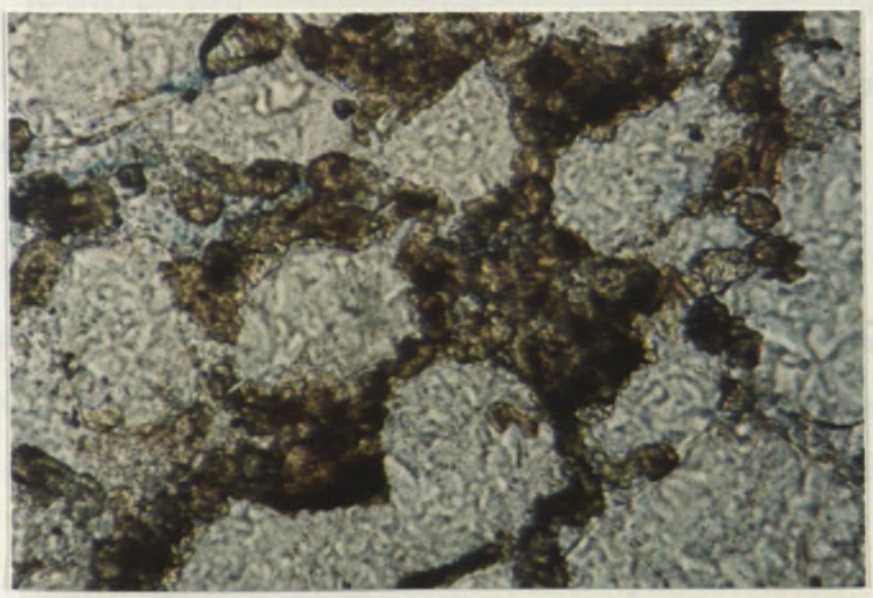

0.1 mm

associated with samples rich in argillaceous fragments. Carbonates occur as pore-filling and grain-replacive varieties (Figures 3.12E and F). Some feldspar grains and rock-fragments are found to be preferentially replaced by carbonates, in some cases beyond original grain-type recognition (Figure 3.12E). Retention of former grain outlines (dust lines), ghost remnants of cleavage traces and insoluble residue help or permit identification of the mineralogical or genetic nature of the replaced or partly replaced grains. Feldspar grains were observed to be attacked preferentially along cleavage traces which facilitated fluid contact by exposing larger surface areas. Cleavage and twin planes are the areas of highest surface energy (Hurst, 1981) and are likely to be attacked preferentially. Corrosion of quartz grains by carbonates was also noticed in some samples. A brief description of the mode of occurrence of the common diagenetic minerals follows.

Silica cement

Two forms of authigenic quartz cement were observed in the Surat Basin succession: one in the form of syntaxial overgrowth around detrital quartz grains (Figures 3.13C-D and 3.20A-D) and the other as pore-filling and less commonly grain-replacive microcrystalline aggregates of druzy quartz ranging in size from 5 to 20 um (Figures 3.13B, H and I). The volumetric importance of the latter variety, however, is not significant.

All relatively quartz-rich sandstones are to some extent characterized by the presence of quartz overgrowth. The degree of quartz cementation is more pronounced in the Precipice Sandstone than in the Hutton Sandstone while the Gubberamunda Sandstone has less than both of these - a trend that follows the degree of their respective compositional maturity (cf. Figure 2.3). The general absence of syntaxial quartz overgrowth in the labile sandstones may suggest that the detrital quartz grains of the quartzose facies themselves provide the source of silica to

be deposited within pore spaces of the same rock unit. This observation may help resolve the enigma of the source of the silica (as opposed to other possible sources such as feldspar dissolution, shale dewatering, transformation of smectite to illite etc., cf. Blatt, 1979). It has also been observed that, other factors being equal, syntaxial quartz overgrowth is more pronounced in the coarser-grained sandstones than in the finer-grained ones. The development and amount of authigenic quartz (if any) in the latter may be offset by their proneness to pressure solution, an observation consistent with the findings of Heald (1956), Fuchtbauer (1967) and Houseknecht (1984).

Silica cementation in the form of syntaxial quartz overgrowths has been found to be arrested in some formations where thick clay-coatings are present on the detrital quartz grains (Figures 3.13A and F). However, overgrowths were not completely prevented due presumably to the fact that small uncoated areas can act as a nucleation sites and subsequent lateral grain-margin-parallel growth can completely engulf the detrital grain boundaries giving the common appearance of dust rims/clay-coats commonly visible under the petrographic microscope (Figures 3.13 D, E and J). The concept of a critical nucleation percentage of clay in a sandstone necessary to prevent quartz overgrowth as suggested by Almon (1981, p. 206) generally holds true only for a variety of authigenic silica cementation, i.e., syntaxial overgrowth. Likewise the idea put forward by some workers (e.g., Pittman and Lumsden, 1968; Heald and Laresee, 1974; Tillman and Almon, 1979) that a thick clay-coat can prevent quartz overgowth or more generally silica cementation (and thereby preserve high porosity) is not wholly supported by the present study. In many Surat Basin sandstones clay-coats have retarded quartz overgrowth but have not prevented it as can be seen in the quartzose petrofacies (Figures 3.13D, E and J). On the other

Figure 3.13. Thin-section and SEM photomicrographs showing various aspects of silica cementation.

A: Thin-section photomicrograph showing absence of quartz overgrowths due to thick clay-coating around the detrital quartz grains. Hutton Sandstone, GSQ Roma 8/52, depth - 782.78 m. Plane light.

B: Thin-section photomicrograph of intergranular microcrystalline quartz. The detrital grains in this sample are coated with smectite-illite clays (best seen under the SEM), and silica cement was subsequently deposited in the form of druzy quartz rather than syntaxial overgrowth. See text for explanation. Hutton Sandstone, GSQ Roma 8/65, depth - 926.03 m. Crossed polars.

C: Concomitant pressure solution and quartz overgrowth cementation resulting in an apparently welded texture. Evergreen Formation, GSQ Mitchell 2/59, depth - 853.86 m. Crossed polars.

D and E: Thin-section photomicrographs of syntaxial quartz overgrowth in the Hutton Sandstone. Note the 'dust-rims' which presumably are discontinuous in 3-dimensions. D - GSQ Mitchell 2/47, depth - 725.86 m, Crossed polars. E - GSQ Roma 8/65, depth - 926.03 m, Plane light.

F: SEM photomicrograph showing selective quartz overgrowth formation on those parts of detrital quartz grains where clay-coat is absent. Evergreen Formation, GSQ Chinchilla 4/31, depth - 965.36 m.

G: SEM photomicrograph showing varieties of silica cementation: in the form of syntaxial overgrowth on detrital quartz grains that lack clay-coatings, and as authigenic microcrystalline clusters of druzy quartz apparently without any seed crystals (centre-right). Siliceous debris probably acted as nucleation sites for the druzy quartz crystals which appear to have grwon on or within a substrate of rosettes of authigenic chlorite. Evergreen Formation, GSQ Chinchilla 4/31, depth - 965.36 m.

H and I: SEM photomicrographs showing druzy quartz crystals within a dissolution pore (H) and intergranular pores (I). Note also the pore-lining smectite which was formed prior to silica precipitation. Evergreen Formation, GSQ Chinchilla 4/36, depth - 1055.77 m.

J: SEM photomicrograph of quartz overgrowths. Imperfections in chlorite clay-coating on detrital quartz grain has led to numerous separate optically continuous outgrowths (as distinct from overgrowth; cf. McBrdie et al, 1987) of microcrystalline quartz (note uniform orientation of the crystals). Subsequent sideways growth of the outgrowths can engulf the clay-coat and lead to development of a continuous overgrowth through lateral coalescence of the outgrowth crystals. This would give the clay-coat the appearance of a dust line commonly discernible under petrographic microscope. Hutton Sandstone, GSQ Roma 8/48, depth - 734.55 m.

K: SEM photomicrograph showing loosely spaced microcrystalline quartz on a detrital grain. These druzy quartz crystals with random crystallographic orientations probably are not connected to the grain on which they sit (in contrast to J) and constitute a common form of silica cementation in quartz-poor stratigraphic units. Evergreen Formation, GSQ Chinchilla 4/31, depth - 426.81 m.

A

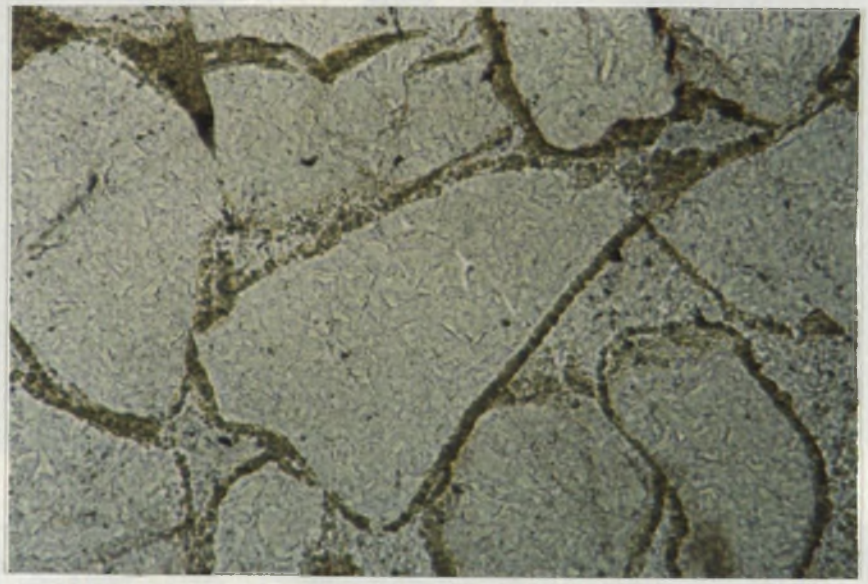

0.1 mm

B

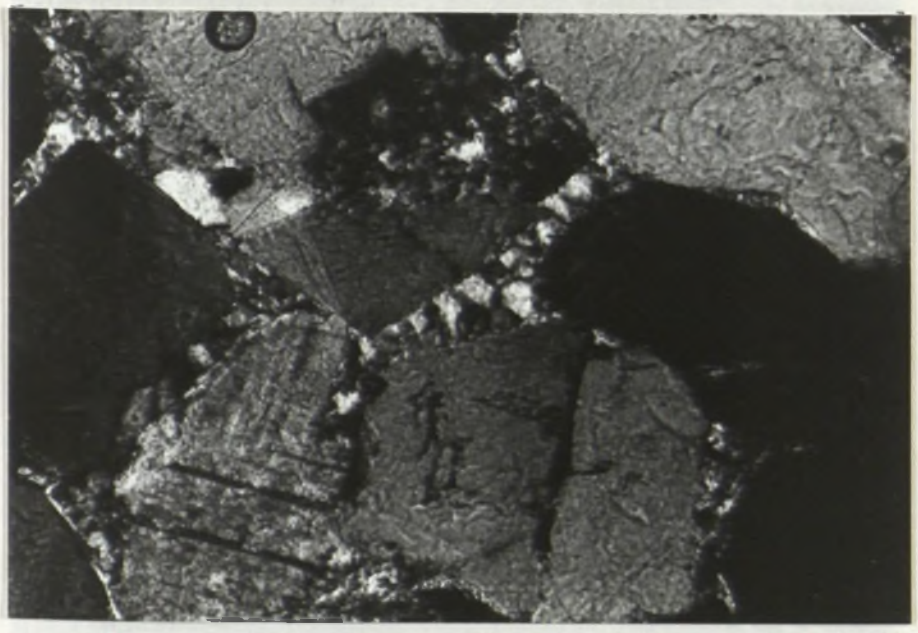

0.1 mm

C

0.1 mm

D

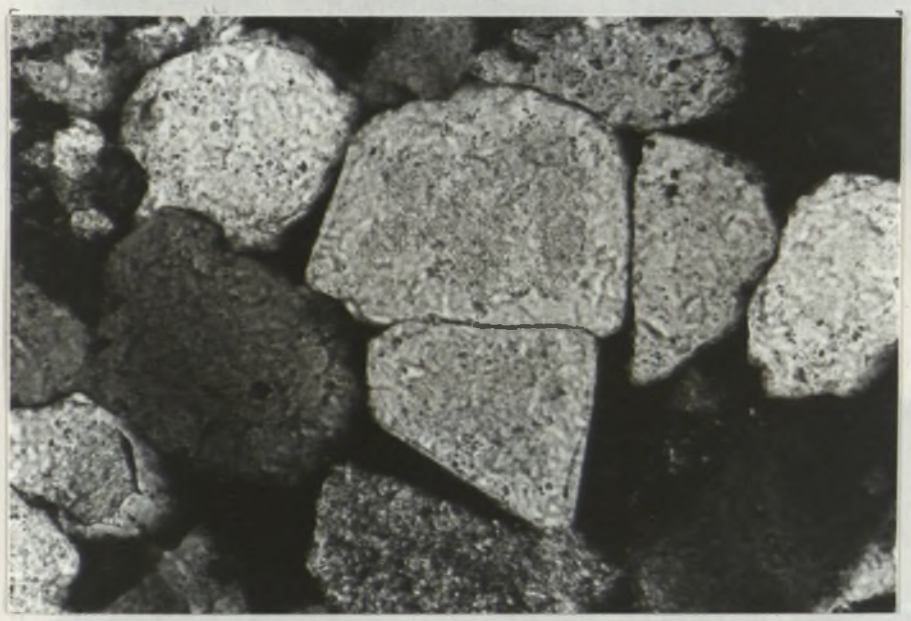

0.1 mm

E

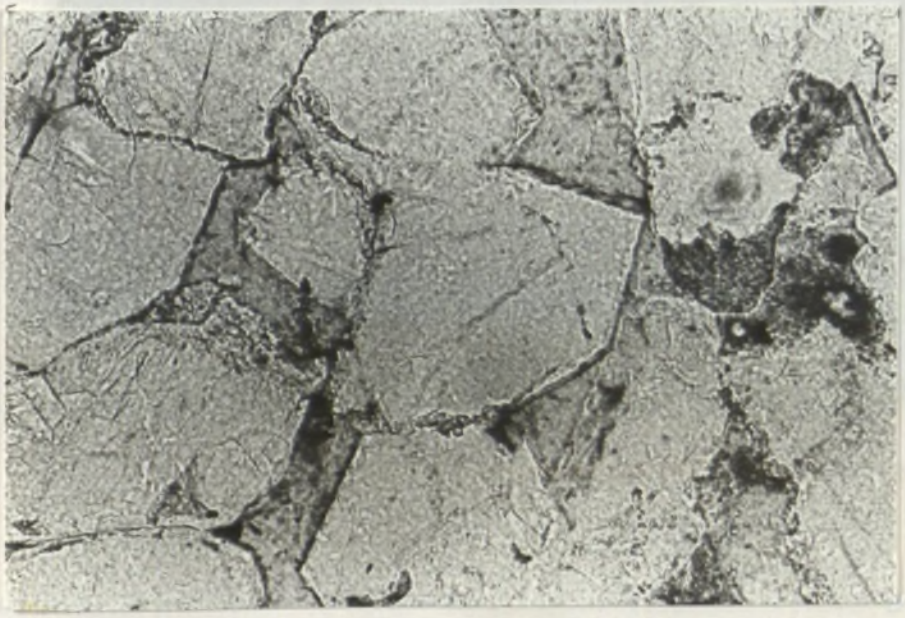

0.1 mm

F

G

H

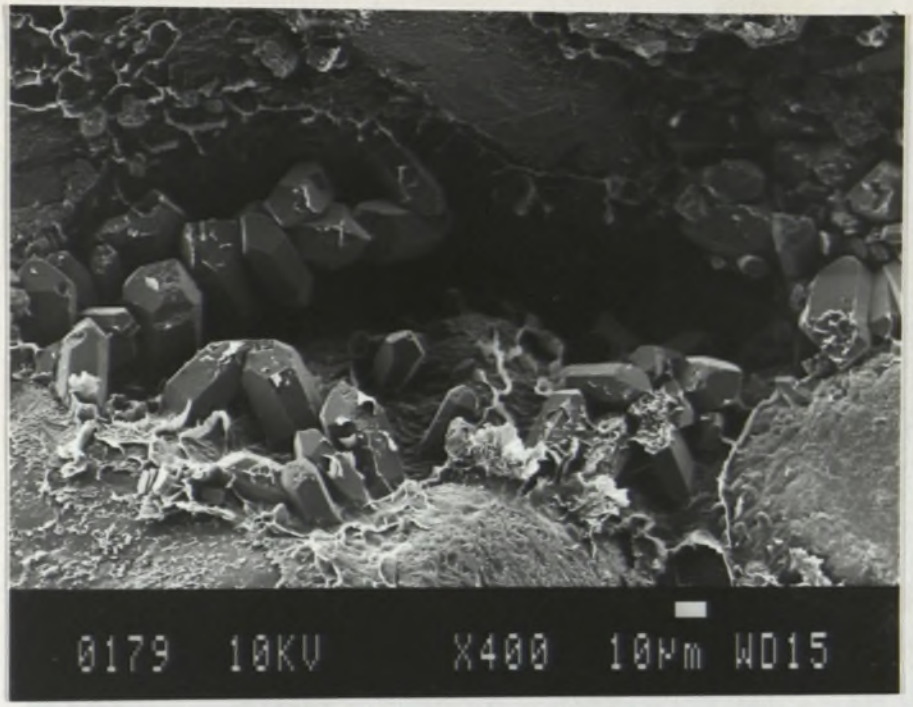

I

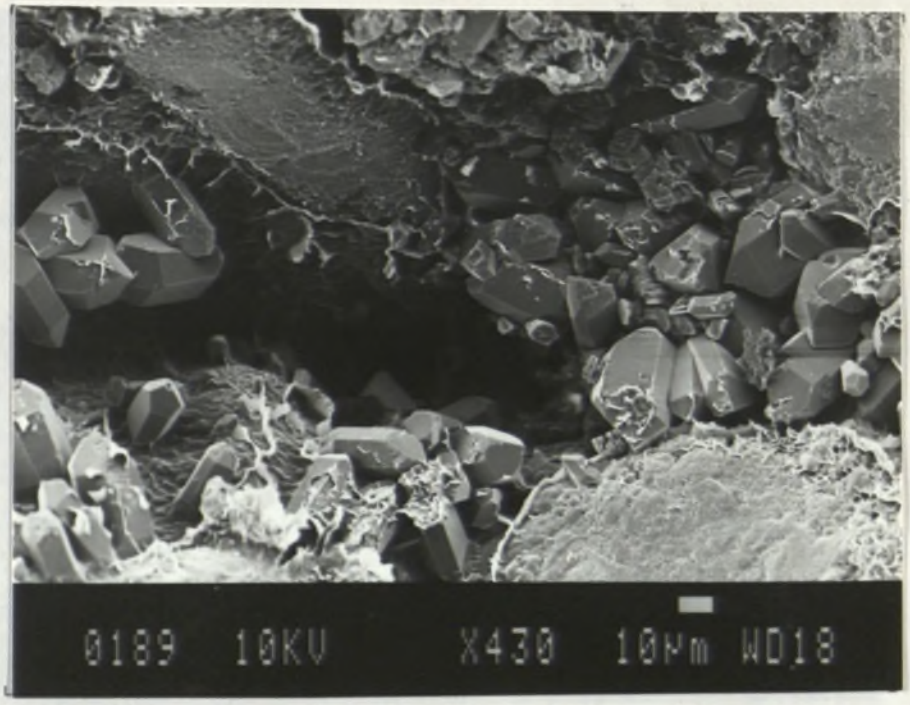

J

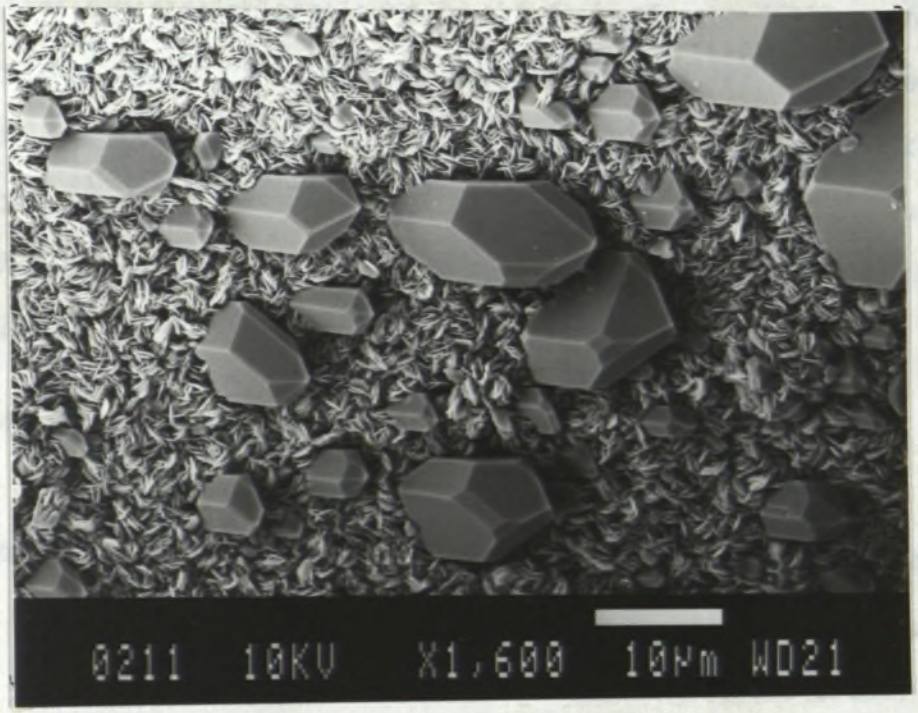

K

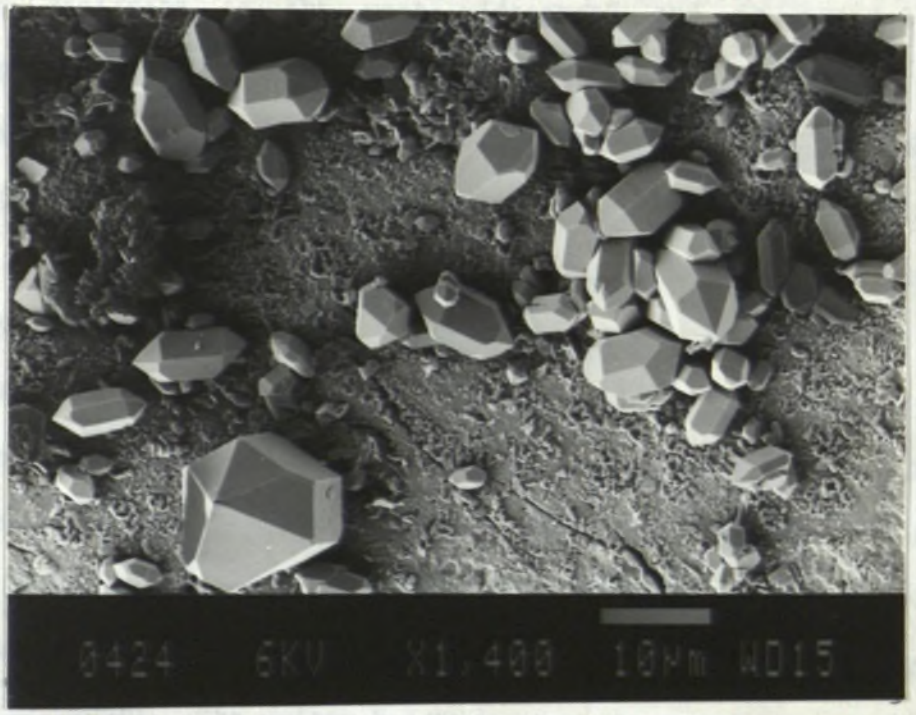

hand, in the labile facies which is characterised by considerable amounts of interstitial matrix and relatively thick clay-coatings on detrital grains, silica cementation continued in the form of pore-filling and grain-replacive microcrystalline aggregates (Figure 3.13B, G-K). It appears that the availability and concentration of dissolved silica in the pore water (presumably derived in this case from the breakdown products of volcanolithic grains) is more critical in silica cementation than the presence of clay-coats on detrital grains.

Clay minerals

The effect of the diagenetic clay mineral assemblage on various petrophysical properties has been discussed in Chapter 4. A brief discussion of the major authigenic clays with reference to their mode of occurrence and likely formative conditions of growth follows below.

Kaolinite

Among the authigenic clay minerals present in the Surat Basin succession kaolinite is the most widespread and is present in all stratigraphic units but is volumetrically more important in the mineralogically mature quartzose units (Figures 4.1, 4.3A-B and 4.10). Shelton (1964) in a world-wide survey found that authigenic kaolinite is present in sandstones of diverse mineralogic composition ranging from quartzarenite through arkose to litharenite and in geologic age ranging from Ordovician to Miocene. Although kaolinite is found to occur in both modern terrestrial and marine depositional environments (Grim, 1968, p. 529, 544-548; Millot, 1970, p. 135-234) and palaeoenvironments (Shelton, 1964), Shelton (ibid.) points out that there might be an initial association of kaolinite with the terrestrially deposited sandstones (see also Keller, 1970). The writer believes that the presence of authigenic kaolinite indicates association with relatively fresh water of low pH at

any stage of the geologic history. Its presence may be indicative either of the initial depositional or postdepositional geochemical environments. Once formed kaolinite can exist over a relatively wide range of pH (from 5.1 to 8.3; cf. Shelton, 1964). The chemistry of pore-water evolves through time, and authigenesis of minerals is the response to the changing geochemical environment. The presence of authigenic kaolinite in the Surat Basin sandstones is interpreted here to be the product of Cainozoic meteoric water invasion; kaolinite tends to be preferentially associated with less saline water (Shelton, ibid.) which is exemplified by the fresh formation water of the Surat Basin sandstones (Exon, 1976, p. 61; Habermehl, 1980).

The mode of fluid flow and the crystallographic habits of kaolinite

Facies-controlled initial porosity and permeability are believed to be two of the critical parameters in controlling the mode of fluid flow which in turn influences diagenetic alterations be it cementation or dissolution. Mass transfer of fluid and dissolved chemical species in sedimentary rocks takes place by two principal means: fluid flux and diffusion, the latter much slower than the former. The mode of mass transport is known to control the paragenetic sequence of authigenic phases (Almon and Drumsteller, 1978), but it also presumably controls the crystallographic habits and size of the authigenic minerals. For example, it has been observed that in the Surat Basin succession kaolinite formed in the coarse-grained sandstones is larger in crystal size (10-15 um) and is characterised by irregular/corroded grain outlines (Figures 3.14A and D) as distinct from the noticeably finer-grained (5-10 um) and euhedral kaolinite in the finer-grained sandstones (Figures 3.14B, E and F). The latter variety can hardly be recognised on the optical microscope; under higher magnification it has the appearence of clots of powder and can be

Figure 3.14. Thin-section and SEM photomicrographs of different types of kaolinite.

A: Thin-section photomicrograph showing the coarse-grained 'skeletal' kaolinite (terminology of Hurst and Irwin, 1982). Gubberamunda Sandstone, GSQ Mitchell 2/21, depth - 299.30 m. Crossed polars.

B: Thin-section photomicrograph of fine-grained 'powdery' pore-filling kaoilinite. Gubberamunda Sandstone, GSQ Roma 8/21, depth - 324.30 m. Plane light.

C: Thin-section photomicrograph showing the fan-shaped variety of kaolinite derived in this example from the alteration of mica (evidence) of which lies just outside the frame of the photomicrograph). Westbourne Formation, GSQ Mitchell 2/23, depth - 324.83 m. Crossed polars.

D: SEM photomicrograph of the fan-shaped variety of coarse-grained 'skeletal' kaolinite. Mooga Sandstone, GSQ Roma 8/5, depth - 135.69 m.

E and F: SEM photomicrographs of fine-grained euhedral kaolinite. Note the contrast in crystal-size compared to Figure 3.14D and euhedral crystal habit. The kaolinite mineralogy of some of these samples as well as others not illustrated here is confirmed by electron microprobe (cf. Appendix 2.6), XRD (Appendix 2.3), and EDX (Appendix 2.2.1) analyses. E - Hutton Sandstone, GSQ Roma 8/52, depth - 774.16 m, F - Evergreen Formation, GSQ Chinchilla 4/31, depth - 965.36 m.

A

0.1 mm

B

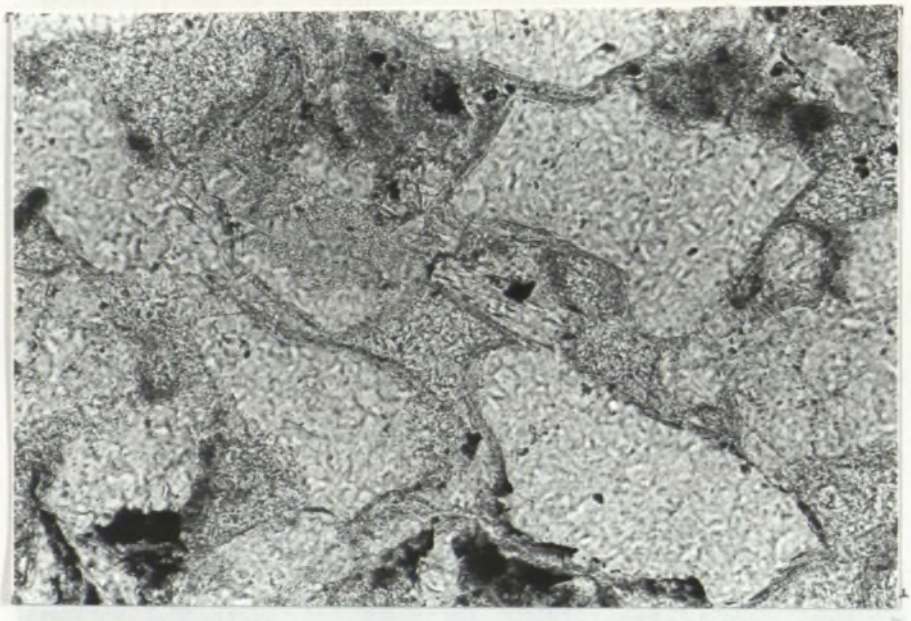

0.1 mm

C

0·1 mm

D

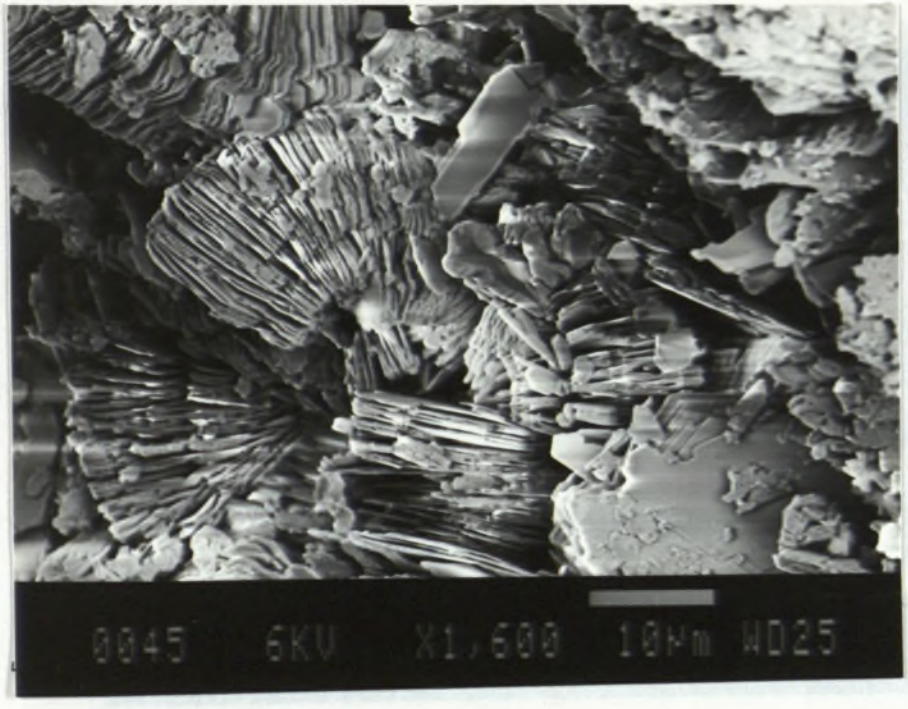

E

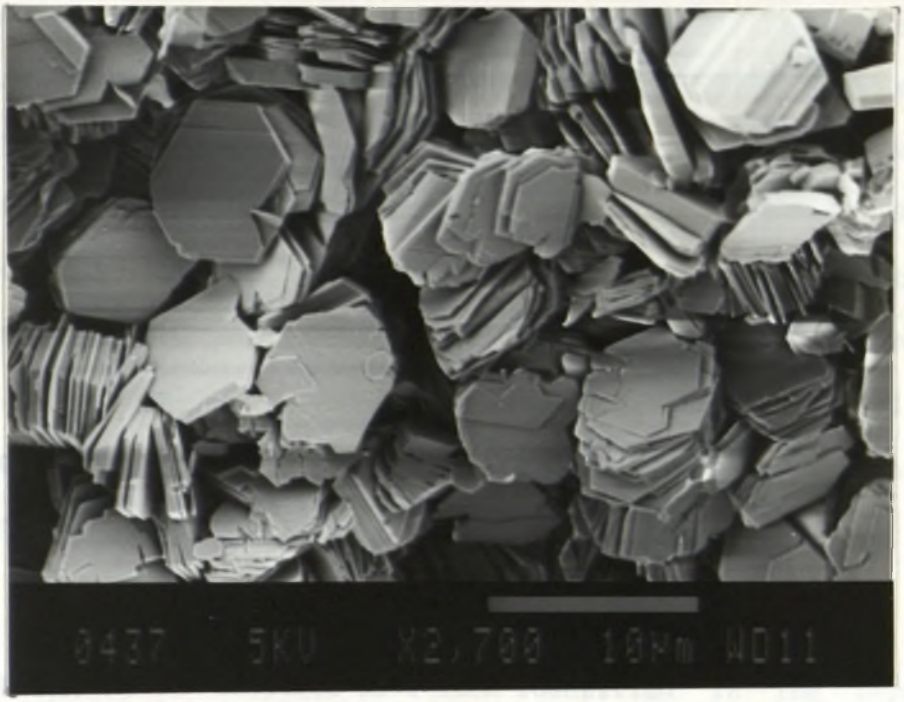

F

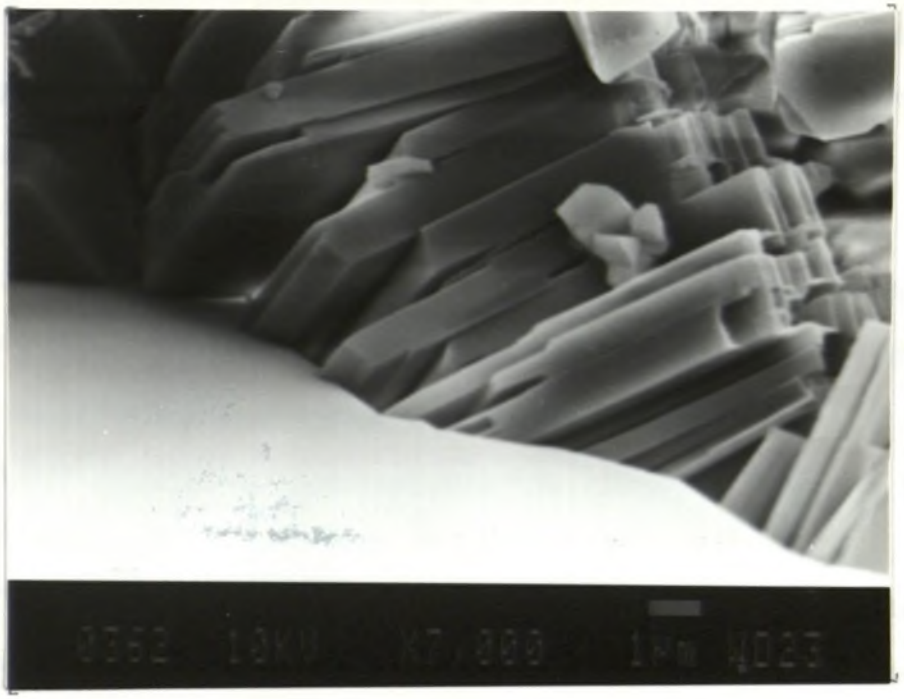

confused with interstitial matrix or altered aphanitic rock-fragments/pseudomatrix (Figure 3.14 B). By contrast, the coarser-grained kaolinite is readily discernible on the petrographic microscope and in places is so coarse that its crystalline mosaic contributes to the intercrystalline effective porosity as evidenced by its patchy uptake of the blue epoxy resin during thin-section preparation (Figure 3.19C). Some of the coarse-grained kaolinite with characteristic fan-shaped outlines are derived from the alteration of muscovite and also possibly biotite (Figure 3.14 C). Presence of such authigenic kaolinite of distinctive crystallographic habits and size as a function of sandstone grainsize is also reported by Hurst and Irwin (1982).

Smectite

Two types of smectite have been identified in the Surat Basin sandstones. The volcanolithic Cretaceous sandstones are characterized by Fe-rich smectite (nontronite, cf. X-Ray diffractogram, Figure 3.15) with typical green color in thin-section (plane light) and may be confused with chlorite (Figure 3.16A-B). These nontronite crystals have a conspicuous 'hairy' appearance in thin-section, grown perpendicular to the grain-surface, and commonly bridge across pore-constrictions to cause dramatic reduction of permeability while still maintaining excellent porosity (Figures 3.16A-C). This nontronite presumably formed soon after deposition as evidenced by the rather loose sand-grain packing and generally relatively high pre-cement porosity (up to 18%) (Figures 3.16A and B). In SEM photomicrographs this variety of smectite is seen to comprise a dense cluster of delicate laths/blades and is referred to here as "blade-nontronite" (Figure 3.16C). The size of individual crystal is typically 5 to 10 um in long dimension and less than 0.5 um in thickness. The other type of smecite is represented by montmorillonite as suggested by XRD

Figure 3.15. X-ray diffractograms of nontronite. Note peak shift after glycolation (G) and the disappearance of the inter-layer water after heating at 500°C for one hour (H). The original peak at 14.98 A° (A) is replaced by one at 9.82 A° (H). A - air dried, G - glycolated, H - heated. Griman Creek Formation. GSQ Surat 3/11, depth - 147 m.

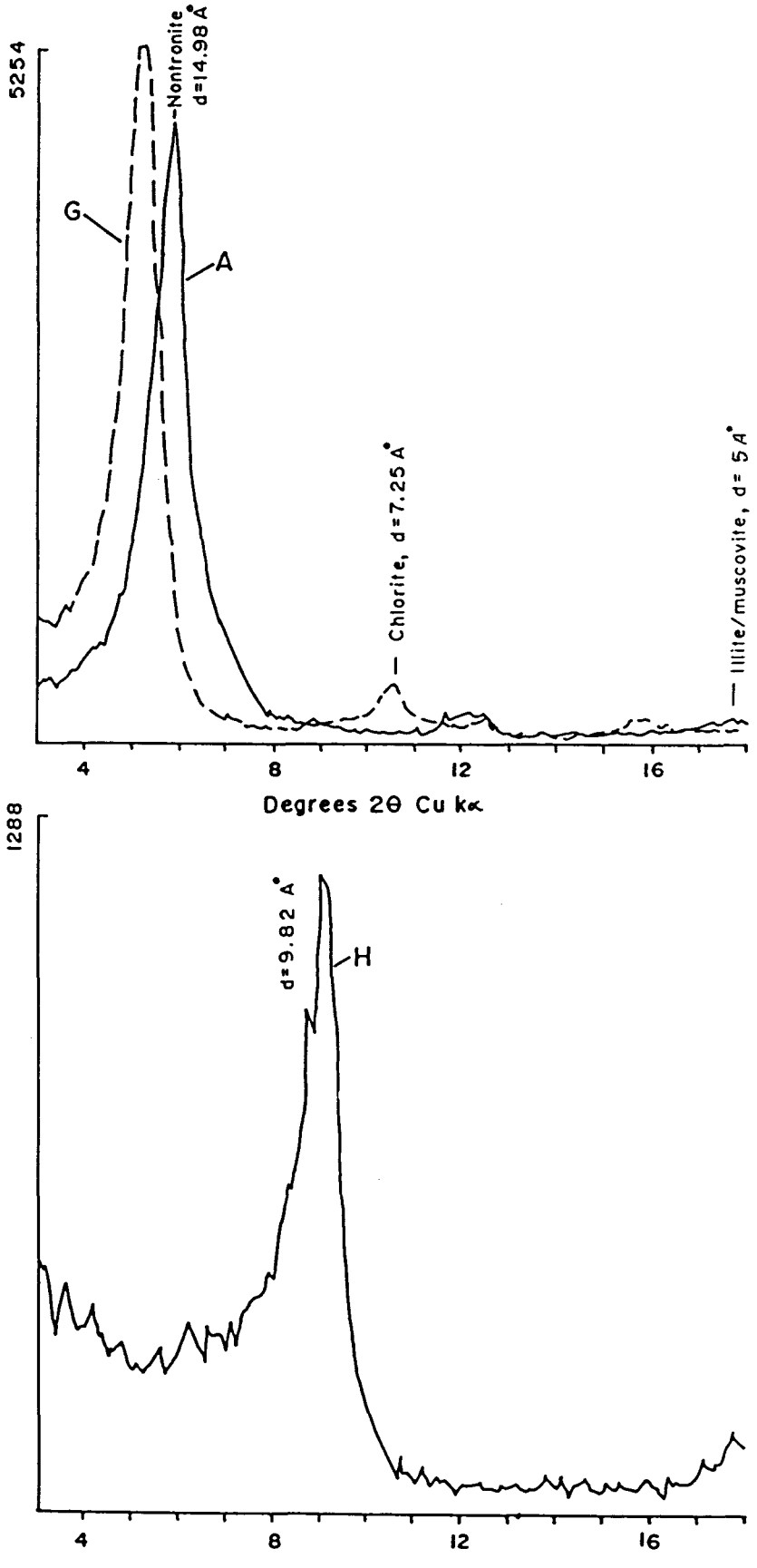
5254
Nontronite
d=14.98 Å
G
A
Chlorite, d=7.25 Å
Illite/muscovite, d= 5 Å
4
8
12
16
Degrees 2θ Cu kα
1288
d=9.82 Å
H
4
8
12
16

analyses (cf. Appendix 2.3) and typically occurs as grain-coats that under the SEM have the appearance of a reticulate or honeycomb-like meshwork of wrinkled, wisp-shaped and laterally-connected blades or curvilinear sheets and serrated laths (Figures 3.17A-F). This honeycomb-like meshwork obviously gives rise to an extremely high aggregate surface area. In some places the crystals also form web-shaped bridges across pores, possibly involving more illitic lath-shaped outgrowths of the more smectitic base (Figures 3.17B-C). Wholesale temperature-induced illitization of smectite as reported by Hower et al (1976) from the Gulf Coast has not been observed in the Surat Basin sandstones, consistent there with the low levels of organic maturity of the intercalated mudrocks. Smectite starts to transform into mixed-layer smectite-illite at a level of organic maturity equivalent to Ro = 0.5% (Powell et al, 1978).

Chlorite

The chlorites in the Surat Basin sandstones occur as rosette-style aggregates of plate- or disc-shaped crystals coating detrital grains (Figures 3.13J and 3.16D) and less commonly also occurring as loosely spaced pore-filling aggregates. The size of individual crystals is typically much smaller relative to those of the nontronite with long dimensions being in the order of 3-6 um and thickness in the order of 0.1-0.2 um (compare Figures 3.16C and 3.16D). In thin-section the crystals are pale green and occur as grain-coats (Figure 3.13 A) which being very thin, can go unnoticed in routine petrographic analysis unless higher magnification is used. Their detrimental effect on permeability is less severe than that of nontronite and montmorillonite .

Figure 3.16. Thin-section and SEM photomicrographs of authigenic nontronite and chlorite.

A and B: Thin-section photomicrographs showing the Fe-rich 'hairy' nontronite grain-coats. The samples have respectively 26 and 29% core porosities and 22 and 35 md permeabilities. A - Griman Creek Formation, GSQ Surat 3/12, depth - 153.90 m. Plane light. B - Griman Creek Formation, GSQ Surat 3/13, depth - 161.50 m. Plane light.

C: SEM photomicrograph of 'blade-nontronite'. Core porosity - 28%, permeability - 0.60 md. Griman Creek Formation. GSQ Surat 3/9, depth - 113.20 m.

D: SEM photomicrograph showing the characteristic rosettes of chlorite in a grain-coat. Core porosity - 16.6%, permeability - 0.19 md. The very little permeability of this sample is due to the presence of other diagenetic clays, notably pore-filling kaolinite. Hutton Sandstone, GSQ Roma 8/52, depth - 782.78 m.

A

0.1 mm

B

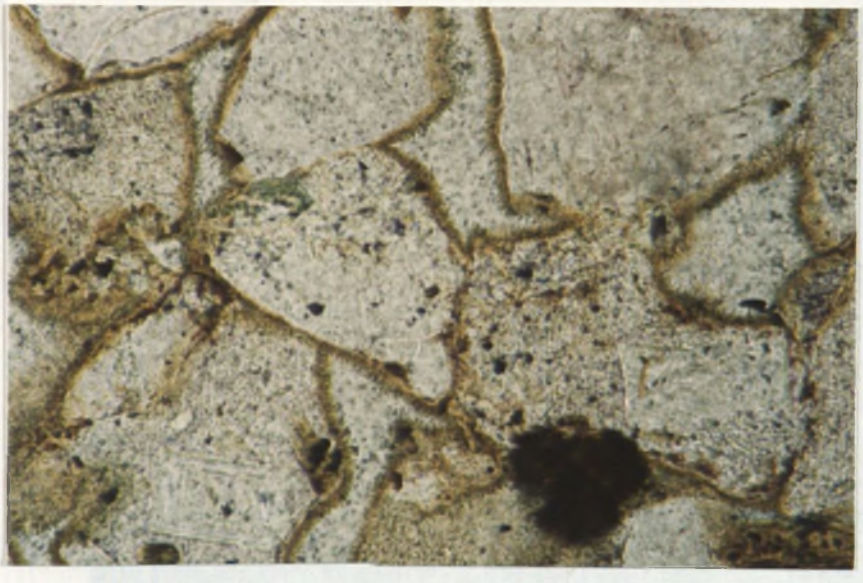

0.1 mm

C

D

Figure 3.17. SEM photomicrographs illustrating various aspects of authigenic smectite (montmorillonite).

A: Smectite grain-coatings. Note their absence at places of former grain contacts (top-centre and bottom-right) attesting to the authigenic nature of the clay. The lath-shaped crystal terminations also bridge pores (upper-left). Gubberamunda Sandstone, GSQ Chinchilla 4/3, depth 65.69 m.

B: Enlarged view of right hand side of A. Note the characteristic anastomosing or reticulate meshwork pattern with curved, elongate, and laterally-linked shhet-like crystals resulting in an extremely high surface area.

C: Lath-shaped terminations of ?mixed-layer illite-smectite. Such terminations cause drastic reduction of permeability and can break loose and subsequently block pore constrictions during drilling, testing and hydrocarbon production causing further reduction of permeability. Evergreen Formation, GSQ Chinchilla 4/36, depth - 1055.77 m.

D: Honeycomb-like smectite with serrated edge. Note also the web-shaped bridge at the centre and lower-left of the photomicrograph. Walloon Coal Measures, GSQ Chinchilla 4/20, depth - 681.34 m.

E: Enlarged view of the grain in centre of A illustrating the enormous surface area that offers great resistance to fluid flow.

F: Smectite grain-caoting showing flaky serrated terminations which make them prone to break loose during turbulent fluid flow causing formation damage. Evergreen Formation, GSQ Chinchilla 4/31, depth - 965.00 m.

A

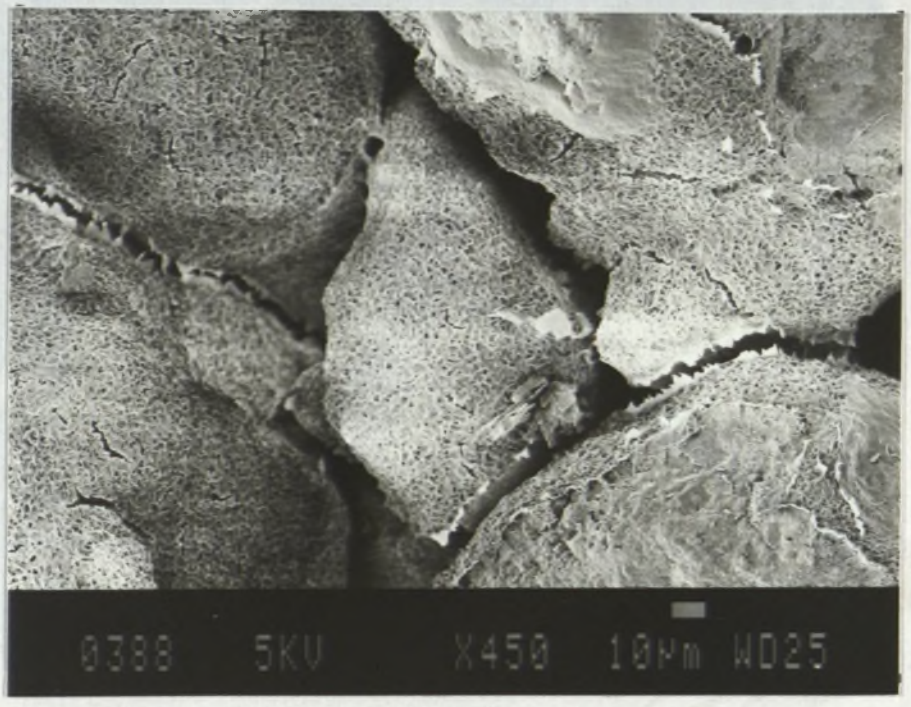

B

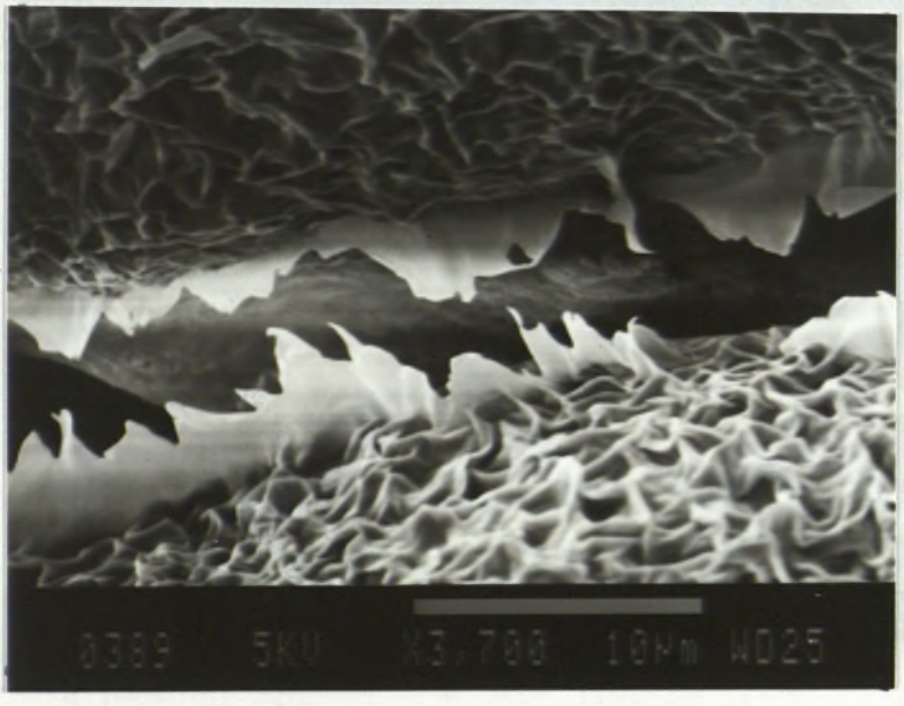

C

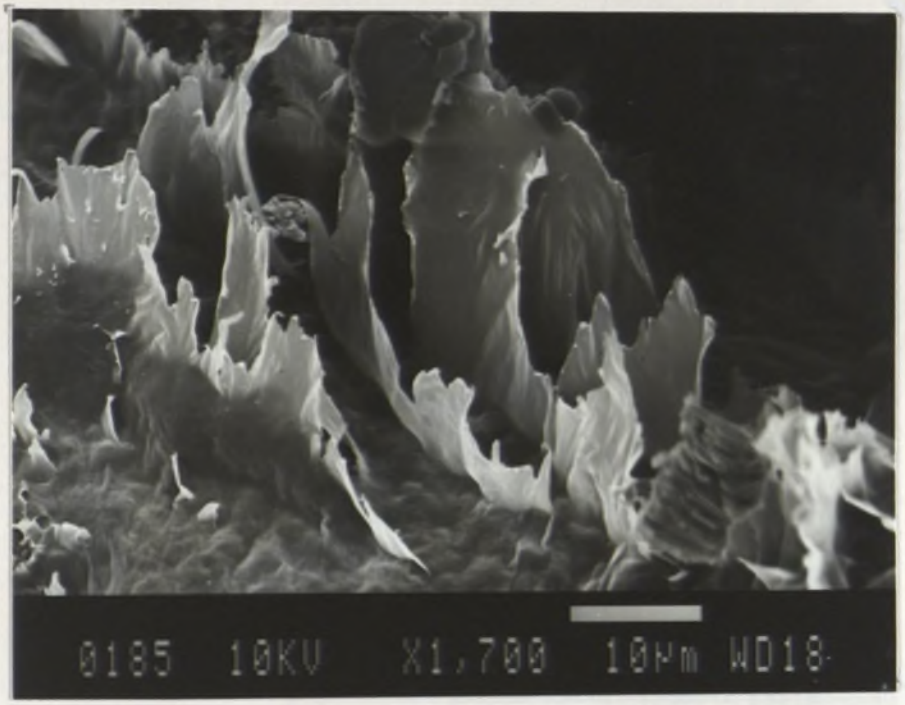

D

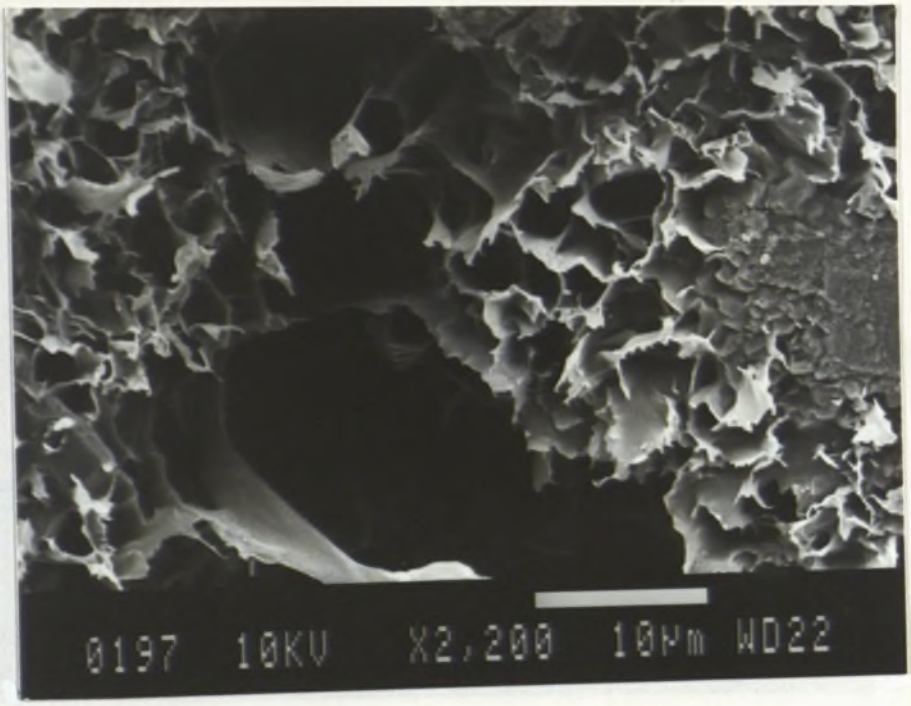

E

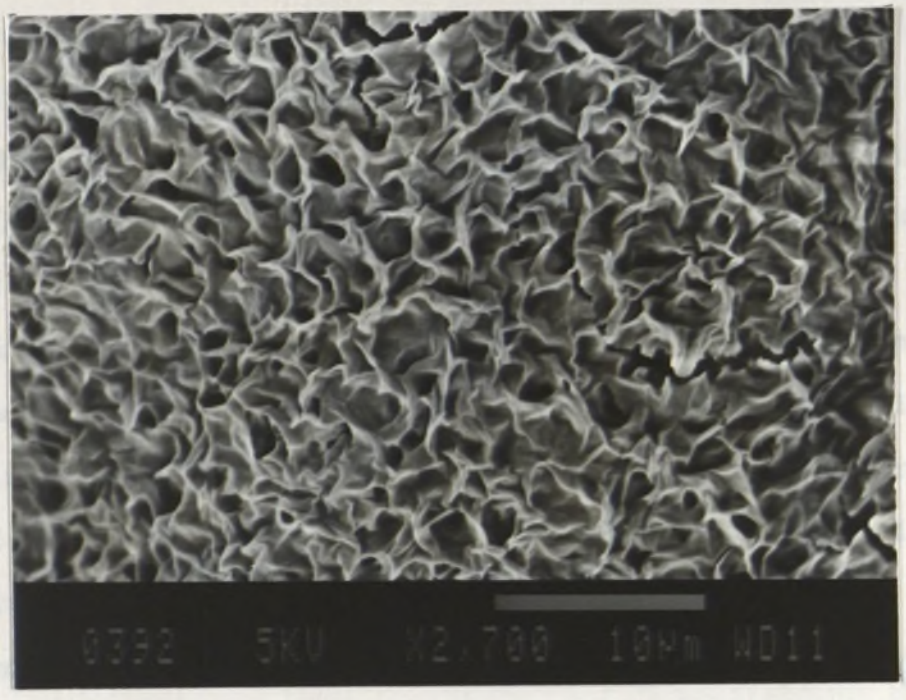

F

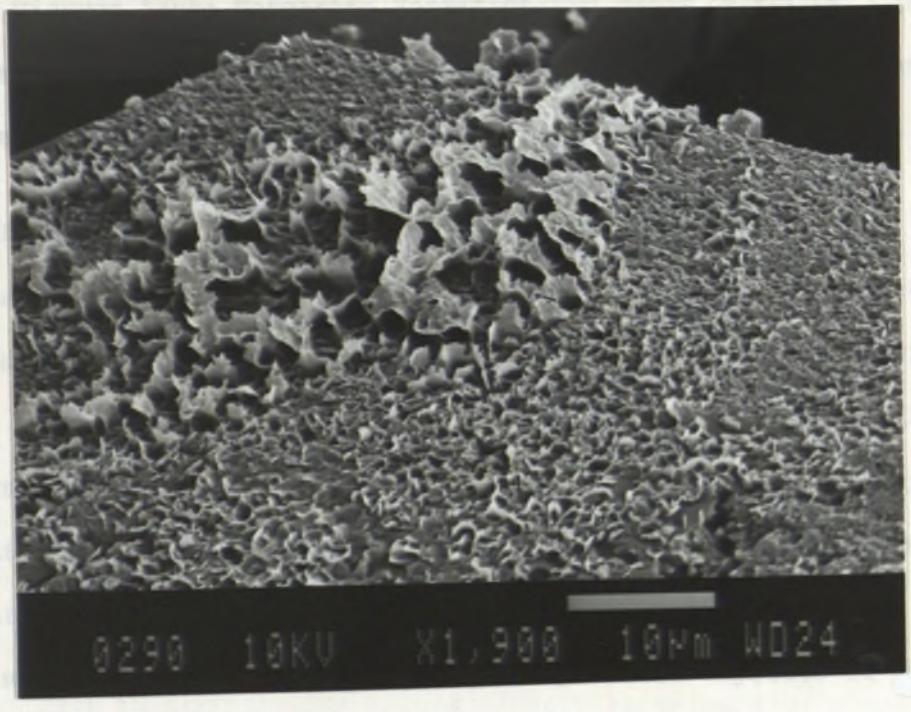

Zeolites

Authigenic zeolite is reported here for the first time from the Surat Basin succession in Queensalnd. Slansky (1984) has however noted the occurrence of zeolite of the heulandite-clinoptilolite group from the Doncaster Member of the Wallumbilla Formation in the NSW part of the basin. Zeolites found in this study occur as pore-filling and grain-coating aggregates in the Griman Creek and Wallumbilla Formations of the Rolling Downs Group (see also Chapter 5). It is very fine-grained and can easily be overlooked in routine petrographic analysis which may explain its non-mention in the earlier reconnaissance and semi-quantitative petrographic studies of these formations by Houston (1972). Under higher magnification the zeolite is seen to comprise stubby tabular crystals ranging in size from 10 to 40 um filling pore spaces and sporadically replacing volcanic rock-fragments and feldspars (Figures 5.3D and E). It has rather low birefringence and high negative relief. This zeolite very much resembles the authigenic heulandite illustrated by Gilbert and McAndrews (1948) from the upper Miocene Santa Margarita Formation/San Pablo Group in California. Electron microprobe and EDX analyses confirm its composition as heulandite (Appendices 2.4 and 2.2 respectively).

TYPES OF POROSITY

Porosity is here arbitrarily subdivided into two broad categories: microporosity having pore diameters <20 um and macroporosity with pore diameters ⩾20 um. This arbitrary classification does not imply that pore diameteres <20 um are impermeable to epoxy resin. While a ⩾20 um pore may be identifiable in routine thin-section petrographic analysis (under high magnification) the microporosity can be resolved only under the SEM and consists mainly of intercrystalline porosity within deposits of diagenetic minerals, between cement crystals and detrital grains and within altered

framework grains (rock-fragments, micas, feldspars etc.). Microporosity is calculated as the difference between the quantitatively measured core porosity and quantitatively measured thin-section porosity. Additionally, porosity is genetically classified as primary, consisting mainly of the intergranular variety, and secondary which is again subdivided into subcategories as shown in Figure 3.18. Most of the secondary porosity observed in the Surat Basin sandstones is of the moldic (grain-dissolution) type (Figures 3.19A-D) with variable amounts of intragranular (cf. Figures 3.12A-B and 3.19C) and some secondary intergranular cement-dissolution porosity. It is very difficult if not impossible in some cases to ascertain whether an instance of moldic porosity is the result of direct dissolution of framework grains or dissolution of earlier grain-replacive cement (cf. Hayes, 1979). Therefore, no distinction was attempted between these two varieties of moldic porosity. Additionally because secondary intergranular porosity mimics primary porosity, it is difficult to identify it as the one rather than the other in some cases but an attempt was nevertheless made wherever possible to distinguish it (diagnostic operational criteria are discussed below). Secondary intergranular porosity derived from dissolution of interstitial matrix (in contrast to dissolution of pore-filling cement) was likewise not possible to identify with any degree of confidence. Some shrinkage porosity was also observed and occurs mostly within glauconie pellets (Figure 3.19E), particularly in the lower part of Griman Creek Formation, the Wallumbilla Formation and the upper part of the Bungil Formation. Very minor amounts of fracture porosity (both grain- and rock-fracture; cf. Appendix 1.9) were also observed in some stratigraphic units (such as the Orallo Formation and the Walloon Coal Measures) associated mainly with very fine-grained sandstones rich in argillaceous matrix. Variable amounts of intragranular porosity are present in some stratigraphic units containing abundant

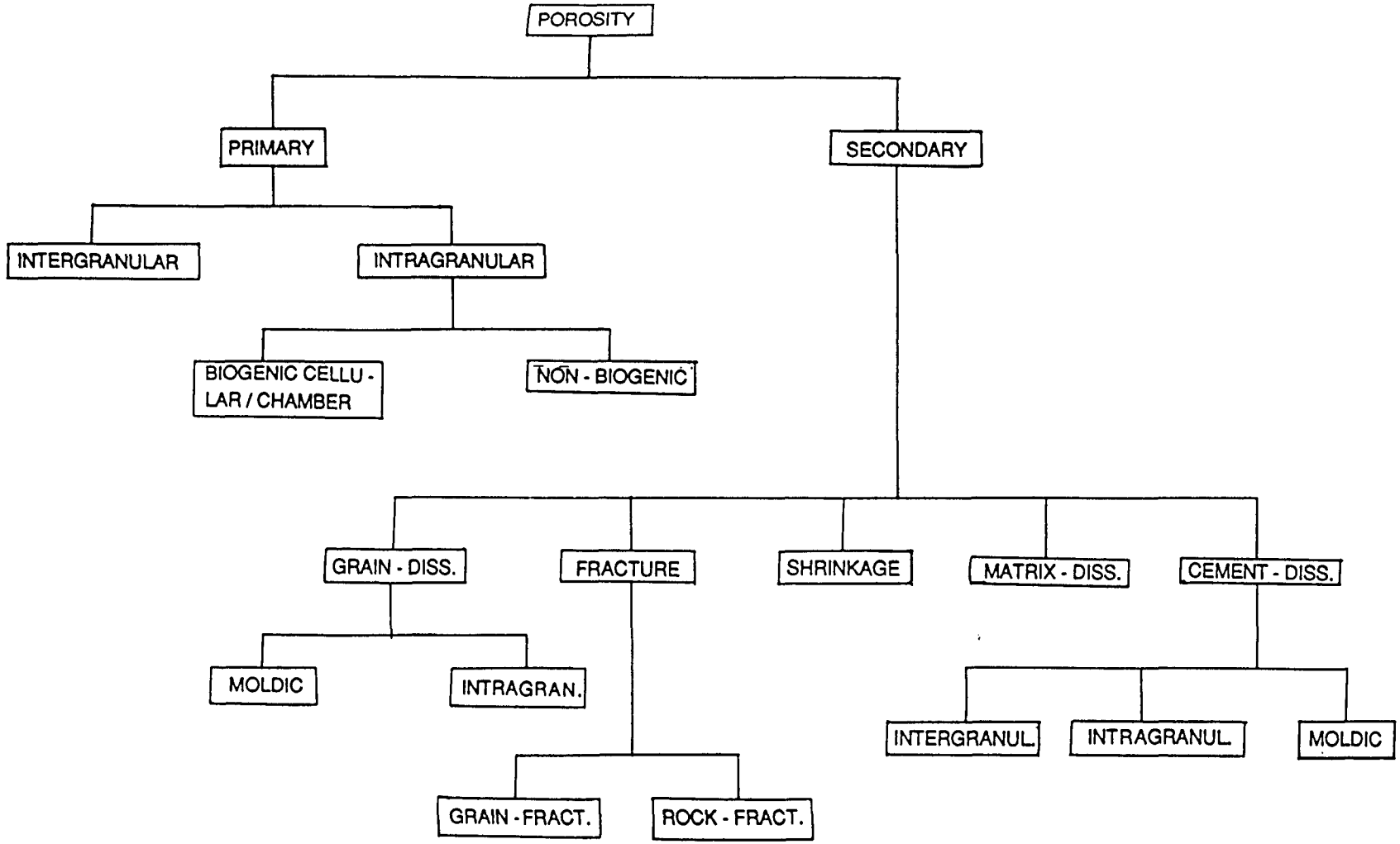

Figure 3.18. A genetic classification of porosity types in sandstones. Modified after Schmidt and McDonald (1979b).

Figure 3.19. Thin-section photomicrographs showing different pore-types. Pore spaces are defined by blue coloured resin. Plane light.

A and B: Moldic porosity formed by the dissolution of framework grains. Diagnostic criteria for its recognition include the inhomogeneity of packing, oversized pores, and presence of remnants of partially leached grains. Hutton Sandstone, GSQ Roma 8/48, depth - 734.55 m; and GSQ Roma 8/46, depth - 713.68 m.

C: Intragranular pore within skeletal feldspar (centre). Intergranular spaces are occupied by coarse-grained kaolinite. Note the effective porosity within the pore-filling kaolinite as indicated by the pervasive uptake of the blue resin during thin-section preparation. Orallo Formation, GSQ Mitchell 2/17, depth - 253.62 m.

D: Presence of both intergranular and moldic (centre-right) pores give rise to a well-connected pore system with very good permeability (core porosity = 23.4%, permeability = 375 md). Note the packing inhomogeneity (left and right of photo) and the remnant intergranular pore-filling calcite (red stained area) which are suggestive of a secondary origin of the intergranular porosity. Hutton Sandstone, GSQ Roma 8/60, depth - 876.21 m.

E: Shrinkage porosity within a glauconie pellet (centre of photo) as defined by nontronite grain-coating preserving oroginal outline of the detrital grain. Griman Creek Formation. GSQ Surat 3/12, depth - 153.90 m.

A

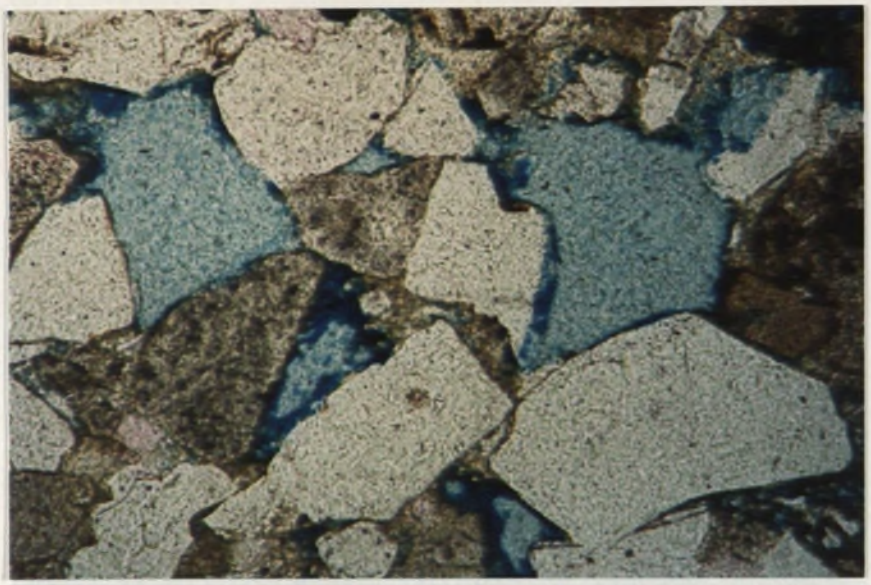

0·1 mm

B

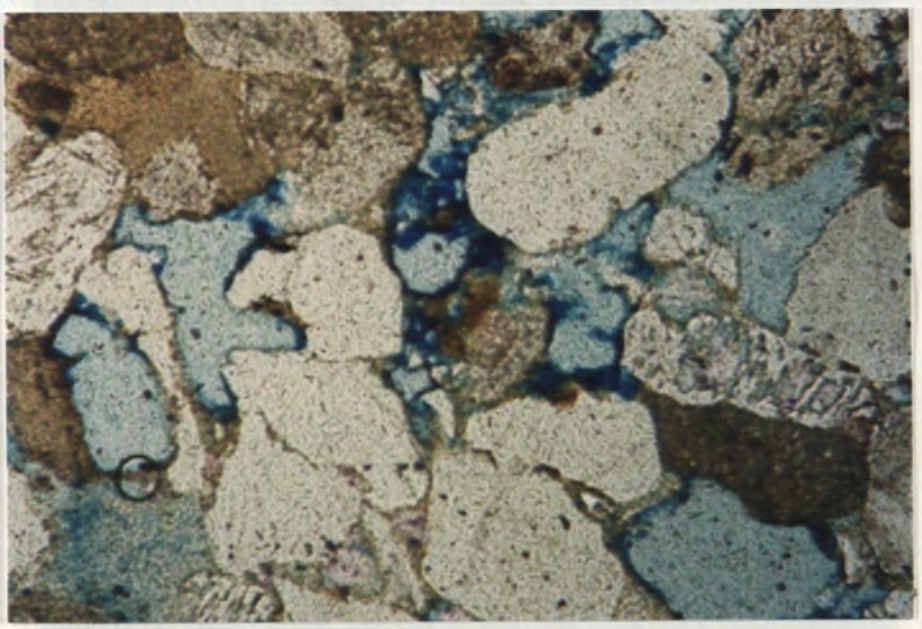

0·1 mm

C

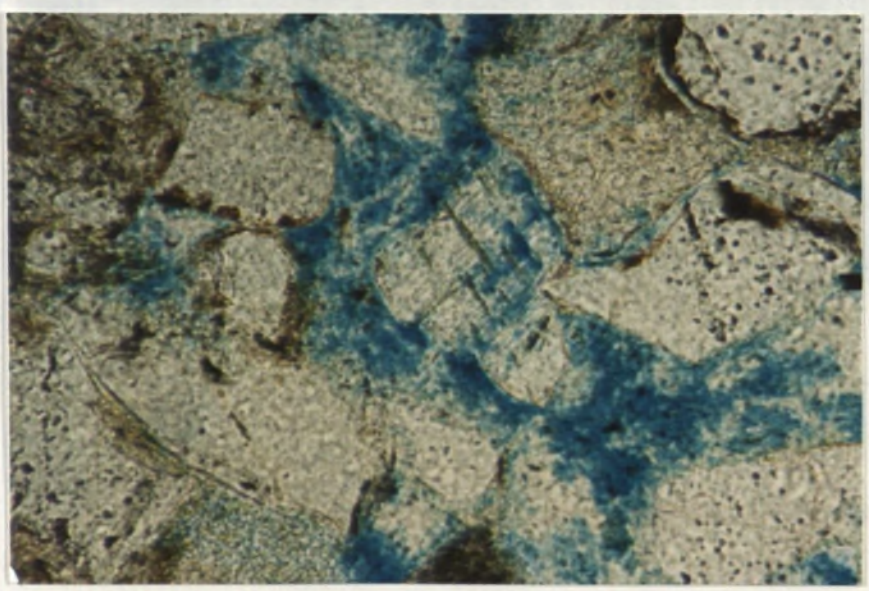

0·1 mm

D

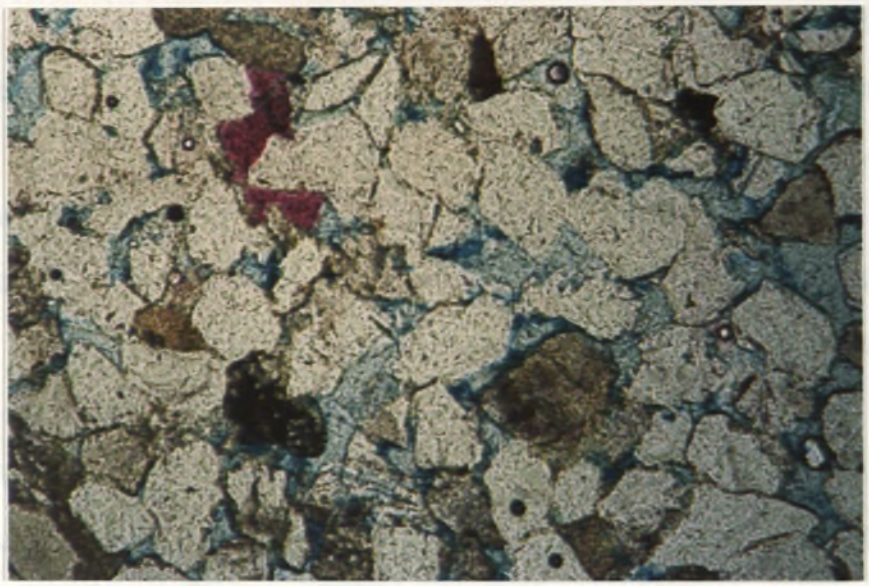

0·1 mm

E

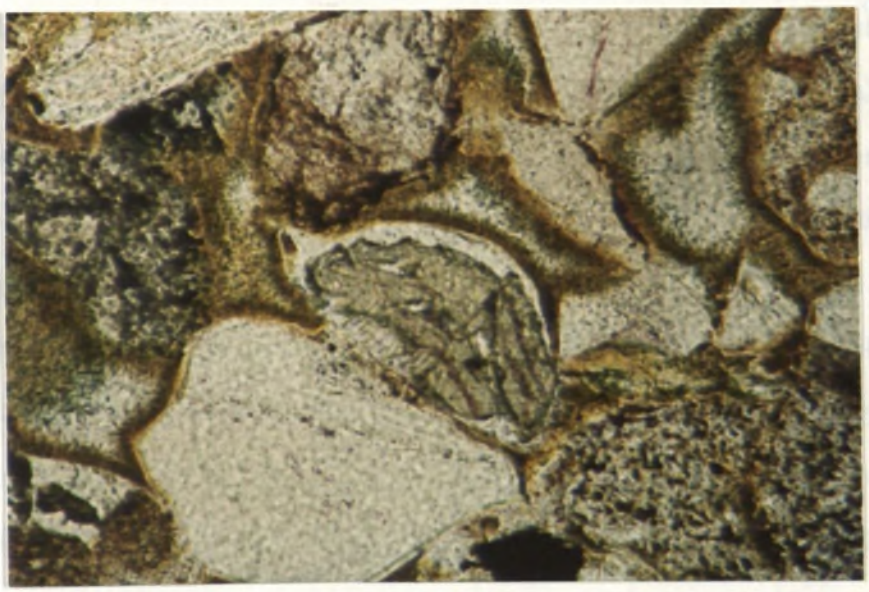

0·1 mm

feldspars (e.g., the Gubberamunda Sandstone; Figures 3.12A-B and 3.19C).

Identification of secondary porosity

Secondary porosity was identified using the thin-section criteria of Schmidt et al (1977), Schmidt and McDonald, (1979b) and Shanmugam (1985a, 1985b) and the SEM criteria of Burley and Kantorowicz (1986). Thin-section petrographic criteria include:

1) partial dissolution; 2) molds; 3) inhomogeneity of packing; 4) oversized pores; 5) elongate pores; 6) corroded grains; 7) intraconstituent pores; and 8) fractured grains, (cf. Schmidt et al, 1977; Schmidt and McDonald, 1979b). Secondary grain-dissolution porosity (GDP) is easier to distinguish from the secondary intergranular porosity (IGP) (resulting from dissolution of pore-filling cement/matrix; cf. Figure 3.18) since the latter commonly mimics primary porosity. In the absence of any remnant intergranular cement, secondary IGP can be impossible to identify in thin-section. However, more commonly secondary IGP is accompanied by variable amounts of GDP in which case an intelligent assessment about presence of both can be made. Also, if the inferred secondary cement-dissolution porosity is patchy/localized in distribution (which is commonly the case), inhomogenity of grain-packing observed in neighbouring thin-sections with similar texture and from comparable depth, and in some cases within the scale of the same thin-section, can offer a diagnostic clue. In a most interesting paper on this topic, Burley and Kantorowicz (1986) advocate the use of the SEM for identification of secondary IGP. They argue that secondary IGP formed by the dissolution of carbonate cements leaves corrosion features on quartz grain surfaces and on overgrowths which can best be seen under the SEM. Features similar to those documented by Burley and Kantorowicz (1986) occur in some of the Surat Basin sandstones examined with the SEM and range from regularly shaped (commonly V-shaped) grooves and notches on the surfaces of quartz overgrowths (Figures 3.20A-D)

Figure 3.20. SEM photomicrographs showing geometric V-shaped notch- and groove-like features on quartz overgrowth surfaces. Note the distinction between the very regular geometric shape of these features compared to the ragged ?overgrowth interference marks (e.g., upper-left and lower-left of D) presumably caused by the interpenetration of neighbouring grains. A - Hutton Sandstone, GSQ Mitchell 2/47, depth - 725.86 m. B - Evergreen Formation, GSQ Mitchell 2/49, depth - 853.46 m. C - Gubberamunda Sandstone, GSQ Roma 8/25, depth - 364.71 m. D - Hutton Sandstone, GSQ Roma 8/53, depth - 791.53 m.

A

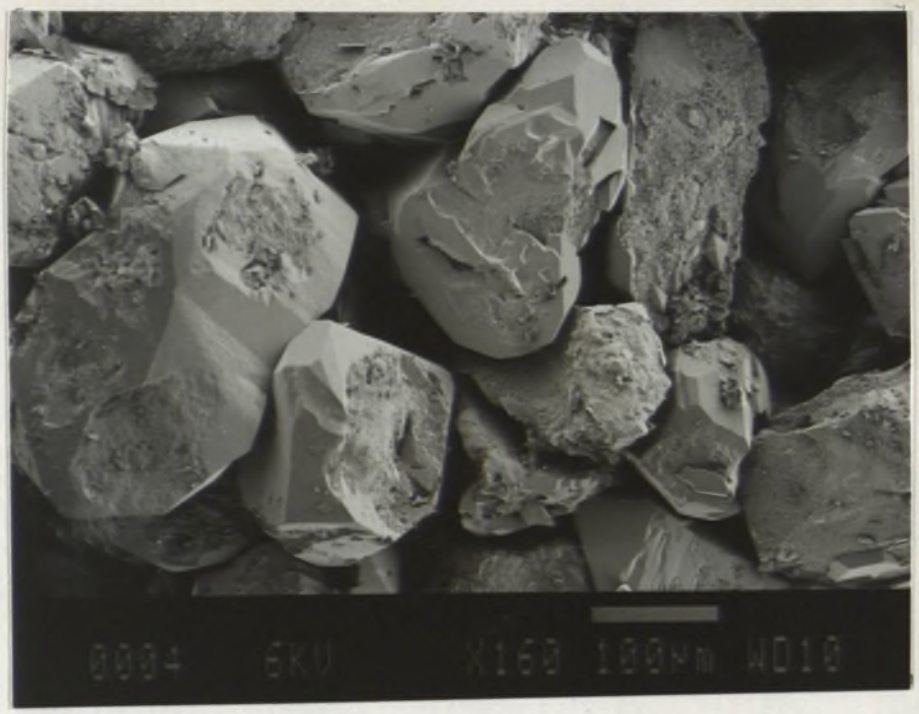

B

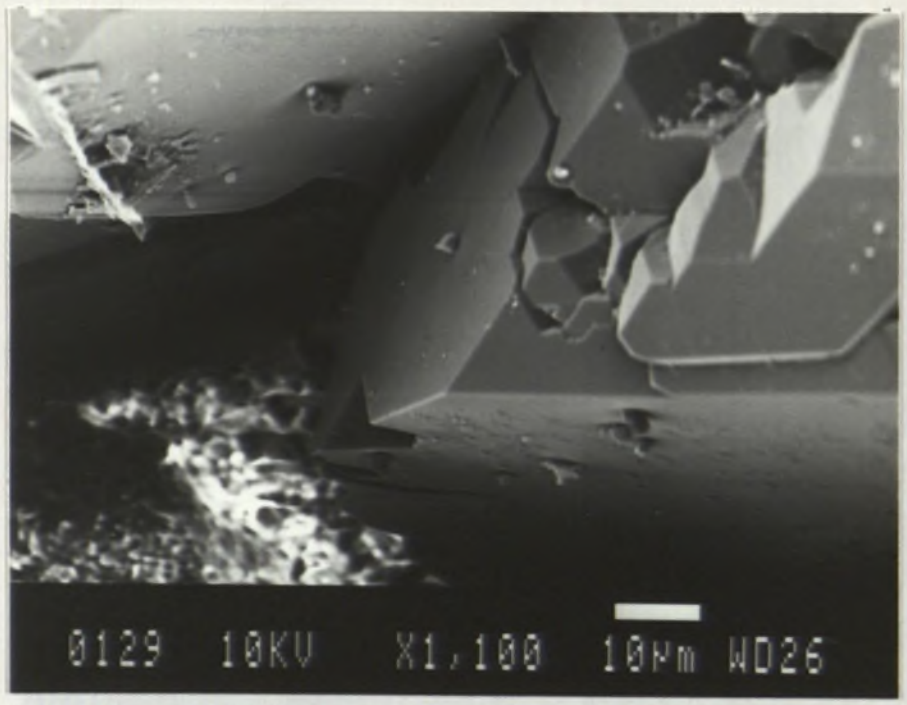

C

D

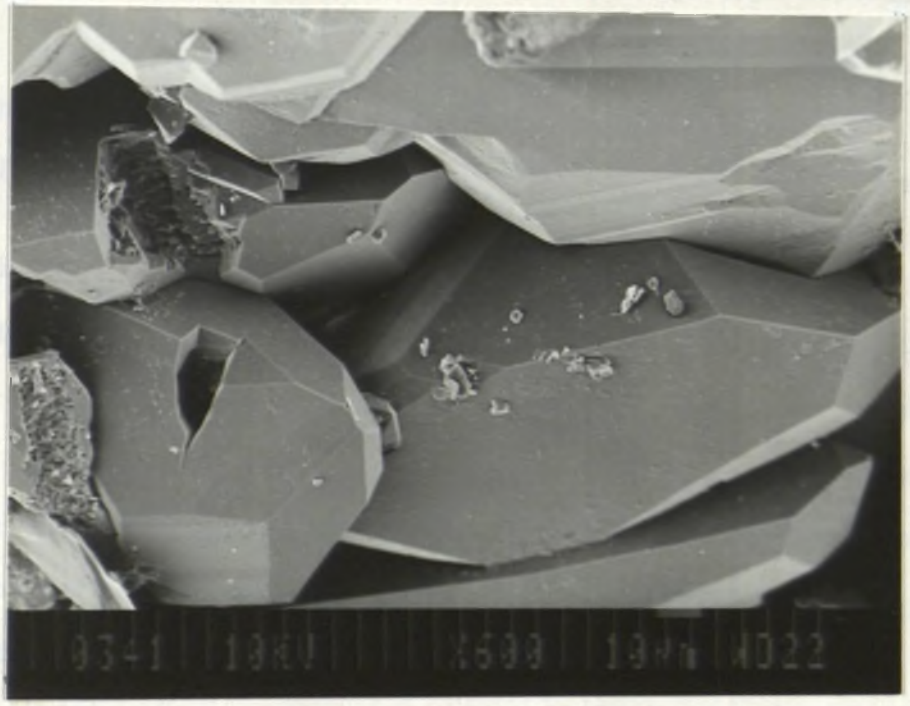

to irregularly-shaped embayments and depressions on the detrital grain-boundaries and overgrowths (these latter features are best seen in thin-section). However, although the V-shaped notches and groove-like features present on quartz overgrowths in the Surat Basin sandstones are comparable in size to the largest example described by Burley and Kantorowicz (1986), they occur as sporadic isolated features rather than in clusters and are of more regular geometric shape. Therefore it is unlikely that the Surat Basin grain-surface features result from the dissolution of carbonate cement and their origin remains unclear. It is possible that interference features somewhat similar to those reported by Burley and Kantorowicz (1986) can be produced in response to interpenetrating overgrowth surfaces on neighbouring quartz grains. Therefore the SEM criteria of Burley and Kantorowicz have been used with caution, but notwithstanding their apparent absence in the Surat Basin rocks, other circumstantial evidence observable in thin-sections such as abundance of grain-dissolution porosity (Figures 3.19A-B), presence of remnant patches of intergranular carbonate cement (Figure 3.19D), packing inhomogeneity within the same thin-section (Figure 3.19D) or in nearby samples etc. permitted elucidation of the genetic-temporal nature of the IGP. However, the writer's estimate of the presence of secondary IGP is likely to err on the conservative side.

Microporosity

Microporosity is a significant contributor to the total core porosity especially in the lithic sandstones rich in interstitial materials. Microporosity is associated mainly with the interstitial materials - both detrital matrix and authigenic phases. Contributions from altered rock-fragments and mica grains (in the latter case, especially those partially altered to fan-shaped kaolinite; cf. Figure 3.14C) is also important. Likewise, altered (sericitized/kaolinitized) feldspars

contribute to the microporosity. Classification of the porosity types together with their plot on the ternary diagram of Pittman (1979a, 1979b; Figure 3.21 herein) was found to be very helpful in assessing their relative importance (see also Chapter 5). The porosity types and their location on the ternary diagram of Pittman show statistically preferred associations with the different polar constituents on a superimposed QFR triange (Figure 3.21; see also Table 3.1). Figure 3.21 shows that the more microporous sandstones are also more lithic, attesting to the fact that altered rock-fragments are the most important contributors to the microporosity as it will be shown below by quantitative analysis. The association is also presumably accentuated by the fact that lithic sandstones are also rich in interstitial (ortho/proto-) matrix and authigenic clays which are other significant contributors to microporosity (Table 3.1).

An empirical algorithm to estimate microporosity

An attempt has been made to formulate an algorithm to empirically derive an estimate of the microporosity from knowledge of the major petrographic grain-type modal analysis categories (cf. Table 3.1). To this end a multiple regression analysis was performed on the Hutton Sandstone (having the highest number of samples) using a SPSSX computer package (PROCEDURE REGRESSION, SPSS Inc, 1983) with microporosity (MICROPOR) as the dependent variable and the following categories as the independent variables: RFRAG (rock-fragments, %), FSPAR (feldspar, %), MICA (detrital mica, %), EPIMAT (epimatrix, %; cf. Dickinson, 1970), ORMAT (ortho/protomatrix, % - interstitial matrix; cf. Dickinson, 1970; see also Appendix 1.1). The outcome of the analysis is shown in Table 3.1. A brief mathematical treatment on the purpose and utility of the multiple regression analysis is located in Chapter 6. As can be seen from Table

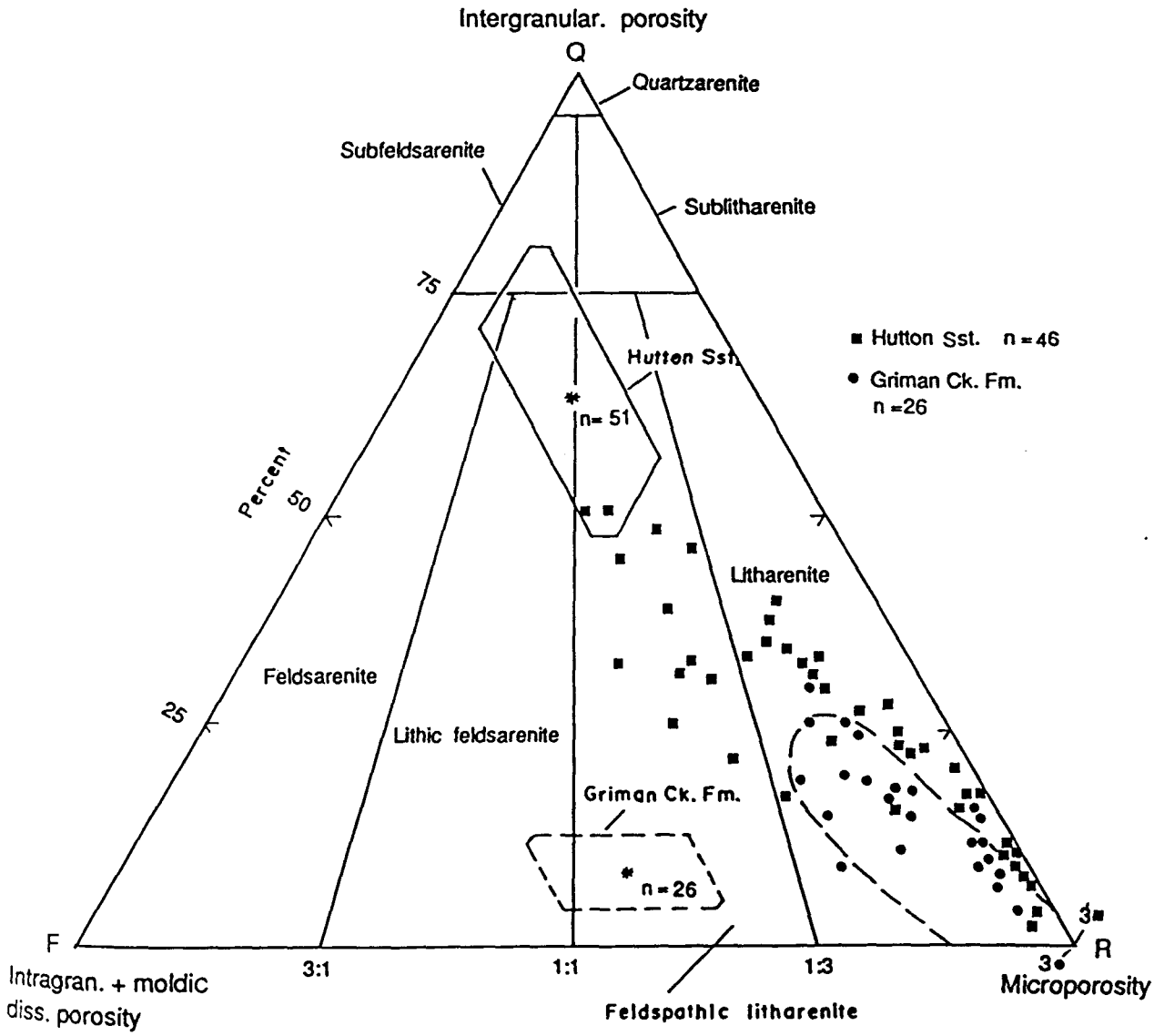

Figure 3.21. Types of porosity in the Hutton Sandstone and Griman Creek Formation superimposed on the QFR compositional triangle. Porosity classification after Pittman (1979a, 1979b). The basal apices of the porosity triangle have been interchanged for ease of comparison. Note that on a first-order level the more lithic sandstones are likely to be more microporous as suggested by the fact that the Griman Creek Formation plots around the microporosity pole. The wider scatter of porosity types in the Hutton Sandstone reflects its wide compositional field. Asterisks and enclosing polygonal envelopes show respectively the compositional means and one standard deviation about the mean (cf. Figures 2.2A and C).

Table 3.1. Correlation matrix, its one-tailed significance, multiple correlation coefficient (R), R^2 and other relevant statiatics of the multiple regression analysis on the Hutton Sandstone with microporosity as the dependent variable.

N of Cases = 51

Correlation, 1-tailed Sig:

	MICROPOR	RFRAG	FSPAR	MICA	EPIMAT	ORMAT
MICROPOR	1.000	.644	.297	.297	.069	.584
	.999	.000	.017	.017	.315	.000
RFRAG	.644	1.000	.265	.085	-.217	.564
	.000	.999	.030	.278	.063	.000
FSPAR	.297	.265	1.000	.261	.238	.120
	.017	.030	.999	.032	.046	.201
MICA	.297	.085	.261	1.000	.031	.624
	.017	.278	.032	.999	.414	.000
EPIMAT	.069	-.217	.238	.031	1.000	-.352
	.315	.063	.046	.414	.999	.006
ORMAT	.584	.564	.120	.624	-.352	1.000
	.000	.000	.201	.000	.006	.999

Variable(s) Entered on Step Number 3.. EPIMAT

Multiple R	.75995
R Square	.57752
Adjusted R Square	.55056
Standard Error	3.05967

Analysis of Variance

	DF	Sum of Squares	Mean Square
Regression	3	601.46991	200.48997
Residual	47	439.99362	9.36157

F = 21.41628 Signif F = .0000

---------- Variables in the Equation ----------

Variable	B	SE B	Beta	Correl	Part Cor	Partial	T	Sig T
RFRAG	.216365	.052834	.470335	.643850	.388262	.512818	4.095	.0002
ORMAT	.234553	.064992	.432205	.583732	.342162	.465817	3.609	.0007
EPIMAT	.714842	.223898	.323456	.069273	.302701	.422170	3.193	.0025
(Constant)	7.749776	1.313585					5.900	.0000

---------- Variables not in the Equation ----------

Variable	Beta In	Partial	Min Toler	T	Sig T
FSPAR	.052002	.073117	.624672	.497	.6214
MICA	-.050452	-.051391	.277415	-.349	.7287

End Block Number 1 PIN = .050 Limits reached.

3.1, SPSSX chose three variables namely, RFRAG, ORMAT and EPIMAT in that order of importance. The multiple correlation coefficient is 0.76 and the algorithm can be used to estimate microporosity with a standard error of 3%. The relationship of microporosity with these variables can be expressed as follows (cf. statistics in Table 3.1):

Microporosity (%) = 7.75 + 0.216 (RFRAG) + 0.234 (ORMAT) + 0.715 (EPIMAT).

It is evident from Table 3.1 that the inclusion of feldspar and mica as predictor variables does not significantly improve the correlation coefficient. It may be mentioned here that in a recent paper Pittman and King (1986) attempted to empirically determine microporosity and offered an algorithm which took into consideration only the sum of Kaolinite and lithics as independent variable. They do not give the correlation coefficient, coefficient of determination or the standard error of estimate. They did not comment explicitly on the presence or absence of matrix in their samples but if it is present then it is surprising that they have excluded it as a predictor variable since it is considered a significant contributor of microporostity.

CORE POROSITY AND THIN-SECTION POROSITY RELATIONSHIPS

Core porosity is found to be consistently higher than thin-section porosity in the Surat Basin sandstones (Figure 3.22), as might be expected from similar studies in other basins. Core porosities can range from 5 to 15% in samples where thin-section porosity is negligible (not discernible; Figure 3.22). The higher porosity recorded by the conventional helium-injection core porosity measuring technique and its poor correlation with measured thin-section porosity may be due to the following factors:

1) thin-section samples were not always taken from exactly the same place from where core plugs were taken;

2) because of the very small size of the helium molecule it can penetrate

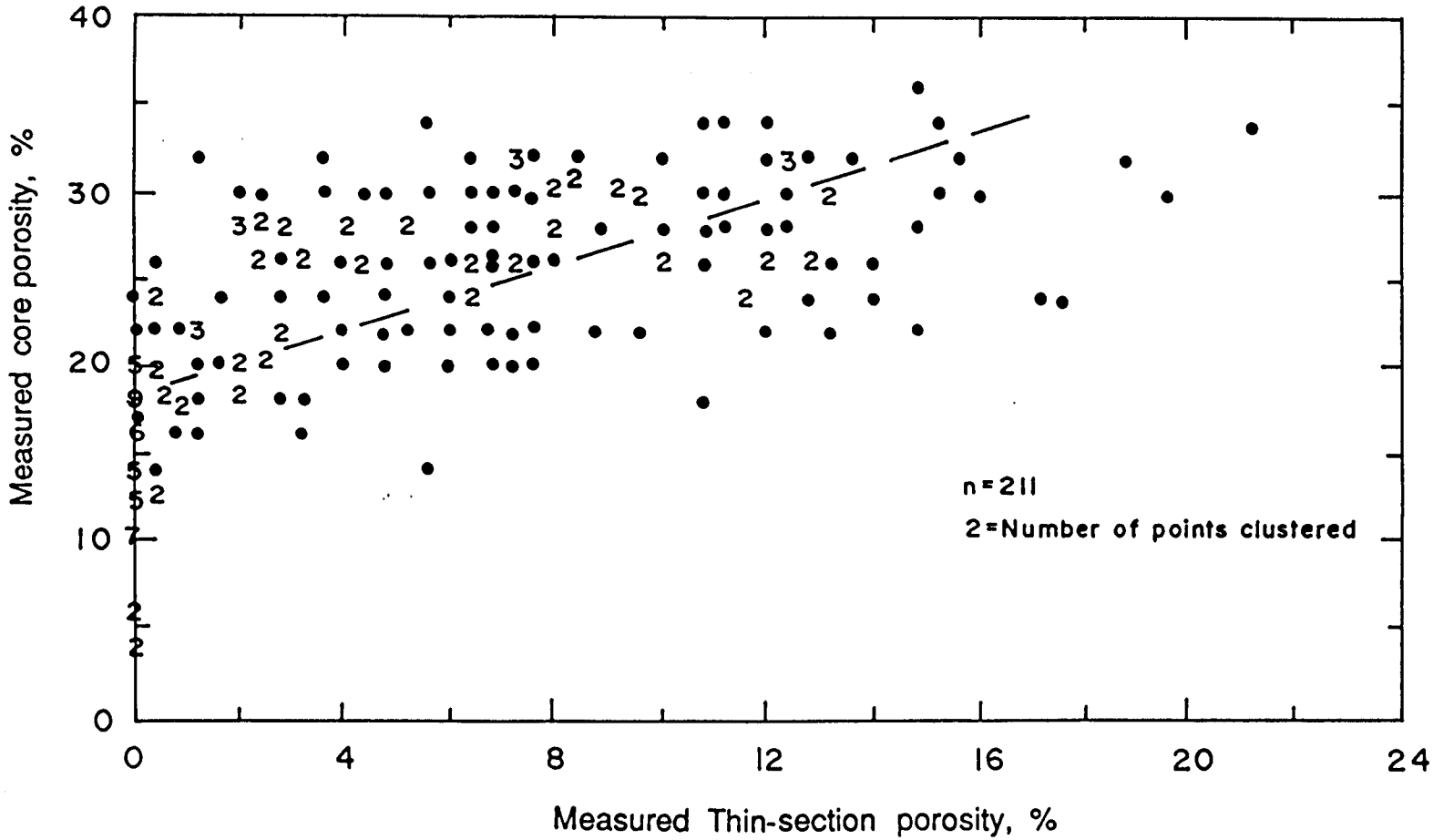

Figure 3.22. Plot of core porosity against thin-section porosity of the Surat Basin sandstones (all formations) with computed regression line. Correlation coefficient (r) = 0.65, r^2 = 0.43, standard error of estimate (s.e.) = 5.13, intercept (A) = 18.31, slope (B) = 0.87, significance (sig.) = 0.0000. A more detailed version of this plot which differentiates the quartzose and labile petrofacies is shown in Appendix 8.2.

the smallest of pores (e.g., intercrystalline micropores in the diagenetic clays/cement and other micropores within detrital matrix and altered framework grains) thereby giving higher values of core porosity;

3) the curved edges of the grain/cement - pore boundaries as observed in the 30 um-thick thin-sections result in the underestimation of the pore space to the advantage of the solid phase present, be it detrital grain or cement. This phenomenon, called the 'Holmes effect' (Hilliard, 1968), is particualrly important in the finer-grained and more poorly-sorted rocks (see also Halley, 1978).

POROSITY - PERMEABILITY RELATIONSHIPS

The relationships between core porosity and permeability and thin-section porosity and permeability for all formations are shown in Figures 3.23 and 3.24 respectively (plots of core porosity against permeability for each individual formation are documented in Appendix 2.7). The pattern of wide scatter between core porosity and permeability can be attributed to reservoir inhomogeneity as evidenced by the occurrence of much microporosity in some samples which contributes little, if any, to the permeability. Additionally, contribution to permeability by secondary porosity is variable and is dependent on the degree of interconnection with other pore types. Another component which possibly contributes to the scatter between thin-section porosity and permeability is that thin-sections were not in every case made from exactly the same place from where core plugs were taken for the porosity and permeability measurements. It is appropriate to mention here that thin-section porosity shows an exponential relationship with log permeability (Figure 3.24) which suggests that after attaining a certain threshold value, further increase in thin-section porosity does not increase log permeability significantly, presumably due to the fact that once a critical coordination number (cf.

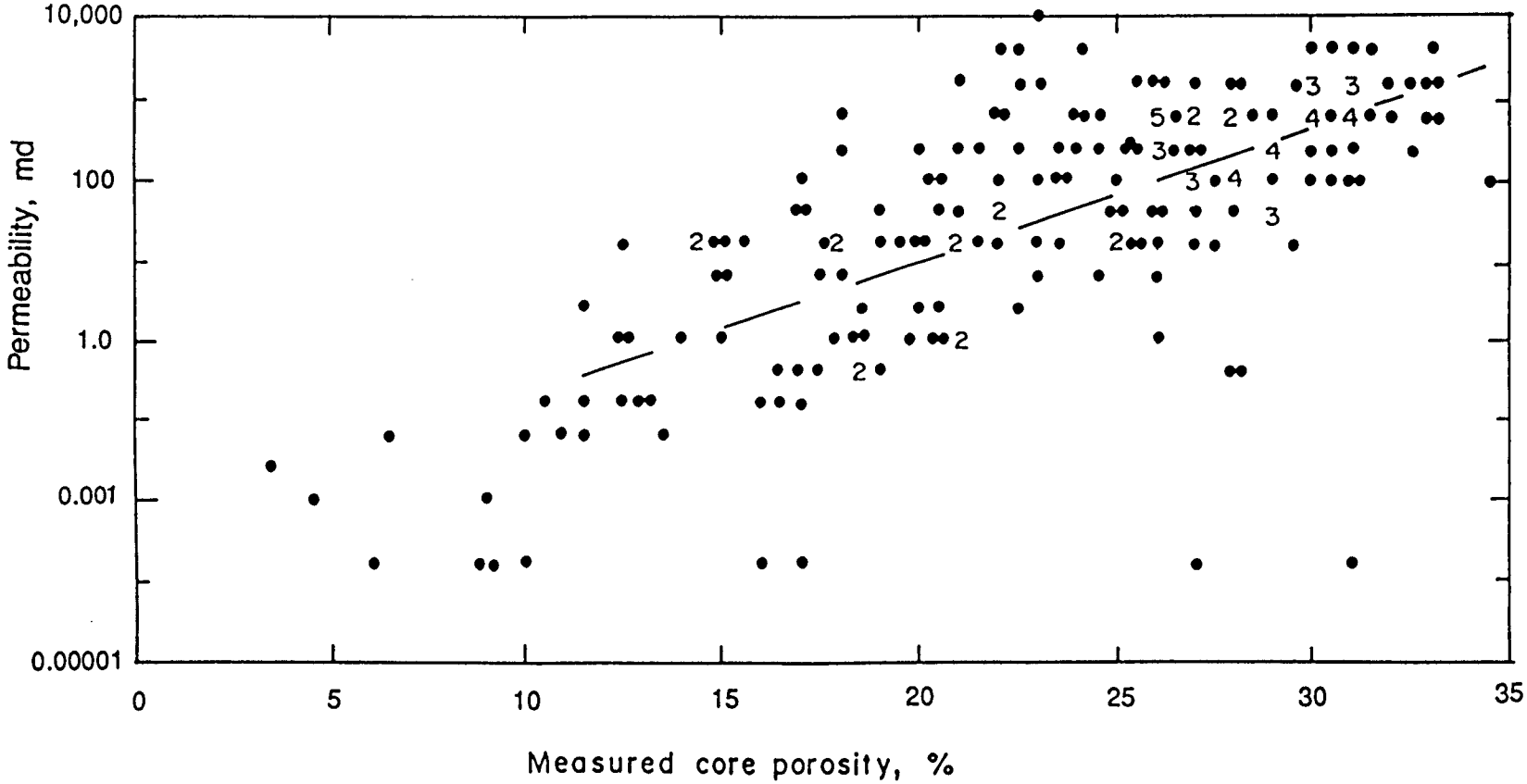

Figure 3.23. Plot of measured core porosity against permeability of the Surat Basin sandstones (all formations) with computed regression line. n = 211, r = 0.73, r^2 = 0.53, s.e. = 1.11, A = -2.54, B = 0.17, sig. = 0.0000. Statistical notations as in Figure 3.22. A more detailed version of this plot which differentiates the quartzose and labile petrofacies is shown in Appendix 8.3.

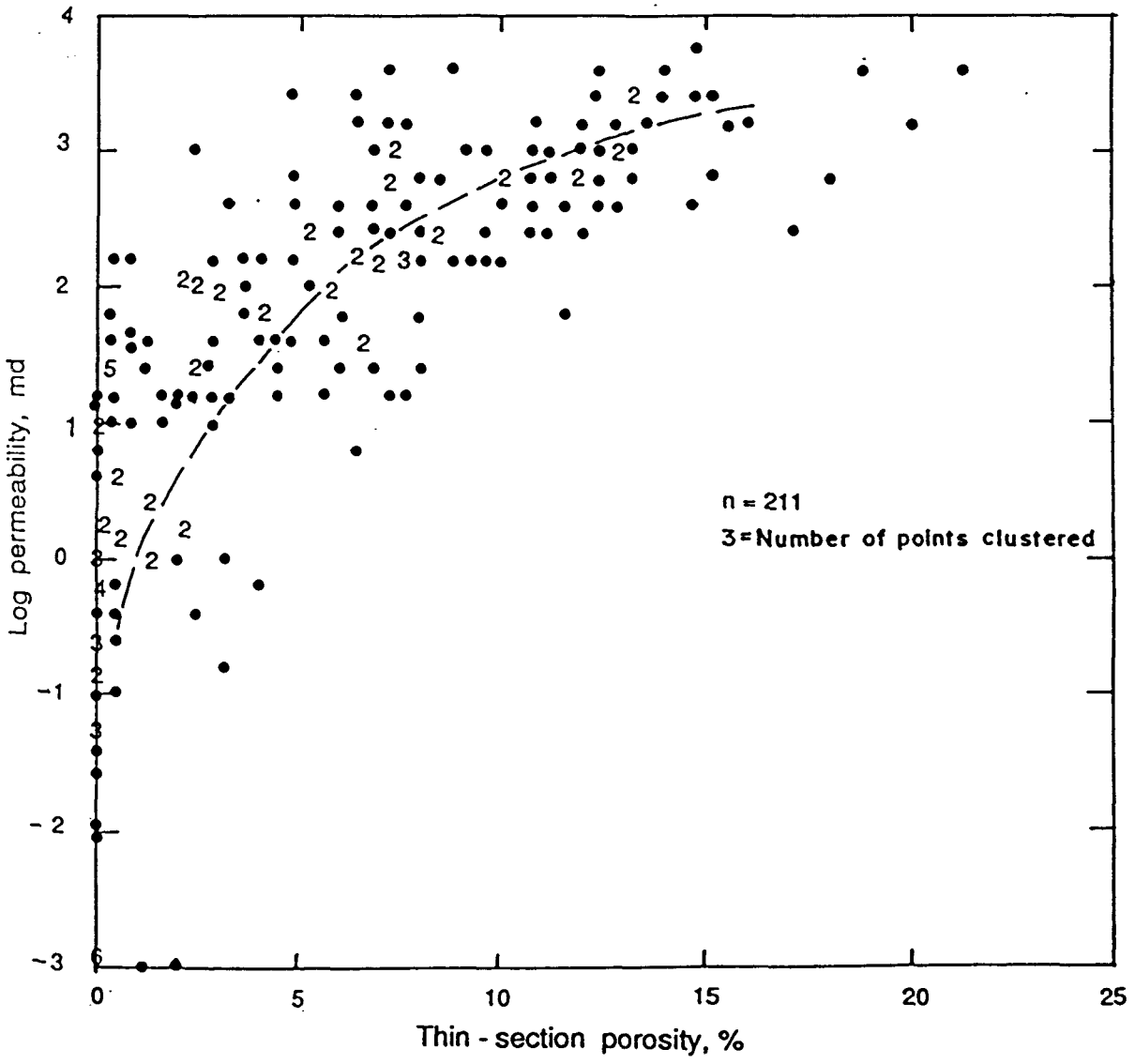

Figure 3.24. Plot of measured thin-section porosity against permeability of the Surat Basin sandstones (all formations). The curve is best visual fit. A more detailed version of this plot which differentiates the quartzose and labile petrofacies is shown in Appendix 8.4.

Wardlaw, 1980) is achieved further increase in the degree of pore interconnection does not significantly enhance shortening of fluid flow-paths. A log-log plot results in a linear relationship with a better correlation coefficient and standard error of estimate (Figure 3.25).

SECONDARY POROSITY: IMPORTANCE AND POSSIBLE MECHANISMS OF FORMATION

Importance of secondary porosity in the Surat Basin succession

A plot of thin-section porosity against depth is shown in Figure 3.26. A considerable proportion of the thin-section porosity in some formations comprises secondary porosity (Figures 3.27 and 3.28). That a considerable proportion of thin-section porosity comprises secondary dissolution porosity can be seen by comparing Figures 3.26 and 3.27 where it is evident that the pattern of distribution of thin-section porosity against depth (Figure 3.26) faithfully follows that of secondary porosity against depth (Figure 3.27). The importance of secondary porosity (as a proportion of thin-section porosity), however is more rigorously illustrated in Figure 3.28 which shows the distribution of secondary porosity index (SPI) against depth. SPI is here defined as the ratio of the total secondary porosity to the total thin-section porosity. It shows how much of the total macroporosity (as a fraction of thin-section porosity) is secondary in origin. In the whole stratigraphic column of the Surat Basin, the porosity in 14.4% of all samples showing more than zero thin-section porosity (n = 181) comprises 100% secondary porosity (SPI = 1), and 13.3% of all cases show no secondary porosity. The porosity in the rest of the samples is a combination of both primary and secondary porosity (cf. Appendix 2.5.1). Figure 3.29 shows the stratigraphic distribution of thin-section porosity which mimics that of secondary porosity index (Figure 3.30). A visual comparison of Figures 3.29 and 3.30 illustrates that on a first-order level the highest secondary porosity

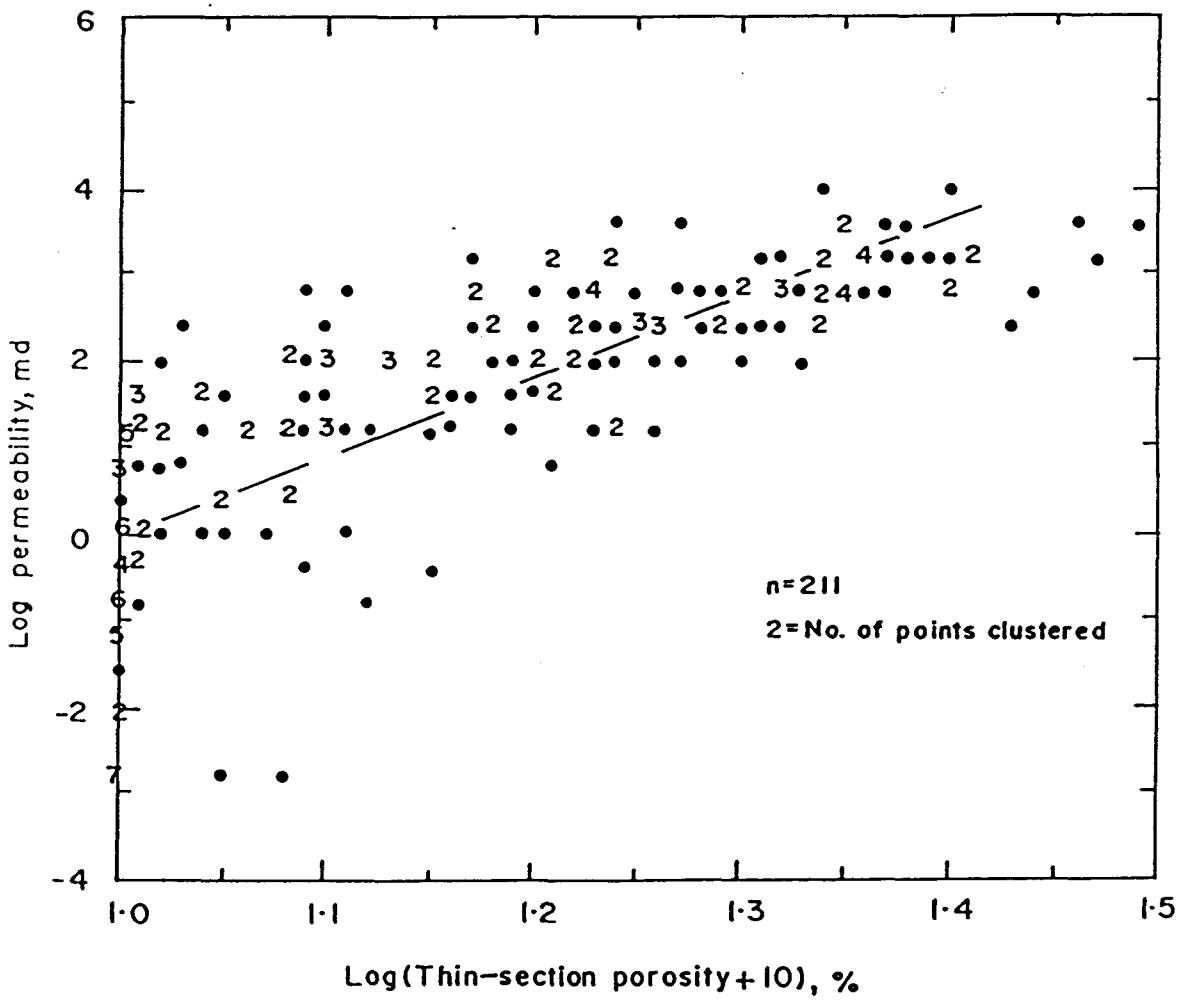

Figure 3.25. A log-log plot of thin-section porosity and permeability of the Surat Basin sandstones (all formations). To overcome the zero thin-section porosity in certain cases, a constant (10) is added to all the porosity values. Note better linear relationship compared to the semi-log plot in Figure 3.24. The regression line is computed. $r = 0.77$, $r^2 = 0.59$, s.e. = 1.03, A = -9.07, B = 9.04, sig. = 0.0000. Statistical notations as in Figure 3.22. See Appendix 8.5 for a more detailed version of this plot which differentiates the quartzose and labile petrofacies.

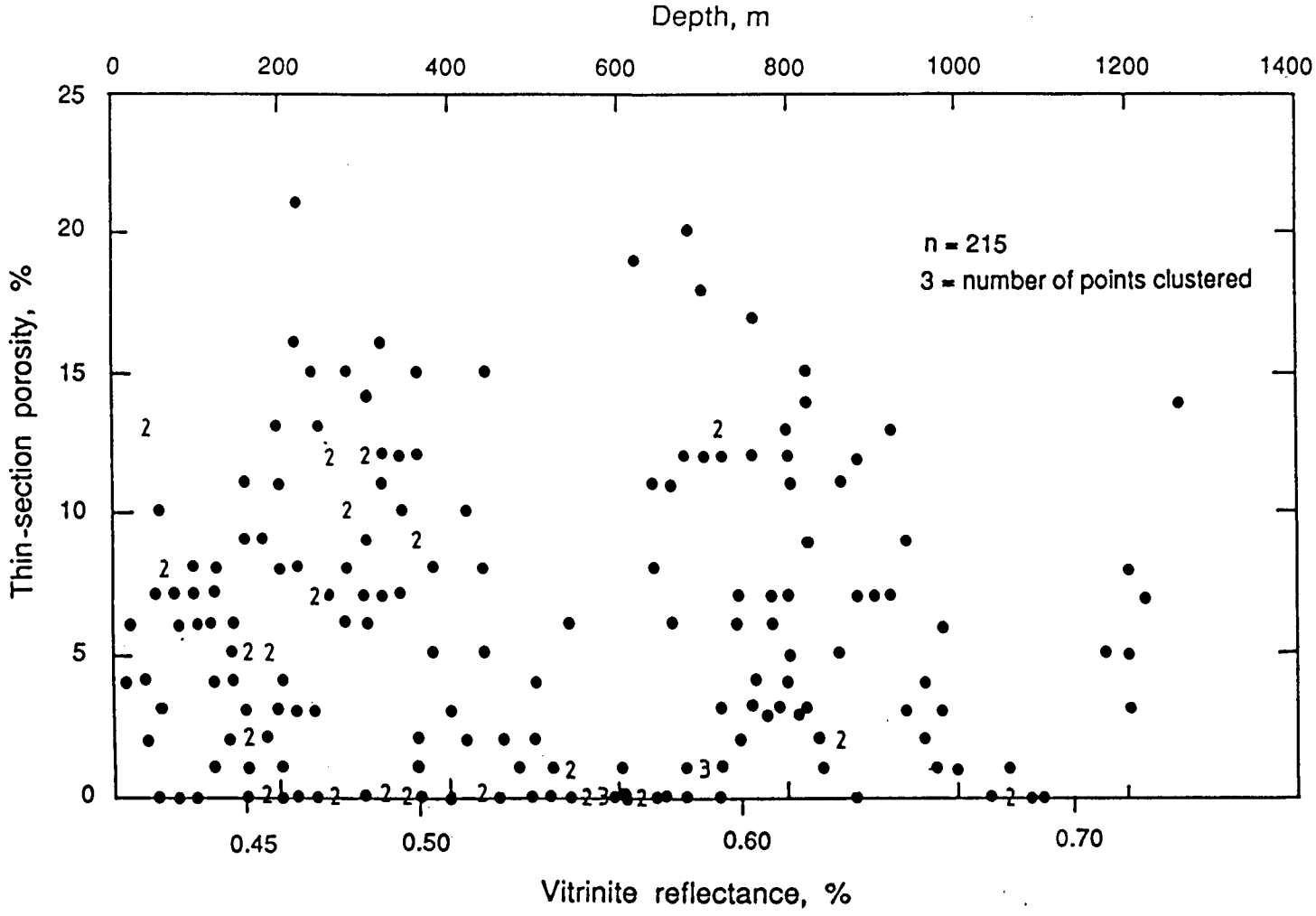

Figure 3.26. Thin-section porosity - depth relationship of the Surat Basin sandstones (all formations). Vitrinite reflectance scale is calculated from the R_o - depth regression equation (Appendix 2.8.1), based on reflectance data from GSQ Mitchell 2, GSQ Roma 8, GSQ Chinchilla 4, and GSQ Taroom 17. See Appendix 8.6. for a more detailed version of this plot which differentiates the quartzose and labile petrofacies.

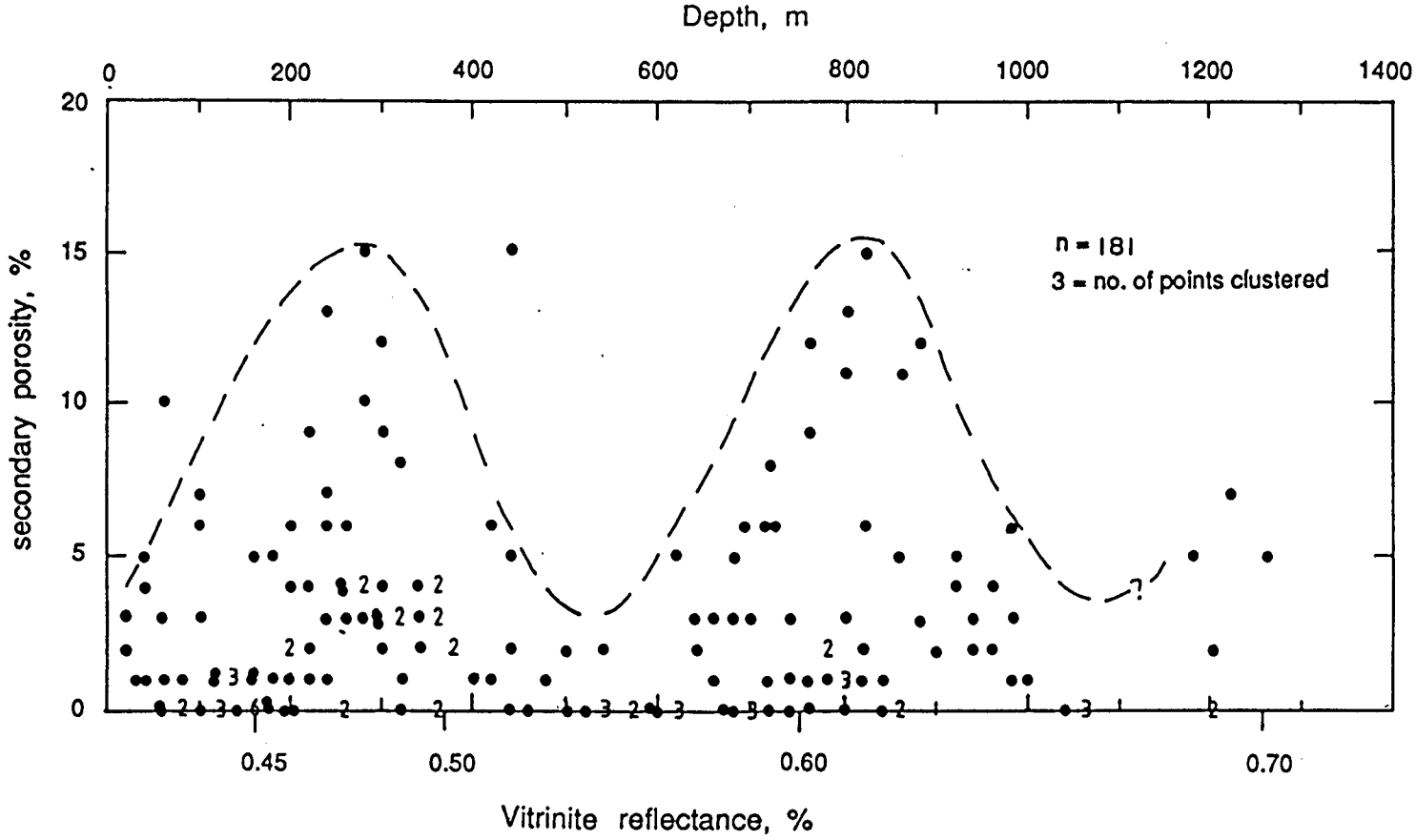

Figure 3.27. Plot of secondary dissolution porosity against depth of the Surat Basin sandstones (all formations) superimposed on vitrinite reflectance. Vitrinite reflectance scale as for Figure 3.26. Plot excludes all samples with zero thin-section porosity. A more detailed version of this plot which differentiates the quartzose and labile petrofacies is shown in Appendix 8.7.

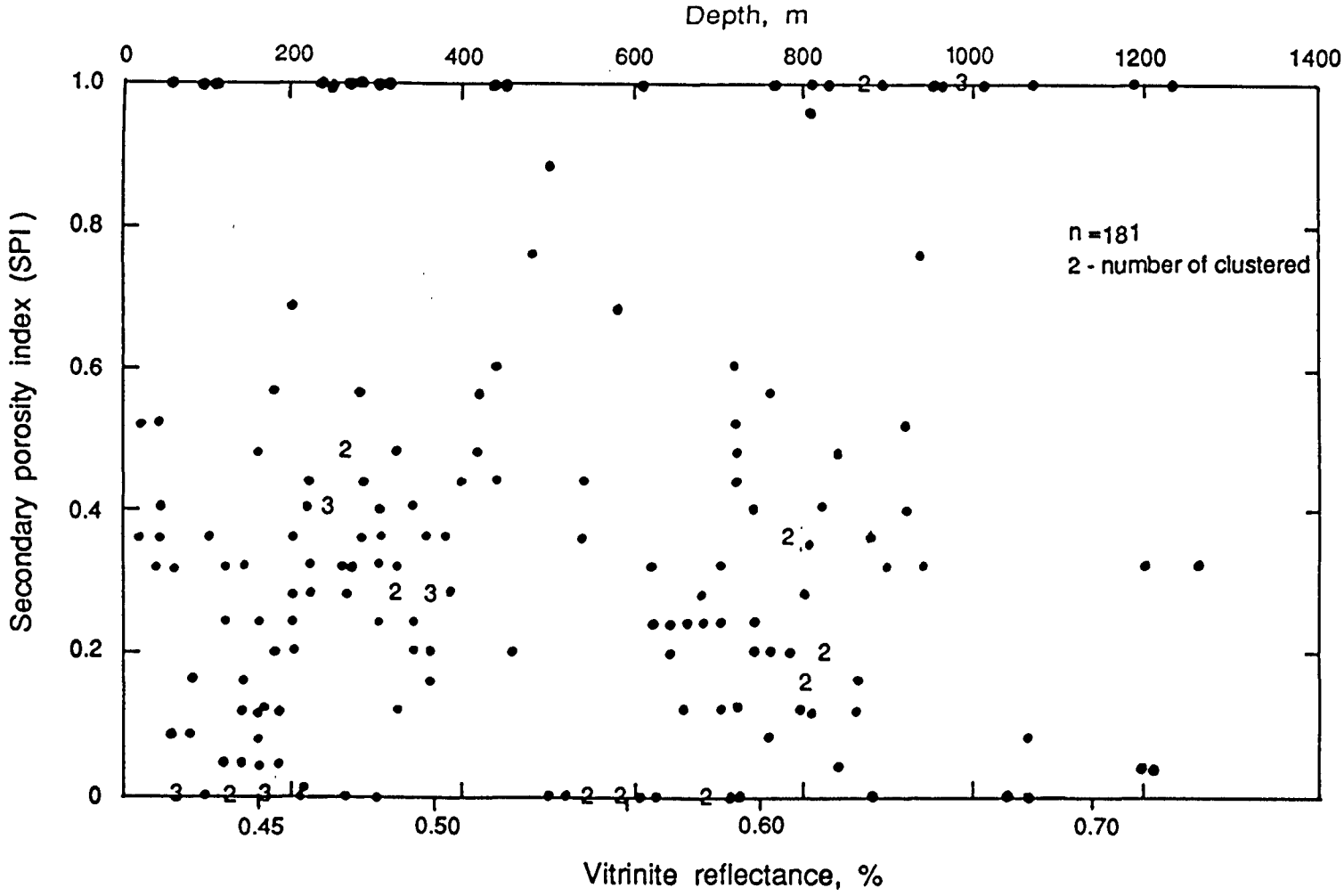

Figure 3.28. Plot of secondary porosity index (SPI) of the Surat Basin sandstones against depth (all formations). Vitrinite reflectance scale as in Figure 3.26. A more detailed version of this plot which differentiates the quartzose and labile petrofacies is shown in Appendix 8.8.

Figure 3.29. Means (asterisks) and bars defined by plus and minus one standard deviation of secondary porosity in different stratigraphic units of the Surat Basin succession. The means and standard deviations in this figure (and in Figure 3.30) are not statistically rigorous values because the data sets constitute a constant sum which is therefore constrained. Although the fields defining standard deviation are statistically meaningless they are measures of dispersion of the data and are useful in visually illustrating the contrast in populations. Stratigraphic units: 1 - Precipice Sandstone, 2 - Evergreen Formation, 3 - Hutton Sandstone, 4 - Walloon Coal Measures, 5 - Springbok Sandstone, 6 - Westbourne Formation, 7 - Gubberamunda Sandstone, 8 - Orallo Formation, 9 - Mooga Sandstone, 10 - Bungil Formation, 11 - Wallumbilla Formation and Surat Siltstone (taken together), 12 - Griman Creek Formation.

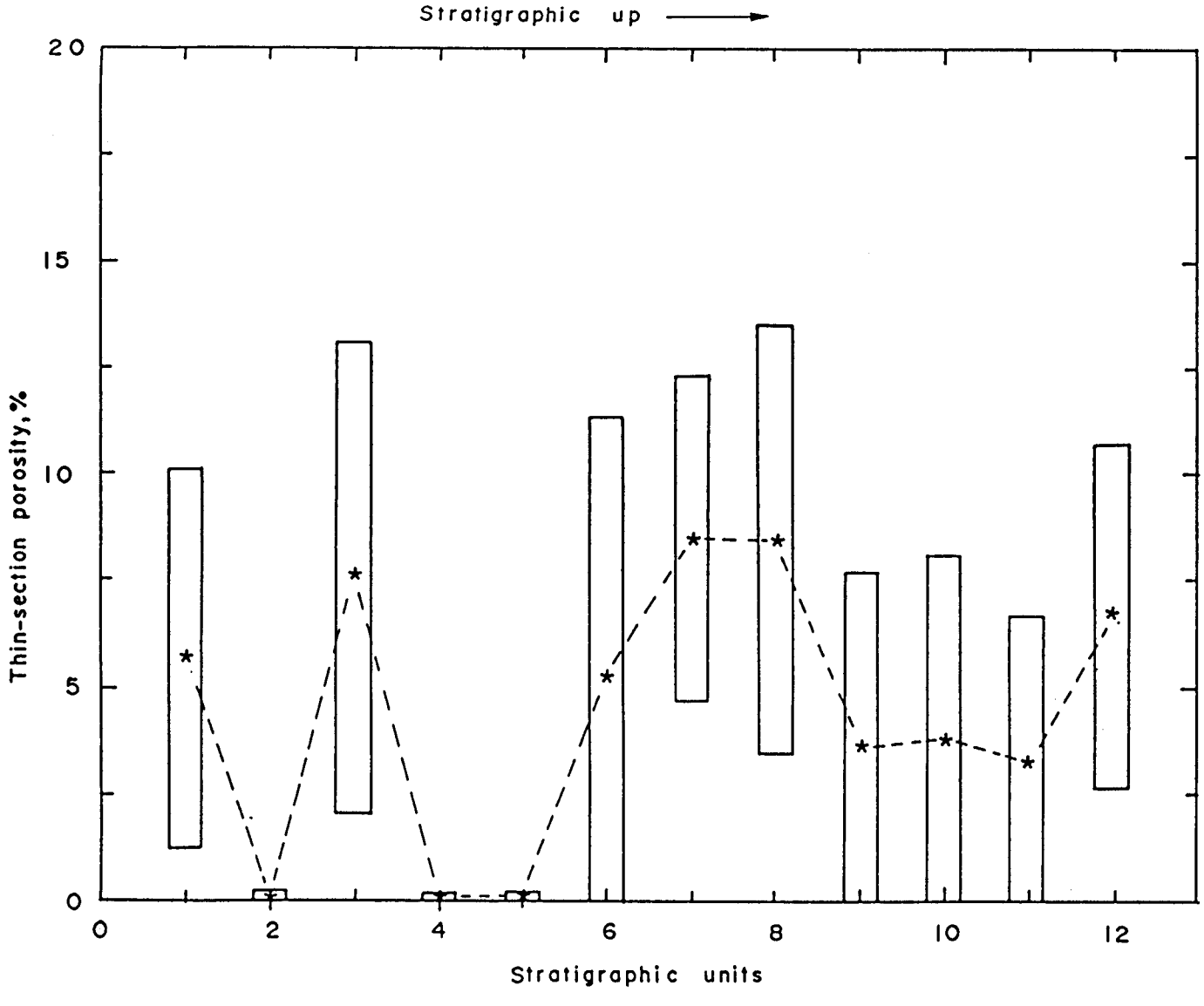
Stratigraphic up
20
15
10
5
0
Thin-section porosity, %
0
2
4
6
8
10
12
Stratigraphic units

Figure 3.30. Stratigraphic distribution of SPI in the Surat Basin sandstones (all formations). Symbols as for Figure 3.29.

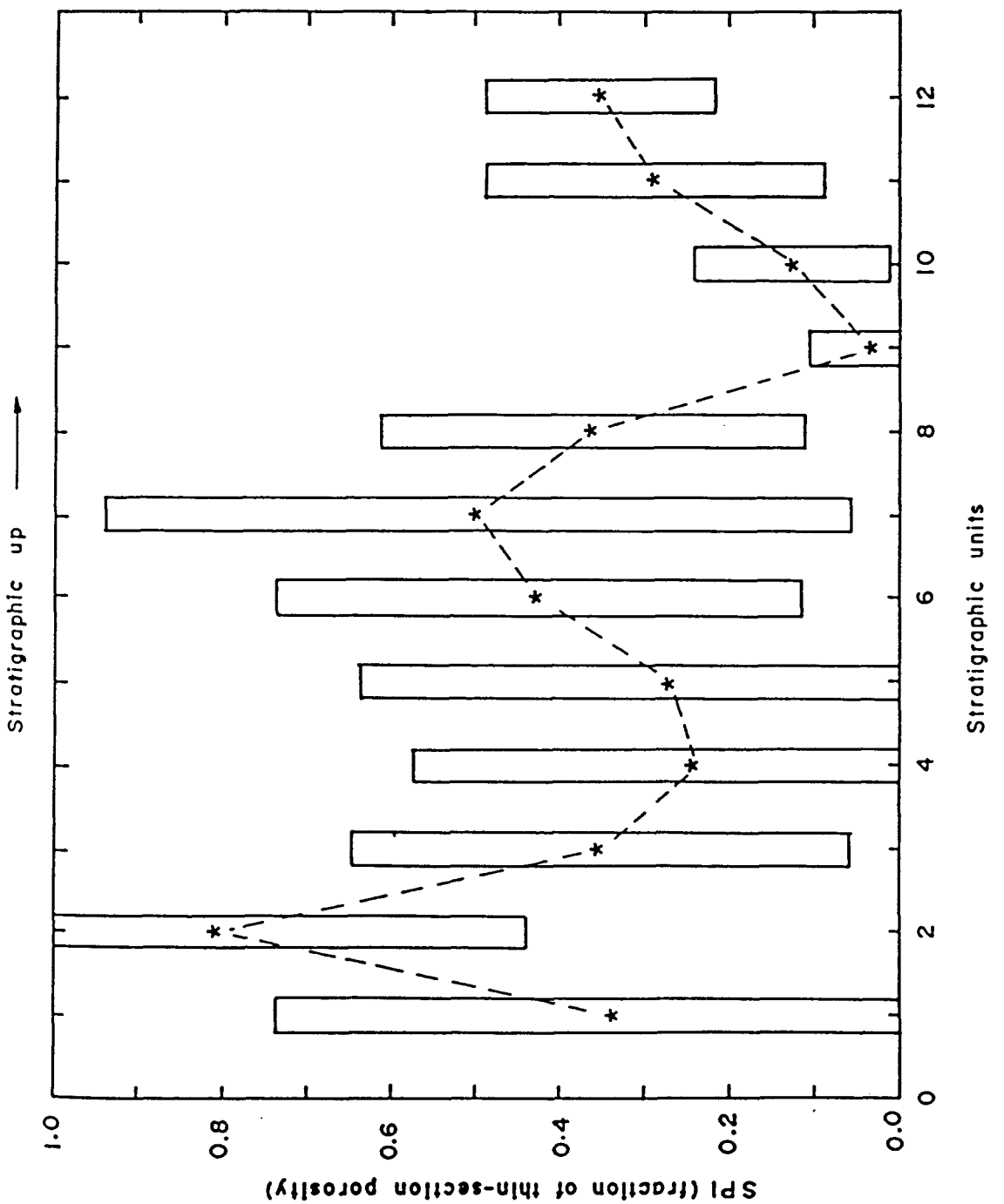
Stratigraphic up
SPI (fraction of thin-section porosity)
1.0
0.8
0.6
0.4
0.2
0.0
0
2
4
6
8
10
12
Stratigraphic units

occurs in formations displaying high thin-section (and primary) porosity. The Evergreen Formation is an exception, which despite showing very low thin-section porosity, has the highest SPI suggesting presumably an overriding influence of organic maturation products (discussed in text later) compared to the influence of original depositional porosity (and texture) on secondary porosity development.

Secondary porosity in other basins

The development of secondary porosity at depth and the resulting deviation from the normal porosity-depth relationship was first predicted by Proshlyakov (1960) and was subsequently documented by Savkevich (1969) (Figure 3.31). Since then the presence of secondary porosity has been increasingly recognised in reservoirs of different ages and from different localities around the world; moreover, some hydrocarbon fields such as the giant Prudhoe Bay Field have been attributed to reservoirs formed by the wholesale generation of secondary porosity (Schmidt and McDonald, 1979c). Shanmugam (1985a) reported that secondary porosity is the dominant type of porosity in major sandstone reservoirs worldwide (as much as 70% of total porosity) ranging in age from Cambrian to Pleistocene. The estimated importance of secondary porosity would probably be even higher given the difficulty in recognising certain of its varieties (e.g., intergranular cement-dissolution type).

Mechanisms of secondary porosity development

To account for the ubiquitous secondary porosity in many hydrocarbon reservoirs various mechanisms have been put forward by many workers. Dissolution caused by maturation products of organic matter from the intercalated mudrocks is by far the most popular. However, more than one mechanism might be operating in specific basins. The idea that the organic maturation products that form prior to hydrocarbon generation create

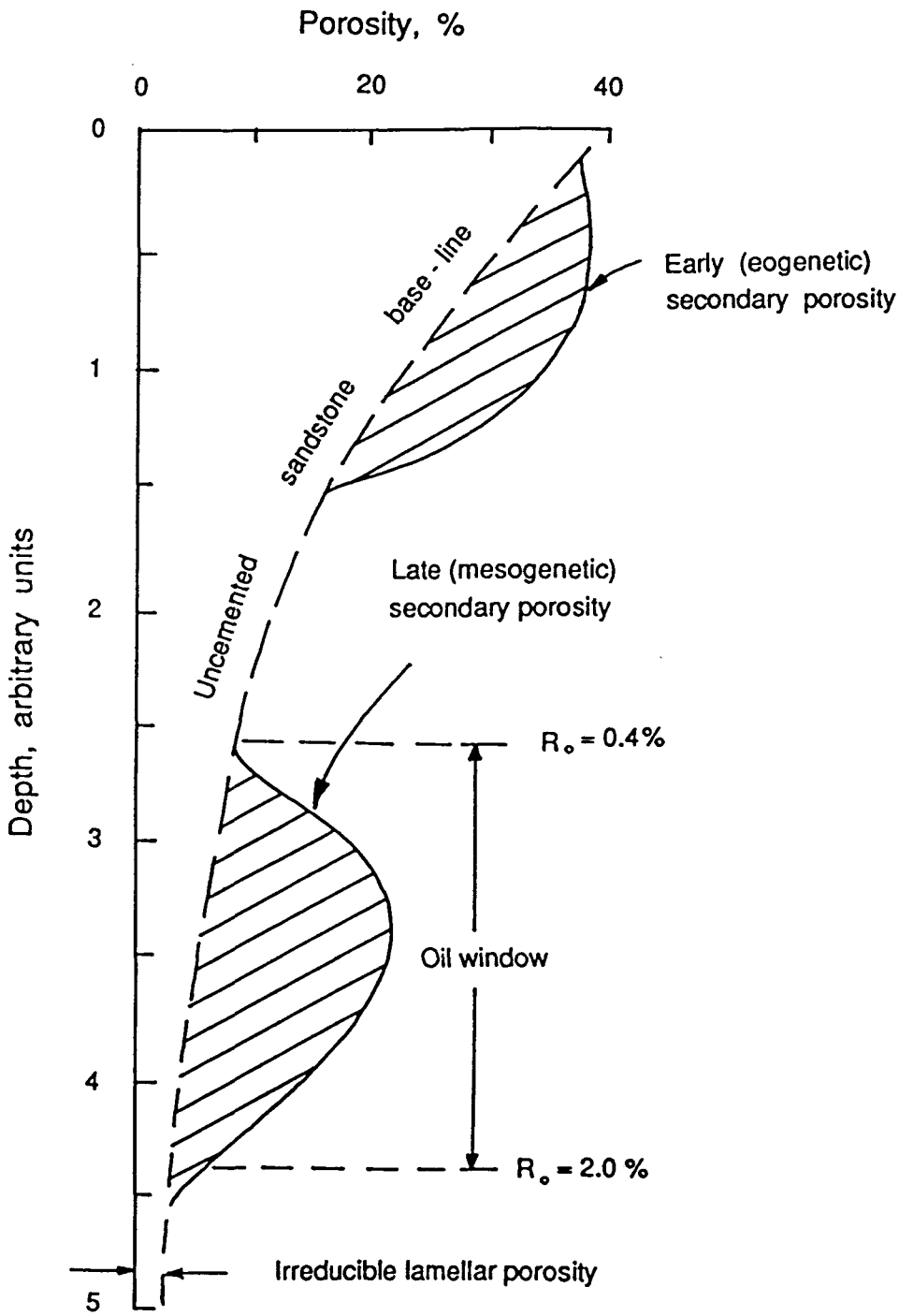

Figure 3.31. Schematic diagram showing the geologic evolution of sandstone porosity. Modified from Savkevich (1969), Hayes (1979) and Schmidt and McDonald (1979a).

secondary porosity was first suggested by Chepikov et al (1961). The work of these Soviet researchers went largely unnoticed until Schmidt and McDonald (1979a) and Hayes (1979) in independent parallel studies came to the same conclusion that most of the porosity in many hydrocarbon reservoirs from around the world comprises secondary porosity and that it is created by the products of organic maturation expelled from the intercalated mudrocks. Surdam et al (1984), Surdam and Crossey (1985), Crossey et al (1986) and Edman and Surdam (1986) proposed that mobility/complexing of aluminium (which determines the aluminosilicate dissolution) can be increased by several orders of magnitude in some organic acids (e.g., mono and difunctional carboxylic acids) and phenolic solutions which are believed to be produced by the thermal degradation of kerogen prior to hydrocarbon generation. These acids also dissolve carbonates. Carothers and Kharaka (1978) have reported anions of such organic acids in oil-field waters from California and the Gulf Coast. The peak production of these organic acids occurs between 80° C and the onset of hydrocarbon generation (120°C) (Figure 3.32). Thermal and bacterial degradation of these organic acids may produce CO_2 which (as carbonic acid) may also acount for the dissolution of carbonates and feldspars. Consequently, enhancement and/or preservation of porosity prior to hydrocarbon generation is a natural consequence of a subsiding pile of sediments comprising sandstones and organic-rich mudrocks.

Secondary porosity development controlled by burial depth in the Surat Basin

In the Surat Basin there is evidence to suggest that the product of organic maturation is one of the most important mechanisms of secondary porosity development at depth, as indicated by the secondary porosity - depth relationship superimposed on vitrinite reflectance (Figure 3.27).

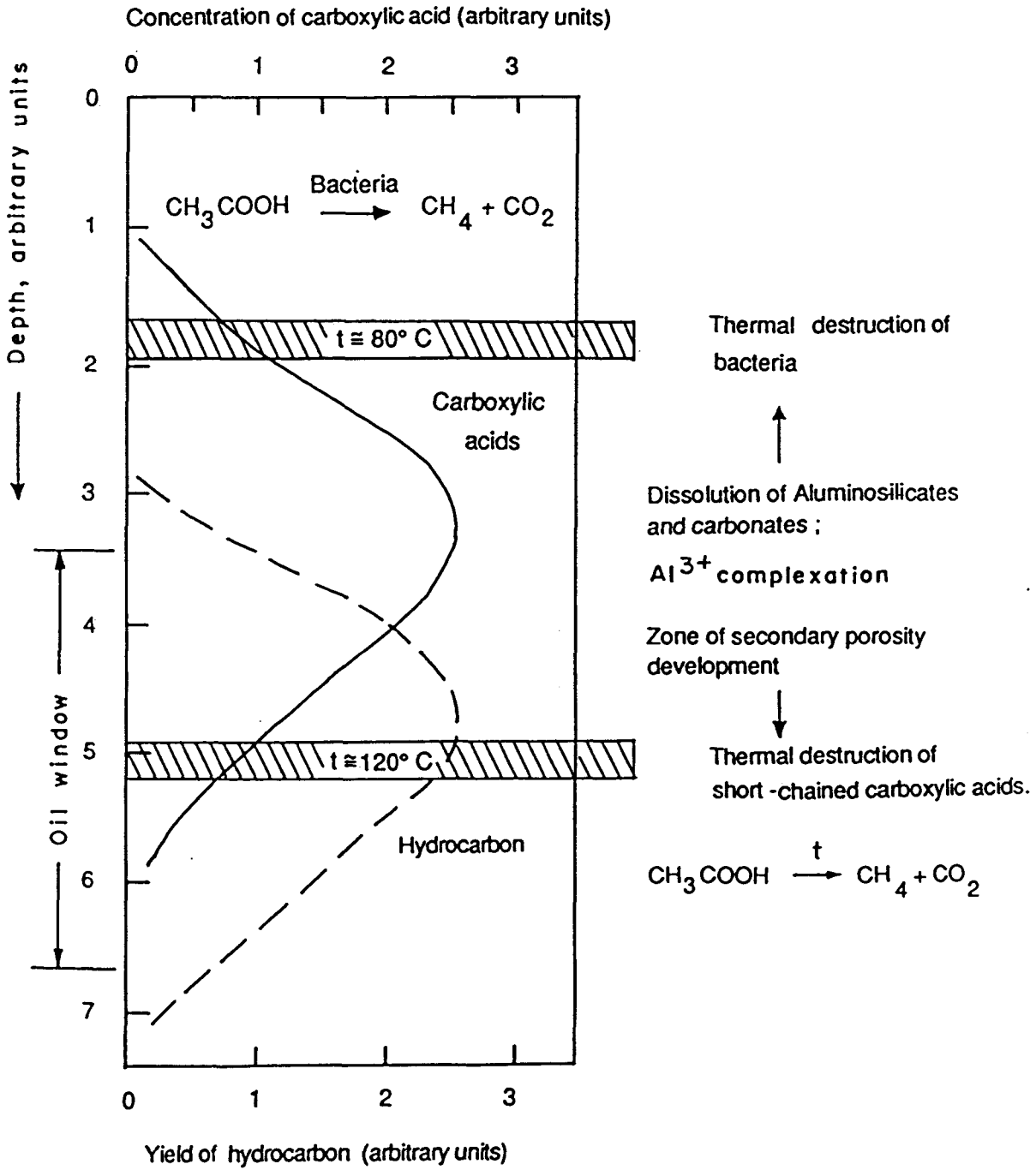

Figure 3.32. Schematic diagram showing the the zone of maximum secondary porosity development at depth as a function of carboxylic acid concentration. Location of the oil window is shown for comparison. Modified after Carothers and Kharaka (1978).

It is interesting to note that there are two distinct zones of occurrence of increased secondary porosity: one at depths corresponding to vitrinite reflectance values of 0.45-0.50% and the other at depths corresponding to reflectance values between 0.60-0.65% (Figure 3.27). These zones of maximum secondary porosity development are roughly discordant to the gross stratigraphy/structure of the basin (Appendix 2.5.2). The permeability - depth relationship (Figure 3.33) roughly follows that between secondary porosity and depth (Figure 3.27) suggesting that, on the whole, secondary porosity forms part of the effective porosity and contributes to permeability (Figure 3.33). The possible genetic significance of the two zones of enhanced porosity and permeability in the Surat Basin succession is addressed in the following section.

The role of kerogen type on levels of thermal maturity

The hydrocarbon generation window (including oil and wet gas) has been accepted at a level of organic maturity equivalent to R_o = 0.5 - 0.6% to 1.5 - 2.00% (Tissot and Welte, 1978, p. 70, 335-350; Waples, 1980, p. 108) but over the years these models have been modified by many workers mainly to account for the presence of commercial quantities of hydrocarbon in specific basins with much lower levels of organic maturity (Powell et al, 1978; Snowdon and Powell, 1982). It has been known that different types of kerogen reach the threshold of intense hydrocarbon generation at different levels of thermal maturity (Powell and Snowdon, 1983; Tissot, 1984). In a basin comprising organic matter with more than one type of kerogen/maceral (which is the case with the Surat Basin and is characteristic of most petroliferous basins), hydrocarbon generation takes place in different phases/episodes corresponding to the different levels of thermal maturity. As has been shown in Chapter 8, the Surat Basin organic matter is represented mainly by two types of kerogen: hydrogen-poor typical

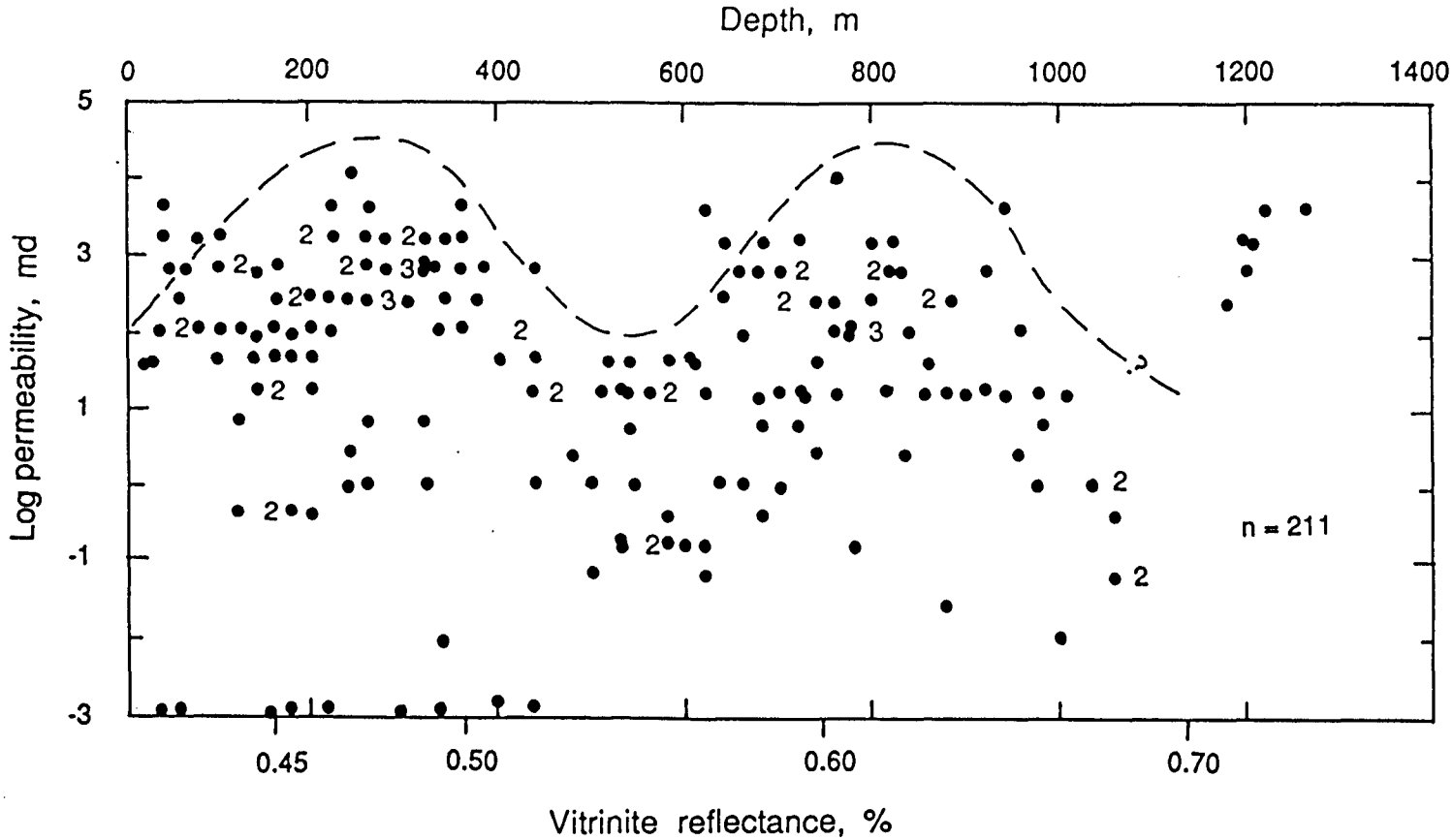

Figure 3.33. Permeability - depth relationship of the Surat Basin sandstones (all formations) superimposed on vitrinite reflectance. Vitrinite reflectance scale as for Figure 3.26. See Appendix 8.9. for a more detailed version of this plot which differentiates the quartzose and labile petrofacies.

type III vitrinitic kerogen and the more hydrogen-rich type II kerogen represented by the liptinitic/exinitic macerals. The implication for the episodic nature of hydrocarbon generation lies in the fact that certain liptinite-rich macerals (e.g., resinite and suberinite) have recently been shown to reach the ceiling of the hydrocarbon window at a much lower level of thermal maturity than conventional wisdom might otherwise have suggested (Snowdon and Powell, 1982; Powell and Snowdon, 1983; Shanmugam, 1985c; Khorasani, 1987; see also Chapter 8). Products of organic maturation, as it will be shown below, constitute potent agents of secondary porosity development and the previously-mentioned two zones of secondary porosity development corresponding to different ranges of Ro may be indicative of the two phases of oil/gas generation as would be expected for hydrocarbon source rocks containing two different types of kerogen. Additionally bacterial degradation of organic matter at shallow depth is known to create various organic acids and CO_2 (along with CH4; Tissot and Welte, 1978) and they might also have contributed to the formation of secondary porosity in the immature zone lying above the conventional oil window (Figure 3.27). Schematically a kerogen molecule can be thought of as consisting of an inner aromatic core surrounded by an aliphatic portion to which various oxygen-containing groups such as carboxylic (-COOH), phenolic (-OH), ketone (>CO), methoxyl ($-OCH_3$) and ester (-COOR) are peripherally attached (Figures 3.34 and 3.35). With increasing time - temperature (burial) the different functional groups are detached giving rise to various acids, ketones, esters and phenols (Figure 3.34). Surdam and Crossey (1985) pointed out that the peak concentration of organic acids (at 80-120°C) coincides in time, temperature and space with mixed-layer smectite/illite ordering reactions in shales (100-110°C) (see also Powers, 1967 and Burst, 1969). Flux of water due to illitization of smectite (and/or compaction) will mobilize these organic acids to adjacent sandstones dissolving not

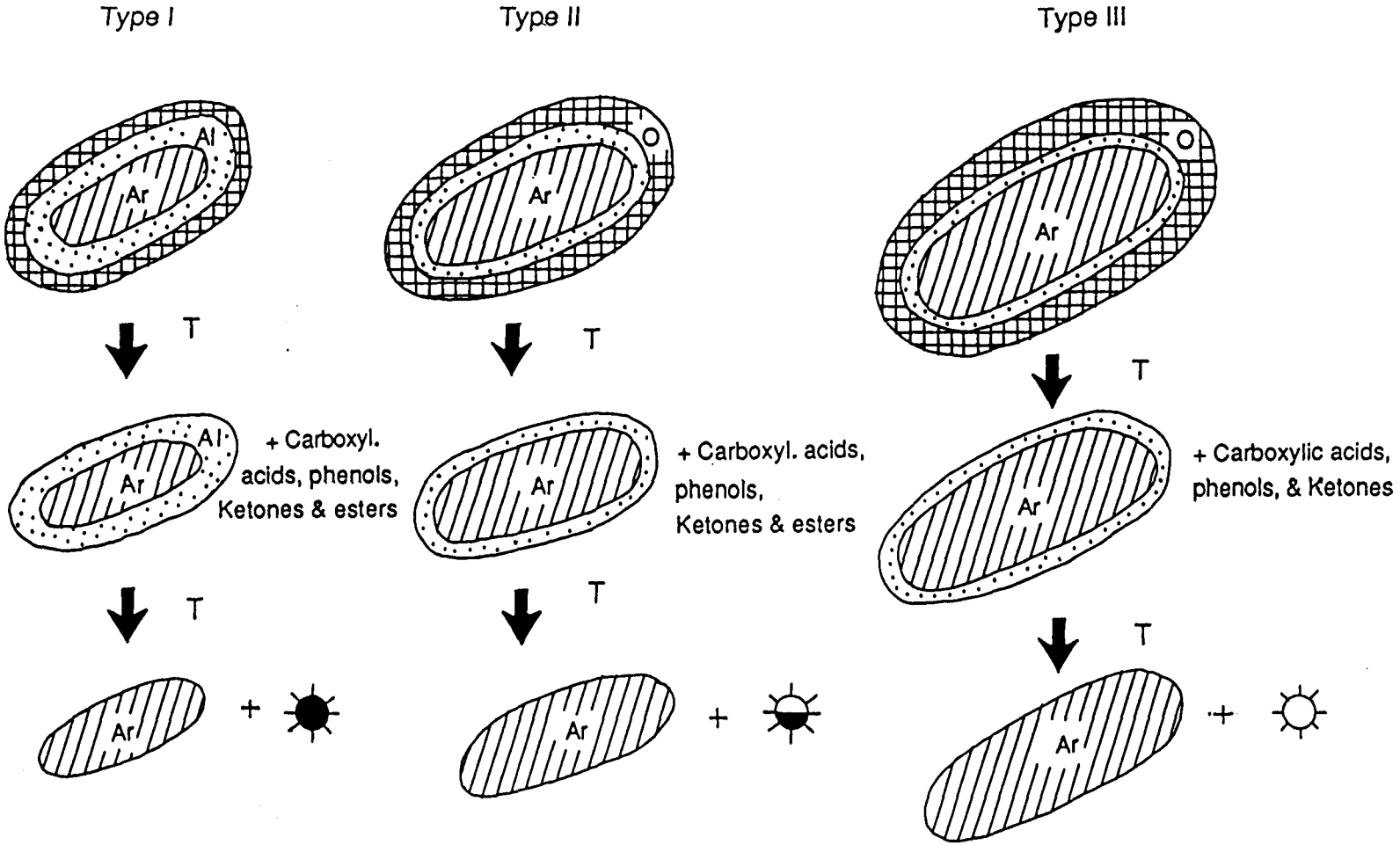

Figure 3.34. Schematic diagram showing the general composition and evolutionary pathways of different types of kerogen as a function of thermal maturation with the concomitant liberation of various functional groups prior to hydrocarbon generation. Ar - aromatic core, A - aliphatic rim, O - oxygen-bearing rim, ☼ - gas, ✹ - oil and gas. Note the relative abundance of aliphatics, aromatics and different oxygen-bearing groups and the resulting types of generated hydrocarbons. Modified from Erdman and Surdam (1986).

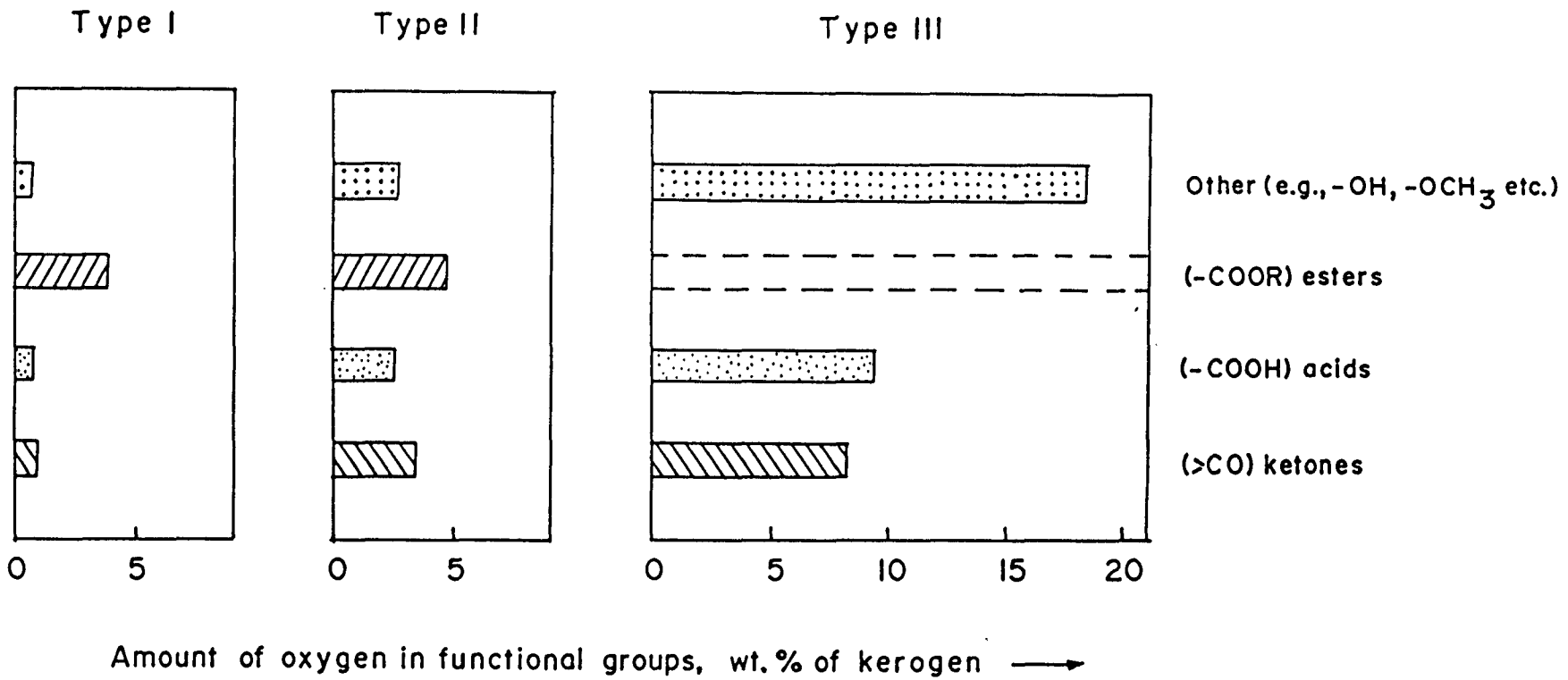

Figure 3.35. Amounts of oxygen engaged in various functional groups in different types of immature kerogens. From Tissot and Welte (1978, fig. II 4.13) based on studies by Robin (1975). Note the absence of ester groups in type III kerogen.

only aluminosilicates but also carbonates. Carbonates are dissolved in carboxylic acid solution over a pH range from 5 to 9 (Surdam et al, 1984, figure 9B). Thus the presence of these organic acids alone can explain some of the secondary porosity resulting from dissolution of intergranular/grain-replacive carbonates and framework grains.

The effect of kerogen type on secondary porosity development

The type of organic matter will have a profound effect on the nature and amount of corrosive products formed prior to hydrocarbon generation. As type III kerogen is highly oxygen-rich, it will provide the highest amount of carboxylic acids, ketones, phenols and other oxygen-containing compounds (Figure 3.35). The chemistry of individual products will affect the solubility of silicate minerals, as noted by Huang and Keller (1970) and Surdam and Crossey (1985). Surdam and Crossey (1985) cite works of Mason (1983) who found that the total dissolved liquid effluent resulting from condensation of coal gasification comprises mostly (85-90%) phenols and the rest carboxylic acids. Some phenols are known to have increased the solubility of aluminosilicates by three orders of magnitude (Surdam and Crossey, ibid.). Hence a dramatic dissolution reaction may be expected to occur in sandstones juxtaposed with thermally mature mudrocks rich in coaly/woody type III organic matter. Type III kerogen has the highest amount of oxygen-containing functional groups (Figure 3.34) and the amount of acidic and phenolic components produced by it are also very high compared to the other kerogen types (Figure 3.35). The coal and dispersed organic matter of the Evergreen Formation of the Surat Basin is moderately oxygen-rich (Golin and Smyth, 1986) and the underlying Bowen Basin coals and coaly organic matter are very rich in inertinite with variable amounts of vitrinite (Figure 3.36). Vitrinite and inertinite, which are commonly equated with type III kerogen (Figure 3.34), are the most oxygen-rich

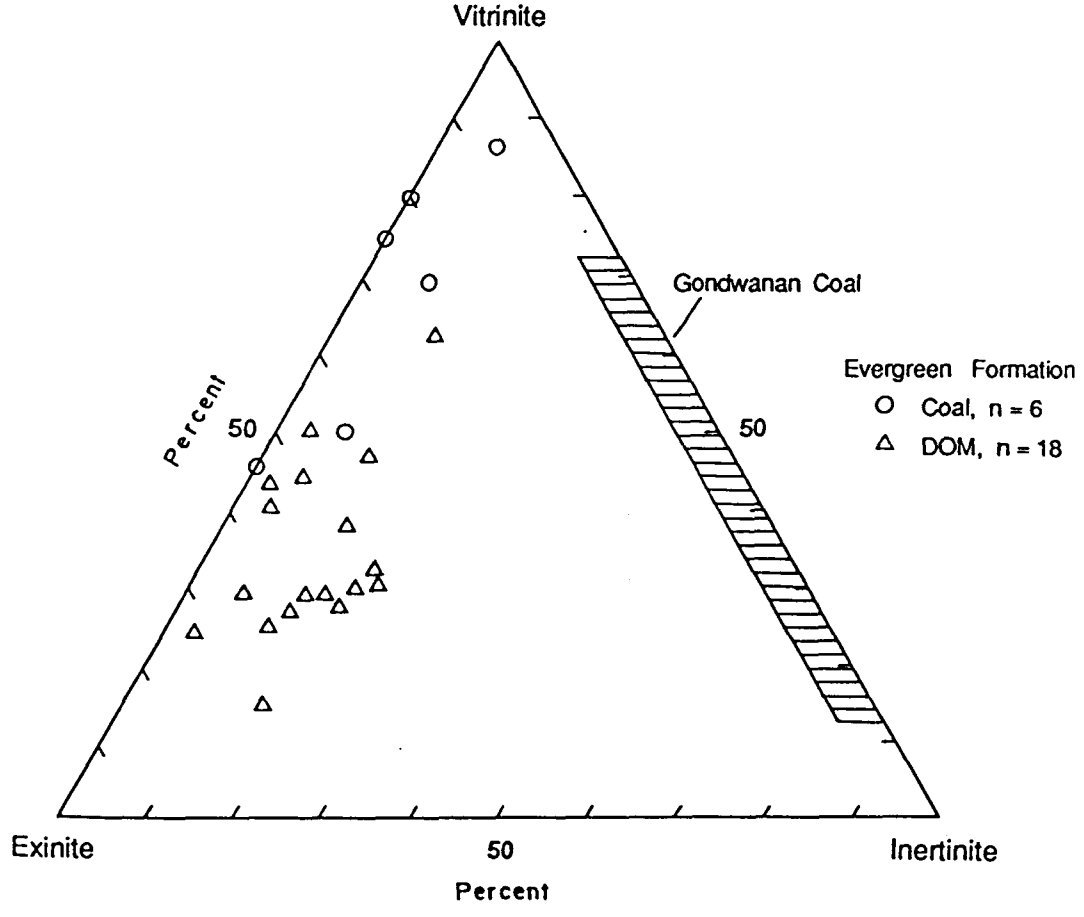

Figure 3.36. Maceral composition of the Evergreen Formation, Surat Basin, and of Permian coals of the underlying Bowen Basin. Composition of the Evergreen Formation after Golin and Smyth (1986); Gondwanan coal maceral composition based on data from Cook (1975) and Stach et al (1982, p. 117-198).

macerals. If products of organic maturation are valid agents of dissolution porosity, under comparable circumstances secondary porosity may be expected to be volumetrically more important in basins rich in coaly/woody type III organic matter (cf. Chapter 8). Additionally, type III organic matter would produce enormous quantities of CO_2 after thermal decarboxylation of various oxygen-containing groups, such as carboxylic acids, phenols, ketones etc, or by the bacterial degradation of these organic components above the intense zone of acid formation (Figure 3.32). The acidic environment due to CO_2 is an active agent for the dissolution of carbonates and aluminosilicates (Schmidt and McDonald, 1979a; Siebert et al, 1984). The amount of CO_2 generated from organic maturation is dependent on the kerogen type and is highest for type III kerogen (Figure 3.37). So the dissolution of framework grains/cements and the complexing of aluminium by organic acids and hence the creation/preservation of secondary porosity at depth will be more important in clastic successions rich in hydrogen-poor and oxygen-rich type III organic matter.

The role of meteoric flushing

The second most important mechanism of secondary porosity development in the Surat Basin sandstones is probably meteoric washing which commenced after the inception of the Great Artesian System in the Tertiary (Bowering, 1982). Flushing of CO_2-charged water is active at present in the Great Artesian Basin as exemplified by the high dissolved CO_2 content and very low salinity of the formation waters. In some shallowly-buried units (above the oil window) meteoric flushing is believed to be the principal agent of secondary porosity development (cf. Arditto, 1982, 1983).

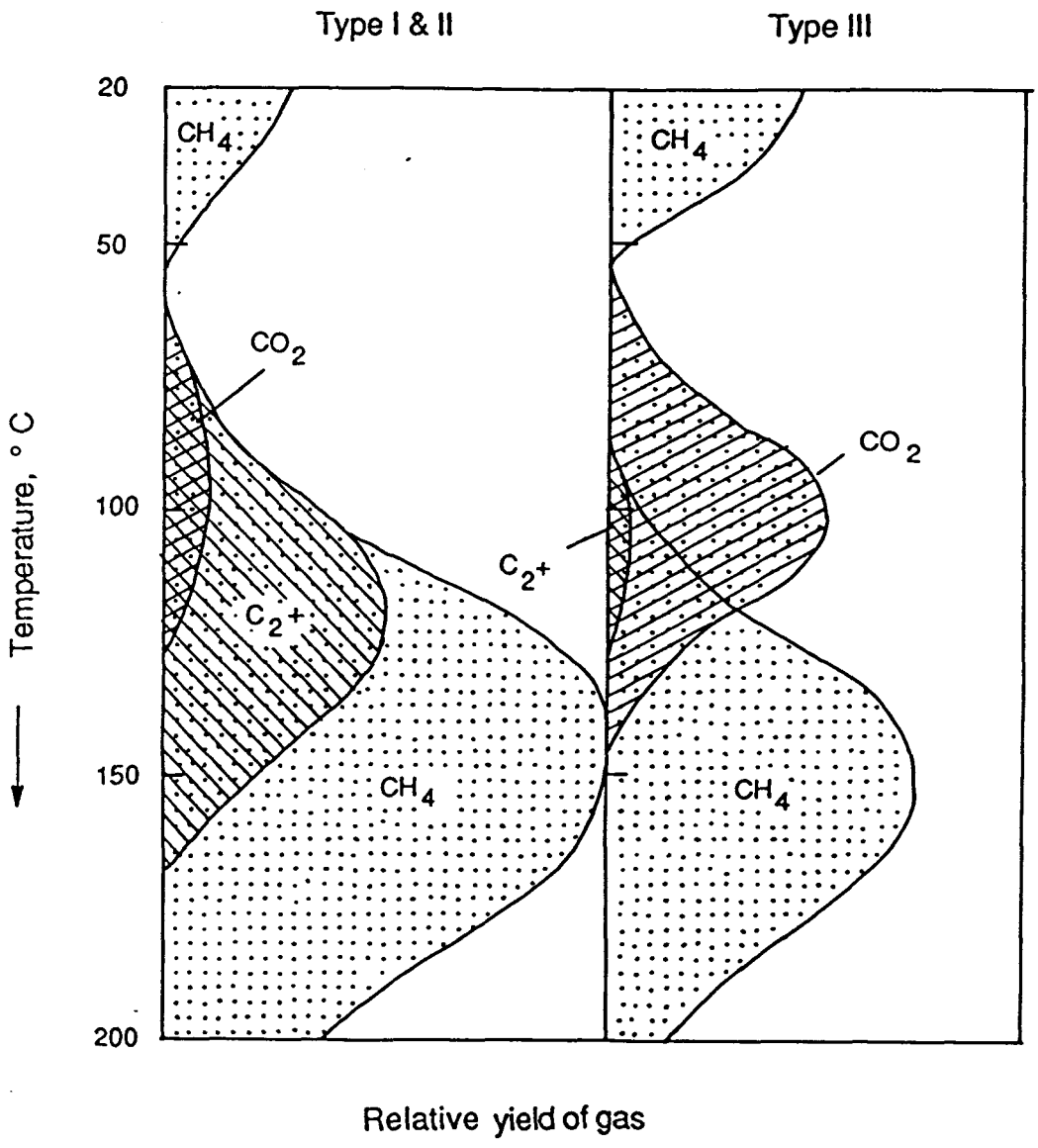

Figure 3.37. Relative yield of gases from different types of organic matter. C_{2+} represents hydrocarbons heavier than CH_4 in gas phase. Yield of liquid hydrocarbon would follow the pattern of C_{2+} gases. From Hunt (1979, fig. 5-6).

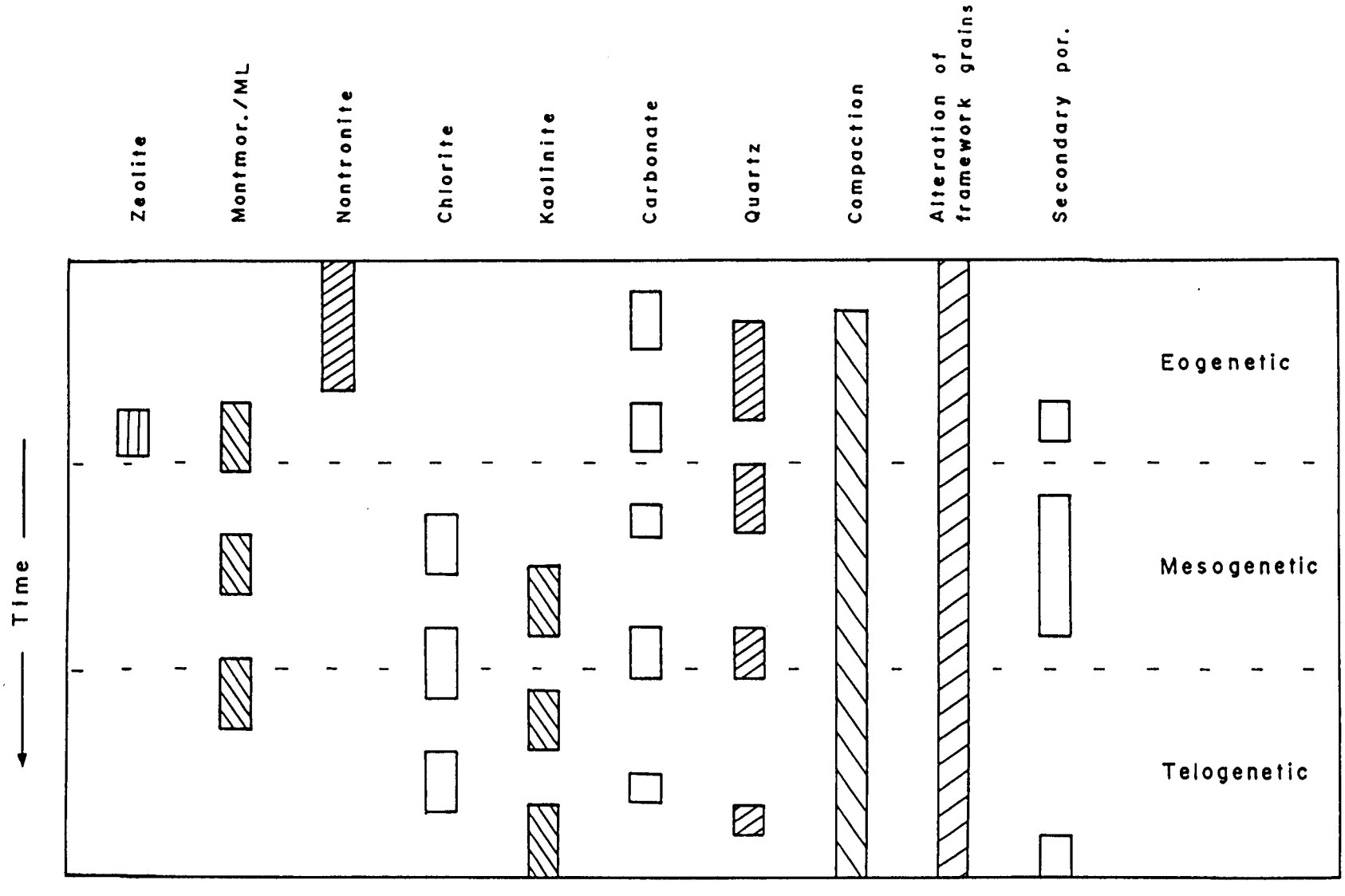

Figure 3.38. Inferred paragenetic sequence of diagenetic events in the Surat Basin sandstones. The development of secondary dissolution porosity due to meteoric flushing of the basin is depicted at bottom-right in the telogenetic stage of the basin's history. See text for additional expalnation. ML - Mixed-layer smectite-illite.

PARAGENETIC SEQUENCE

A paragenetic sequence of diagenetic events has been established (Figure 3.38) using thin-section petrographic criteria (e.g., cement-stratigraphy, packing, minus-cement porosity, geometry of distribution of authigenic minerals etc.). Figure 3.38 shows that compaction and cementation are the two diagenetic processes which were active throughout most of the geologic history of the sediment body, whereas much of the secondary dissolution porosity was developed when it reached the threshold of the oil window (mesogenetic zone in Figure 3.38). However, although compactional processes were active throughout this history, the temporal pattern of cementation, involving as it does several mineral species, was discontinous and episodic. The meteoric flushing is a comparatively recent phenomenon in the geologic history of the basin (Bowering, 1982; cf. Figure 3.38) but is believed to be an important contributor to the secondary porosity development in view of the high fluid flow rate in a geologically short period of time.

CONCLUSIONS

1. The destruction of primary depositional porosity of the Surat Basin sandstones was accomplished principally by compaction with cementation causing ubiquitous, volumetrically minor porosity reduction.

2. Whereas the effect of compaction is more pronounced in the lithic sandstones, authigenic cements occur ubiquitously in formations of either detrital composition - labile and quartzose.

3. Emplacement of various authigenic mineral species commonly reduced effective (macro) porosity, and certain varieties of them (notably clays) significantly increased microporosity and decreased permeability.

4. In some places cementation (especially by carbonates) relatively early during the history of sediment burial arrested compactional porosity

loss. Subsequent dissolution of the cement and framework grains created secondary porosity.

5. The present-day porosity of the Surat Basin sandstones is a combination of both primary and secondary dissolution porosity, the latter being volumetrically more prevalent than the former.

6. Two mechanisms are mostly responsible for the creation of secondary porosity in the Surat Basin clastics: various maturation products expelled from the intercalated organic-rich mudrocks prior to hydrocarbon generation, and flushing by CO_2-charged meteoric water after the inception of the Grat Artesian System in the Tertiary.

7. The zones of maximum development of secondary porosity correlate well with specific values of vitrinite reflectance and are attributed to the time-temperature-induced maturation products of organic matter.

REFERENCES

Almon, W. R., and Drumsteller, D. K., 1978, Delineations of trends in reservoir quality., SPE 7507, 53rd Annual Fall Technical Conf. and exhibition of the Soc. Petrol. Engrs. of Amer. Inst. Min. Metall. Houston, 1978.

Almon, W. R., 1981, The impact of diagenesis on reservoir stimulation and management., Petrol. Expln. Soc. Austral. distinguished lecture series., 383 p.

Arditto, P. A., 1982, Deposition and diagenesis of the Jurassic Pilliga Sandstone in the southeastern Surat Basin, New South Wales. Jour. Geol. Soc. Austral., v. 29, pp. 191-203.

Arditto, P. A., 1983, Mineral-groundwater interactions and the formation of authigenic kaolinite within the southeastern intake beds of the Great Australian (Artesian) Basin, N.S.W. Sediment. Geol., v. 35, pp. 249-261.

Athy, L. F., 1930, Density, porosity and compaction of sedimentary rocks, AAPG Bull., v. 14, pp. 1-24.

Atwater, G. I., and Miller, E. E., 1965, The effect of decrease in porosity with depth on future development of oil and gas reserves in South Louisiana. (Abs.), AAPG Bull, v. 49, pp. 334.

Beard, D. C., and Weyl, P. K., 1973, Influence of texture on porosity and permeability of unconsolidated sand. AAPG Bull., v. 57/2, pp. 349-369.

Blatt, H., 1979, Diagenetic processes in sandstones., In Scholle, P. A., and Schluger, P. R., (eds.), Clastic diagenesis., SEPM Sp. Publ. 26, pp. 141-157.

Bowering, O. J. W., 1982, Hydrodynamics and hydrocarbon migration - a model for the Eromanga Basin. Austral. Petrol. Expln. Assoc. Jour., v. 22, pp. 227-236.

Burley, S. D., and Kantorowicz, J. D., 1986, Thin-section and SEM textural criteria for the recognition of cement-dissolution porosity in sandstones. Sedimentology, v. 33, pp. 587-604.

Burst, F. J., 1969, Diagenesis of Gulf Coast clayey sediments and its possible relation to petroleum migration. AAPG Bull, v. 53/1, pp. 73-93.

Carothers, W. W., and Kharaka, Y. K., 1978, Aliphatic acid anions in oil field waters - implications for the origin of natural gas. AAPG Bull, v. 62, pp. 2441-2453.

Chepikov, K. P., Yermolova, Y. P., and Orlova, N. A., 1961, Corrosion of quartz grains and examples of the possible effect of oil on the reservoir properties of sandy rocks. Doklady Academy of Sci., USSR, Earth Sci. Section, v. 4, pp. 1111-1113 (in English).

Connan, J., 1974, Time-temperature relation in oil genesis. AAPG Bull., v. 58, pp. 2516-2521.

Cook, A. C., 1975, The spatial and temporal variation of the type and rank of Australian coals. In Cook, A. C. (ed.), Australian Black Coal, Australas. Inst. Min. Metall., Illawara Br., ABC Symp., Wollongong, pp. 63-84.

Crossey, L. J., Surdam, R. C., and Lahann, R., 1986, Application of organic/inorganic diagenesis to porosity prediction. in Gautier, D. L. (ed.),, Roles of organic matter in sediment diagenesis. SEPM Sp. Publ., 38, pp. 147-155.

Cummins, W. A., 1962, The greywacke problem., Liverpool and Manchester Geol. Jour., v. 3, pp. 51-72.

Davies, D. K., and Ethridge, F. G., 1975, Sandstone composition and depositional environments. AAPG Bull., v. 59/2, pp. 239-264.

Dickinson, W. R., 1970, Interpreting detrital modes of greywacke and arkose. Jour. Sed. Petrol., v. 40, pp. 695-707.

Dickinson, W. R., 1985, Interpreting provenance relations from detrital modes of sandstones. In G. G. Zuffa (ed.), Provenance of arenites. D. Reidel Publ. Co, Dordrecht/Boston/Lancaster, pp. 333-361.

Dow, W. G., 1977, Kerogen studies in geochemical interpretations. Jour. Geochem. Expln., v. 7, pp. 79-99.

Edman, J. D., and Surdam, R. C., 1986, Organic-inorganic interactions as a mechanism for porosity enhancement in the Upper Cretaceous Ericson Sandstone, Green River Basin, Wyoming. In Gautier, D. L., (ed.), Roles of organic matter in sediment diagenesis. SEPM Sp. Publ. 38, pp. 85-109.

Exon, N. F., 1976, Geology of the Surat Basin in Queensland. Bureau Min. Res. Bull. 160, 160 p.

Exon, N. F., and Burger, D., 1981, Sedimentary cycles in the Surat Basin and Global changes in sea level. Bureau Min. Res. Jour. Austral. Geol. Geophy., v. 6, pp. 153-159.

Fraser, H. J., 1935, Experimental study of the porosity and permeability of clastic sediments. Jour. Geol., v. 43, pp. 910-1010.

Fuchtbauer, H., 1967, Influence of different types of diagenesis on sandstone porosity., Proc. 9th World Petrol. Congress., pp. 359-369.

Fuchtbauer, H., 1974, Some problems of diagenesis in sandstones. Bull. Centre Rech., Pan - SNPA, v. 8/1, pp. 391-403.

Galloway, W. E., 1974, Depositional and diagenetic alteration of sandstone in Northeast Pacific arc-related basins: implications for greywacke diagenesis. Geol. Soc. Amer. Bull., v. 85, pp. 379-390.

Galloway, W. E., 1979, Diagenetic control of reservoir quality in arc-

derived sandstones: implications for petroleum exploration. Scholle, P. A., and Schluger, P. R., (eds.), Aspects of diagenesis. SEPM Sp. Publ. 26, pp.251-262.

Gilbert, C. M., and McAndrews, M. G., 1948, Authigenic heulandite in sandstone, Santa Cruz County, California. Jour. Sedim. Petrol., v. 18, pp. 91-99.

Golin, V., and Smyth, M., 1986, Depositional environment and hydrocarbon potential of the Evergreen Formation, ATP 145 P, Surat Basin, Queensland. Austral. Petrol. Expln. Assoc. Jour., pp. 156-171.

Graton, L. C., and Fraser, H. J., 1935, Systematic packing of spheres with particular relation to porosity and permeability. Jour. Geol., v. 43/8, pp. 785-909.

Griffiths, J. C., 1967, Scientific method in analysis of sediments. McGraw Hill, New York, 508 p.

Grim, R. E., 1968, Clay mineralogy. McGraw-Hill, New York. 596 p.

Habermehl, M. A., 1980, The Great Artesian Basin, Australia. Bureau Min. Res. Jour. Austral. Geol Geophy., v. 5, pp. 9-38.

Halbouty, M. T., King, R. E., Klemme, M. D., Dott, R. H., and Meyerhoff, A. A., 1970, Factors affecting formation of giant oil and gas fields and basin classification. In Halbouty, M. T., (ed.), Geology of giant petroleum fields. AAPG Mem. 14, pp. 528-555.

Halley, R. B., 1978, Estimating pore and cement volumes in thin-sections. Jour. Sed. Petrol., v. 48, pp. 642-650.

Hammerlindl, D. J., 1971, Predicting gas reserves in abnormally pressured reservoirs. 46th An. Fall meeting of the Soc. Petrol. Engrs., Amer. Inst. of Min. Metall., Paper SPE 3479, 7p.

Harris, N. B., 1988, Controls on porosity of Jurassic sandstones of northwest Europe. AAPG Bull., v. 72/2, pp. 194 (Abs.).

Hawkins, J. W., and Whetten, J. T., 1969, Graywacke matrix minerals: hydrothermal recations with Columbia River sediments. Science, v. 166, pp. 868-870.

Hayes, J. B., Harms, J. C., and Wilson, T. Jr., 1976, Contrasts between braided and meandering stream deposits, Beluga and Sterling Formations (Tertiary), Cook Inlet, Alaska. In Miller, T. P., (ed.), Recent and ancient sedimentary environments in Alaska. Alaska Geol. Soc., Anchorage, Alaska., pp. J1-J27.

Hayes, J. B., 1979, Sandstone diagenesis - the hole truth., In Scholle, P. A., and Schluger, P. R., (eds.), Aspects of diagenesis. SEPM Sp. Publ. 26, pp. 127-140.

Heald, M. T., 1956, Cementation of Simpson and St. Peter sandstones in parts of Oklahoma, Arkansas and Missouri. Jour. Geol., v. 64, pp. 16-30.

Heald, M. T., and Larese, R. E., 1974, Influence of coatings on quartz cementation. Jour. Sedim. Petrol., v. 4, pp. 1269-1274.

Hilliard, J. E., 1968, Measurement of volume in volume. In DeHoff, R. T., and Rhines, F. N., (eds.), Quantitative microscopy. McGraw Hill, New York, 422 p.

Houseknecht, D. W., 1984, Influence of grain size and temperature in intergranular pressure solution, quartz cementation and porosity in a quartzose sandstone. Jour. Sedim. Petrol., v. 54, pp. 348-361.

Houseknecht, D. W., 1987, Assessing the relative importance of compaction processes and cementation to reduction of porosity in sandstones. AAPG Bull., v. 71/6, pp. 633-642.

Houston, B. R., 1972, Petrology of subsurface samples of Mesozoic arenites of the Bowen and Surat Basins. In Gray, A. R. G. (ed.), Stratigraphic drilling in the Surat and Bowen Basins, 1967-70., Geol. Survey Qld. Rpt. 71, pp. 89-98.

Hower, J., Eslinger, E. V., Hower, M. E., and Perry E. A., 1976, Mechanism of burial metamorphism of argillaceous sediments: I Mineralogical and chemical evidence. Geol. Soc. Amer. Bull., v. 87, pp. 725-737.

Huang, W. H., and Keller, W. D., 1972, Organic acids as agents of chemical weathering of silicate minerals. Nature, Physical Sci., v. 239, pp. 149-151.

Hunt, J. M., 1979, Petroleum geochemistry and geology. Freeman, San Francisko, 617 p.

Hurst, A. R. 1981, A scale of dissolution of quartz and its implications for diagenetic process in sandstones. Sedimentology., v. 28, pp. 451-460.

Hurst, A., and Irwin, H., 1982, Geological modeling of clay diagenesis in sandstones. Clay minerals. v. 17, pp. 5-22.

Johnston, D. D., and Johnson, R. J., 1987, Depositional and diagenetic controls on reservoir quality in First Wilcox Sandstone, Livingston Field, Louisiana. AAPG Bull., v. 71/10, pp. 1152-1161.

Keller, W. D., 1970, Environmental aspects of clay minerals. Jour. Sed. Pet., v. 40/3, pp. 788-854.

Khorasani, G. K., 1987, Oil-prone coals of the Walloon Coal Measures, Surat Basin, Australia. In Scott, A. C. (ed.), Coal and coal-bearing strata: recent advances. Geol. Soc. Sp. Publ. 32, pp. 303-310.

Klemme, H. D., 1972, Heat influences size of giants. Parts 1 and 2., Oil and Gas Jour., v. 70/29-30, pp. 136-144/76-78.

Klemme, H. D., 1975, Geothermal gradients, heat flow and hydrocarbon recovery. In Fischer, G. A., and Judson, S. (eds.), Petroleum and global tectonics. Princeton Univ. Press., pp. 251-304.

Lopatin, N. V., 1971, Temperature and geologic age as factors in coalification. Izvestia Akademii Nauk SSSR, Seriya Geologischeskaya., n. 3, pp. 95-106 (in Russian).

Loucks, R. G., Dodge, H. M., and Galloway, W. E., 1984, Regional controls on diagenesis and reservoir quality in Lower Tertiary sandstones along the Texas Gulf Coast. In McDonald, D. A., and Surdam, R. C., (eds.), Clastic Diagenesis. AAPG Mem. 37, pp. 15-45.

McBride, E. F., Land, L. S., and Mack, L. E., 1987, Diagenesis of eolian and fluvial feldspathic sandstones. Norphlet Formation (Upper Jurassic), Rankin County, Mississippi, and Mobile County, Alabama. AAPG Bull., v. 71/9, pp. 1019-1034.

Mason, J. M., 1983, Hydrophillic organic compounds produced during underground coal gasification. Unpub. M.Sc thesis., Univ. Wyoming. 73 p. (Non vide).

Mathisen, M. E., 1984, Diagenesis of Plio-Peistocene non-marine sandstones, Cagayan Basin, Philippines: early development of secondary porosity in volcanic sandstones. In McDonald, D. A., and Surdam, R. C., (eds.), Clastic diagenesis. AAPG Mem. 37, pp. 177-193.

Maxwell, J. C., 1964, Influence of depth, temperature and age on porosity of quartzose sandstone. AAPG Bull., v. 48/5, pp. 697-709.

Millot, G., 1970, Geology of clays. Chapman & Hall, London. 429 p.

Nagtegaal, P. J. C., 1978, Sandstone framework instability as a function of burial diagenesis. Jour. Geol. Soc. London., v. 135, pp. 101-105.

Noon, T. A., and Coote, S. M., 1983, Review of departmental stratigraphic drilling in Queensland. Qld. Govt. Min. Jour. v. 84/985, pp. 417-453.

Pettijohn, F. J., Potter, P. E., Siever, R., (1972), Sand and sandstone. Springer-Verlag, Berlin - Heidelberg - NewYork. 618 p.

Pigott, J. D., 1985, Assessing source rock maturity in frontier basins: importance of time, temperature, and tectonics. AAPG Bull., v. 69/8, pp. 1269-1274.

Pittman, E. D., and Lumsden, D. N., 1968, Relationship between chlorite coatings on quartz grains and porosity, Spiro Sand, Oklahoma. Jour. Sedim. Petrol., v. 38, pp. 668-670.

Pittman, E. D., 1979, Porosity, diagenesis and productive capability of sandstone reservoirs. In Scholle, P. A., and Schluger, P. R., (eds.), Clastic diagenesis. SEPM Sp. Publ. 26, pp. 159-173.

Pittman, E. D., 1979b, Recent advances in sandstone diagenesis. Ann. Rev. Earth Planet. Sci., v. 7, pp. 39-62.

Pittman, E. D., and King, G. E., 1986, Petrology and formation damage control, Upper Cretaceous sandstone, offshore Gabon. Clay

Minerals. v. 21, pp. 781-790.

Powell, T. G., Foscols, A. E., Gunther, P. R., and Snowdon, L. R., 1978, Diagenesis of organic matter and fine clay minerals: a comparative study. Geochem. Cosmochem. Acta, v. 42, pp. 1181-1197.

Powell, T. G., and Snowdon, R. L., 1983, A composite hydrocarbon generation model. Erdol und Kohle, Erdgas, Petrochemie vereinigt mit Brennstoff-chemie, v. 36, pp. 163-169.

Powers, C. M., 1967, Fluid release mechanisms in compacting marine mudrocks and their importance in oil generation. AAPG Bull., v. 51/7, pp. 1240-1254.

Proshlyakov, B. K., 1960, Reservoir properties of rocks as function of their depth and lithology. Geologya nefti i gaza. v. 4, n. 12, pp. 24-29, Assoc. Tech. Service Trans. RJ 3421.

Pryor, W. A., 1973, Permeability-porosity patterns and variations in some Holocene sand bodies., AAPG Bull., v. 57/1, pp. 162-189.

Rittenhouse, G., 1971, Mechanical compaction of sands containing different percentage of ductile grains: a theoretical approach. AAPG Bull., v. 55/1, pp. 92-96.

Robin, P., 1975, Characterisation de kerogenes at del leur evolution par spectroscopie infrarouge. Dissert. Univ. Cath. Louvain. (Non vide).

Roll, A., 1974, Langfristige reduktion der machtigigkeit von sedimentgesteinen und ihre auswirkung - eine ubersight. Geol. Jahrbuch, part A, v. 14, pp. 2-76.

Rosenfield, M. A., 1949, Some aspects of porosity and cementation. Producers monthly, v. 13, pp. 39-42.

Rubey, W., and Hubbert, M. K., 1959, Role of fluid pressure in mechanisms of overthrust faulting II: overthrust belt in geosynclinal area of western Wyoming in light of fluid pressure hypothesis. Geol. Soc. Amer. Bull., v. 70, pp. 167-206.

Savkevich, S. S., 1969, Variation in sandstone porosity in lithogenesis (as related to the prediction of secondary porous oil and gas reservoirs). Doklady, Academy of Sci., USSR. Earth Sci. Section., v. 184, pp. 161-163, (in English).

Schatz, J. F., Ahmed, U., and Caroll, H. M., 1982, Reservoir performance-changes due to inelastic deformation. Soc. Petrol Engrs. Paper 10670, SPE symposium on formation damage control, Lafayette, LA.,

Scherer, M., 1987, Parameters influencing porosity in sandstones: a model for sandstone porosity prediction. AAPG Bull., v. 71/5, pp. 485-491.

Schmidt, V., McDonald, D. A., and Platt, R. L., 1977, Pore geometry and reservoir aspects of secondary porosity in sandstones. Bull. Can. Petrol. Geol., v. 25/2, pp. 271-290.

Schmidt, V., and McDonald, D. A., 1979a, The role of secondary porosity in the course of sandstone diagenesis. In In Scholle, P. A., and Schluger, P. R., (eds.),, Aspects of diagenesis. SEPM Sp. Publ. 26, pp. 175-207.

Schmidt, V., and McDonald, D. A., 1979b, Texture and recognition of secondary porosity in sandstones. In Scholle, P. A., and Schluger, P. R., (eds.), Aspects of diagenesis. SEPM Sp. Publ. 26, pp. 209-225.

Schmidt, V., and McDonald, D. A., 1979c, Secondary porosity in the course of sandstone diagenesis. AAPG contg. educ. course note ser. 12, 125 p.

Schmoker, J. W., 1984, Empirical reaction between porosity and thermal maturity: an appraisal to regional porosity prediction., AAPG Bull., v. 68, pp. 1697-1703.

Sclater, J. G., and Christie, P. A. F., 1980, Continental stretching: an explanation of the post-mid-Cretaceous subsidence of the central North Sea Basin. Jour. Geophy. Res., v. 85, pp. 3711-3739.

Selley, R. C., 1978, Porosity gradients in North Sea oil-bearing sandstones. Jour. Geol. Soc. London., v. 135, pp. 119-132.

Selley, R. C., 1985, Elements of Petroleum Geology. Freeman, New York, 449 p.

Shanmugam, G., 1985a, Significance of secondary porosity in interpreting sandstone composition. AAPG Bull., v. 69/3, pp. 378-384.

Shanmugam, G., 1985b, Types of porosity in sandstones and their significance in interpreting provenance. In Zuffa, G. G. (ed.), Provenance of arenites, D. Reidel Publ. Co., Dordrecht/Boston/Lancaster, pp. 115-137.

Shanmugam, G., 1985 c, Significance of coniferous rain forests and related organic matter in generating commercial quantities of oil, Gippsland Basin, Australia. AAPG Bull., v. 69/8, pp. 1241-1254.

Shelton, J. W., 1964, Authigenic kaolinite in sandstones. Jour. Sedim. Petrol., v. 34, pp. 102-111.

Siebert, R. M., Moncure, G. K., and Lahann, R. W., 1984, A theory of framework grain dissolution in sandstones. In McDonald, D. A., and Surdam, R. C., (eds.), Clastic diagenesis. AAPG Mem. 37, pp. 163-175.

Siever, R., 1983, Burial history and diagenetic reaction kinetics. AAPG Bull, v. 67, pp. 684-691.

Snowdon, R. L., and Powell, T. G., 1982, Immature oil and condensate - modification of hydrocarbon generation model for terrestrial organic matter. AAPG Bull., v. 66/6, pp. 775-788.

Sprunt, E. S., and Nur, A., 1977, Destruction of porosity through pressure solution. Geophysics., v. 42, pp. 726-741.

SPSS Inc., 1983, SPSSX user guide. McGraw-Hill, New York, 806 p.

Stach, E., Mackowsky, m. Th., Teichmuller, M., Taylor, G. G., Chandra, D., and Teichmuller, R. 1982, Coal Petrology. Gebrunder Borntraeger, Berlin, 452 p.

Surdam, R. C., Boese, S. W., and Crossey, L. J., 1984, The chemistry of secondary porosity., In McDonald, D. A., and Surdam R. C., (eds.), Clastic diagenesis. AAPG Mem. 37, pp. 127-149.

Surdam, R. C., and Crossey, L. J., 1985, Organic-inorganic reactions during progressive burial: key to porosity and permeability enhancement and preservation. Phil. Trans. Royal Soc. London, v. A315, pp. 135-156.

Tillman, R. W., and Almon, W. r., 1979, Diagenesis of Frontier Formation offshore bar sandstones, Spearhead Ranch Field, Wyoming. In Scholle, P. A., and Schluger, P. R., (eds.), Aspects of diagenesis. SEPM Sp. Publ. 26, pp. 337-378.

Tissot, B. P., and welte, D. H., 1978, Petroleum formation and occurrence. Springer-Verlag, Berlin - Heidelberg - NewYork, 527 p.

Tissot, B. P., 1984, Recent advances in petroleum geochemistry applied to hydrocarbon exploration. AAPG Bull. v. 68/5, pp. 545-563.

Waples, D. W., 1985, Geochemistry in petroleum exploration. Intern.Human Res. Dev. Corp., Boston. 232 p.

Wardlaw, N. C., 1976, Pore geometry of carbonate rocks as revealed by pore casts and capillary pressure. AAPG Bull., v. 60, pp. 245-257.

Wardlaw, N. C., 1980, The influence of pore structure in rocks on the entrapment of oil. In Miall, A. D. (ed.), Facts and principles of world petroleum occurrence., Can. Soc. Petrol. Geol. Mem. 6, pp. 193-208.

Weller, J. M., 1959, Compaction of sediments. AAPG Bull, v. 43, pp. 273-310.

Wood, J. R., and Surdam, R. C., 1979, Application of convective-diffusion models to diagenetic processes. In In Scholle, P. A., and Schluger, P. R., (eds.), Aspects of diagenesis. SEPM Sp. Publ. 26, pp. 243-250.

Zieglar, S. S., and Spotts, J. H., 1978, Reservoir and source-bed history of Great Valley, California. AAPG Bull., v. 62, pp. 813-826.

CHAPTER 4: RESERVOIR PROPERTIES OF SOME SURAT BASIN SANDSTONES AS A FUNCTION OF DIAGENETIC CLAY-MINERAL ASSEMBLAGE: IMPLICATIONS FOR HYDROCARBON EXPLORATION AND EXPLOITATION

RESERVOIR PROPERTIES OF SOME SURAT BASIN SANDSTONES AS A FUNCTION OF DIAGENETIC CLAY-MINERAL ASSEMBLAGE: IMPLICATIONS FOR HYDROCARBON EXPLORATION AND EXPLOITATION

ABSTRACT

A study of the geologic evolution of porosity and permeability of the Surat Basin sandstones shows that authigenic clay minerals of different species are invariably present, either singly or in preferred associations, in all stratigraphic formations. Reservoir quality is found to be reduced by the presence of these diagenetic mineral assemblages, the extent of which reduction depends upon the amount, type, crystallographic habits and geometry of distribution of the clay minerals within the reservoirs. Improper engineering practices during drilling, testing and completion in these formations may further deteriorate the reservoir quality leading even to bypassing of potential productive zones. Moreover, recognition of any spatial trend of the occurrence of the authigenic clays, be it geographic or stratigraphic, can be instrumental in the discovery of the commonly elusive and subtle diagenetic-permeability traps. This is deemed critical for the Surat Basin which has stepped into its mature phase of hydrocarbon exploration: most likely the present level of production can be sustained and further reserves increased only through the discovery of subtle traps since most of the available structures have already been drilled.

INTRODUCTION

Diagenesis is a complex interaction of a variety of physico-chemical processes which may be broadly divided into two different pathways - one which destroys porosity and the other which preserves or enhances it. Sandstones are deposited with an initial porosity of 30-40% which is

gradually reduced with depth of burial as a result of compaction and precipitation/growth of diagenetic minerals.

Detrital mineralogy, depositional and post-depositional physico-chemical environments exert a first-order influence on the suite of authigenic minerals. In the Surat Basin there is distinct segregation of the diagenetic mineral assemblage as a function of the detrital sandstone composition. In this basin the stratigraphy is that of an intercalation and interfingering of two distinct suites of petrofacies: quartzose and labile/volcanogenic - a characteristic feature of many arc-related foreland basins (cf. Chapters 2 and 9). The quartzose facies is characterised by the presence of pore-filling authigenic kaolinite epimatrix (terminology of Dickinson, 1970) and quartz overgrowths whereas the labile facies is dominated by smectite, mixed-layer smectite-illite (and/or some illite), zeolite, Chlorite and minor kaolinite (Figure 4.1; see also Exon, 1976, and Slansky, 1984).

Clay minerals within the sandstones can be classified into two distinct groups: allogenic or detrital, and authigenic or diagenetic. Their modes of occurrence are schematically shown in Figure 4.2. Detrital clay can occur either as interstitial matrix which is pervasive such that all pores are filled with it, or else as intercalated laminae. Both dispersed matrix and clay laminae are impermeable and act as vertical permeability barriers. Detrital clay minerals are generally concentrated in bedding-parallel zones which tend to effect directional permeability (i.e. drastically reducing the vertical permeability). In the horizontal direction permeability remains unaffected by such anisotropy involving the distribution of detrital clay. Sand-sized allogenic clay-aggregates in argillaceous rock-fragments, biogenic pellets and rip-up clasts can be treated as framework grains. Contrastingly, diagenetic clay minerals occur as loosely-spaced pore-fillings, pore-linings and pore-bridgings (Figures

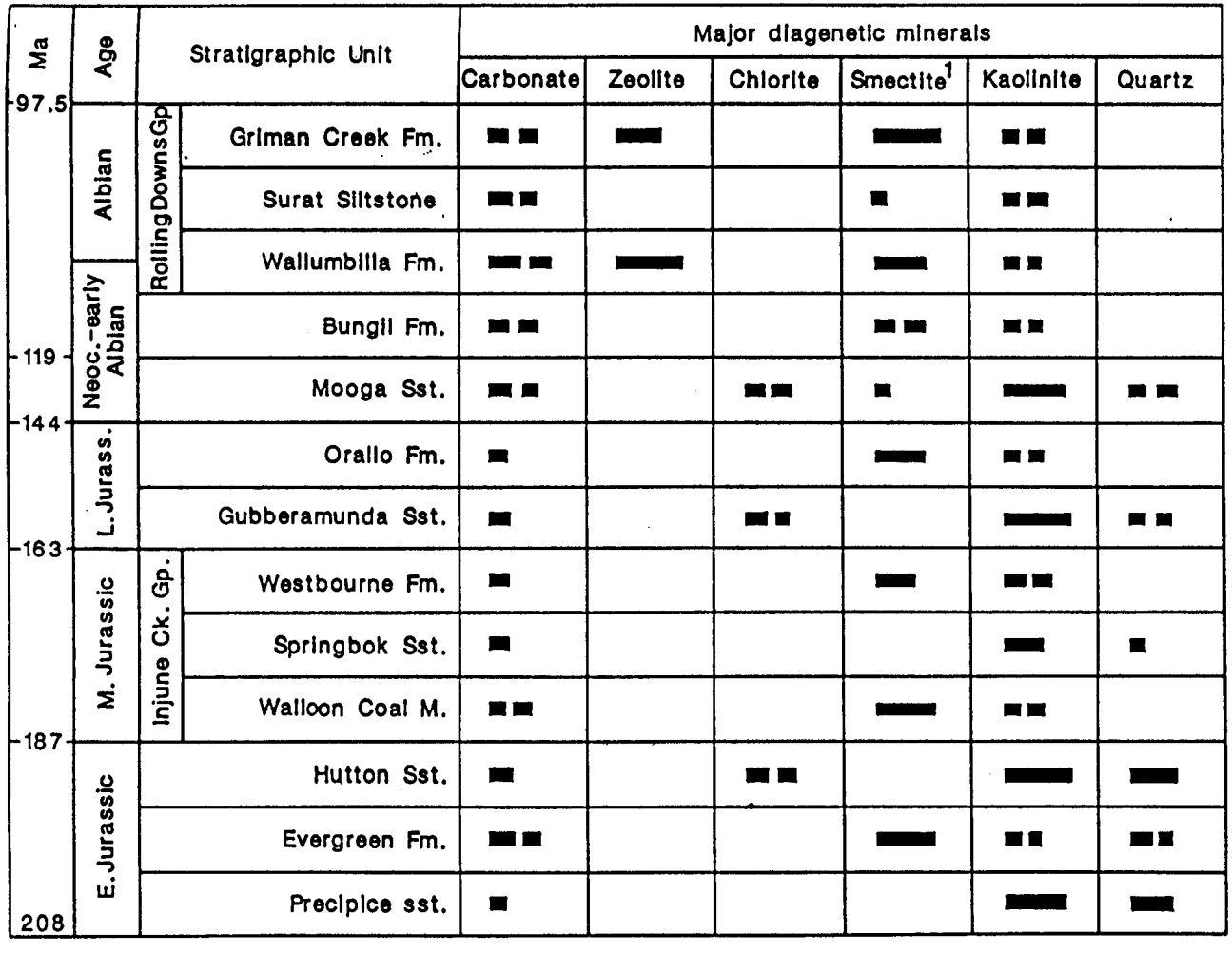

Figure 4.1. Stratigraphic distribution of major authigenic minerals in the Surat Basin sandstones. Broken bars indicate patchy distribution and length of bars indicates relative abundance of the authigenic phases. 1 - includes montmorillonite, nontronite, and mixed-layer smectite-illite.

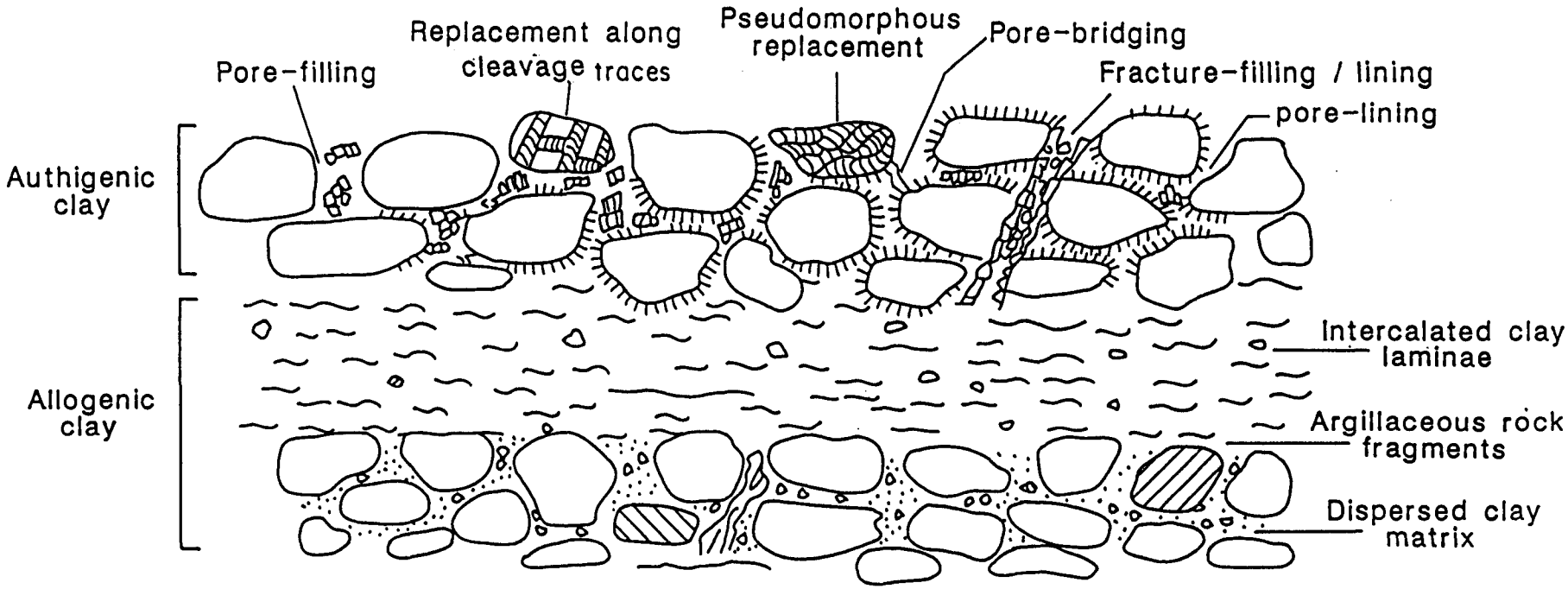

Figure 4.2. Modes of occurrence of authigenic and allogenic clays. After Pittman and Thomas (1979).

4.2 and 4.3). They also occur as alteration products or pseudomophs of labile grains. Authigenic clay minerals are invariably present in the Surat Basin sandstones and affect the reservoir properties in a more varied and complicated fashion.

A glossary of the various mathematical symbols and text mnemonics used in this Chapter is given in Appendix 3.1.

DIAGENETIC CLAYS AND POROSITY - PERMEABILITY RELATIONSHIPS

Füchtbauer (1967) was one of the first workers to note the difference in porosity-permeabilty relationships of sandstone reservoirs as a function of the proportion and type of diagenetic minerals present. In the sandstone suites of the Surat Basin such relationships were confirmed. For instance, within the Hutton Sandstone, samples containing <3% kaolinite show a very good correlation between porosity and permeability with little scatter of the data points whereas samples with ⩾3% kaolinite show poorer correlation and wider scatter (Figure 4.4). The difference in porosity-permeability relationships can be explained by the fact that pores and pore-throats in well- to moderately-sorted sandstones with little or no interstitial clay exhibit even geometric distribution which results in turn in the porosity and permeability being interdependent. Presence of interstitial clay leads to the poor pore-throat sorting (PTS) and consequently porosity becomes less interdependent with the permeability. The different porosity-permeability is not only due to the different proportions of authigenic clays but also on their modes of occurrence within the pore system as shown in individual samples in Figure 4.3. Figure 4.6 shows such relationships in two sandstone suites of comparable textures but diffferent type of authigenic clays. It shows that at comparable porosity, nontronite-cemented sandstones are likely to be less permeable than kaolinite-bearing sandstones (see also Figure 4.7). Such

Figure 4.3. SEM photomicrographs showing the different morphology and modes of distribution of diagenetic clays. Bottom photomicrograph in each page illustrates detail of field of view in top photomicrograph. Scales defined by bar.
A and B: Loosely-spaced pore-filling kaolinite. Mooga Sandstone, GSQ Roma 8/5, ϕ = 29%, k = 46 md, M_z = 3.12ϕ, σ = 0.80ϕ, d = 132.69 m.
C and D: Pore-lining chlorite rosettes. The horizontal bands on quartz overgrowth faces (lower-left of C) are due to charging effect. Hutton Sandstone, GSQ Roma 8/52, ϕ = 16.6%, k = 0.19 md, M_z = 1.92ϕ, σ = 0.85ϕ, d = 782.78 m.
E and F: Pore-lining/briding smectite (montmorillonite). Walloon Coal Measures. GSQ Chinchilla 4/20, ϕ = 17.2%, k = 0.60 md, M_z = 1.88ϕ, σ = 0.50ϕ, d = 681.34 m.
G and H: Pore-lining and pore-bridging chlorite. Note the absence of chlorite on grain contacts attesting to the authigenic origin of the clay. Griman Creek Formation. GSQ Surat 3/9, ϕ = 28%, k = 0.60 md, M_z = 2.57ϕ, σ = 0.65ϕ, d = 113.20 m.
ϕ = porosity, k = permeability, M_z = mean grainsize (in phi units), σ = grainsize sorting (phi standard deviation), d = depth of sample below surface, m.

A

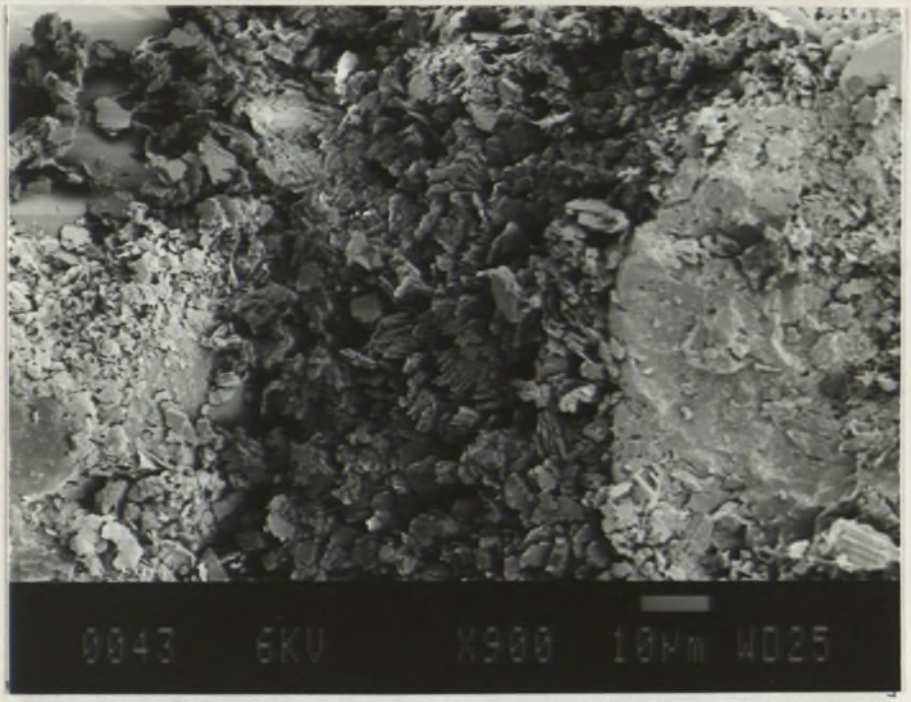

B

C

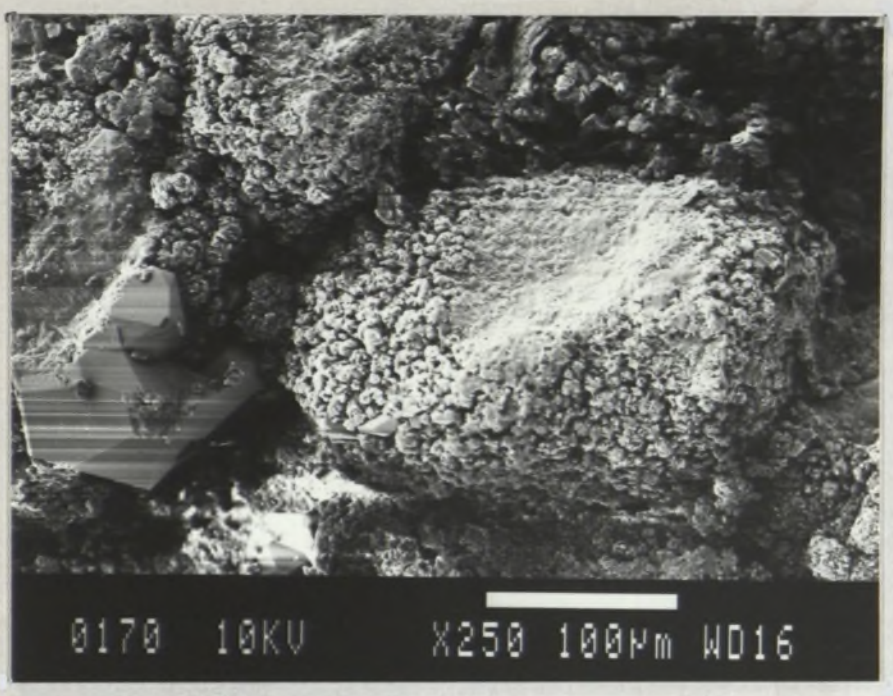

D

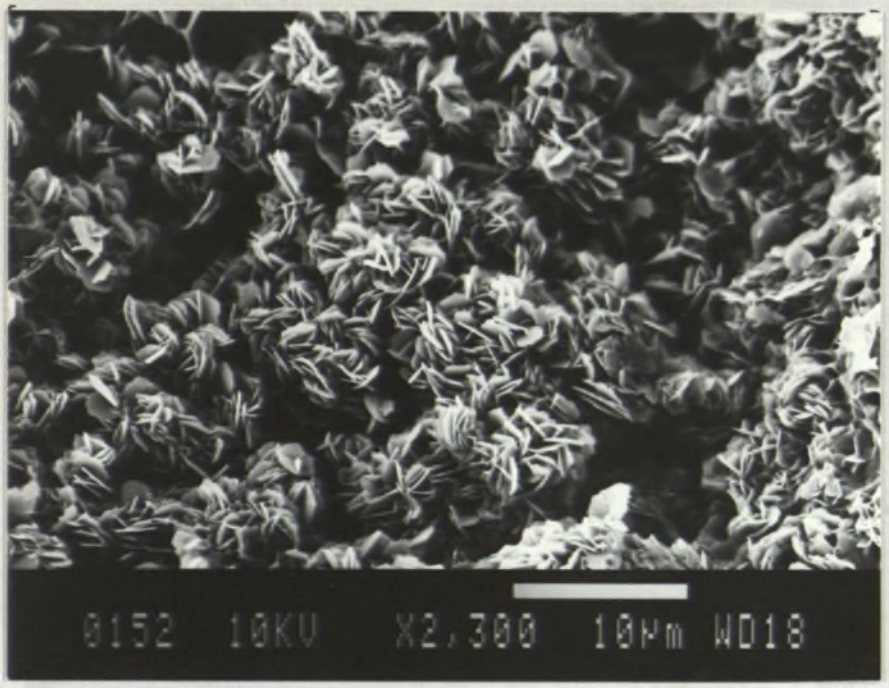

E

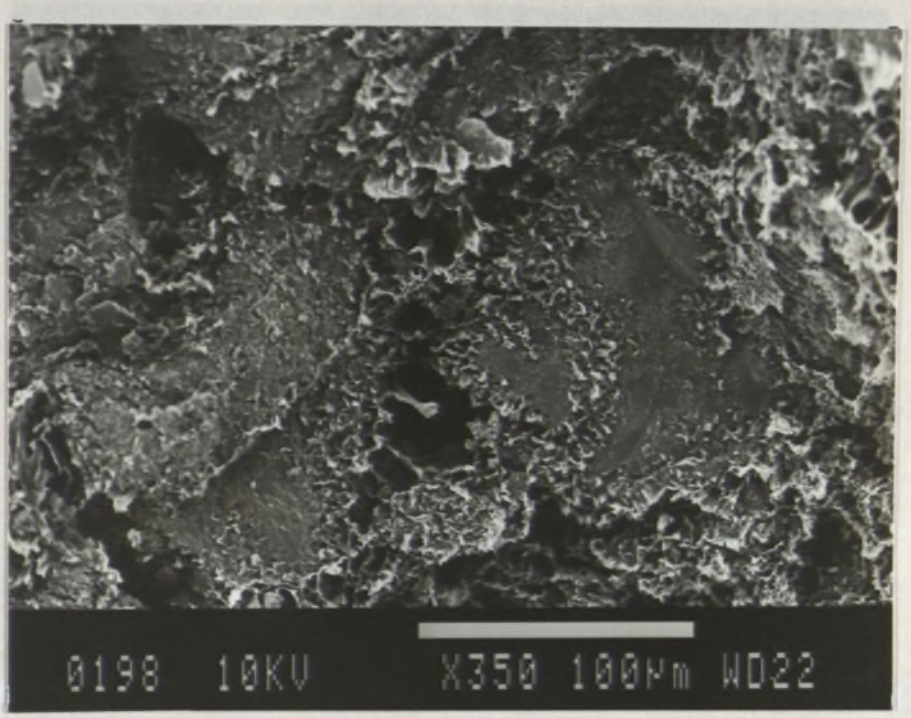

F

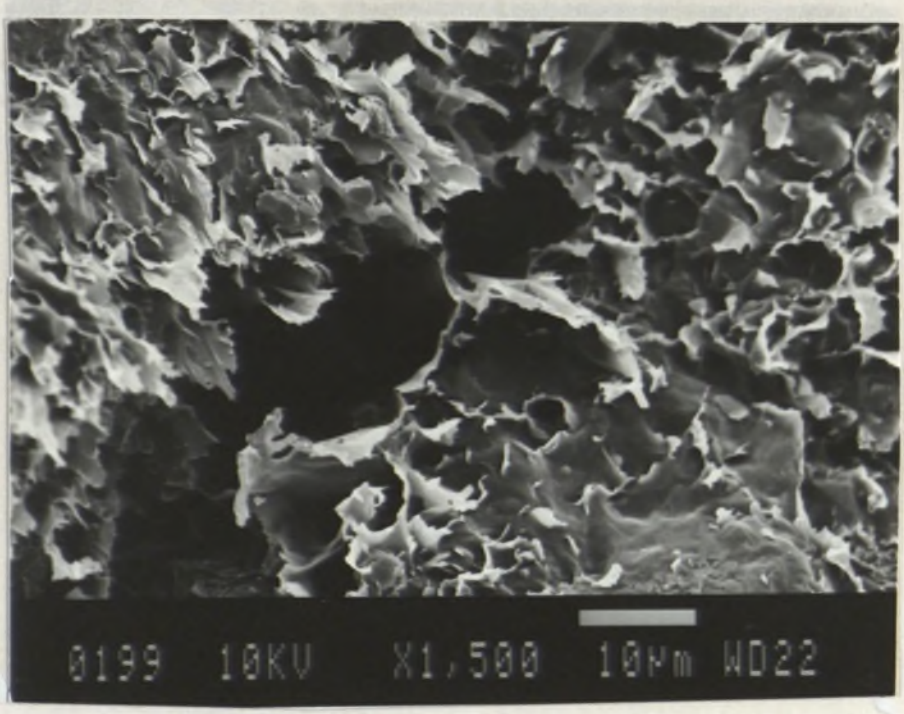

G

H

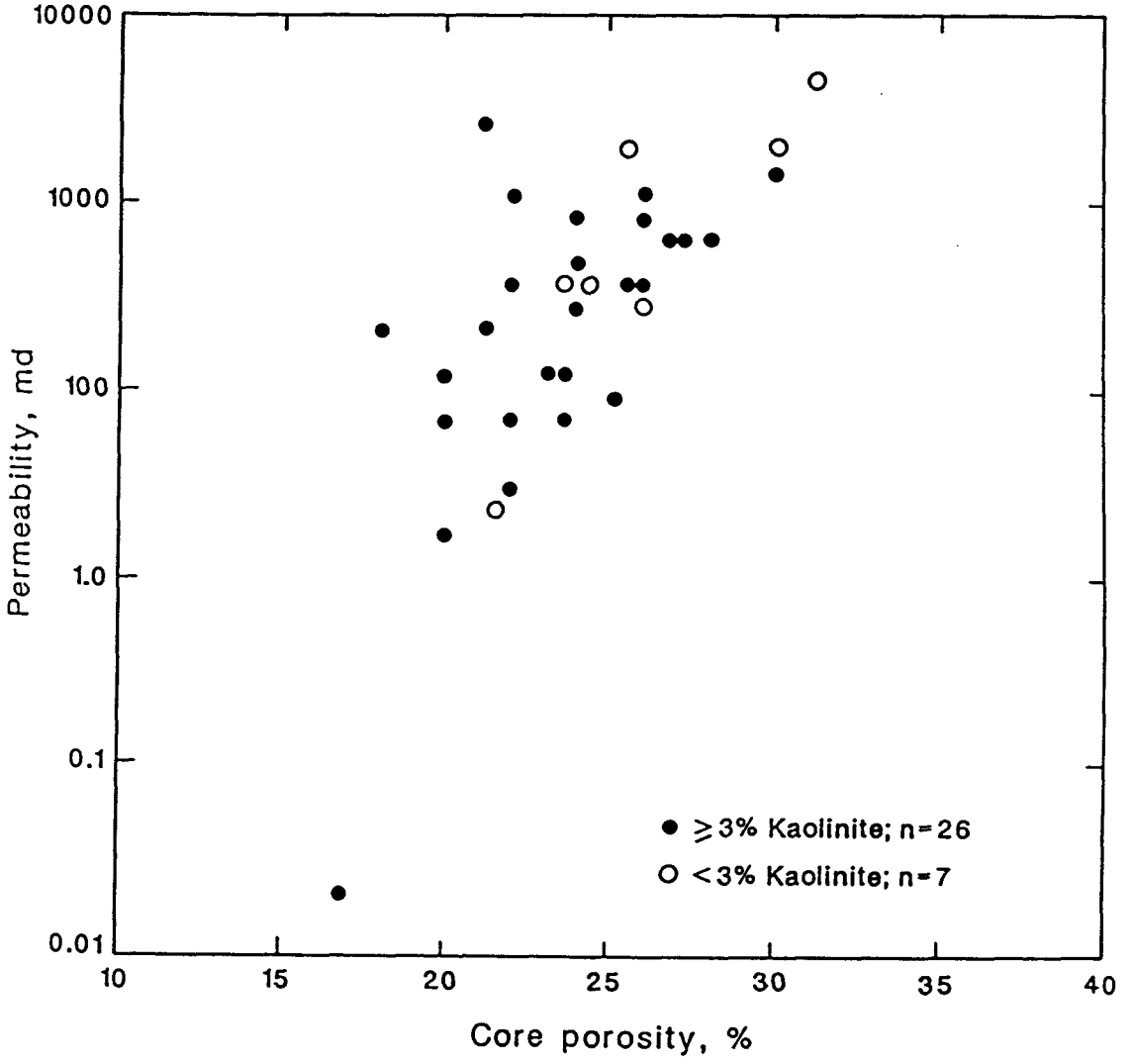

Figure 4.4. Porosity - permeability plots of some Hutton Sandstone samples containing different amounts of authigenic kaolinite. Samples are of comparable grainsize (medium- to fine-grained, moderately sorted). Data from GSQ Mitchell 2, GSQ Roma 8, and GSQ Chinchilla 4.

Figure 4.5. SEM photomicrographs showing microporosity within different species of diagenetic minerals.
A: Pore-filling kaolinite. Evergreen Formation, GSQ Mitchell 2/59, d = 853.86 m.
B and C: Pore/grain-coating late diagenetic chlorite. Hutton Sandstone, GSQ Roma 8/52, d = 782.78 m.
D and E: Pore-lining/grain-coating early diagenetic blade-like/reticulate nontronite. Griman Creek Formation, GSQ Surat 3/9, d = 113.20 and 147.20 m.
F: Microporosity within druzy quartz crystals. Evergreen Formation, GSQ Chinchilla 4/37, d = 1064.88 m.

A

B

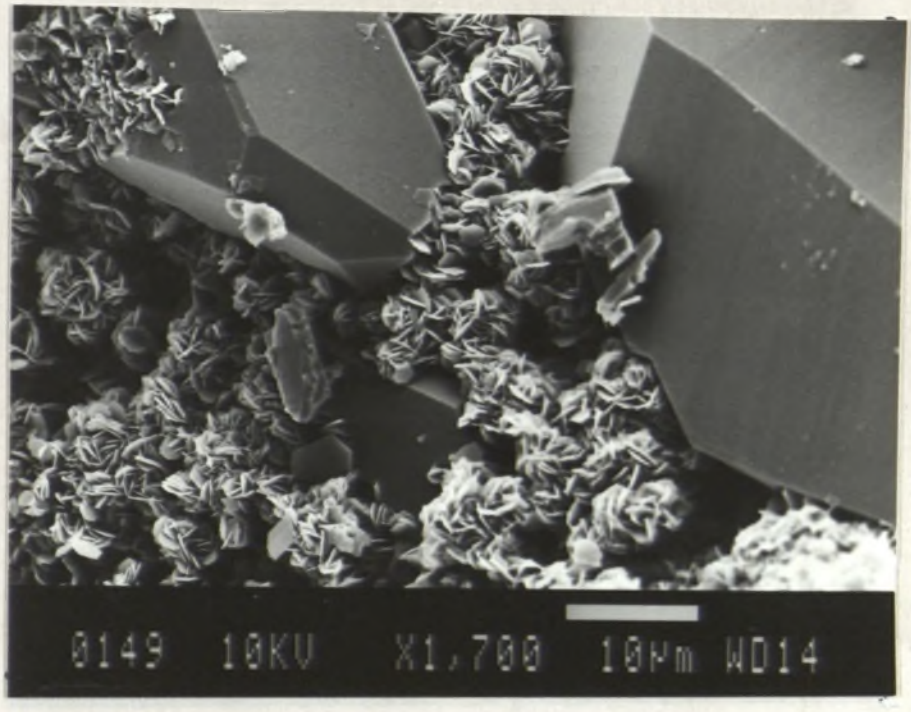

C

D

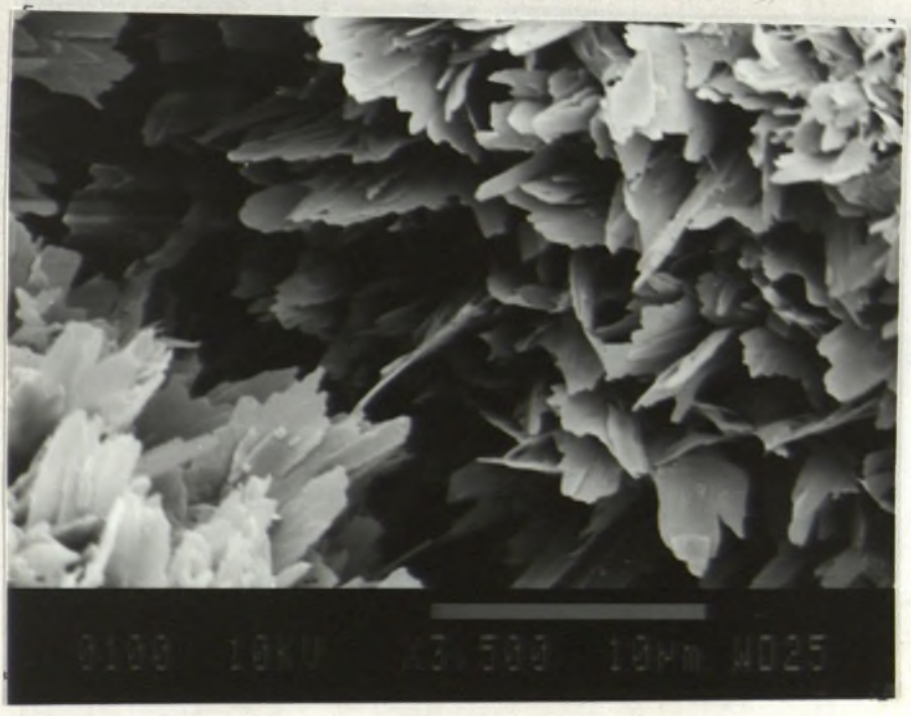

E

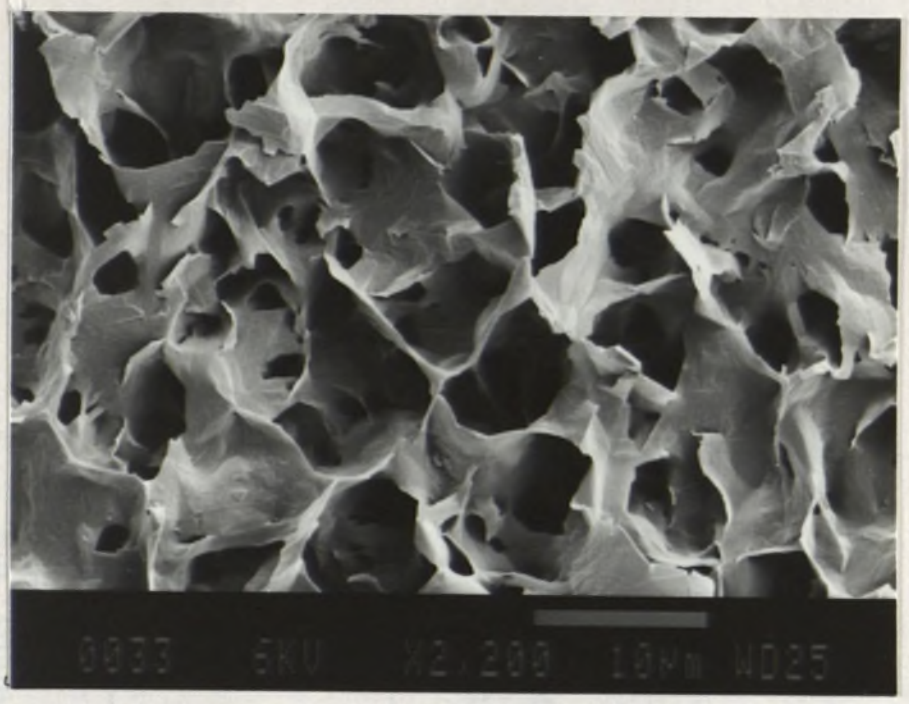

F

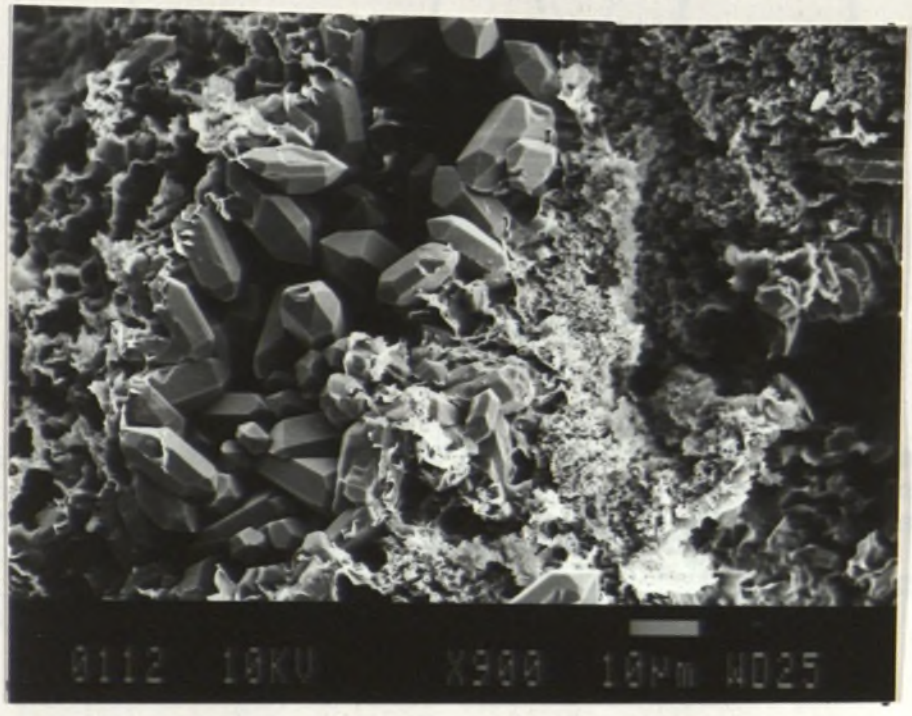

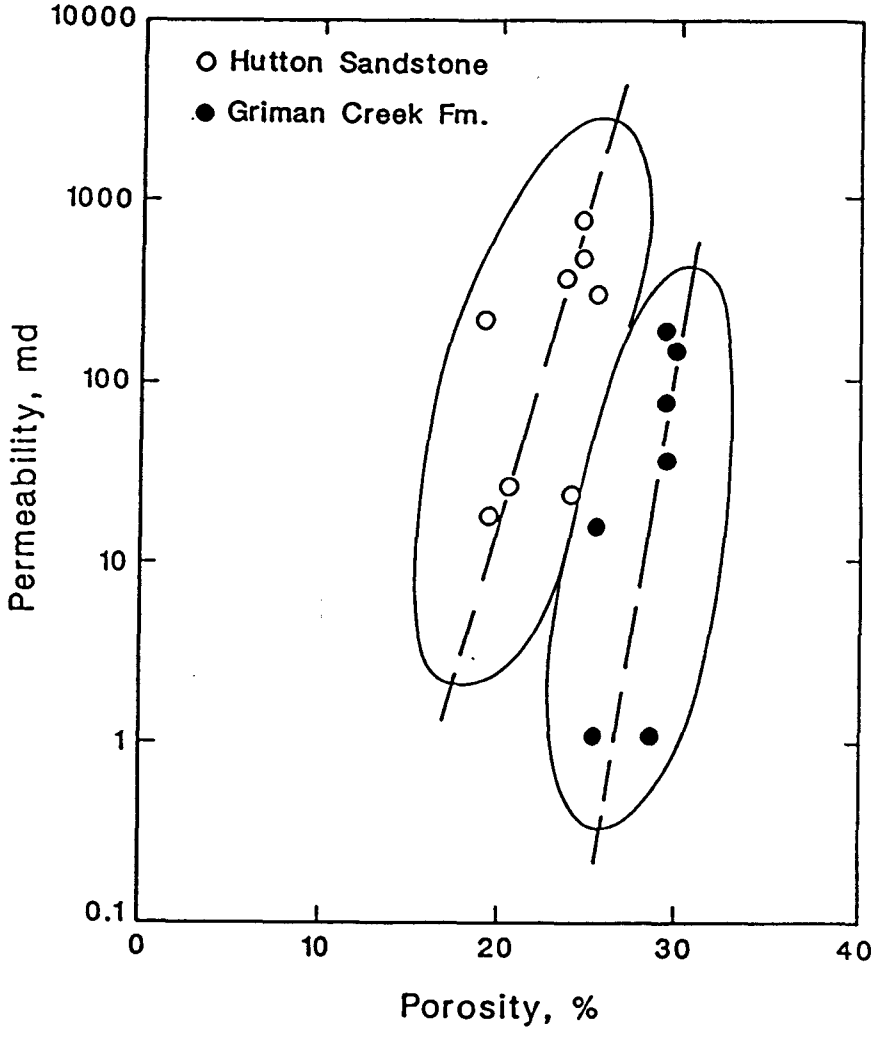

Figure 4.6. Porosity - permeability plot of two formations with comparable texture (medium- to fine-grained, moderately sorted) but characterized by different species of diagenetic clay minerals. Hutton Sandstone contains pore-filling kaolinite whereas Griman Creek Formation contains pore-lining/grain-coating nontronite. Data from GSQ Mitchell 2, GSQ Roma 8, and GSQ Chinchilla 4.

relationships have been confirmed in other basins by many workers (e.g., Stalder, 1973; Neasham, 1977; and Wilson, 1982). Nontronite forms ubiquitous grain-coatings and commonly bridges pores causing drastic reduction in permeability compared to the loosely spaced pore-filling kaolinite.

EFFECT OF DIAGENETIC CLAYS ON PORE-SIZE DISTRIBUTION OF CLASTIC RESERVOIRS

Commonly, diagenetic minerals not only reduce the effective (macro) porosity by clogging pore-space but also increase the proportion of microporosity (Figure 4.5). Micropores are arbitrarily classified here as pores with apertures less than 20 um in diameter although various authors have assigned a lower value (e.g., Gaida et al, 1973; Pittman, 1979). Microporosity is here calculated from the difference between the measured core porosity and the measured thin-section porosity. Microporosity index (MPI) is defined as the ratio of the microporosity to the measured core porosity (cf. Ranganathan and Tye, 1986). In a reservoir with a mixture of both micropores and macropores high water saturation (as much as 60-70%) can prevail. In a water-wet reservoir, water is held tightly to these micropores due to high capillary pressure. Such water is irreducible and consequently a reservoir may produce water-free hydrocarbon without fracturing because the macropores may contain mobile oil while micropores may hold irreducible water. Numerous such cases have been reported in the literature (e.g., Keike and Hartmann, 1973; Schultz, 1979; Almon and Schultz, 1979). Authigenic clay minerals of several species are present, either singly or in preferred associations, in all Surat Basin sandstones. Where their volume is significant (e.g. >3% by volume), abundant micropores of intercrystalline origin will develop (Figure 4.10). In individual samples the amount of authigenic clays (epimatrix) reaches upto 11% on a whole-rock basis (cf. Appendix 1.5) and such high clay content gives rise

Figure 4.7. SEM photomicrographs of two sandstones of very similar texture but having different type and morphology of diagenetic clays. Bottom photograph on each page shows detail of top photograph.
A and B: Pore-filling kaolinite. Hutton Sandstone. Note also the skeletal feldspar at top-right of A. GSQ Mitchell 2/7, ϕ = 26%, k = 799 md, M_z = 2.40Φ, σ = 0.55Φ, MPI = 0.50, d = 725.86 m.
C and D: Pore-lining/bridging nontronite in the Griman Creek Formation. GSQ Surat 3/9, ϕ = 28%, k = 0.60 md, M_z = 2.57Φ, σ = 0.65Φ, MPI = 0.85, d = 113.20 m. Note how the permeabilities (and corresponding MPI's) differ despite the near-identical porosities, grainsize and sorting.

A

B

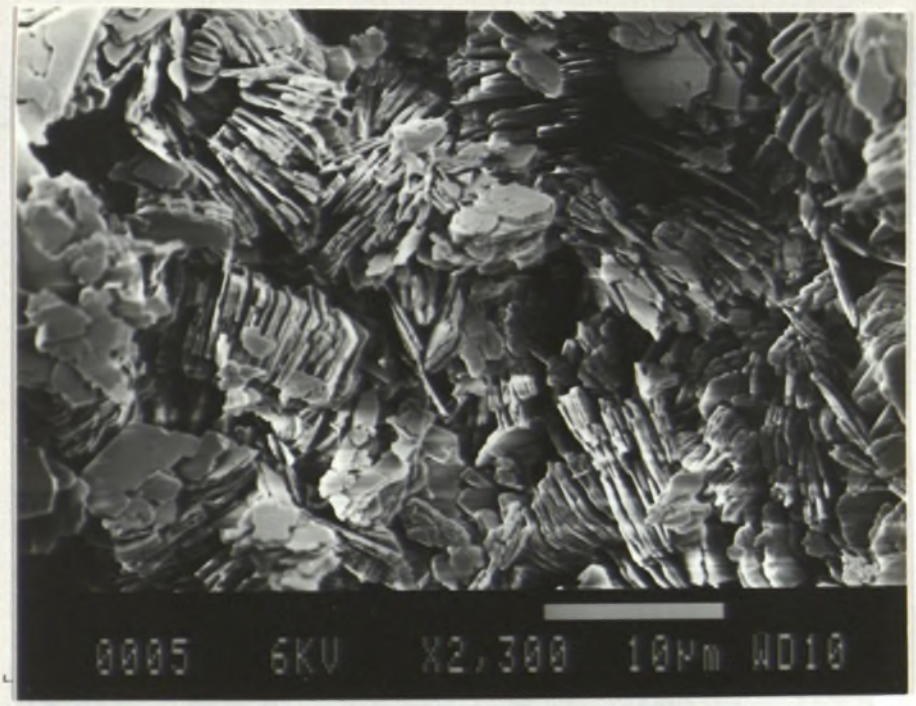

C

D

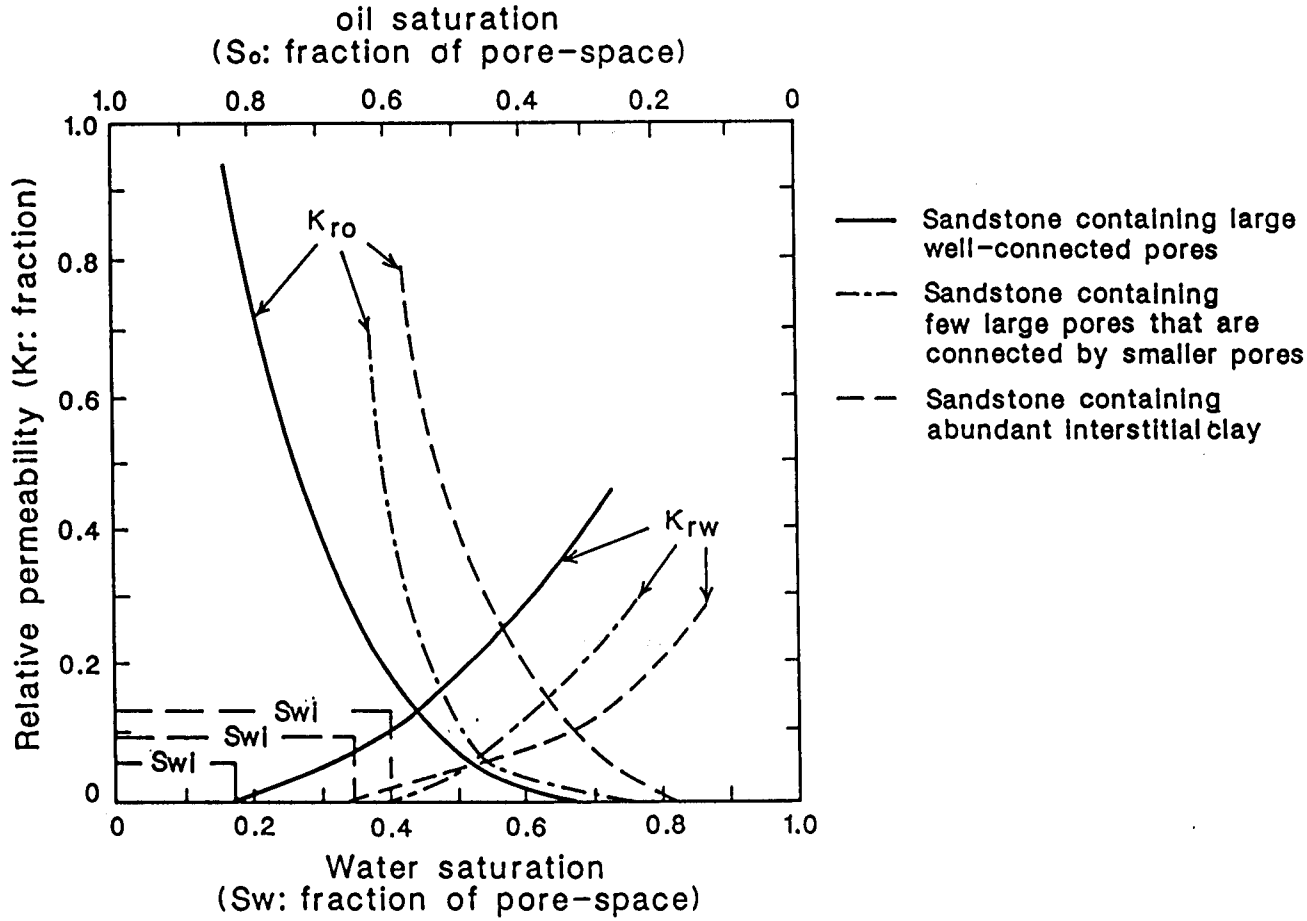

Figure 4.8. Oil-water relative permeability curves of three sandstones of comparable texture. Note how initial water saturation differs in each case. Modified from Mordan and Gordon (1970, figs. 1,3, and 8). K_{ro} - relative permeability to oil; K_{rw} - relative permeability to water; S_{wi} - irreducible water saturation.

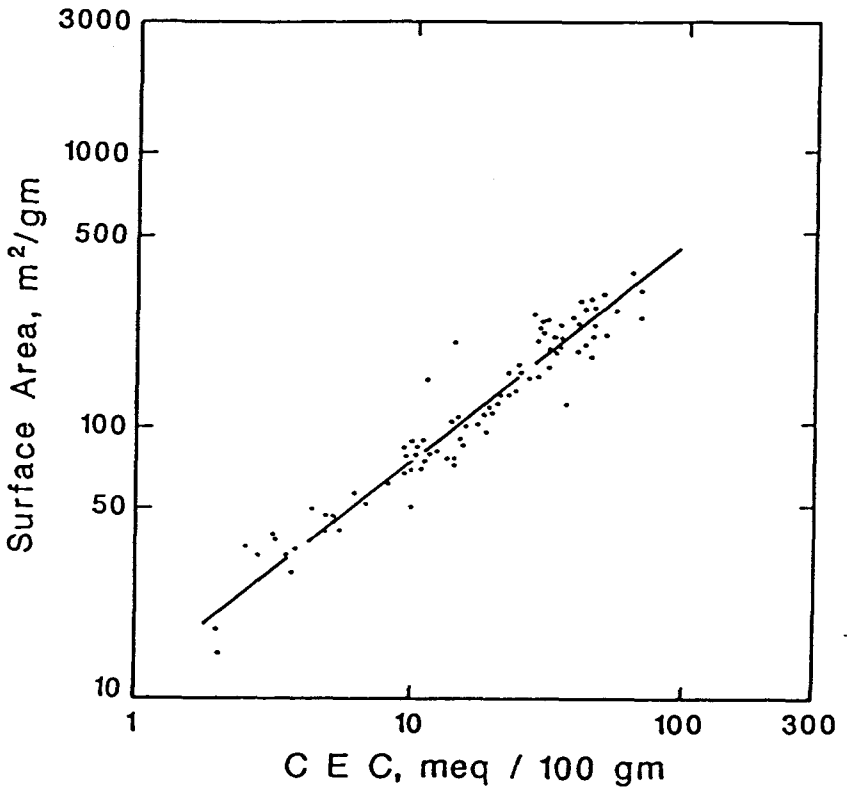

Figure 4.9. Relationship between specific surface area and cation-exchange-capacity (CEC). After Patchet (1975, fig. 2).

Figure 4.10. SEM photomicrographs showing the abundance of microporosity due to the presence of ubiquitous diagenetic clays.
A: Mooga Sandstone, GSQ Roma 8/5, ϕ = 29%, k = 46 md, M_z = 3.12Φ, σ = 0.80Φ, MPI = 0.78, d = 135.69 m, epimatrix = 3.1%.
B: Gubberamunda Sandstone. GSQ Roma 8/26, ϕ = 31.7%, k = 623 md, M_z = 1.87Φ, σ = 0.53Φ, MPI = 0.77, d = 324.30 m, epimatrix = 3.4%.
Late diagenetic chlorite grain-coats in B have not bridged the pores leaving a fairly well interconnected pore system whereas the pervasive kaolinite in A has virtually chocked all pore constrictions. This is apparent in their permeability values.

A

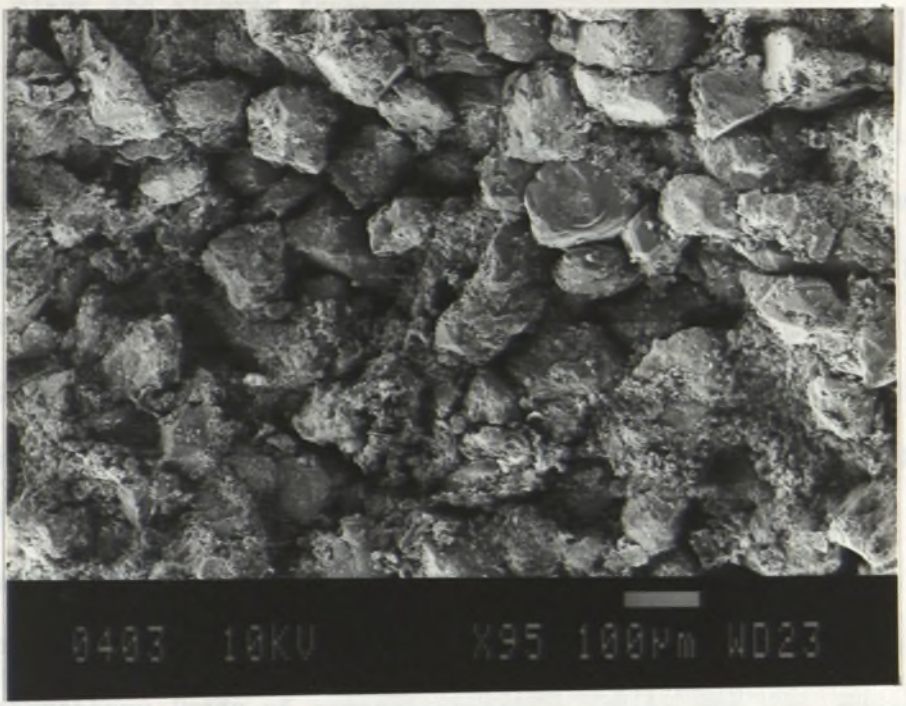

B

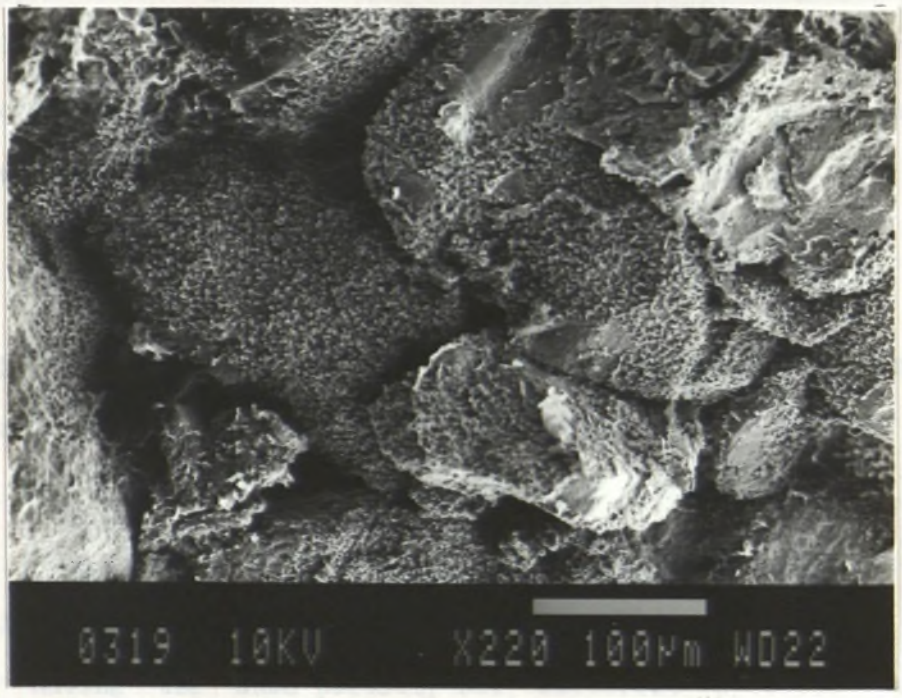

to high microporosity index. High MPI is also due to the presence of allogenic clays and altered framework grains (cf. Chapter 3). In samples containing little allogenic clays (cf. Figures 4.10A-B), high MPI may be attributed mainly to the microporosity within the authigenic phases. High MPI also gives rise to poor pore-throat sorting. Although the total heleium-injection porosity may not be reduced drastically by the presence of diagenetic clays (due to the smaller molecular size and hence extreme penetrating ability of helium even into micropores), conventional nitrogen-permeabilty shows dramatic reduction. In such sandstones core porosity records optimistically high values.

Reduction in permeability as a result of diagenetic clays is not only a function of the amount of the diagenetic clay present but also the type(s), morphology (mode of crystallographic habit) and the geometry of its distribution within the sandstone body because all these attributes affect the resistance to flow (Stalder, 1973). Diagenetic clays increase the specific surface area of the pore volume which exerts higher resistance to fluid flow, thus causing permeability reduction. This is well explained by the Kozeny-Carman equation which relates permeabilty to porosity and specific surface area (Scheidegger, 1963):

$$K = \frac{\phi^3}{5(1-\phi^2)S^2} \qquad (4.1)$$

where k = permeability, ϕ = porosity, and S = specific surface area. This equation, as a first approximation, can be rewritten as

$$K = C.\frac{\phi}{S^2} \qquad (4.2)$$

where c is a constant. From equation (4.2) it is evident why two sandstones having the same porosity but different specific pore-space surface areas have quite different permeabilty. Authigenic clay minerals

also increase the tortuosity making the sandstones prone to turbulent fluid flow at higher flow rates. Further reduction in permeability may occur through dislodgement of fine clay particles and their mechanical concentration within and hence choking of the pore-throats. This is very characteristic of loosely-spaced kaolinite and less commonly so of chlorite and illite.

RELATIVE PERMEABILITY AND WATER SATURATION

The change in pore geometry as a result of diagenetic clay precipitation significantly affects the relative permeability curves (Figure 4.8). Sandstones containing large interconnected pores will have high initial relative permeability to oil (K_{ro}) and two-phase flow will occur over a wide range of water saturation (S_w) (irreducible water saturation (S_{wi}) in such a case is very low; usually 20-30%). Contrastingly, reservoirs with high interstitial clay content show a completely different relative permeability curve characterised by low initial K_{ro} and high S_{wi} (usually >30%) resulting in the two-phase fluid flow in a smaller range of S_w (Figure 4.8).

S_w is a critical petrophysical criterion for formation evaluation. It is generally calculated by the Archie method (Pirson, 1963):

$$S_w = \left(\frac{R_o}{R_t} \right)^{1/n} = \left(\frac{R_w \cdot \phi^{-m}}{R_t} \right) = \left(\frac{F \cdot R_w}{R_t} \right)^{1/n} \qquad (4.3)$$

where R_o = electrical resistivity of formation 100% saturated with water, ϕ = porosity, m = cementation exponent, n = saturation exponent (n = 1.8 for shaly sandstones and 2.0 for non-shaly sandstones), F = formation resistivity factor, R_w = resistivity of formation water and R_t = resistivity of undisturbed formation (i.e., reservoir areas beyond the zone flushed by drilling mud-filtrate). Sandstones containing authigenic clay minerals with high specific surface areas (e.g., smectite and illite; cf.

Table 4.1) give higher conductivity and the electric-log-derived water saturation appears anomalously high which may lead to the bypassing/abandoning of a potential reservoir even though most of the water is irreducible and the formation could produce water-free hydrocarbons.

Dependence of permeability on S_{wi} can be expressed by the empirical formula of Timur (1968):

$$K = \frac{\phi^{4.4}}{S_{wi}^{2}} \tag{4.4}$$

or by Wyllie and Rose's (1950) formula:

$$K = c_1 \cdot \frac{\phi^{3}}{S_{wi}^{2}} \tag{4.5}$$

where c_1 = constant which depends on hydrocarbon gravity. Equating (4.2) and (4.4) it follows that

$$S_{wi} = a_1 \cdot S_o \cdot \phi^{1.2} \tag{4.6}$$

Alternatively, from (4.2) and (4.5) we derive

$$S_{wi} = a_2 \cdot S_o \cdot \phi \tag{4.7}$$

where a_1 and a_2 are constants. Equations 4.6 and 4.7 show the the linear dependence of irreducible water saturation on specific surface area.

Another important aspect of sandstones containing interstitial clay minerals is their high cation-exchange capacity (CEC) which gives rise to their high conductivity. CEC of clay minerals is generally attributed to the following factors (Grim, 1968):

1. the broken bonds around the edges of the silica-alumina units give rise to unsatisfied charges which are balanced by adsorbed cations. The number of broken bonds and CEC due to this cause increases with decreasing clay particle size. In kaolinite for instance, broken bonds may be the major cause of CEC.

2. Substitution of Al^{3+} for Si^{4+} in the tetrahedral sheet and Mg^{++} and other bivalent cations for AL^{+++} in the octahedral sheets results in the unbalanced charges.

3. The hydrogen of the exposed hydroxyl can be replaced by cations which might be exchangeable (Grim, 1968, p. 193-195).

CEC is directly proportional to the specific surface area (Figure 4.9) which is due partly to the increase in the number of broken bonds (negative charges) with decreasing grainsize (Grim, 1968).

In respect to the CEC of the clay minerals, smectite has the highest value followed by illite and chlorite (Table 4.1) - a trend consistent with the average grainsize of these minerals. The least CEC associated with kaolinite may be due to its typically large grainsize, readily discernible in thin-sections as tiny booklets of pseudohexagonal crystals. Of the non-clay authigenic minerals zeolite has the highest CEC (Table 4.1) and this has implications for the Cretaceous Rolling Downs Group sediments where zeolite occurs as a common interstitial diagenetic mineral (Figure 4.1).

Table 4.1. Cation-exchange capacity and specific surface area of some common diagenetic minerals (after Grim, 1968).

	CEC (meq/100gm)	Surface area $(m^2/gm)/(m^2/cc)$
Smectite	80 - 150	82/173
Illite	10 - 40	113/284
Chlorite	10 - 40	---
Kaolinite	3 - 15	22/53
Zeolite	100 - 300	---
Quartz*	---	$1.5 \cdot 10^{-5}/3.9 \cdot 10^{-5}$

* Depends on grainsize.

FORMATION DAMAGE AND RESERVOIR MANAGEMENT

The presence of interstitial clays within the reservoir significantly affects the drilling, completion and production procedures. Smectite (including montmorillonite and nontronite) and mixed-layer smectite-illite are fresh-water-sensitive, so drilling and completion in the potentially productive zone may have to be performed with oil- or KCl-based mud. This applies to the Jurassic Evergreen Formation where smectite and mixed-layer smectite-illite are the dominant clay minerals (Figure 4.1). The quartoze facies of the Surat Basin (e.g., the Jurassic Precipice and Hutton Sandstones) are characterized by loosely-spaced pore-filling kaolinite (Figure 4.7A-B) which may be mechanically dislodged and move with fluids to eventually form bridges that block the pore-throats. Kaolinite also may cause varying degree of impaired permeability on contact with fresh-water probably as a result of colloidal dispersion (Pittman and King, 1986). Chlorite (and possibly illite), if loosely-attached (Figures 4.5C-D), may also give rise to similar clogging of pore constrictions. Bridging is dependent on the clay-particle size, amount of fines (dislodged clays) and pore-throat size. In these formations migration of dislodged fines during drilling is the main problem but it can be tackled with clay stabilizers such as polyhydroxy aluminum[1] (Almon and Davis, 1981). To avoid turbulent flow, the drilling mud should have low gel content, and the time for running in and pulling out of the drilling string should be maximized to avoid pressure surge. Duff (1986) recommends that drill stem tests (DST) in these Surat Basin formations be performed at a pressure surge not exceeding 500 psi (3445 Kpa) in order to prevent severe turbulence which may dislodge the interstitial kaolinite and lead to pore-space clogging. Apart from the migration of dislodged fines (e.g., kaolinte, illite and chlorite), fresh-water-sensitive clays (e.g., smectite and mixed-layer clays) and acid-sensitive clays (e.g., nontronite and chlorite), water

1 These days organic cationic polymers are preferred to polyhydroxy aluminum because the former are strongly absorbed on the surface of clay, and are not affected by acid and do not change wettability.

saturation in and around the drill-hole can increase dramatically as a result of imbibition of drilling- and completion-fluids (i.e., water blocking) with the consequent reduction of permeability to oil and gas (Spencer, 1985). This is likely to occur at the pore-throats which are made smaller (i.e., to capillary-size) by the prior presence of authigenic minerals. Likewise, chemical additives may cause precipitation of compounds (including mineral phases) during acidizing and hydraulic fracturing, thus causing further deterioration of the reservoir quality.

Acidizing and hydraulic fracturing with HCl and/or HF should take into account that Fe-bearing authigenic minerals such as nontronite, chlorite, siderite, ankerite, ferroan calcite and ferroan dolomite may precipitate CaF_2, $Fe(OH)_3$, and secondary silica. A chelating agent (such as citric acid) and an oxygen-scavenging agent may be used to prevent it (Pittman and Thomas, 1979; Almon, 1981).

Although swelling clays can expand up to 40 times their normal size, this is probaly not a severe problem in the Surat Basin since the formation water is very fresh (cf. Habermehl, 1980) and the authigenic clays are probably in equilibrium with the formation water. In situations where swelling can occur (cf. Evergreen Fm.), drilling may require a mud system with low fluid loss into the formation. Moreover, any fluid loss in to the formation should carry sufficient cations such as K^+, Mg^{++}, and Ca^{++} to inhibit any clay swelling.

RESPONSE OF GEOPHYSICAL WELL LOGS AS A FUNCTION OF AUTHIGENIC CLAYS

One of the adverse effects of the presence of authigenic clay in a reservoir is its anomalously high S_w calculated from electric logs. There are two sources of anomalously high S_w calculated from electric logs in formations containing authigenic clays. High conductivity associated with clay surfaces gives rise to a lower value of R_t, and R_w measured in the

productive zone may be completely different from its value in the non-productive zone; this is evident from the Archie formula (Equation 4.3). To calculate R_t in formations containing interstitial clays, commonly Waxman-Smits formula (Waxman and Smits, 1968) is used which takes into account the high CEC due to formation 'shaliness':

$$\frac{1}{R_t} = \frac{1}{F^*}\left(\frac{1}{R_w} + BQ_v\right) = \frac{1}{F^* \cdot R_w} + \frac{BQ_v}{F^*} \qquad (4.8)$$

where F^* is a limiting formation factor measured for very small R_w which approximates the F of a clean formation with the same porosity; Q_v = cation-exchange capacity in meq/cc of pore space; and B = equivalent conductivity of clay exchange.

Authigenic clays are also known to affect SP and resistivity/induction log readings. A small amount of diagenetic clay in a reservoir can cause a negligible decrease in the SP log from an observed or theoretical static SP value and at the same time (due to high surface conductance) reduce resistivity values in the electric logs (Pirson, 1963; Schultz, 1979; Almon and Schultz, 1979). The induction log will be especially affected since it measures the conductivity of the formation. Porosity values calculated from well logs, whether from electric, sonic or radiation logs, are invariably anomalously high because clay particles give rise to an apparent increase in electrical conductivity (due to higher than normal CEC), a decrease in the velocity of sonic waves and an increased emission of captured gamma ray intensity (Pirson, 1963, p. 275).

The effect of formation 'shaliness' on many log responses depends on the amount of clay present and its physical properites such as CEC and specific surface area. CEC values of clays is directly related to their capacity to absorb and hold water. Clays of the smectite group have the greatest capacity to absorb water and also have the highest CEC values

(Table 4.1). Kaolinite and chlorite have very low CEC values, and their capacity to hold irreducible water is also low. Several logging tools such as resistivity, sonic, SP, and neuclear-magnetic-resonance are also affected by the way the clay is distributed in the formation (Schlumberger, 1972).

Porosity type (macro vs intercrystalline micro, whether within the diagenetic or detrital clay or within the altered labile grains) will affect the readings of shallow laterologs used to measure the invasion by mud-filtrate. The resistivity of formation water is usually an order of magnitude less than that of the mud-filtrate. During drilling and completion, formations containing significant microporosity will not have their irreducible water flushed by the drilling mud, thus giving rise to relatively low R_{xo} (resistivity of the zone flushed by mud-filtrate). This happens due to the retention of the low-resistivity connate-water (Keith and Pittman, 1983). This problem, however, may not be so severe in the Surat Basin in view of the relatively fresh nature of the formation water (Habemehl, 1980).

HEIGHT OF THE OIL-COLUMN

As mentioned previously, diagenetic clays lead to poor PTS. PTS is the standard deviation of the pore-throat radius and varies from 1.0 (perfect) to 8.0 (essentially no uniformity/sorting) (Jennings, 1987). The significance of PTS lies in the rock's ability to accept oil saturation. Numerically high (i.e., poor) PTS is an indicator of low oil saturation (high water saturation). In rocks with good (i.e., numerically low) PTS when a threshold buoyancy pressure is obtained oil will rapidly saturate the available porosity up to the maximum capacity. Rocks with poor PTS require a buyoancy pressure increase over a much broader range (due to high capillary pressure) to obtain the same level of oil saturation. Hence poor

PTS will cause a long transitional oil/water zone in the oil-column (Jennings, 1987). This is especially true for kaolinite which is present in varying proportions in the principal reservoir sandstones of the Surat Basin. In practice oil-column-height values can be used to determine the minimum trap relief, either structural or stratigraphic, to obtain a specific oil saturation (e.g. 50% or 70% etc.) at the top of the trap. Table 4.2 shows the relationship between PTS, permeability and the minimum height of the oil-column relative to trap-relief for some actual hydrocarbon reservoirs. As can be seen from the Table 4.2, a sandstone having moderate permeability but poor PTS will need a high-amplitude/relief trap for oil accumulation to be commercially viable. In other words, if two traps of similar closure, whether structural or stratigraphic have different amounts of diagenetic clays - say for instance one with <3% kaolinite (and moderate PTS) and the other with >3% kaolinite (and poor PTS) then the trap with the higher kaolinite content will have lower oil saturation than the other at comparable structural levels (Figure 4.11).

Dependence of the height of the oil-column (measured from the free-water level (FWL)) on pore-throat radius is also evident from the modified Hobson equation (Berg, 1975):

$$Z_o = 2\gamma \left[\frac{1}{r_t} - \frac{1}{r_p} \right] / g(\rho_w - \rho_o) \qquad (4.9)$$

where Z_o = is the height of the oil-column, γ = interfacial tension between oil and water, r_t, r_p = radii of the pore-throats and pores, g = accelaration due to gravity, and ρ_w, ρ_o = densities of water and oil respectively. From the above equation it follows that a small decrease in the pore-throat radii of the reservoir rock can give rise to a higher oil-column (i.e., relative to FWL).

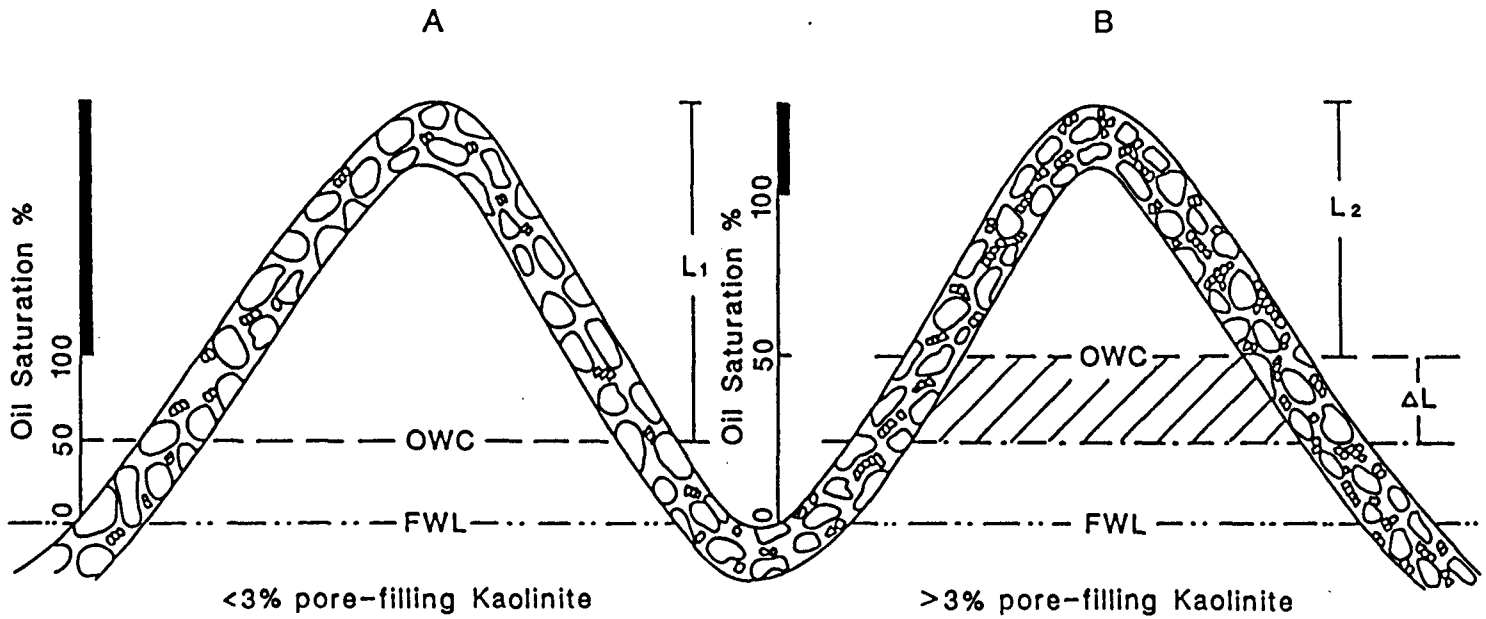

Figure 4.11. Schematic diagram showing the importance of interstitial diagenetic clays on the length of oil-columns in two adjacent structural traps (A and B). The amount of shortening of the oil-column (ΔL) is hatchured. Note also the long transitional oil/water contact (OWC) in trap B. OWC is drawn arbitrarily at 50% oil saturation (S_o). FWL - free-water level. Solid bar on vertical scale represents 100% oil saturation. See text for more explanation.

DIAGENETIC-PERMEABILITY TRAPS

Perhaps one of the most important implications of the digenetic-clay-induced capillary pressure difference is the formation of stratigraphic traps. In the literature they are commonly referred to as diagenetic or permeability traps (e.g., Webb, 1974; Wilson, 1977; Schneeflock, 1978). A knowlege of any spatial trend in the diagenetic overprint, be it a geographic or stratigraphic trend, can be critical in identifying these subtle and commonly elusive traps. The degree to which permeability deteriorates does not have to be significant, for even reservoir-quality sandstones may form effective barriers to oil migration (Berg, 1975). The diagenetic component has been found to be important in the trapping mechanisms of the many hydrocarbon fields in the Surat Basin, especially in the Roma Shelf area (cf. Martin, 1976). Diagenetic/permeability traps are rather common in low-permeability tight-gas reservoirs and can even give rise to such unconventional traps as 'inverted pools' where reservoirs commonly yield water-free gas in the downdip parts changing updip through a gas/water transition zone to a gas-free water zone (Masters, 1979, 1984; Cant ,1983; Spencer, 1985).

Table 4.2. Relationship between permeability, pore-throat sorting (PTS) and the minimum height of the oil-column relative to free-water level (FWL) and trap-relief of some actual hydrocarbon reservoirs (slightly modified from Jennings, 1987).

Permeability (md)	PTS	Min. height of the oil-column/ minimum trap closure (m).	
		50% oil satn.	75% oil satn.
0.5	1.2	50	65
10	4.2	20	40
350	1.2	2	2.5

TILTED OIL/WATER CONTACT

Another implication of the diagenetic-clay-induced capillary pressure difference within the reservoir rock is the occurrence of tilted oil/water contacts. Although they have been attributed to hydrodynamic flow of the formation fluids (Hubbert, 1953; Dahlberg, 1982) they can also result from sheer lateral change in porosity-permeability affecting the capillary pressure (Arps, 1964). These changes affect the length of the transition zone in different limbs of the trap resulting in a tilted oil/water contact. Identifying the type of tilting can be critical to successful economic development of an oil field. If lateral change in diagenetic trend which may give rise to changes in capillary pressure are not recognised then incorrect well locations might result from the improper application of the hydrodynamic theory. It may be mentioned here that tilting of the contact can occur also by loss of porosity-permeability due to continued diagenesis in the water-bearing reservoir rock below the oil/water or gas/water contacts if hydrocarbon is entrapped early in the geologic history. Subsequent structural movement may tilt the hydrocarbon/water interface without any hydrodynamic and capillary-pressure component. These 'frozen-in' hydrocarbon pools are, however, another type of diagentic trap (Webb, 1974; Wilson, 1977).

CONCLUSIONS

Authigenic clay minerals are present in varying proportions in all stratigraphic units of the Surat Basin succession. They adveresly affect such petrophysical parameters as porosity, permeability and water saturation. They increase the microporosity and water saturation, and reduce effective porosity and permeability. Porosity-permeability relationships in different formations are affected by the presence of different type and proportions of authigenic minerals. Some of these

mineral species are water- and acid sensitive whereas others are prone to effect migration of fines problems. A comprehensive understanding of the type, amount, crystallographic habit and mode of occurrence of the diagenetic mineral assemblage in sandstone reservoirs is vital for formation evaluation, successful drilling, testing, completion and enhanced recovery processes of hydrocarbons. Knowledge of this kind can be useful in the deliberate search for stratigraphic traps even in the early phase of exploration. This is critical for the Surat Basin which has stepped into its mature phase of hydrocarbon exploration since most of the obvious structures have been drilled.

REFERENCES

Almon, W. R., 1981, The impact of diagenesis on reservoir stimulation and management. Petrol. Expln Soc. Austral. distinguished lecture series. 383 p.

Almon, W. R., and Davies, D. K., 1981, Formation damage and crystal chemistry of clays. In Almon, W. R. (ed.) The impact of diagenesis on reservoir stimulation and management. Petrol. Expln Soc. Austral. distinguished lecture series., pp. 307-331.

Almon, W. R., and Schultz, A. L., 1979, Electric log detection of diagenetically altered reservoirs and diagenetic traps. Trans. Gulf. Coast Assoc. Geol. Soc., v. 29, pp. 1-10.

Arps, J. J., 1964, Engineering concepts useful in oil finding. AAPG Bull., v. 48, pp. 157-165.

Berg, R. R., 1975, Capillary pressure in stratigraphic traps. AAPG Bull., v. 59/6, pp. 939-956.

Cant, D. G., 1983, Spirit River Formation - a stratigraphic-diagenetic trap in the Deep basin of Alberta. AAPG Bull., v. 67/4, pp. 577-587.

Coote, S. M., 1986, Departmental stratigraphic drilling in Queensland, 1983 to 1986. Qld. Govt. Min. Jour., v. 87, n. 1017, pp. 306-326.

Dahlberg, E. C., 1982, Applied hydrodynamics in petroleum exploration. Springer-Verlag, 171 p.

Dickinson, W. R., 1970, Interpreting detrital modes of greywacke and arkose. Jour. Sedim. Petrol., v. 40, pp. 695-707.

Duff, P. G., 1986, Possible formation damage due to kaolinite in the Surat Basin, Bureau Min. Res. Unpubl. Rpt., 2p.

Exon, N. F., 1976, Geology of the Surat Basin in Queensland. Burea Min. Res. Bull. 166, 160 p.

Fuchtbauer, H., 1967, Influence of different types of diagenesis on sandstone porosity, Proc. 7th World Petrol. Cong., pp. 359-369.

Gaida, K. H., Ruhl, W., and Zimmerle, W., 1973, Rasterelektronmicroskopiche untersuchungen des porenraumes von sandsteinen, Erdoel Erdgas Zeitschrift, v. 89, pp. 336-343.

Grim, R. E.,1968, Clay mineralogy. McGraw-Hill Book Co., New York, 596 p.

Habermehl, M. A., 1980, The Great Artesian Basin, Australia. Burea Min. Res. Jour. Geol. Geophy. v. 5, pp. 9-38.

Hubbert, M. K., 1953, Entrapment of petroleum under hydrodynamic condition. AAPG Bull., v. 37, pp. 1954-2026.

Jennings, J. B., 1987, Capillary pressure techniques: application to exploration and development geology. AAPG Bull., v. 71/10, pp. 1196- 1209.

Keike, E. M., and Hartmann, D. J., 1973, Scanning electron microscope application to formation evaluation. Trans. Gulf Coast Assoc. Geol. Soc., v. 3, pp. 60-67.

Keith, B. D., and Pittman, E. D., 1983, Bimodal porosity in oolitic reservoir - effect on productivity and log response, Rodessa Limestone (Lower Cretaceous), East Texas Basin. AAPG Bull., v. 9. pp. 1391-1399.

Martin, K. R., 1976, Sedimentology of the Precipice Sandstone, Surat Basin, Queensland. Unpubl. Ph.D thesis. Univ. Qld., 224 p.

Masters, J. A., 1979, Deep basin gas trap, Western Canada. AAPG Bull., v. 63, pp. 152-181.

Masters, J. A., 1984, Lower Cretaceous oil and gas in the Deep basin of Western Canada. In Masters, J. A., (ed.) Elmworth - case study of a Deep basin gas field. AAPG Mem. 38, pp. 1-33.

Morgan, J. T., and Gordon, D. T., 1970, Influence of pore geometry on water-oil relative permeability. Jour. Petrol. Tech., pp. 1199-1208.

Neasham, J. W., 1977, The morphology of dispersed clay in sandstone reservoirs and its effect on sandstone shaliness, pore space, and fluid flow properties. Paper 6858, Soc. Petrol. Engrs.

Noon T. A., and Coote, S. M., 1983, Review of stratigraphic drilling in Queensland. Qld. Govt. Mining Jour., v. 84/985, pp. 417-453.

Patchet, J. G., 1975, An investigation of shale conductivity. The log Analyst., v. 16/6, pp. 3-20.

Pirson, S. J., 1963, Handbook of well log analysis for oil and gas formation evaluation. Prentice-Hall Inc., Englewood Cliffs, 326 p.

Pittman, E. D., 1979, Porosity, diagenesis and productive capability of sandstone reservoirs. In Scholle, P. A., and Schluger, P. R. (eds.) Clastic diagenesis. SEPM Sp. Publ. 26, pp. 159-173.

Pittman, E. D., and Thomas, J. B., 1979, Some applications of scanning electron microscopy to the study of reservoir rock. Jour. Petrol. Tech., pp. 1375-1380.

Pittman, E. D., and King, G. E., 1986, Petrology and formation damage control, Upper Cretaceous sandstone, offshore Gabon. Clay Minerals., v. 21, pp. 781-790.

Ranganathan, V., and Tye, R. S., 1986, Petrography, diagenesis, and facies controls on porosity in Shanon sandstone, Hartzog Draw Field, Wyoming. AAPG Bull., v. 70/1, pp. 56-69.

Scheidegger, A. E., 1963, The physics of flow through porous media. McMillan, New York, 313 p.

Schlumberger Ltd., 1972, Schlumberger log interpretation, vol.1 - principles. New York, 112 p.

Schneeflock, R., 1978, Permeability traps in Gatchell (Eocene) sands of California. AAPG Bull., v.62/5, pp. 848-853.

Schultz, A. L., 1979, Electric log evidence for hydrocarbon production and trapping in sandstones possessing diagenetic clay minerals. Bull. Houston Geol. Soc., pp. 4-7.

Slansky, E., 1984, Clay mineralogy, in Hawke, J. M., and Cramsie, J. W., (eds.) Contributions to the geology of the great Artesian Basin in New South Wales. Geol. Survey NSW Bull. 31, pp. 179-203.

Spencer, C. W., 1985, Geologic aspects of tight gas reservoirsin the Rocky Mountain region. Jour. Petrol. Tech., pp. 1308-1314.

Stalder, P. J., 1973, Influence of crystallographic habit and aggregate structure of authigenic clay minerals on sandstone permeability. Geolog. Mijn., v. 52/4, pp. 217-220.

Timur, A., 1968, An investigation of permeability, porosity and residual water saturation relationships. Soc. Profess. Well Log Anal. Annual symp. paper J., 18 p.

Waxman, M. H., and Smits, L. J. M., 1968, Electrical conductivities in oil-bearing shaly sands. Soc. Petrol. Engrs. Jour., v. 8, pp. 107-122.

Webb, J. E., 1974, Relation of oil migration to secondary clay cementation, Cretaceous sandstones, Wyoming. AAPG Bull., v. 58/11, pp. 2245-2249.

Wilson, H. H., 1977, "Frozen-in" hydrocarbon accumulations or diagnetic traps - exploration targets. AAPG Bull., v. 61/4, pp. 483-491.

Wilson, M. D., 1982, Origins of clays controlling permeability in tight gas sands. Paper 9843, Soc. Petrol. Engrs.